

U.S. DEPARTMENT OF COMMERCE
National Technical Information Service

AD-A028 314

REXOR ROTORCRAFT SIMULATION MODEL
VOLUME I. ENGINEERING DOCUMENTATION

LOCKHEED-CALIFORNIA COMPANY

PREPARED FOR
ARMY AIR MOBILITY RESEARCH AND DEVELOPMENT
LABORATORY

JULY 1976

232111

USAAMRDL-TR- 76-28A



REXOR ROTORCRAFT SIMULATION MODEL
Volume I - Engineering Documentation

ADA 028314 : Lockheed California Co.
P.O. Box 551
Burbank, Calif. 91520

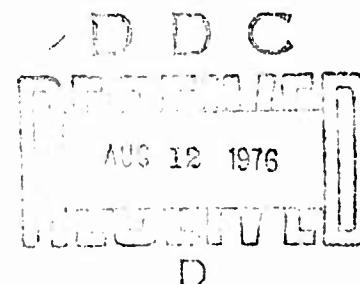
July 1976

Final Technical Report

Approved for public release;
distribution unlimited.

Prepared for

U. S. Army Aviation Systems Command
P.O. Box 209
St. Louis, Mo. 63166



EUSTIS DIRECTORATE
U. S. ARMY AIR MOBILITY RESEARCH AND DEVELOPMENT LABORATORY
Fort Eustis, Va. 23604

REPRODUCED BY
NATIONAL TECHNICAL
INFORMATION SERVICE
U. S. DEPARTMENT OF COMMERCE
SPRINGFIELD, VA. 22161

Unclassified

SECURITY CLASSIFICATION OF THIS PAGE (When Data Entered)

REPORT DOCUMENTATION PAGE		READ INSTRUCTIONS BEFORE COMPLETING FORM
1. REPORT NUMBER USAAMRDL-TR-76- 28A	2. GOVT ACCESSION NO.	3. RECIPIENT'S CATALOG NUMBER
4. TITLE (and Subtitle) REXOR ROTORCRAFT SIMULATION - Volume I, Engineering Documentation		5. TYPE OF REPORT & PERIOD COVERED Final Technical Report
7. AUTHOR(s) W.D. Anderson, F. Conner, P. Kretsinger, J.S. Reaser		6. PERFORMING ORG. REPORT NUMBER LR 27463
9. PERFORMING ORGANIZATION NAME AND ADDRESS Lockheed California Company PO Box 551 Burbank, Calif. 91520		8. CONTRACT OR GRANT NUMBER(s) DAAE11-66-C-3667(H)
11. CONTROLLING OFFICE NAME AND ADDRESS U.S. Army Aviation Systems Command P.O. Box 209 St. Louis, Missouri 63166		10. PROGRAM ELEMENT, PROJECT, TASK AREA & WORK UNIT NUMBERS
14. MONITORING AGENCY NAME & ADDRESS (if different from Controlling Office) Eustis Directorate U.S. Army Air Mobility R&D Laboratory Fort Eustis, Virginia 23604		12. REPORT DATE July 1976
		13. NUMBER OF PAGES 303
		15. SECURITY CLASS. (of this report) Unclassified
		15a. DECLASSIFICATION/DOWNGRADING SCHEDULE
16. DISTRIBUTION STATEMENT (of this Report) Approved for public release; distribution unlimited.		
17. DISTRIBUTION STATEMENT (of the abstract entered in Block 20, if different from Report)		
18. SUPPLEMENTARY NOTES Volume I of three volumes.		
19. KEY WORDS (Continue on reverse side if necessary and identify by block number) Aerodynamics Rotorcraft Simulation Matrix Representation Airfoil Tables Helicopters Rotors Nonlinear Models Computer Programs Blade Dynamics Digital Computers Inplane Damping		
20. ABSTRACT (Continue on reverse side if necessary and identify by block number) This report describes a rotorcraft nonlinear simulation called REXOR, and is divided into three volumes. The first volume is a development of rotorcraft mechanics and aerodynamics. The second is a development and explanation of the computer code required to implement the equations of motion. The third volume is a user's manual, and contains a description of code input/output as well as operating instructions.		

SECURITY CLASSIFICATION OF THIS PAGE (When Data Entered)

REXOR has been implemented on IBM 360 and CDC 6000 series equipment. The operating instructions are primarily based on the 360 equipment usage with additional instructions to show use on the 6000 series equipment.

[illegible]

2.

SECURITY CLASSIFICATION OF THIS PAGE(When Data Entered)

TABLE OF CONTENTS

Section		Page
	LIST OF ILLUSTRATIONS	8
	LIST OF TABLES	10
1	INTRODUCTION	11
1.1	SCOPE OF THE REXOR PROGRAM	11
1.2	REXOR CAPABILITIES	11
1.3	IMPROPER APPLICATION OF RFXOR	14
1.4	THE REXOR REPORT AND ITS USE	14
2	BACKGROUND	16
2.1	THE DERIVATION OF REXOR	16
2.2	GROWTH OF CAPABILITY	16
3	BASIC COMPUTATIONAL IDEA	17
3.1	MODAL SOLUTION - OVERVIEW	17
3.2	ENERGY METHODS DEVELOPMENT	17
3.3	CALCULATION OF ROTOR MODE DISPLACEMENTS, VELOCITIES AND ACCELERATIONS	18
3.4	OUTPUT	19
4	SYMBOLS	20
4.1	SUBSCRIPTING NOTATION	20
4.1.1	Blade Number	20
4.1.2	Mode Number	20
4.1.3	Mode Type	20
4.1.4	Generalized Mass, Damper, Spring, Forces	21
4.1.5	Forces and Moments	21
5	COORDINATE SYSTEMS AND TRANSFORMATIONS	22
5.1	INTRODUCTION	22
5.2	COORDINATE SETS	22
5.2.1	Fuselage Coordinates	22
5.2.2	Hub Coordinates	22

TABLE OF CONTENTS (Continued)

Section		Page
5.2.3	Rotor Coordinates	25
5.2.4	Blade Coordinates	25
5.2.5	Blade Element Coordinates	29
5.2.6	Freestream (Earth) Set	29
5.2.7	Gyro Coordinates	29
5.2.8	Swashplate Coordinates	34
5.3	DEGREES OF FREEDOM	34
5.3.1	Vehicle or Rigid Body	34
5.3.2	Rotor	36
5.3.3	Shaft or Pylon Bending	36
5.3.4	Blades	37
5.3.5	Swashplate	40
5.3.6	Gyro	42
5.4	GENERAL MOTION AND COORDINATE TRANSFORMATIONS	42
5.4.1	General Case of Space Motion	42
5.4.2	Coordinate Transformations - Euler Angles	46
5.4.3	Angular Velocities and Accelerations - General	50
5.5	RELATIVE MOTIONS AND TRANSFORMATIONS USED IN THE EQUATIONS OF MOTION	53
5.5.1	Hub Motion in Inertial Space	53
5.5.2	Fuselage Motion in Inertial Space	60
5.5.3	Motion of Rotor Coordinate Axis	63
5.5.4	Blade Coordinate Relative to Rotor Coordinates	65
5.5.5	Blade Element Motion	67
5.5.6	Swashplate Motion	107
5.5.7	Direct Feedback Control System Gyro Motion	110
5.5.8	Blade Feathering Motion	111
6	EQUATIONS OF MOTION	117
6.1	INTRODUCTION	117
6.2	ENERGY APPROACH TO DEVELOPMENT OF EQUATIONS OF MOTION	117

TABLE OF CONTENTS (Continued)

Section		Page
6.3	ITERATIVE CONCEPT AND EQUATION SET SOLUTION METHOD . . .	123
6.4	OVERVIEW OF ROTOR-BLADE MODEL	140
6.4.1	Concept of Modes	140
6.4.2	Blade Bending - Modal Variable	140
6.4.3	Adapting Modal Description to Variable Geometry . . .	141
6.4.4	Blade Mode Generation	143
6.4.5	Modal Coefficients	144
6.4.6	Independent Blades	144
6.4.7	Blade Element Aerodynamic Forces - Overview	145
6.4.8	Blade Torsional Response	145
6.4.9	Radial Integration	145
6.5	EQUATION SYSTEM DEVELOPMENT	145
6.5.1	Reference to Base Operation Matrix	145
6.5.2	Organization by Degrees of Freedom	146
6.5.3	Partial Derivatives	147
6.5.4	Generalized Masses	151
6.5.5	Generalized Forces	152
6.6	BLADE BENDING AND TORSION EQUATIONS	152
6.6.1	Blade Radial Summation	152
6.6.2	Partial Derivatives	152
6.6.3	Generalized Masses	163
6.6.4	Generalized Forces	168
6.6.5	Quasi-Static Blade Torsion	173
6.6.6	Quasi-Static Pitch Horn Bending	175
6.7	ROTOR TILT EQUATIONS	176
6.8	SHAFT BENDING EQUATIONS	178
6.8.1	Prime Contributions From Fuselage	178
6.8.2	Partial Derivatives	178
6.8.3	Generalized Masses	179
6.8.4	Generalized Forces	182

TABLE OF CONTENTS (Continued)

Section		Page
6.9	PRINCIPAL REFERENCE AXIS EQUATIONS	183
6.9.1	Nonzero Contributions From Most Vehicle Mass Elements	183
6.9.2	Partial Derivatives	184
6.9.3	Generalized Masses	187
6.9.4	Generalized Forces	187
6.10	SWASHPLATE EQUATIONS	199
6.10.1	Use as a Pure Swashplate or a Feathering Feedback Control Gyro	199
6.10.2	Partial Derivatives	200
6.10.3	Generalized Masses	202
6.10.4	Generalized Forces	208
6.10.5	Control Inputs	220
6.11	CONTROL GYRO EQUATIONS	221
6.11.1	Introduction	221
6.11.2	Partial Derivatives	222
6.11.3	Generalized Forces	222
6.11.4	Control Gyro Feedback	228
6.11.5	Summary Description of Phase Angles	233
6.12	ENGINE EQUATIONS	235
6.12.1	Rotor Azimuth and Rotation Rate	235
6.12.2	Engine Model	235
6.12.3	Partial Derivatives	237
6.12.4	Generalized Masses	238
6.12.5	Generalized Forces	240
7	AERODYNAMICS	241
7.1	INTRODUCTION	241
7.1.1	Aerodynamic Forces Producing Surfaces Considered . .	241
7.1.2	Use of Forces Generated	241

TABLE OF CONTENTS (Continued)

Section	Page
7.2	MAIN ROTOR 241
7.2.1	Overview 241
7.2.2	Concept of Rotor Inflow Model 242
7.2.3	Blade Element Velocity Components 252
7.2.4	Coefficient Table Lookup - Overview 263
7.2.5	Blade Element and Rotor Aerodynamic Loads Summary . . 266
7.3	INTERFERENCE TERMS 267
7.3.1	Nature of the Phenomenon 267
7.3.2	Rotor to Wing/Fuselage 267
7.3.3	Rotor to Horizontal Tail 269
7.3.4	Wing to Horizontal Tail 270
7.3.5	Data Sources 270
7.4	BODY LOADS 271
7.4.1	Nonrotating Airframe Airloads 271
7.4.2	Component Additional Airloads 275
7.5	TAIL ROTOR 276
7.5.1	Formulations 276
7.5.2	Airloads - Control Settings 283
7.6	PROPELLER 283
7.6.1	Formulations 283
7.6.2	Airloads - Control Settings 285
8	REFERENCES CITED 288
	LIST OF SYMBOLS 290

LIST OF ILLUSTRATIONS

Figure		Page
1-1	Block Diagram Model Description	12
5-1	Coordinate Systems Fuselage Set	23
5-2	Coordinate Systems Fuselage Axis to Airmass	24
5-3	Coordinate Systems - Hub (Nonrotating Shaft Top to Fuselage Axis (Flexible Shaft)	26
5-4	Coordinate Systems - Hub Axis to Airmass	27
5-5	Coordinate Systems - Rotor, Blade, and Blade Element Sets	28
5-6	Coordinate Systems - Blade Element Set	30
5-7	Coordinate Systems - Freestream (Earth) to Hub Axis	31
5-8	Coordinate Systems - Trajectory Path to Freestream Axis	32
5-9	Coordinate Systems - Control Gyro and Swashplate Sets to Reference Sets	33
5-10	Degrees of Freedom	35
5-11	First Inplane Mode	39
5-12	First Flap Mode	39
5-13	Second Flap Mode	39
5-14	Blade, Pitch Horn and Feather Hinge Geometry	41
5-15	General Case of Space Motion in Terms of Moving Coordinate Axes x, y, z and Inertial Axes X, Y, Z	43
5-16	Rotational Displacement of a Coordinate System	48
5-17	Relationship of Euler Angle and Coordinate System Angular Rates	51
5-18	Blade Element CG/Origin Location in Blade Coordinates	69
5-19	Effect of Blade Twist on Location of Blade Element CG/Axis System Origin	69
5-20	Blade Precone Angle, β_0	71
5-21	Blade Sweep, τ_0 , and Blade Droop, γ	71
5-22	Introduction of Blade 1/4 Chord Offset, Y_{jog} and Z_{jog} With Respect to Precone Line	72
5-23	Point p and Feathering Axis Precone β_{FA}	74
5-24	Static Feather Bearing Geometry	77

LIST OF ILLUSTRATIONS (Continued)

Figure		Page
5-25	Blade Static Pretwist, ϕ_{TW} and Elastic Twist, ϕ_T	84
5-26	Neutral Axis vs Blade Radius.	101
5-27	Pitch Horn Blade Feathering Phase Angle	114
6-1	Equation Solution Loop	128
6-2	Teetering Rotor Mass Matrix Modifications	177
6-3	Swashplate Friction	210
6-4	Tension-Torsion Pack Geometry	212
6-5	Control Axis	216
6-6	Effect of Stiction of Feedback Lever Displacement	230
6-7	Phasing For Direct-Flap Feedback Control System	234
6-8	Engine Model and Torque-Speed Characteristics	236
7-1	Blade Loading Distributions in Hover	243
7-2	Induced Velocity Distribution as a Function of Wake Angle (Forward Flight)	244
7-3	Incremental Area for Shaft Moment Integration	246
7-4	Typical Shape of Longitudinal Factor Curve	251
7-5	Dynamic Stall-Lift Coefficient vs Angle-of-Attack Hysteresis Loop	262
7-6	Dynamic Stall - Moment Coefficient vs Angle-of-Attack Hysteresis Loop	264
7-7	Trivariant Linear Interpolation	268
7-8	Overall Tail Rotor Geometry	277
7-9	Tail Rotor Blade Element Detail	277
7-10	Propeller - Fuselage Geometry	284
7-11	Typical Non Dimensional Propeller Data	286

LIST OF TABLES

Table		Page
6-1	Blade Generalized Masses	164
6-2	Generalized Masses	180
6-3	Generalized Forces	182
6-4	Principal Axis Generalized Masses	188
6-5	Principal Axis Generalized Forces	195
6-6	Swashplate Generalized Masses	203
6-7	Engine Generalized Masses	239

1. INTRODUCTION

1.1 SCOPE OF THE REXOR PROGRAM

REXOR is a rotorcraft analysis tool which has resulted from applying an interdisciplinary math modeling philosophy, Reference 1. The REXOR math model has been written for a single four-bladed, gyro-controlled, hingeless-rotor helicopter with additional capability for analysis of teetering or hinge-offset rotor systems with conventional controls and two or four blades. This helicopter may be conventional in design, winged, or compounded. The specific analysis is limited to a maximum of four blades, but it can be expanded to include more blades by following the detailed mechanical derivation procedure established for the analysis. The model is broken down into the three major categories shown in Figure 1-1. These categories are the control system, the rotor, and the body.

Figure 1-1 indicates the manner in which these components are related to one another as utilized in the analysis. The analysis is the simulation of an entire aircraft, which includes a detailed dynamic description of the rotor and control system as well as a conventional six-degree-of-freedom body dynamic description which operates in two modes identified as TRIM and FLY. In the TRIM mode, the aircraft is constrained to a prescribed static flight condition while the controls are activated and the rotor is allowed to respond to obtain a force and moment equilibrium of the aircraft at that static condition. In the FLY mode the entire aircraft is free to respond dynamically to a maximum of 30 degrees of freedom to control inputs or to any other arbitrary inputs such as gusts. Pilot inputs can be any single or multiple control manipulation in the form of simple steps or pulses, doublets, stick stirs, or other transient input within the capabilities of the control system simulated. As a result, transient loads and resulting aircraft and rotor dynamic response can be obtained. For correlation purposes, actual flight test control motions can be used as input to provide comparative response data. For specialized applications, an analytic autopilot may be used to control the flight path of the aircraft. Additionally, gust inputs and other types of external excitations could be applied directly to the rotor and/or airframe.

1.2 REXOR CAPABILITIES

REXOR is a detailed rotorcraft math model simulation with particular emphasis on the main rotor mechanics. The program is particularly valuable in a detailed exploration of rotor characteristics of proposed designs, in identifying problem areas and verifying fixes in flight test development programs. A case history is given in Reference 2.

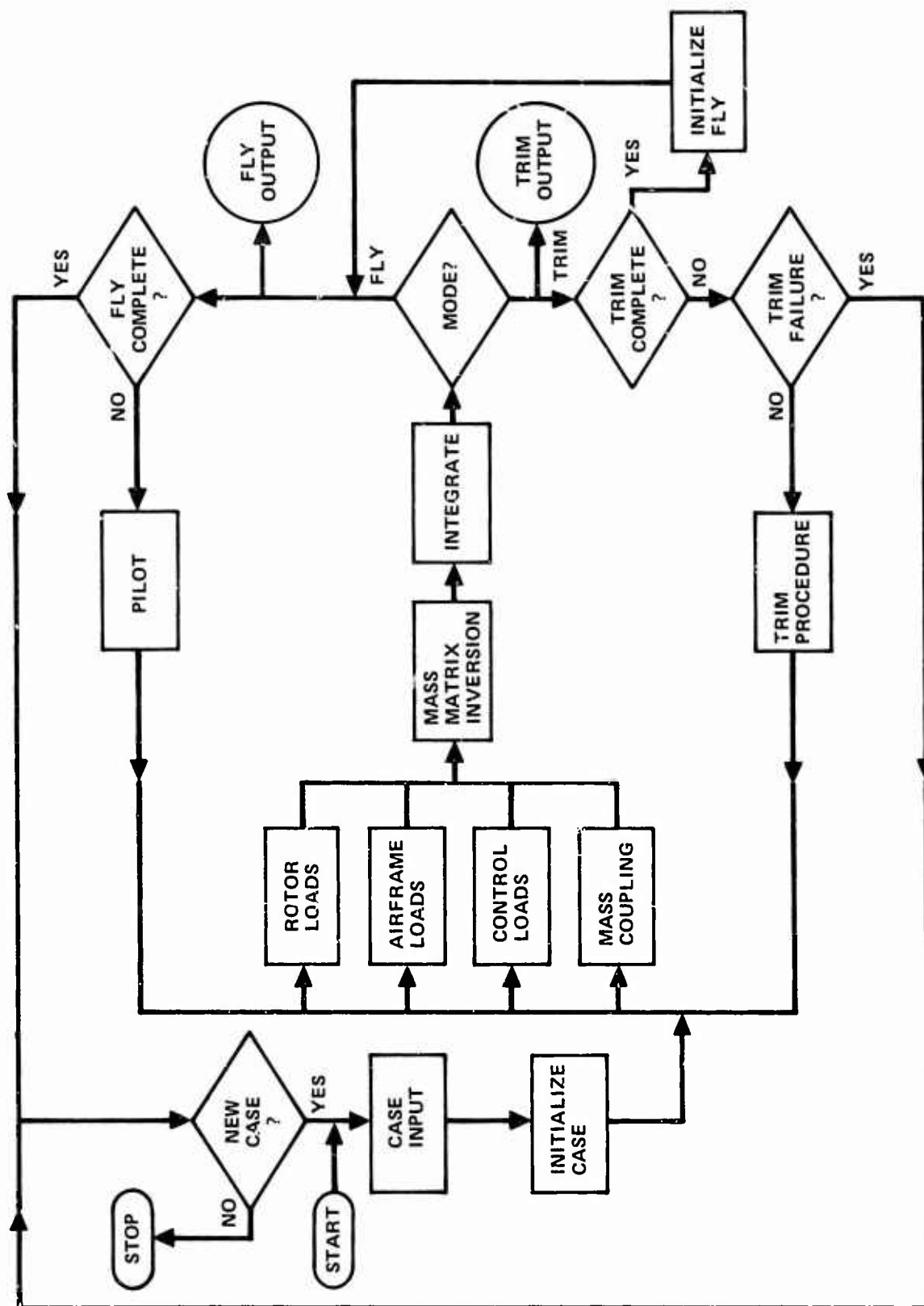


Figure 1-1. Block Diagram Model Description

Typical REXOR applications are listed below.

Dynamics:

- Rotor stability in regions below 4P as function of flight speed, maneuvers, rotor rpm, nonlinear blade aerodynamics
- Rotor/body sensitivity and dissipation capacity as a function of gusts and pilot control inputs
- Effects of design parameters (mechanical and elastic couplings, controls, etc.) on rotor stability and load sensitivity
- Correlation and check of specialized dynamic models.

Handling Qualities:

- Vehicle response to pilot control inputs for vehicle flight conditions, speed, altitude, rotor rpm, design parameter variations
- Vehicle stability as function of speed, rotor rpm, flight conditions, design parameters
- Effect of design parameter variations on handling qualities
- Development and checking of handling qualities models.

Failure Analysis:

- Effect of loss of one inplane damper on subsequent flight time history
- Blade projectile hit and ensuing events
- Blade strike and resulting rotor track.

Performance:

- Correlation and independent check of performance models, particularly in regions of highly nonlinear blade aerodynamic operation (retreating blade stall and compressibility effects)
- Develop data for performance models for use in nonlinear areas

Loads:

- Steady-state rotor loads as a function of rotor rpm, flight velocity, control trim settings
- Dynamic rotor loads as a function of rotor rpm, flight velocity, vehicle maneuvers, pilot control inputs
- Rotor/fuselage clearances as a function of speed, vehicle maneuvers, rotor rpm, pilot control inputs, flight configuration
- Rotor/fuselage/wing design characteristics requirements as functions of maneuver load factor, control commands (see Reference 3).

1.3 IMPROPER APPLICATION OF REXOR

While REXOR is capable of performing a number of analysis tasks, the program range of use is certainly not all inclusive. Examples of types of use where REXOR either wouldn't work well or would be impractical are given below.

REXOR is an extensive math model and, as such, may consume a considerable amount of computer time to execute a case. Therefore, the program is not intended as a parametric design analysis tool, but rather as a device to verify the correctness of a parametric selection process.

REXOR does not treat blade-to-blade vortex interaction. This condition limits the validity of the vibration solution in the transition flight regime.

REXOR typically uses twenty or less blade radial stations. The computer blade deflections show good correlation to measured data with this modeling. However, since shear is a first derivative, and moment is a second derivative of deflection data, care needs to be exercised in their use (Reference 4).

1.4 THE REXOR REPORT AND ITS USE

This report is presented in three volumes.

- Volume I

A development of rotorcraft mechanics and aerodynamics including a derivation of the equations of motion from first principles.

- Volume II

The development and explanation of the computer code required to implement the equations of motion.

- Volume III

A user's manual containing a description of code input/output and instructions to operate the program.

Volume I is intended to be a self-sufficient guide to the math development of the equations of motion and is the reference background as such. Volume II gives the location of computation elements, and serves to locate elements for inspection or modification. Volume III presents normal program operation plus troubleshooting guide material required for day-to-day program use.

2. BACKGROUND

2.1 THE DERIVATION OF REXOR

The REXOR analysis is the result of a natural evaluation of capability arising from a desire to develop a rotorcraft handling qualities analysis. This required a model of a complete aircraft which, as it was refined, exhibited unique advantages for analysis of dynamic stability, loads and performance. The eventual outgrowth is an interdisciplinary analysis with broad areas of application.

The initial development effort was called Rotor Junior (Reference 5). This program had a reasonably detailed nonrotating airframe representation, but used a steady-state representation for the main and tail rotors. (Bailey T Coefficients, Reference 6.) A major rework of this program especially in the main rotor led to Rotor Senior. Here the dynamic response of rotating blades was calculated (References 7 and 8). Many simplifying assumptions were made in the construction of the blade dynamics. Starting afresh in this area plus a general overhaul of the model by an interdisciplinary team of specialists led to Revised and Extended Rotor Senior or REXOR. A key feature was incorporating the solution of generalized force equations for incremental accelerations using a generalized mass matrix, and thus coupling of all the degrees of freedom.

2.2 GROWTH OF CAPABILITY

The original model (Rotor Junior) was intended strictly for stability derivatives. With the addition of blade dynamics, some evidence of and useful insight into subharmonic rotor instability problems was obtained (Rotor Senior). With the advent of very detailed blade and blade interface modeling, many new design problem areas have been avoided, and deficiencies of existing designs corrected (REXOR).

3. BASIC COMPUTATIONAL IDEA

3.1 MODAL SOLUTION - OVERVIEW

The aircraft is described dynamically in approximately thirty fully-coupled degrees of freedom. In addition to the six degrees of freedom of the hub principal reference axes, the fuselage is related to the rotor hub through rotor rotational speed, shaft pitch, and shaft roll degrees of freedom. The control gyro/swashplate combination has three degrees of freedom. Motion of each of the four main rotor blades is described by three coupled flapwise and inplane modes and a pitch horn bending degree of freedom which couples blade feathering to the control gyro or swashplate. These four degrees of freedom per blade make sixteen for the four blades.

The blade modes are primitive modes in that they are determined from a lumped parameter analysis of a rotating cantilever blade at a selected rotor speed and collective blade angle, hereafter referred to as the reference feather angle. The generalized stiffness matrix is computed using these rotating modes and contains only the structural stiffness of the blades and hub. This formulation ensures proper internal and external force and moment balance. The modal deflections outboard of the feather hinge are rotated through the actual feather angle less the reference feather angle. Thus, blade element deflections outboard of the feathering hinge due to modal displacements are defined to remain aligned with a coordinate axis system which is orthogonal to a plane containing the instantaneous deformed feather axis and rotated through the instantaneous feather angle less the reference feather angle. As a result, the internal strain energy in the blade due to unit modal displacements is invariant with variation in blade angle. This technique permits the highest resolution of motion and forces for the blade with an assumed mode solution for a given number of modes.

3.2 ENERGY METHODS DEVELOPMENT

The equations of motion for REXOR are developed from Lagrange's equations, which is an energy approach. If one can express the kinetic, potential, and dissipative energies of a system in addition to the work done by external forces, then Lagrange's equations provide a powerful method for developing the equations of motion.

The dynamic equations of motion are written in matrix form as

$$- [A] \{\ddot{q}\} + \{G\} = 0 \quad (3-1)$$

where $[A]$ is approximately a 30 by 30 matrix of generalized mass elements, $\{\ddot{c}\}$ is a column matrix of accelerations of the generalized coordinates and $\{G\}$ is a column matrix derived from the Lagrangian energy functions, dissipation function and generalized forces, which take the form:

$$\{G\} = - [B] \{\dot{q}\} - [C] \{q\} + [Q] \{f(t)\} \quad (3-2)$$

The equations of motion are solved as a time history at rotor azimuth angle increments required to provide a stable solution for the highest frequency mode present in the solution.

3.3 CALCULATION OF ROTOR MODE DISPLACEMENTS, VELOCITIES AND ACCELERATIONS

In a rotor simulation of this type, it is difficult to compute the proper displacement velocities and accelerations, and associated inertia and aerodynamic forces and moments which are required for high resolution of the blade feathering moments. This requires exacting aerodynamic data as well as a precise statement of the inertial loadings. To establish the feathering moments due to these loads, the relationship between the feather axis and the point of application of the loads must be precisely determined. This is accomplished by a very accurate analytic construction of the undeformed blade and a superposition of the blade elastic bending on this shape. In order to achieve the highest resolution of the predicted blade shape and feather axis position, the blade modes are defined at approximately the trim collective blade angle. The blade static position is also constructed at this blade angle. Blade element displacements, velocities, and accelerations are then computed from the combined static shape, the elastic blade motion, and blade feathering with respect to the reference feather angle.

The aerodynamic description used in the analysis is composed of a rotor inflow model, nonlinear steady and unsteady blade element aerodynamics, nonlinear body aerodynamic characteristics, rotor/body aerodynamic interference, and auxiliary airloads from the tail rotor and propeller. The auxiliary airloads are contained in modular subroutines and are functions of advance ratio and propeller and tail rotor collective pitch. The main rotor downwash effect on the wing and horizontal tail angles of attack is an empirical function of rotor thrust and advance ratio. The nonlinear body aerodynamics may be inputted as tables of actual wind tunnel test data.

The aircraft primary control systems are simulated from the pilot control levers operating through a boost system in all control axes. Gearing and gains in the control path are inputs to the analysis and may be easily changed for studying the effects of design changes in the control system.

Control servos are simulated by first-order lags with rate limits and with soft and hard physical stops. Control stiffnesses in collective and cyclic pitch axes of the main rotor are included in the dynamic equations of motion.

3.4 OUTPUT

The analysis is a time-history solution of the equations of motion. The standard output format provides plots of up to 40 output parameters in TRIM and 60 in FLY. In addition, a tabulation is provided at the end of each mode of operation. The analysis also provides plot capability at the end of TRIM to show loads at various points in the system over a single rotor revolution on an expanded linear scale. These loads are harmonically analyzed and the harmonic components printed out.

In addition to the tabbed or plotted time-history output in the FLY mode, a tape or disc pack record can be made at selected time points for use in a fast Fourier transform analysis. The record pickup interface and FFT are not supplied as part of REXOR, but are included by the user to match the computation facility used. The FFT analysis gives a quantitative evaluation of the mode/member oscillation in question. Accurate damping ratio and resonant frequency data are available from this procedure.

4. SYMBOLS

The notation used in REXOR generally follows what could be termed NASA notation. In general:

- Axis systems use a right-hand triad X, Y, Z
- Rotations about these axes are also a right-hand triad θ, ϕ, ψ
- Rotation rates, again a right-hand triad, are p, q, r
- Velocity components of X, Y, Z are u, v, w .

4.1 SUBSCRIPTING NOTATION

Subscripting is used as a rule in REXOR to further identify a variable. Superscripts except in a few column vectors are reserved to denote raising to a power. The subscripting can mean:

- Type of element; F for fuselage, SP for swashplate, TR for tail rotor, R for rotor, etc.
- Coordinate system reference; BLn for blade axis, H for hub axis, R for rotor axis, etc.
- Modal identifiers.

4.1.1 Blade Number

The blade modal identifier typically is of the form A_{mn} . Where n is the blade number.

4.1.2 Mode Number

Also from A_{mn} , m is the mode number, and is keyed to the symbol A . A represents blade bending modes (3). Therefore m can be 1 to 3.

4.1.3 Mode Type

Other than blade bending the remaining blade mode is torsion, and is separately identified as β_{PHn} . Nonblade modes are identified by the direction and subscripted axis of motion. Examples are ψ_R for rotation of the rotor and θ_S for longitudinal shaft bending.

4.1.4 Generalized Mass, Damper, Spring, Forces

The generalized masses are denoted as M doubly subscripted by the two modes active for that mass. Examples are $M_{\phi S \phi S}$ and $M_{Amn \theta_H}$. This

scheme is also used for other elements of the equations of motion, dampers (C), springs (K), forces (F). Note the forces are a column vector and singly subscripted.

4.1.5 Forces and Moments

In the process of forming the equations of motion many subelements of forces and moments are formed, translated and combined. Several layers of subscripting may exist in performing this process. The guidelines to the layering are:

- First layer denotes the direction or axis system that the quantity is formed in. Examples are X and BLE.
- Second is the axis system involved or axis system being translated to, depending on the specification of the first level. The second level may also be specified as 0 or nought, to indicate the value is at the coordinate system origin. This notation is used to show an inertial reference and blade root summation quantities.
- The third layer, usually outside a series of bracketed quantities, shows the blade number being computed, or the overall coordinate system in use for the computation at hand.

5. COORDINATE SYSTEMS AND TRANSFORMATIONS

5.1 INTRODUCTION

Prior to developing the equations of motion, a system of coordinate sets with a description of the elements of the system in these sets and the interrelationship of the sets is required.

5.2 COORDINATE SETS

5.2.1 Fuselage Coordinates (X_F, Y_F, Z_F)

The fuselage set origin is located along the undeflected main rotor shaft line, and at a convenient waterline (the cg for instance). See Figure 5-1. The coordinates form a right-hand triad X_F, Y_F, Z_F . Notations for velocities with respect to earth of these coordinates are either $\dot{X}_F, \dot{Y}_F, \dot{Z}_F$ or u_F, v_F, w_F . A conventional double dot notation is used for acceleration. Euler rotations of the set follow conventional practice of roll right ϕ_F , pitch up θ_F , and yaw right ψ_F . Rates of rotation are either denoted by dot notation or p_F, q_F, r_F . Angular acceleration is double dot notation of the rotation or dot notation of the rates, $\ddot{\phi}_F, \ddot{\theta}_F, \ddot{\psi}_F$ or $\dot{p}_F, \dot{q}_F, \dot{r}_F$.

Numerous aerodynamic terms are referenced to the fuselage set. Figure 5-2 shows the relationship of airflow to this set. The components of airflow, also noted as u_F, v_F, w_F , are defined with respect to the fuselage set by an angle of attack α , and a sideslip angle β . The angle of attack is the arcsin of the ratio of the vertical component and the vector sum of the X and Z components. The sideslip is the Y component of airflow in relation to the total vector airflow sum. The angle of attack is positive (pitch up) of the fuselage set with respect to the airflow. The sideslip is positive (yaw left) for the airflow relative to the set. The airflow is the vector sum of the fuselage set inertial motion and flow fields from other parts of the vehicle, such as main rotor downwash.

5.2.2 Hub Coordinates (Principal reference set) (X_H, Y_H, Z_H)

The hub set origin is at the top of the main rotor mast, but does not rotate with the mast. The mast top location represents the optimum choice as a summing point for loads, and a reference point to track relative positions of model elements with a minimum of algebraic operations.

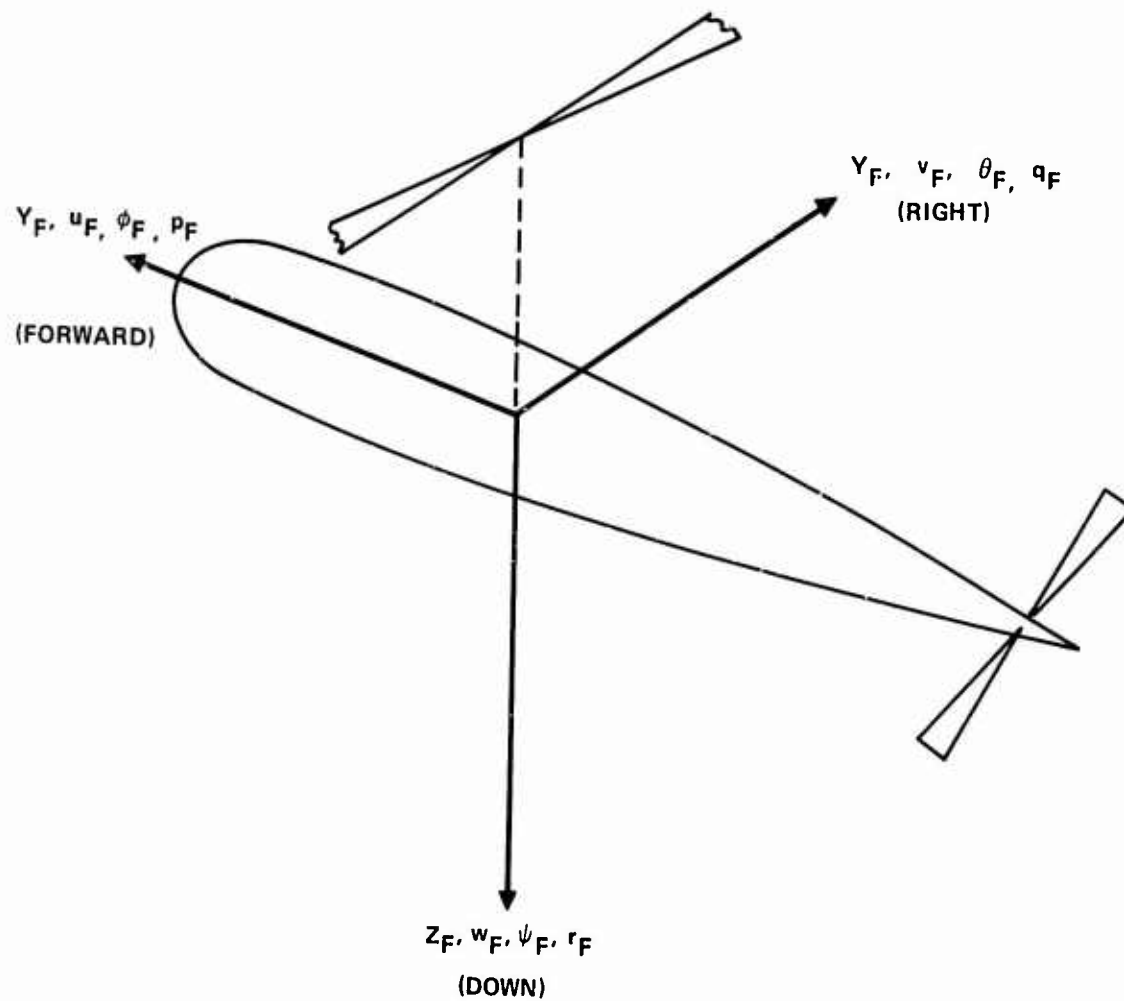
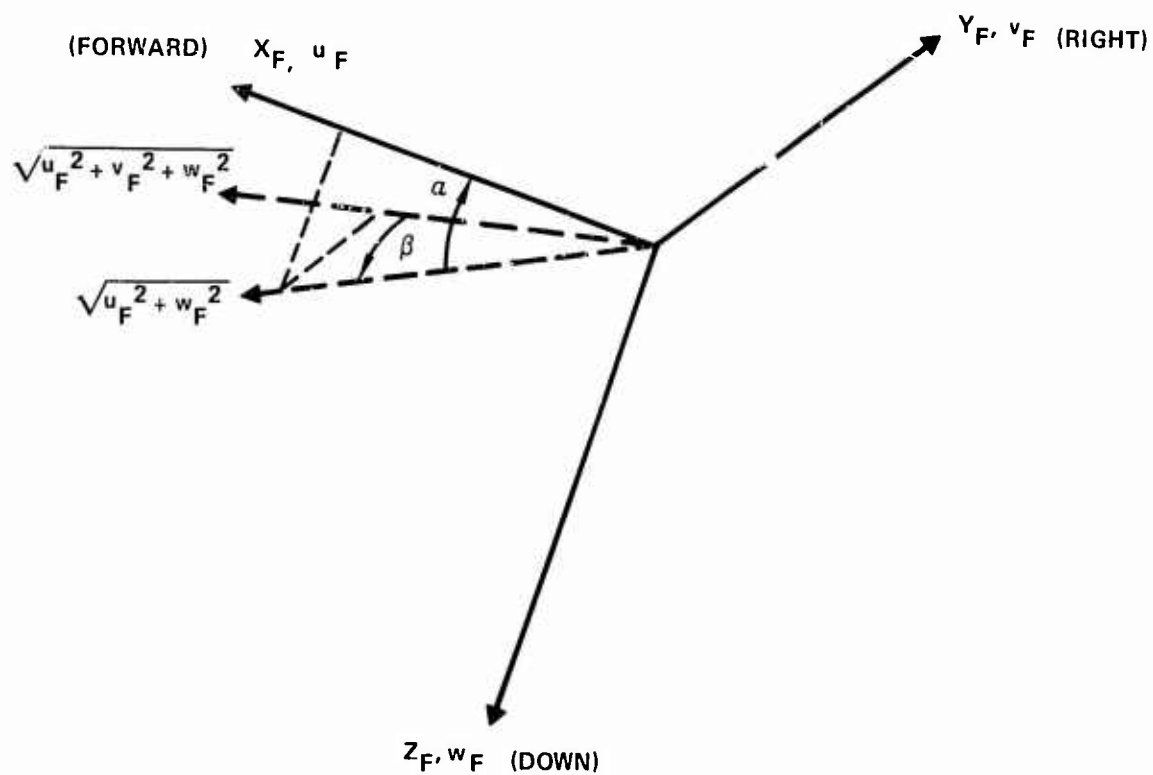


Figure 5-1. Coordinate Systems Fuselage Set



$$\alpha = \sin^{-1} \frac{w_F}{\sqrt{u_F^2 + w_F^2}} ; \beta = \sin^{-1} \frac{v_F}{\sqrt{u_F^2 + v_F^2 + w_F^2}}$$

Figure 5-2. Coordinate Systems Fuselage Axis to Airmass

For an undeflected rotor mast, the hub set origin is in line with the Z_F axis a distance Z_{OF} up from the fuselage set. See Figure 5-3. At this point, the hub set X, Y axes are in the same direction and sense as the fuselage set X, Y .

Due to small angle assumption shaft (S) set bending, the hub set is rotated ϕ_S and θ_S (Euler angles) from the fuselage set. As the hub set is the principal reference axis, the fuselage set rotates under the hub set. The fuselage set origin moves to the right and back for positive ϕ_S and θ_S . The corresponding translations are $(\partial X_F / \partial \theta_S) \theta_S$ and $(\partial Y_F / \partial \phi_S) \phi_S$. The partials are constants, and are zero for a virtual pivot point at the fuselage set origin.

Airflow information is also referenced to the hub set for use in the main rotor aerodynamic calculations. The reference scheme is shown on

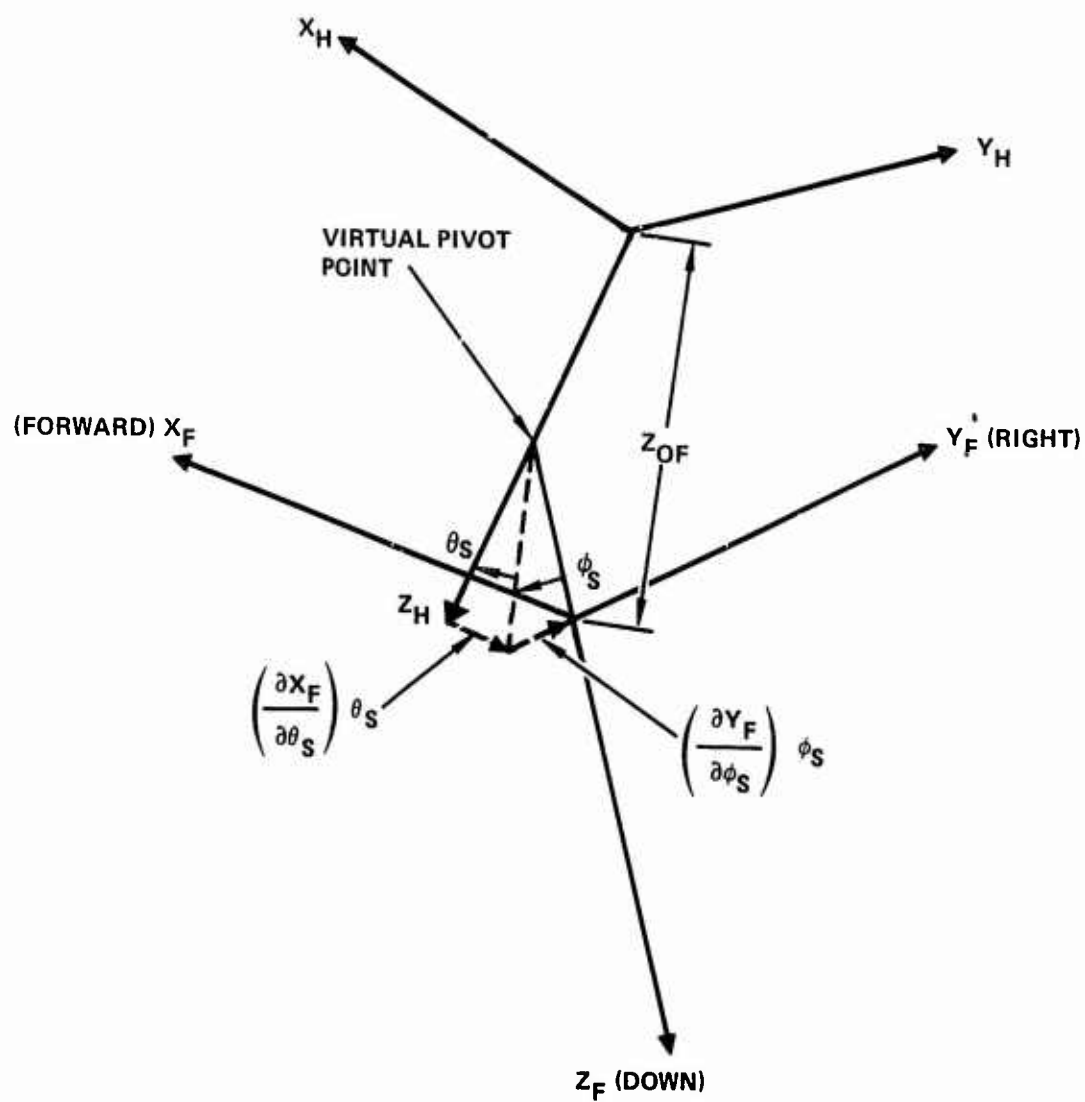
Figure 5-4. For components of airflow u_H, v_H, w_H with respect to the hub set, an angle of attack α_2 , and sideslip ψ are defined. The generation conventions are different from the fuselage airflow reference.

5.2.3 Rotor Coordinates (X_R, Y_R, Z_R)

The undeflected rotor set has the same origin as the hub set and a common Z axis. See Figure 5-5. However, the X_R axis rotates with the blade number 1 reference axis system. The Y_R axis points to the blade number 1 leading edge. The rotation of the rotor set is measured counter-clockwise (CCW) from the $-X_H$ axis by the angle ψ_R . The rotor set serves as a datum basis for blade number one and has a common Z axis with the BLn sets.

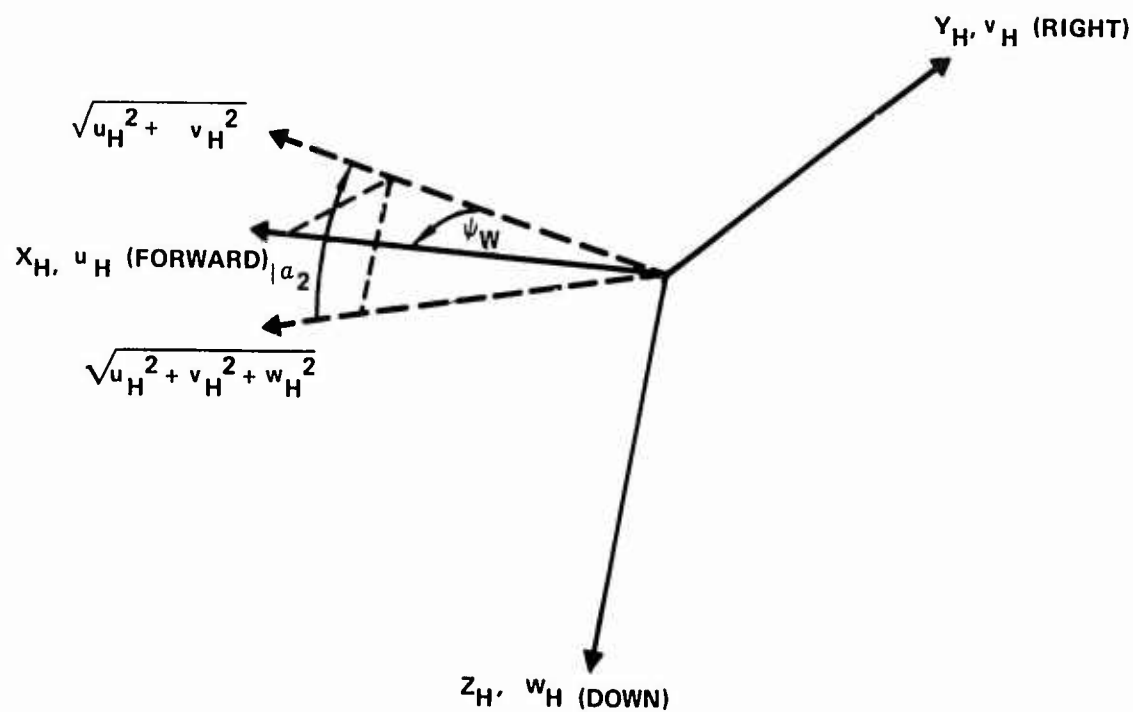
5.2.4 Blade Coordinates ($X_{BLn}, Y_{BLn}, Z_{BLn}$)

To bookkeep the deflections properly of all the main rotor blades, sets equivalent to the rotor set are created for each blade. These are the BLn sets, where n is the blade number (counted clockwise from blade number one). All BLn sets are identical except for an azimuthal rotation $(n-1) \Delta\psi$, where $\Delta\psi$ is the interblade angular spacing. The rotation is about the Z_R axis. Note that BLn sets are rotating coordinates and have a common Z axis.



THERE IS NO YAW (Z) ROTATION BETWEEN H AND F SETS

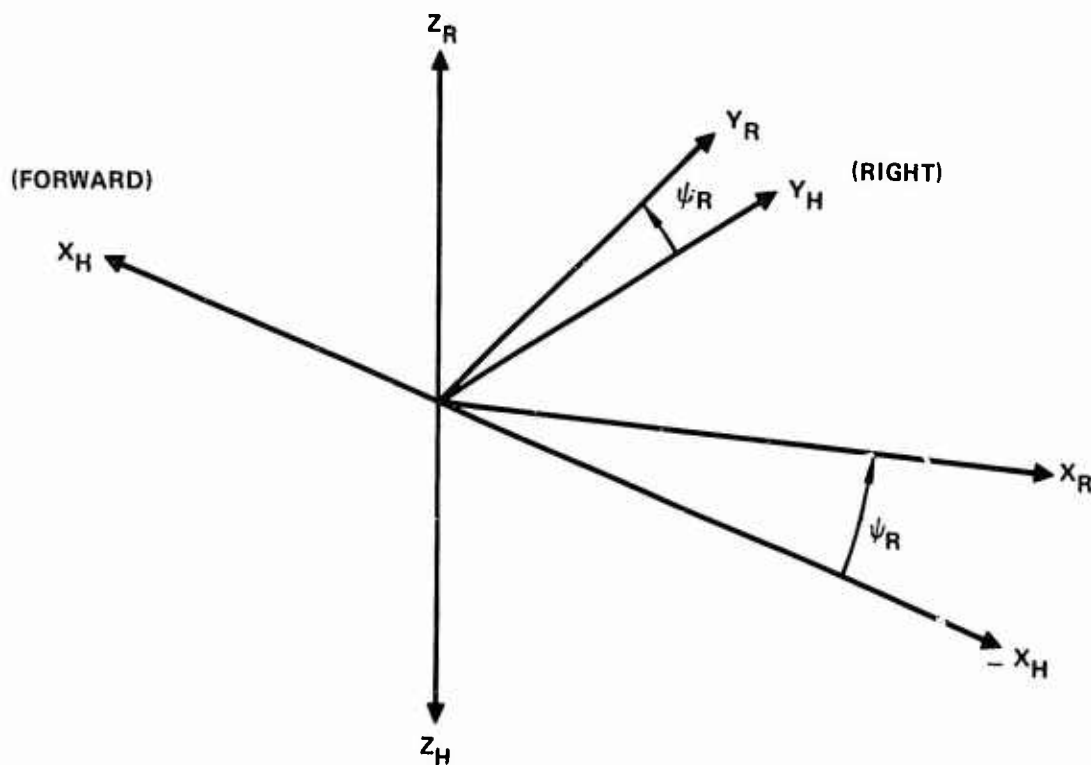
Figure 5-3. Coordinate Systems - Hub (Nonrotating Shaft Top) to Fuselage Axis (Flexible Shaft)



$$\alpha_2 = \sin^{-1} \frac{w_H}{\sqrt{u_H^2 + v_H^2 + w_H^2}} \quad ; \quad \psi_W = \sin^{-1} \frac{v_H}{\sqrt{u_H^2 + v_H^2}}$$

Figure 5-4. Coordinate Systems - Hub Axis to Airmass

a. ROTOR AND HUB AXIS SETS



b. ROTOR AND BLADE AXIS SETS
(DOWN)

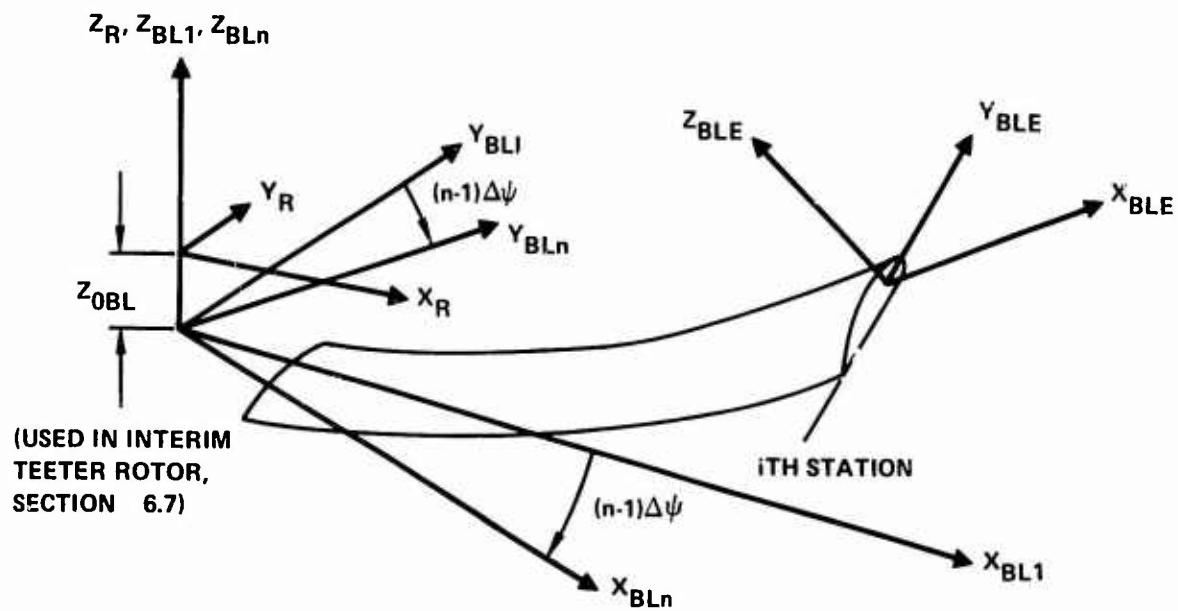


Figure 5-5. Coordinate Systems - Rotor, Blade, and Blade Element Sets

5.2.5 Blade Element Coordinates (X_{BLE} , Y_{BLE} , Z_{BLE})

The blade element set origin is located at the center of gravity of an element of a particular blade. See Figure 5-6. Reference to a column vector subscripted by BLE is used to denote the blade element located by the blade element set origin. The right-hand coordinate triad of this set has the X axis parallel to the local quarter chord line, the Y axis along the chord line toward the leading edge. The Z axis is mutually perpendicular and pointed up. The BLE set is used to track the local feather angle, to develop aerodynamic and dynamic loading terms.

The BLE set origin for each blade element specifies the element c.g. with respect to the quarter chord, and in terms of the BLE directions, i.e., for the Kth element the position coordinates are $SX(K)$ and $SZ(K)$. $SX(K)$ is the blade radial station. Transformations to the neutral, no-stretch axis are made for X deflections. Note: The quarter chord is merely a convenient reference datum, and does not convey any model limitations or assumptions.

5.2.6 Freestream (Earth) Set (X_E , Y_E , Z_E)

The freestream set is essentially the earth or inertial set inasmuch as the axis alignments are the same. However, the freestream set can assume any origin. Thus the use of the set is to reference the local gravity vector and/or an absolute angular displacement or linear velocity acceleration of another set. As shown on Figure 5-7, the Z_E axis points down toward local gravity. Other sets reference to the E set, as the H set shown here, may assume any starting value of roll and pitch such as the trim initial conditions. The relative orientation changes with progressing time of flight.

With the freestream set origin located coincident with the fuselage set, the components of fuselage set velocity in E set are u_E , v_E , w_E . These components combine into a trajectory velocity u_T and path X_T . The trajectory path is yawed right ψ_T and pitched up γ_T from the E set. See Figure 5-8.

5.2.7 Gyro Coordinates (X_G , Y_G , Z_G)

A gyro set is used for modeling an internal, isolated control gyro. This set is shown in Figure 5-9. The G set origin is coincident with the fuselage (F) set origin and has the same sense of direction and rotation. Rotations are measured relative to the fuselage set.

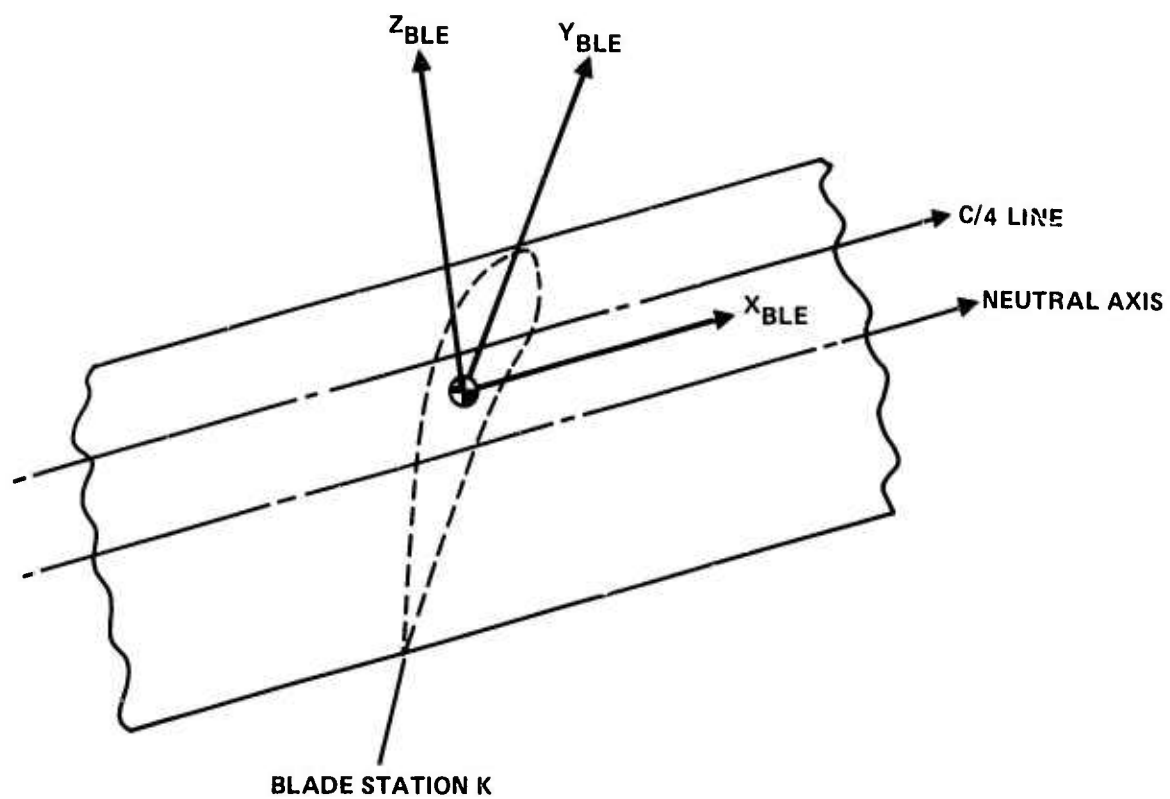


Figure 5-6. Coordinate Systems - Blade Element Set

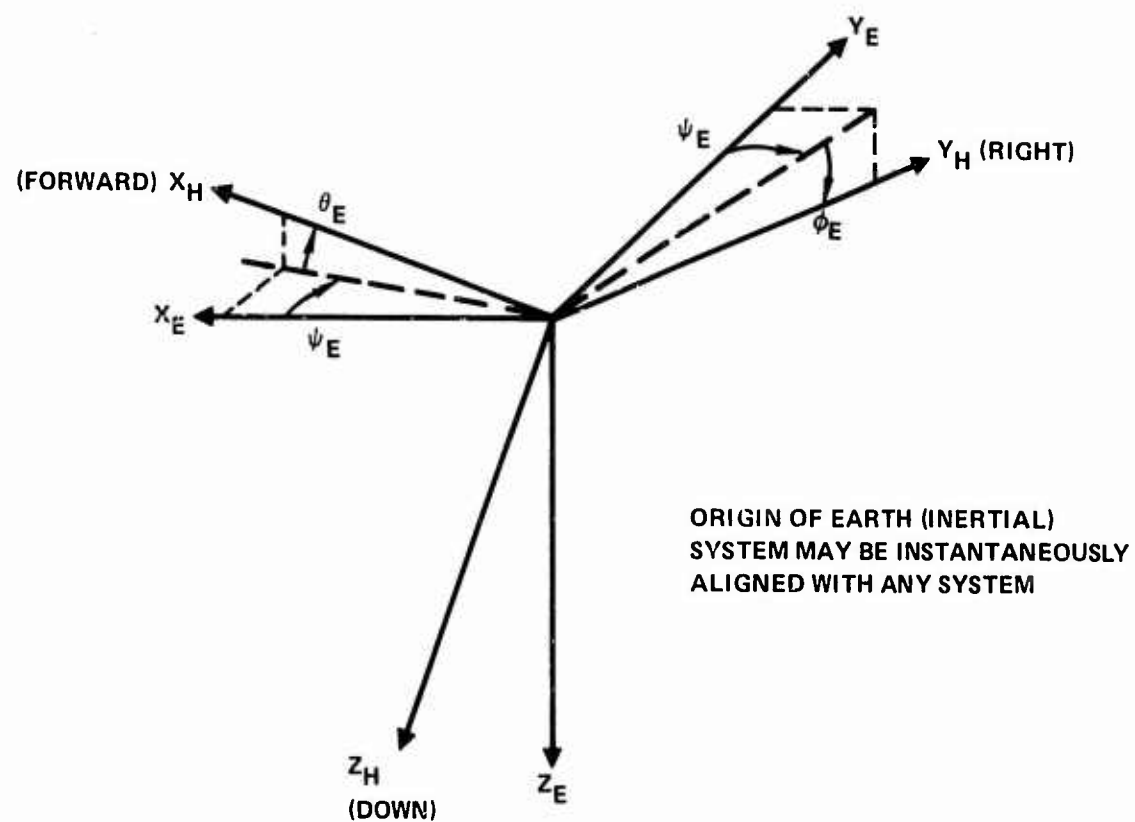
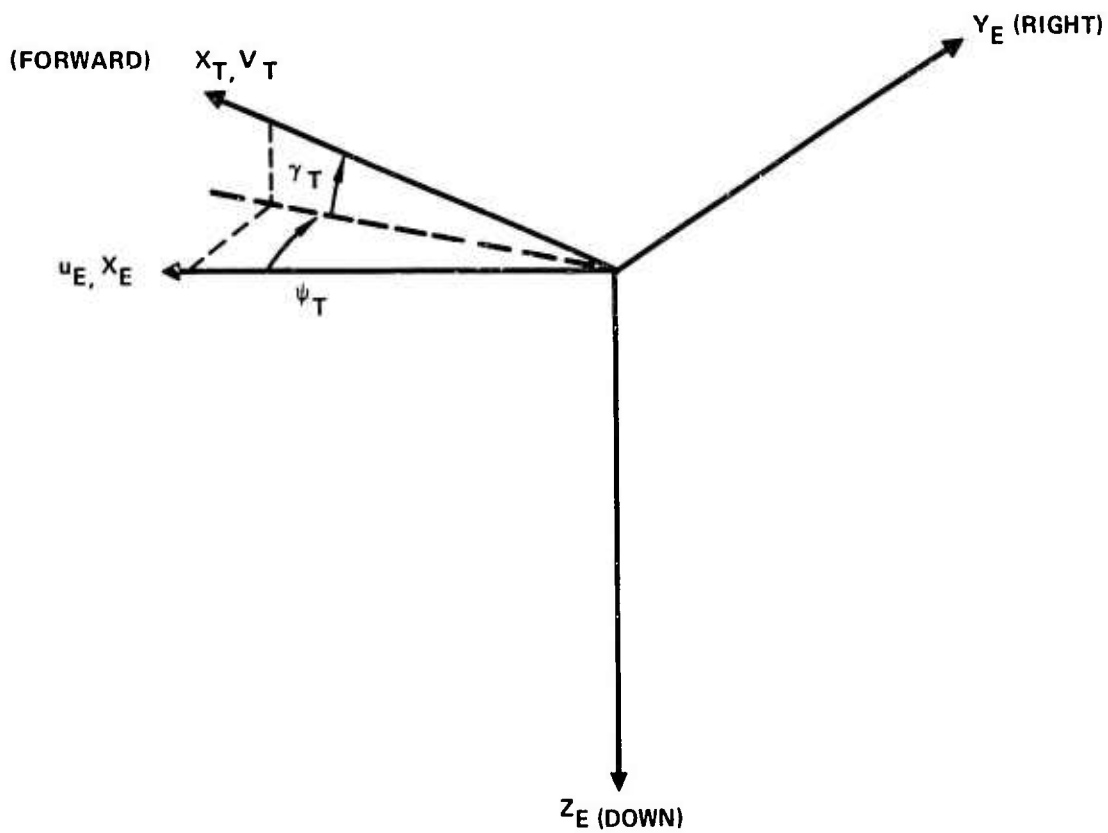


Figure 5-7. Coordinate Systems - Freestream (Earth) to Hub Axis



$$V_T = \sqrt{u_E^2 + v_E^2 + w_E^2}$$

$$\psi_T = \sin^{-1} \frac{v_E}{\sqrt{u_E^2 + v_E^2}} \quad , \quad \gamma_T = \sin^{-1} \frac{w_E}{\sqrt{u_E^2 + v_E^2 + w_E^2}}$$

BY DEFINITION: $v_T, w_T \equiv 0$

Figure 5-8. Coordinate Systems - Trajectory Path to Freestream Axis

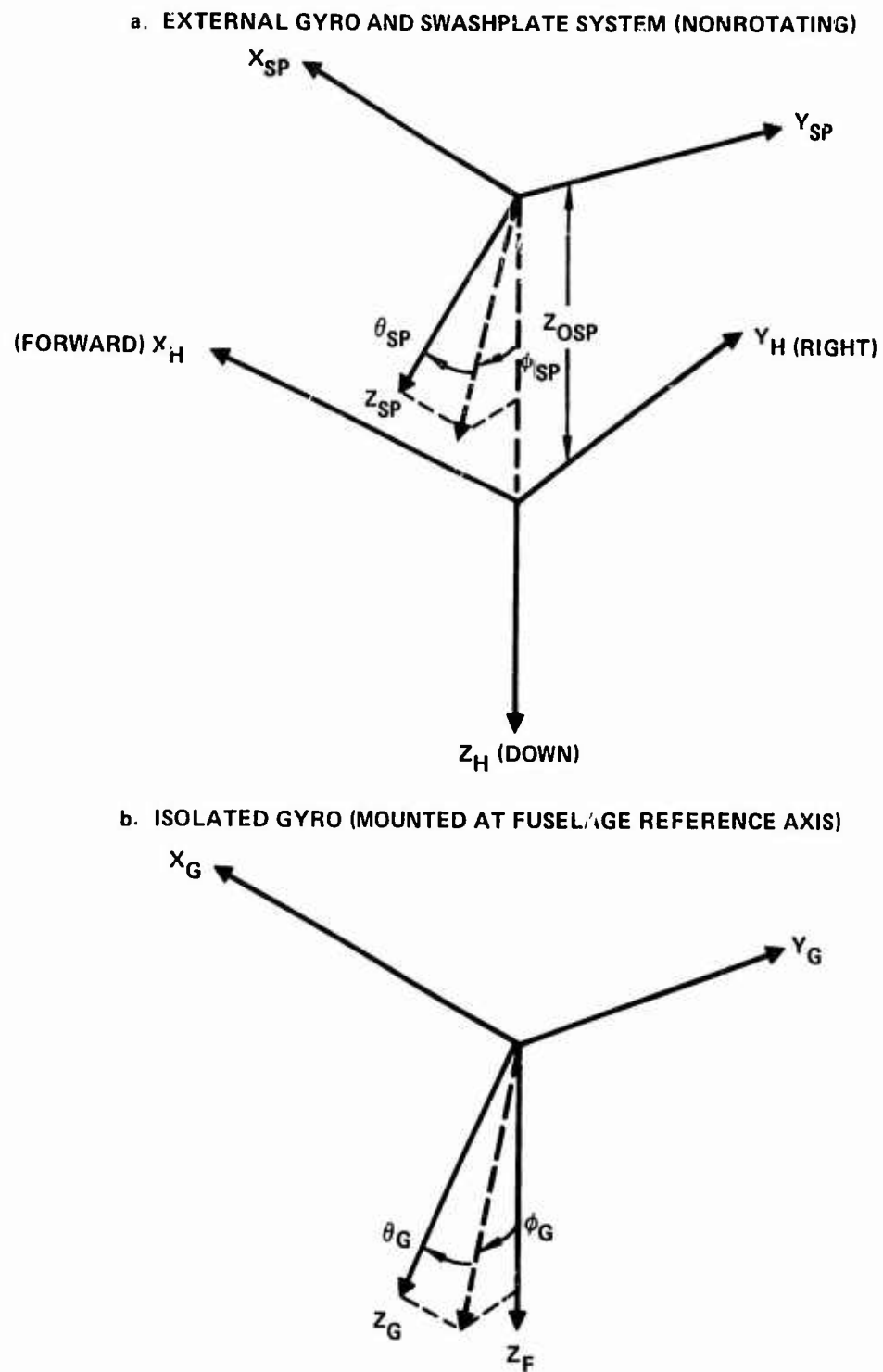


Figure 5-9. Coordinate Systems - Control Gyro and Swashplate Sets to Reference Sets

5.2.8 Swashplate Coordinates (X_{SP} , Y_{SP} , Z_{SP})

The swashplate set serves one of two possible functions. For a conventional control system, or a system using an isolated control gyro (Section 5.2.7), the motion of the set describes the motion of the swashplate. For systems using a control gyro directly in the feathering angle control path, this set describes the control gyro motions.

As shown on Figure 5-9, the SP set origin is located in line with the Z_H axis and above the hub set a distance Z_{OSP} . The SP set does not rotate with the rotor shaft. For no deflection of the SP set, the X and Y axes have the same alignment as the X and Y of the hub set.

5.3 DEGREES OF FREEDOM

The degrees of freedom of the REXOR equations are defined as the generalized coordinate variables of the set of equations of motion to be developed in Section 6. These degrees of freedom fully describe the motion of the physical elements of the modeled helicopter, but each direction of motion of the helicopter may not have a degree of freedom directly associated with it. The physical motions may be described by a series of modal variables (Section 6.4) or through a set of transformations and combinations of the degrees of freedom as developed in Sections 5.4 and 5.5.

The REXOR rotorcraft simulation analysis can be applied to describe the vehicle-rotor-control system dynamic response for up to thirty-two fully-coupled degrees of freedom. These include the normal six rigid body or vehicle degrees of freedom; rotor speed; and additional provisions for up to twenty-three degrees of freedom defining rotor blade motion (one mode per degree of freedom), flexible swashplate and rotor shaft or pylon motion, and a flapping moment feedback control gyro. The equations of motion are written in a general form so that additional degrees of freedom can be added if desired. The current thirty degrees-of-freedom are listed in Figure 5-10, followed by a discussion describing them in detail.

5.3.1 Vehicle or Rigid Body

The six rigid body degrees-of-freedom, three translations, and three rotations are defined as motions of the hub or principal reference axis system, Section 5.2.2, relative to freestream (inertial) reference datum.

Translational displacements (X , Y , Z)_{OH} of the origin of the hub coordinate, and rotational displacements (ϕ , θ , ψ)_H about the hub axes describe these degrees of freedom. See Figure 5-7. As mentioned in Section 5.2.6,

<u>ITEM</u>	<u>SYMBOL</u>	<u>TYPE OF MOTION</u>
MAIN ROTOR HUB AXIS	x_{0H}, y_{0H}, z_{0H} ϕ_H, θ_H, ψ_H	TRANSLATION AND ROTATION WITH RESPECT TO INERTIAL REFERENCE
ROTOR	ψ_R	ROTATION OF ROTOR SET WITH RESPECT TO HUB AXES
SHAFT OR PYLON BENDING	ϕ_S, θ_S	DEFLECTION OF FUSELAGE REFERENCE WITH RESPECT TO HUB AXES
BLADES ($n = 2$ or 4)	A_{1n}, A_{2n}, A_{3n} β_{PHn}	BLADE BENDING MODES AND FEATHER/PITCH HORN BENDING OR TORSION WITH RESPECT TO BLADE ROOT AXES
SWASHPLATE	ϕ_{SP}, θ_{SP} z_{SP}	SWASHPLATE AXES MOTIONS WITH RESPECT TO HUB AXES
GYRO	ϕ_G, θ_G	GYRO (INTERNAL) AXES ROTATION WITH RESPECT TO FUSELAGE AXES

Figure 5-10. Degrees of Freedom

the freestream set may instantaneously assume any reference point; therefore, only the time derivatives of $(X, Y, Z)_{OH}$ and $(\phi, \theta, \psi)_H$ have significance.

In order to locate the direction of the gravity vector relative to the hub, a running calculation of the Euler angles ϕ_E, θ_E, ψ_E must be made. Since these are not degrees of freedom and therefore not calculated in the equations of motion, they must be calculated outside the dynamic equations as the time history proceeds. When the initial orientation of the hub is defined, ϕ_E, θ_E , and ψ_E are known and their changing values may be calculated by integrating the hub rotation rates in the earth or freestream axes.

5.3.2 Rotor

The rotation for the rotor degree of freedom ψ_R is defined as motion of the rotor coordinate system relative to the hub axis system. This is shown in Figure 5-5. This figure also indicates the change from Z down to Z up axis, which is equivalent to a 180-degree positive rotation about the Y axis.

5.3.3 Shaft or Pylon Bending

Shaft or pylon bending degrees-of-freedom are defined as motions of the fuselage coordinates relative to the hub or principal axis system. As shown in Figure 5-3, fuselage translations, X_{OF} and Y_{OF} , are dependent variables which are functions of the two shaft bending Euler rotations, ϕ_S and θ_S . These rotations are about a virtual hinge of the shaft or pylon.

Shaft bending or pylon bending is assumed to be small enough such that displacement along the Z axis is negligible. Thus, when computing the translation of the origin of the fuselage coordinate system in the X_F and Y_F directions due to shaft bending, small angle approximations for the sine and cosine of ϕ_S and θ_S can be used. These translations are thus defined as products, $\left(\frac{\partial Y_F}{\partial \phi_S}\right) \phi_S$ in the Y_F direction and $\left(\frac{\partial X_F}{\partial \theta_S}\right) \theta_S$ in the X_F direction. The partial derivatives represent the distances from the virtual hinge in each axis to the fuselage reference.

5.3.4 Blades

Each blade's motion relative to the rotor coordinate system is defined in terms of four generalized coordinates. These consist of three blade bending modes and a combined feathering, pitch arm bending mode, or a torsion mode.

5.3.4.1 Blade Bending

Blade motion due to blade bending is defined by the following generalized modal coordinates:

A_{1n} : coupled first inplane bending mode

A_{2n} : coupled first flapwise bending mode

A_{3n} : coupled second flapwise bending mode

Ordinarily in a modal analysis, the effects of centrifugal and structural stiffness are lumped together into a generalized stiffness which is simply the modal natural frequency squared times the generalized mass. In contrast to this, the REXOR analysis separately treats the strain energy or structural stiffness in each mode and the stiffening due to the centrifugal force field. This provides the capability of being able to account for the periodic variation of stiffness in the modes due to the reorientation of the centrifugal force field with respect to the blade principal axis due to variations in blade angle. This feature can be important in the study of subharmonic stability where the periodic variation of coefficients may be important, but it also permits being able to make rather large changes in rotor speed and collective blade angle without having to change blade modal data.

Mode shapes and natural frequencies are initially determined for a twisted blade at or near the collective blade angle and rotor speed to be analyzed. Such effects as precone, blade sweep, blade droop, and blade angle variation are included in the REXOR analysis and couple the initially orthogonal modes. The elastic bending contribution due to the modal deflections is calculated relative to the blade's static shape.

As previously noted, the blade modes are initially defined at some reference feathering angle, ϕ_{REF} . As time progresses in the analysis, the blade feather angle varies about this reference position. The mode shapes are correspondingly transformed to account for the difference between the instantaneous feathering angle and the reference feathering angle, at the same time accounting for other

effects such as the static and instantaneous shape of the blades. This yields the modal coefficients (partial derivatives) that relate blade element motion to the blade bending generalized coordinates as a function of time.

The vertical and inplane blade element variational motions, δY_i and δZ_i , can be written as follows:

$$\delta Y_{in} = \frac{\partial Y_i}{\partial A_{1n}} (q_r, t) \delta A_{1n} + \frac{\partial Y_i}{\partial A_{2n}} (q_r, t) \delta A_{2n} + \frac{\partial Y_i}{\partial A_{3n}} (q_r, t) \delta A_{3n} \quad (5-1)$$

and

$$\delta Z_{in} = \frac{\partial Z_i}{\partial A_{1n}} (q_r, t) \delta A_{1n} + \frac{\partial Z_i}{\partial A_{2n}} (q_r, t) \delta A_{2n} + \frac{\partial Z_i}{\partial A_{3n}} (q_r, t) \delta A_{3n} \quad (5-2)$$

where the given or input partial derivatives are the true modal coefficients of the orthogonal modes for the blade in an undeformed shape, with no static geometry accounted for, and at the rotor speed and collective angle for which the blade modes were initially calculated.

The orthogonal bending modes used in the analysis are illustrated in Figures 5-11, 5-12, and 5-13. Observe that the root boundary conditions for the modes may be cantilevered or articulated.

Note that in addition to the normal bending responses, Y_i and Z_i , the spanwise motion of each blade element is also determined, and blade feathering due to pitch-lag and pitch-flap kinematic coupling effects are also accounted for in each blade bending mode. This feathering is added to that due to swashplate motion as is blade feathering due to flexibility.

This modal data is developed to the form used in the blade equations in Section 5.5.5. The discussion of modes is carried on from a math viewpoint in Section 6.4.

5.3.4.2 Pitch Horn Bending - Dynamic Torsion

The remaining mode per blade, pitch horn bending, is comprised of either a blade feathering drive flexibility with a torsionally rigid blade or an uncoupled torsion mode. Examining the first alternative, the swashplate position determines the primary blade

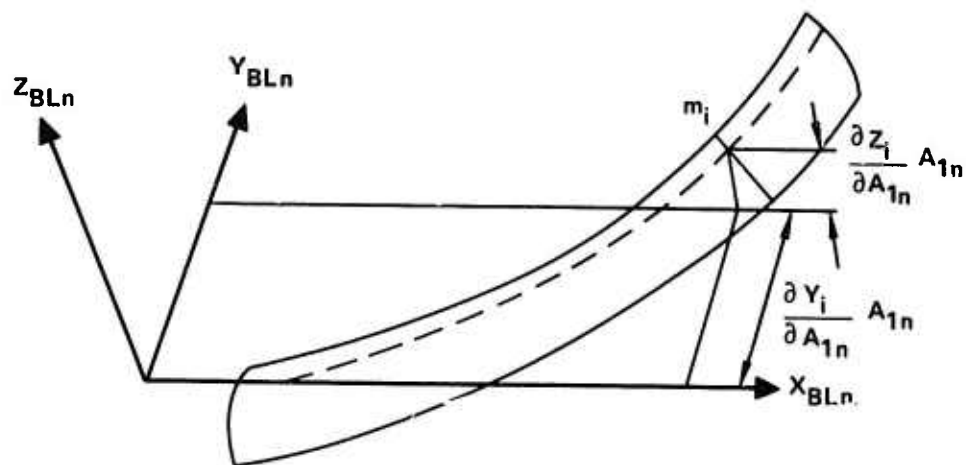


Figure 5-11. First Inplane Mode

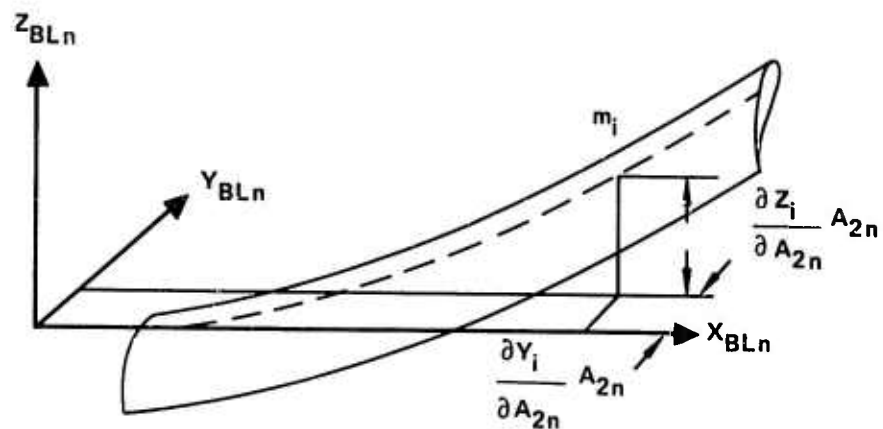


Figure 5-12. First Flap Mode

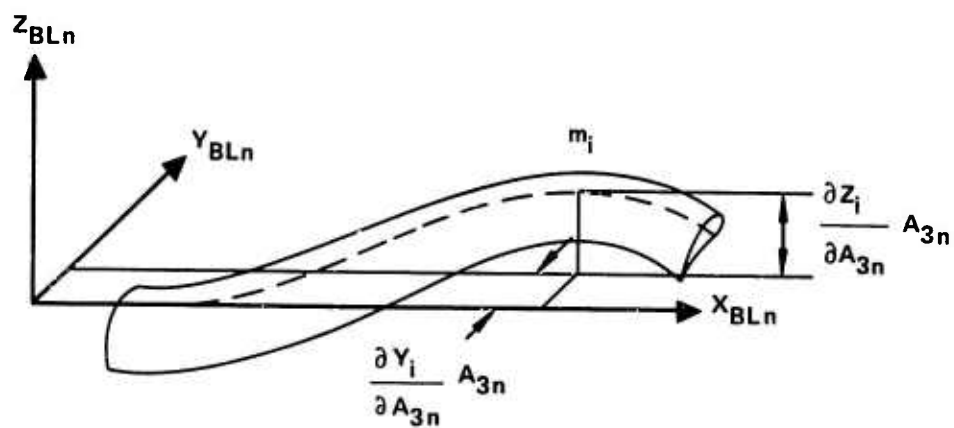


Figure 5-13. Second Flap Mode

feathering motion. In addition, the linkage between the swashplate and the blade (see Figure 5-14) has flexibility in the pitch link, pitch horn, and cuff. The feathering or pitch horn bending degree-of-freedom therefore can be rigid blade feathering motion outboard of the blade cuff coupled with a net inboard stiffness. Inboard of the blade cuff, feathering flexibility results from the pitch link, pitch link bearings, pitch horn, and cuff. The relationship between blade feathering, ϕ_{Fn} , and motion of this degree-of-freedom, β_{PHn} , is

defined as the partial derivative, $\left(\frac{\partial \phi_F}{\partial \beta_{PH}} \right)_n$.

Alternatively, this degree of freedom, β_{PHn} , can be a distributed torsional response of the blade based upon defining an uncoupled dynamic torsion mode. The selection of the degree-of-freedom representation is made on the basis of the type of analysis being performed. The mode defined is uncoupled in the sense that it is not a function of the flapping or lead-lag modes.

An optional quasi-steady torsional response of the blade may be used in conjunction with pitch horn bending. This is superimposed on the rigid blade feathering and permits a distributed torsional response alternative of the blade reacting the spanwise variation of applied torsional moments from aerodynamics, coriolis, and centrifugal force terms. The blade torsional response at the i th blade station is computed from the following equation:

$$\phi_{Ti} = \frac{1}{\tau_T S + 1} \int_{\text{root}}^{x_i} \frac{dx}{GJ(x)} \int_{x_i}^{\text{tip}} M_\phi(x) dx \quad (5-3)$$

where S is the Laplace operator, and τ_T is the time constant associated with blade torsional response. This equation is implemented numerically in the REXOR program.

To aid in program trouble shooting the pitch horn bending representation (with or without quasi-static torsion) may also be operated as a quasi-static degree of freedom without second-order response.

5.3.5 Swashplate

The swashplate has three degrees of freedom: ϕ_{SP} , θ_{SP} , and Z_{SP} . Rotations ϕ_{SP} and θ_{SP} are Euler angles defining the orientation of swashplate

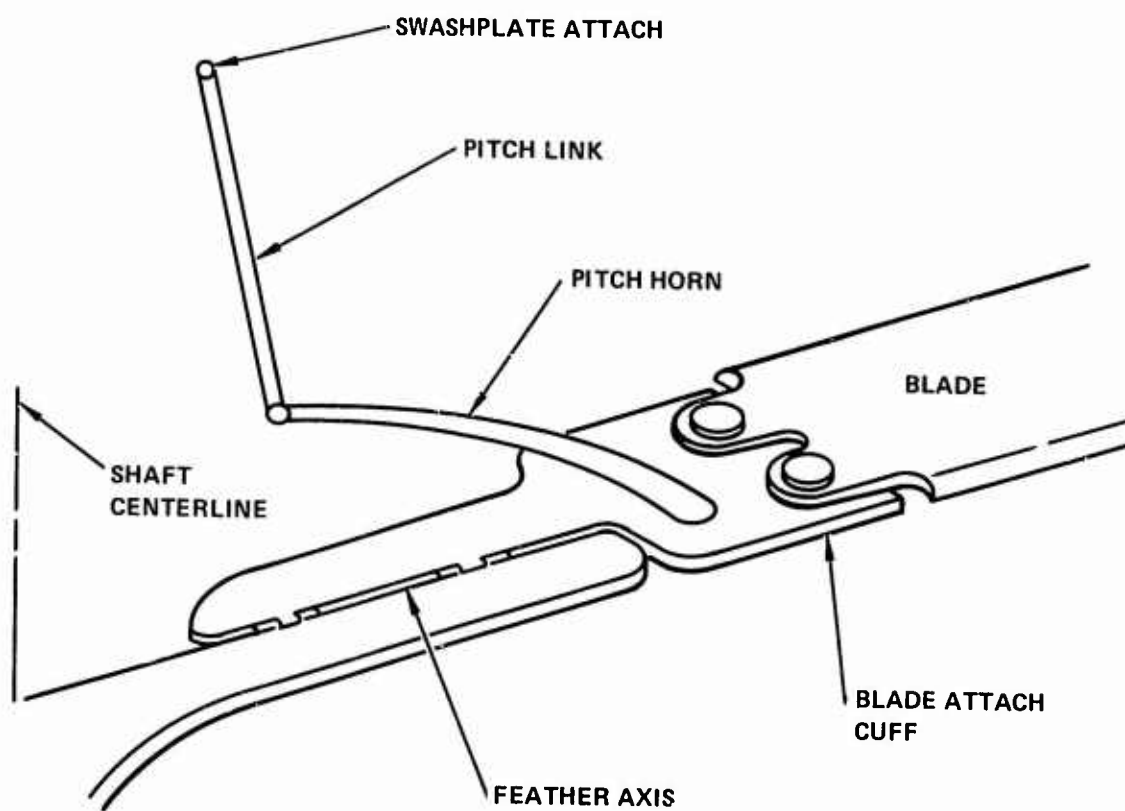


Figure 5-14. Blade, Pitch Horn and Feather Hinge Geometry

coordinates relative to the hub. Likewise, the translation Z_{SP} defines vertical displacement of the swashplate relative to the hub axis. These are shown schematically in Figure 5-9.

In a gyro-controlled feathering moment feedback system, such as the Lockheed concept, the swashplate becomes the control gyro and the swashplate degrees of freedom correspond to the degrees of freedom associated with the control gyro. The selection of this or other control system configurations is optional in the program; fundamentally by data changes in terms of inertias and spring rates.

5.3.6 Gyro

A gyro is included in the present version of the analysis which permits the description of a direct flapping moment feedback-gyro controlled rotor system. As already noted, the inclusion of this control system is a selectable option in the program. The degrees of freedom associated with this gyro are ϕ_G and θ_G , and are Euler angles defining the orientation of the control gyro relative to the fuselage axis system. These degrees of freedom are shown schematically also in Figure 5-9.

5.4 GENERAL MOTION AND COORDINATE TRANSFORMATIONS

In development of the equations of motion, it is convenient to write the forces, moments, velocities, and accelerations in coordinate systems related to separate elements of the system. Consider the concept of general space motion of a particle.

5.4.1 General Case of Space Motion

For the general case of space motion, a particle, p , moves with respect to a reference axis system which is, in turn, in motion with respect to a fixed coordinate system. This is illustrated in Figure 5-15 where the fixed or inertial coordinate system is designated by capital letters X, Y, Z , and the moving coordinate system is designated by lower case letters x, y, z . The moving coordinate system is rotating at an angular velocity, $\vec{\omega}$. The vector $\vec{\omega}$ may, in general, vary in magnitude and direction, both of which can be referenced with respect to the fixed X, Y, Z axes.

Thus, the absolute motion of the particle p , referred to the inertial X, Y, Z axes, is equal to the motion of the particle relative to the moving coordinate axes x, y, z plus the motion of the moving-axis system with respect to inertial space.

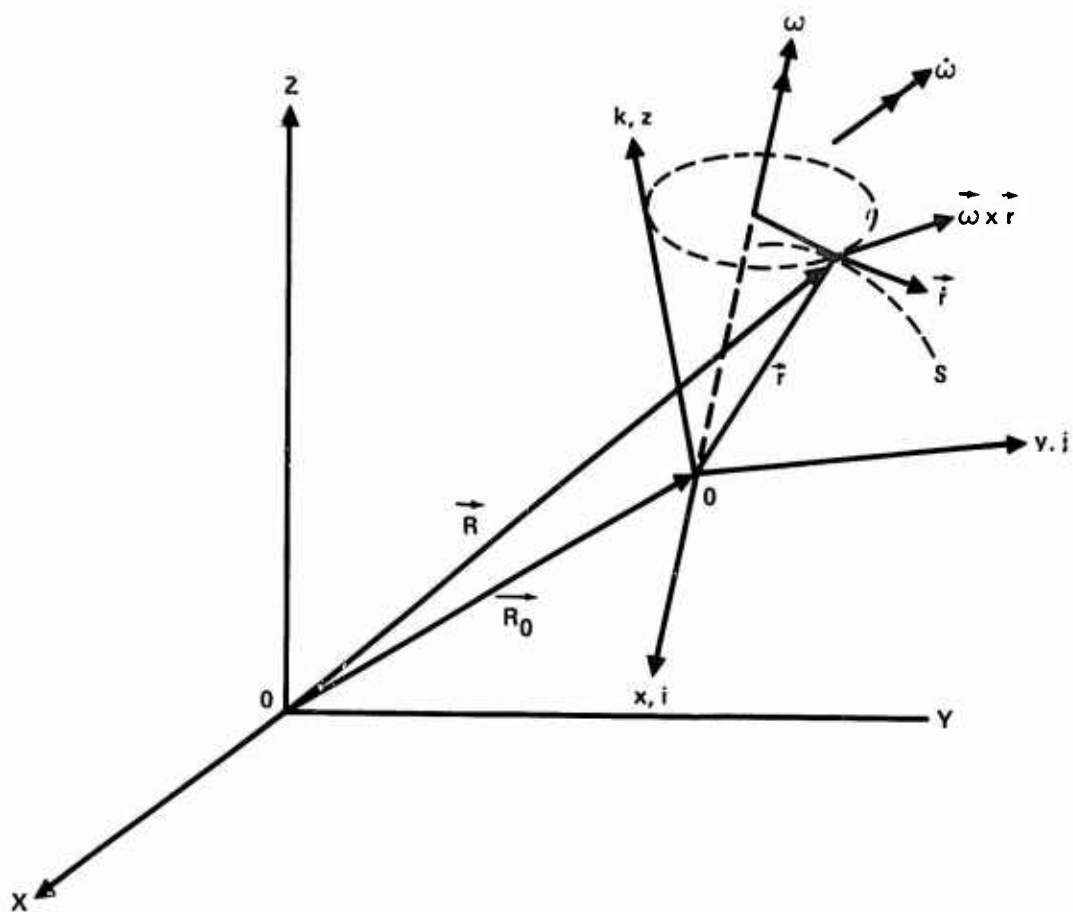


Figure 5-15. General Case of Space Motion in Terms of Moving Coordinate Axes x, y, z and Inertial Axes X, Y, Z

To visualize the motion of the particle p , let its motion with respect to the moving axis system be indicated along a curve s fixed in the moving axis system, x, y, z . An observer sitting on the moving axis system would therefore see only the motion of p along the curve s .

From Figure 5-15, the position of p relative to the x, y, z axes is represented by the vector

$$\vec{r} = x\vec{i} + y\vec{j} + z\vec{k} \quad (5-4)$$

where i, j , and k are unit vectors along x, y, z , and therefore must be treated as variables due to their changing direction. Differentiating \vec{r} results in

$$\dot{\vec{r}} = \dot{x}\vec{i} + \dot{y}\vec{j} + \dot{z}\vec{k} + x\frac{d\vec{i}}{dt} + y\frac{d\vec{j}}{dt} + z\frac{d\vec{k}}{dt} \quad (5-5)$$

Since $\frac{d\vec{i}}{dt} = \vec{\omega} \times \vec{i}$, $\frac{d\vec{j}}{dt} = \vec{\omega} \times \vec{j}$ and $\frac{d\vec{k}}{dt} = \vec{\omega} \times \vec{k}$, this expression can be written as

$$\dot{\vec{r}} = \dot{x}\vec{i} + \dot{y}\vec{j} + \dot{z}\vec{k} + \vec{\omega} \times (x\vec{i} + y\vec{j} + z\vec{k}) \quad (5-6)$$

or

$$\dot{\vec{r}} = \dot{\vec{r}} + \vec{\omega} \times \vec{r} \quad (5-7)$$

In this equation, the first term, $\dot{\vec{r}}$ represents the velocity p relative to the rotating axis, x, y, z . The second term, $\vec{\omega} \times \vec{r}$, is the velocity of the point in the moving coordinate system due to the rotation ω . The absolute or inertial velocity $\dot{\vec{R}}$ of the point p is obtained by adding the velocity of the origin $\dot{\vec{R}}_0$ of the moving axis system to $\dot{\vec{r}}$, or:

$$\dot{\vec{R}} = \dot{\vec{R}}_0 + \dot{\vec{r}} + \vec{\omega} \times \vec{r} \quad (5-8)$$

where

$$\vec{\omega} = p\vec{i} + q\vec{j} + r\vec{k}$$

and

$$\dot{\vec{\omega}} = \dot{p}\vec{i} + \dot{q}\vec{j} + \dot{r}\vec{k}$$

The inertial accelerations of the point p can now be determined by simply differentiating this expression with respect to time. Performing this differentiation yields

$$\ddot{\vec{R}} = \ddot{\vec{R}}_0 + \ddot{\vec{r}} + \vec{\omega} \times \vec{\omega} \times \vec{r} + \dot{\vec{\omega}} \times \vec{r} + 2\vec{\omega} \times \dot{\vec{r}} \quad (5-9)$$

where the terms $\vec{\omega} \times \vec{\omega} \times \vec{r}$ and $\dot{\vec{\omega}} \times \vec{r}$ represent accelerations of the coincident point in the moving axis system, $\ddot{\vec{r}}$ is the acceleration of p relative to the moving axes, x, y, z , and $2\vec{\omega} \times \dot{\vec{r}}$ is the coriolis acceleration which is directed normal to the plane containing the vectors $\vec{\omega}$ and the relative velocity $\dot{\vec{r}}$, as given by the right-hand rule.

The vectors expressed in the preceding equations are in the most general form for defining the motion of a particle moving in a moving coordinate system. All special cases can be deduced from these equations.

For convenience, the time derivative equations can be expanded in matrix form. The inertial or absolute velocity and accelerations of the particle p , written in expanded matrix form, are given by:

$$\begin{Bmatrix} \dot{X} \\ \dot{Y} \\ \dot{Z} \end{Bmatrix}^I = \begin{Bmatrix} \dot{X}_0 \\ \dot{Y}_0 \\ \dot{Z}_0 \end{Bmatrix}^I + \begin{Bmatrix} \dot{x} \\ \dot{y} \\ \dot{z} \end{Bmatrix} + \begin{bmatrix} 0 & -r & q \\ r & 0 & -p \\ -q & p & 0 \end{bmatrix} \begin{Bmatrix} x \\ y \\ z \end{Bmatrix} \quad (5-10)$$

and

$$\begin{Bmatrix} \ddot{X} \\ \ddot{Y} \\ \ddot{Z} \end{Bmatrix}^I = \begin{Bmatrix} \ddot{X}_0 \\ \ddot{Y}_0 \\ \ddot{Z}_0 \end{Bmatrix}^I + \begin{Bmatrix} \ddot{x} \\ \ddot{y} \\ \ddot{z} \end{Bmatrix} + \begin{bmatrix} 0 & -\dot{r} & \dot{q} \\ \dot{r} & 0 & -\dot{p} \\ -\dot{q} & \dot{p} & 0 \end{bmatrix} \begin{Bmatrix} x \\ y \\ z \end{Bmatrix} + 2 \begin{bmatrix} 0 & -r & q \\ r & 0 & -p \\ -q & p & 0 \end{bmatrix} \begin{Bmatrix} \dot{x} \\ \dot{y} \\ \dot{z} \end{Bmatrix} \quad (5-11)$$

Performing the indicated matrix multiplication gives:

$$\begin{Bmatrix} \dot{X} \\ \dot{Y} \\ \dot{Z} \end{Bmatrix}^I = \begin{Bmatrix} \dot{X}_0 \\ \dot{Y}_0 \\ \dot{Z}_0 \end{Bmatrix}^I + \begin{Bmatrix} \dot{x} \\ \dot{y} \\ \dot{z} \end{Bmatrix} + \begin{Bmatrix} zq - yr \\ xr - zp \\ yp - xq \end{Bmatrix} \quad (5-12)$$

and

$$\begin{Bmatrix} \ddot{X} \\ \ddot{Y} \\ \ddot{Z} \end{Bmatrix}^I = \begin{Bmatrix} \ddot{X}_0 \\ \ddot{Y}_0 \\ \ddot{Z}_0 \end{Bmatrix}^I + \begin{Bmatrix} \ddot{x} \\ \ddot{y} \\ \ddot{z} \end{Bmatrix} + \begin{Bmatrix} x(-\dot{r}^2 - \dot{q}^2) + y(p\dot{q} - \dot{r}) + z(p\dot{r} + \dot{q}) + 2\dot{z}q - 2\dot{y}r \\ x(p\dot{q} + \dot{r}) + y(-\dot{r}^2 - \dot{p}^2) + z(q\dot{r} - \dot{p}) + 2\dot{x}r - 2\dot{z}p \\ x(p\dot{r} - \dot{q}) + y(q\dot{r} + \dot{p}) + z(-\dot{p}^2 - \dot{q}^2) + 2\dot{y}p - 2\dot{x}q \end{Bmatrix} \quad (5-13)$$

The same vector development applies to the inertial velocity or acceleration of the reference set. That is, the total derivative is the sum of linear and turning components. The reference for a given coordinate set in REXOR is the inertial reference of the hub axis (principal set) plus the motion of the set in question relative to the hub axis.

5.4.2 Coordinate Transformations - Euler Angles

To describe motions in one coordinate system in terms of motions in another coordinate system, Euler angles ϕ , θ , and ψ with the appropriate subscripts are introduced. These angles can be applied to define the rotation of one coordinate system, x, y, z , relative to another coordinate reference frame, X, Y, Z . Since the development contained in this report utilizes these angles in relating coordinate systems, a brief explanation is given here.

Rotational displacement of a coordinate system can be represented by the three rotational displacements ϕ , θ , and ψ , as shown in Figure 5-16. The order of rotation is not important as long as the sequence selected remains consistent and the reverse order is used when rotating back to the original position. In this analysis, the rotations start with displacement ϕ about the x axis, then a rotation θ about the new y axis, followed by a rotation ψ about the new or final z axis unless geometry or physical considerations of the modeled part dictates another order.

This means the $(X, Y, Z)_a$ coordinates can be rotated into the $(X, Y, Z)_b$ axis system as follows:

$$\begin{Bmatrix} X \\ Y \\ Z \end{Bmatrix}_b = \begin{bmatrix} \cos\psi & \sin\psi & 0 \\ -\sin\psi & \cos\psi & 0 \\ 0 & 0 & 1 \end{bmatrix} \begin{bmatrix} \cos\theta & 0 & -\sin\theta \\ 0 & 1 & 0 \\ \sin\theta & 0 & \cos\theta \end{bmatrix} \begin{bmatrix} 1 & 0 & 0 \\ 0 & \cos\phi & \sin\phi \\ 0 & -\sin\phi & \cos\phi \end{bmatrix} \begin{Bmatrix} X \\ Y \\ Z \end{Bmatrix}_a \quad (5-14)$$

or:

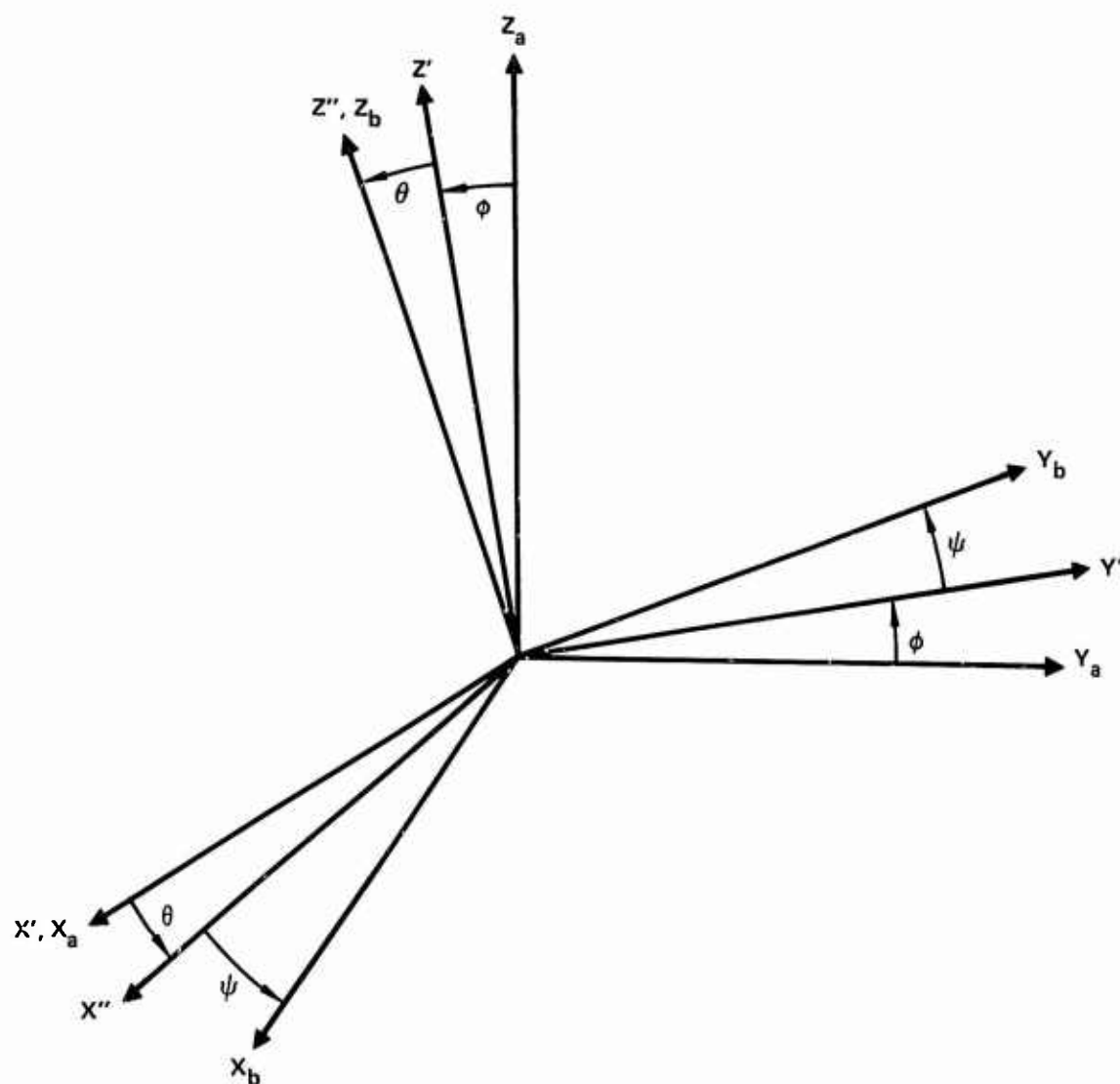
$$\begin{Bmatrix} X \\ Y \\ Z \end{Bmatrix}_b = \begin{bmatrix} T_{a-b} \end{bmatrix} \begin{Bmatrix} X \\ Y \\ Z \end{Bmatrix}_a \quad (5-15)$$

and the inverse transformation can be written as

$$\begin{Bmatrix} X \\ Y \\ Z \end{Bmatrix}_a = \begin{bmatrix} T_{a-b} \end{bmatrix}^{-1} \begin{Bmatrix} X \\ Y \\ Z \end{Bmatrix}_b \begin{bmatrix} T_{b-a} \end{bmatrix} \begin{Bmatrix} X \\ Y \\ Z \end{Bmatrix}_b \quad (5-16)$$

where

$$\begin{bmatrix} T_{a-b} \end{bmatrix} = \begin{bmatrix} \cos\psi & \sin\psi & 0 \\ -\sin\psi & \cos\psi & 0 \\ 0 & 0 & 1 \end{bmatrix} \begin{bmatrix} \cos\theta & 0 & -\sin\theta \\ 0 & 1 & 0 \\ \sin\theta & 0 & \cos\theta \end{bmatrix} \begin{bmatrix} 1 & 0 & 0 \\ 0 & \cos\phi & \sin\phi \\ 0 & -\sin\phi & \cos\phi \end{bmatrix} \quad (5-17)$$



AXES $(X, Y, Z)_b$ DEFINED RELATIVE TO REFERENCE
AXES $(X, Y, Z)_a$ BY EULER ANGLES ϕ, θ, ψ

Figure 5-16. Rotational Displacement of a Coordinate System

and

$$\begin{bmatrix} T_{a-b} \end{bmatrix}^{-1} = \begin{bmatrix} 1 & 0 & 0 \\ 0 & \cos\phi & -\sin\phi \\ 0 & \sin\phi & \cos\phi \end{bmatrix} \begin{bmatrix} \cos\theta & 0 & \sin\theta \\ 0 & 1 & 0 \\ -\sin\theta & 0 & \cos\theta \end{bmatrix} \begin{bmatrix} \cos\psi & -\sin\psi & 0 \\ \sin\psi & \cos\psi & 0 \\ 0 & 0 & 1 \end{bmatrix} \quad (5-18)$$

By inspection, then, it can be seen that

$$\text{inverse of } [T] = \text{transpose of } [T]$$

or

$$\begin{bmatrix} T_{a-b} \end{bmatrix}^{-1} = \begin{bmatrix} T_{a-b} \end{bmatrix}^T = \begin{bmatrix} T_{b-a} \end{bmatrix} \quad (5-19)$$

Carrying out the indicated matrix multiplication yields the transformation matrix $[T]$:

$$\begin{bmatrix} T_{a-b} \end{bmatrix} = \begin{bmatrix} (\cos\psi\cos\theta) & (\sin\phi\sin\theta\cos\psi+\cos\phi\sin\psi) & (-\sin\theta\cos\phi\cos\psi+\sin\phi\sin\psi) \\ (-\sin\psi\cos\theta) & (-\sin\psi\sin\phi\sin\theta+\cos\psi\cos\phi) & (\sin\psi\sin\theta\cos\phi+\cos\psi\sin\phi) \\ (\sin\theta) & (-\cos\theta\sin\phi) & (\cos\phi\cos\theta) \end{bmatrix} \quad (5-20)$$

Using this transformation, the inertial velocities and accelerations of a point or particle be written in one coordinate system in terms of those in the other coordinate system as follows:

$$\begin{Bmatrix} \dot{X} \\ \dot{Y} \\ \dot{Z} \end{Bmatrix}_b^I = \begin{bmatrix} T_{a-b} \end{bmatrix} \begin{Bmatrix} \dot{X} \\ \dot{Y} \\ \dot{Z} \end{Bmatrix}_a^I \quad (5-21)$$

and:

$$\begin{Bmatrix} \ddot{X} \\ \ddot{Y} \\ \ddot{Z} \end{Bmatrix}_b^I = [T_{a-b}] \begin{Bmatrix} \ddot{X} \\ \ddot{Y} \\ \ddot{Z} \end{Bmatrix}_a^I \quad (5-22)$$

and inversely,

$$\begin{Bmatrix} \dot{X} \\ \dot{Y} \\ \dot{Z} \end{Bmatrix}_a^I = [T_{b-a}] \begin{Bmatrix} \dot{X} \\ \dot{Y} \\ \dot{Z} \end{Bmatrix}_b^I \quad (5-23)$$

and

$$\begin{Bmatrix} \ddot{X} \\ \ddot{Y} \\ \ddot{Z} \end{Bmatrix}_a^I = [T_{b-a}] \begin{Bmatrix} \ddot{X} \\ \ddot{Y} \\ \ddot{Z} \end{Bmatrix}_b^I \quad (5-24)$$

5.4.3 Angular Velocities and Accelerations - General

For the general case, consider the coordinates in the previous section, and let $(p, q, r)_a$ and $(p, q, r)_b$ be the respective angular velocities of and about the $(x, y, z)_a$ and $(x, y, z)_b$ axis systems. Also, assume that the Euler angles are varying with time $(\dot{\phi}, \dot{\theta}, \text{ and } \dot{\psi})$ and let $(x, y, z)_a$ be the reference coordinate set with $(x, y, z)_b$ coordinate set moving relative to it. This is illustrated in Figure 5-17.

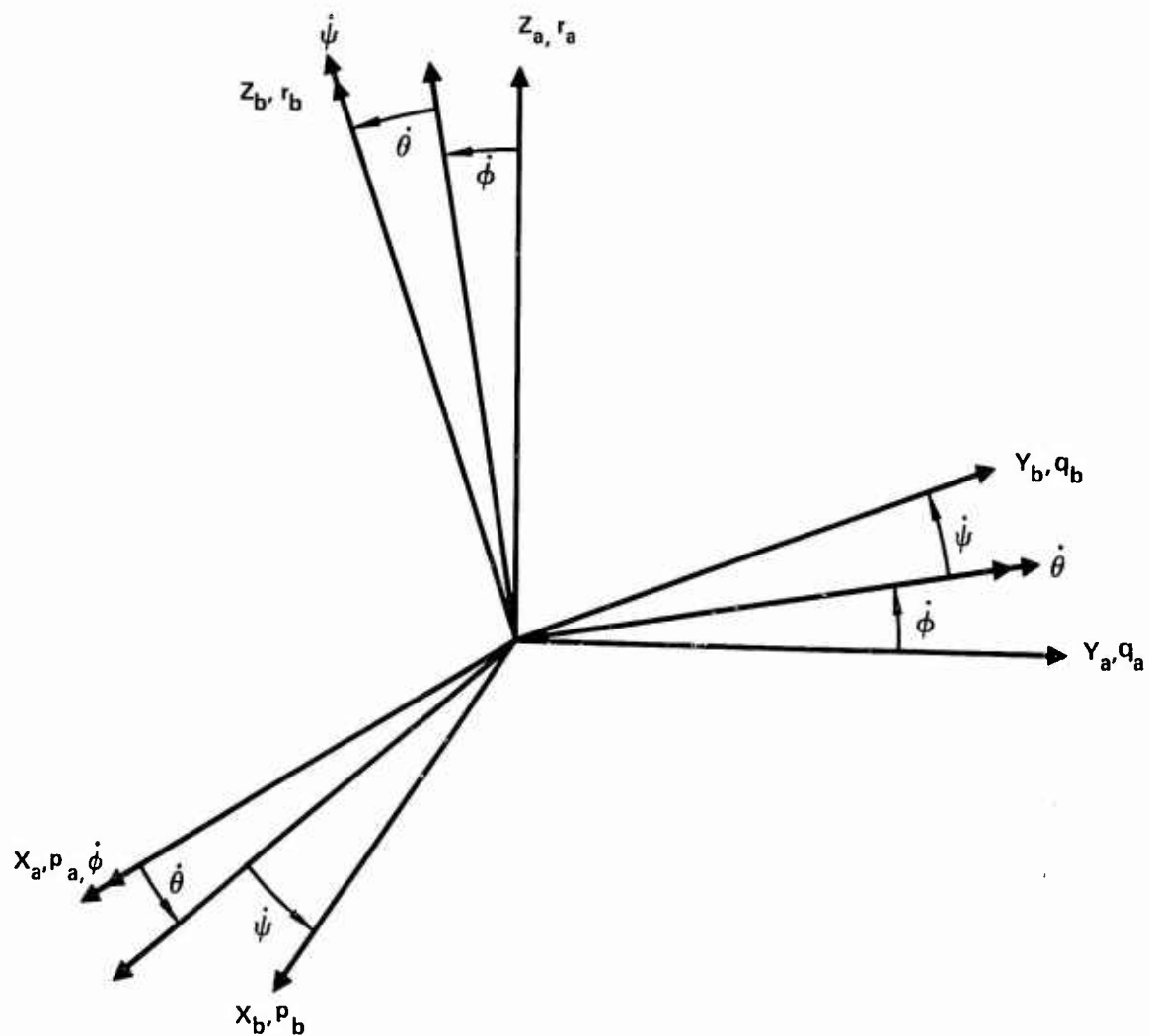


Figure 5-17. Relationship of Euler Angle and Coordinate System Angular Rates

From this figure, the following can be written.

$$\begin{aligned}
 \begin{Bmatrix} p \\ q \\ r \end{Bmatrix}_b &= \begin{Bmatrix} 0 \\ 0 \\ \dot{\psi} \end{Bmatrix} + \begin{bmatrix} \cos\psi & \sin\psi & 0 \\ -\sin\psi & \cos\psi & 0 \\ 0 & 0 & 1 \end{bmatrix} \begin{Bmatrix} 0 \\ \dot{\theta} \\ 0 \end{Bmatrix} + \begin{bmatrix} \cos\theta & 0 & -\sin\theta \\ 0 & 1 & 0 \\ \sin\theta & 0 & \cos\theta \end{bmatrix} \begin{Bmatrix} \dot{\phi} \\ 0 \\ 0 \end{Bmatrix} \\
 &+ \begin{bmatrix} 1 & 0 & 0 \\ 0 & \cos\phi & \sin\phi \\ 0 & -\sin\phi & \cos\phi \end{bmatrix} \begin{Bmatrix} p \\ q \\ r \end{Bmatrix}_a \quad (5-25)
 \end{aligned}$$

Differentiating this expression with respect to time results in angular accelerations $(\dot{p}, \dot{q}, \dot{r})_b$ in terms of the reference coordinate system angular velocities and accelerations. This results in the following:

$$\begin{aligned}
 \begin{Bmatrix} \dot{p} \\ \dot{q} \\ \dot{r} \end{Bmatrix}_b &= \begin{Bmatrix} 0 \\ 0 \\ \ddot{\psi} \end{Bmatrix} + \dot{\psi} \begin{bmatrix} -\sin\psi & \cos\psi & 0 \\ -\cos\psi & -\sin\psi & 0 \\ 0 & 0 & 0 \end{bmatrix} \begin{Bmatrix} 0 \\ \dot{\theta} \\ 0 \end{Bmatrix} + \begin{bmatrix} \cos\theta & 0 & -\sin\theta \\ 0 & 1 & 0 \\ \sin\theta & 0 & \cos\theta \end{bmatrix} \begin{Bmatrix} \dot{\phi} \\ 0 \\ 0 \end{Bmatrix} \\
 &+ \begin{bmatrix} 1 & 0 & 0 \\ 0 & \cos\phi & \sin\phi \\ 0 & -\sin\phi & \cos\phi \end{bmatrix} \begin{Bmatrix} p \\ q \\ r \end{Bmatrix}_a \quad + \begin{bmatrix} \cos\psi & \sin\psi & 0 \\ -\sin\psi & \cos\psi & 0 \\ 0 & 0 & 1 \end{bmatrix} \begin{Bmatrix} 0 \\ \ddot{\theta} \\ 0 \end{Bmatrix} \\
 &+ \dot{\theta} \begin{bmatrix} -\sin\theta & 0 & -\cos\theta \\ 0 & 0 & 0 \\ \cos\theta & 0 & -\sin\theta \end{bmatrix} \begin{Bmatrix} \dot{\phi} \\ 0 \\ 0 \end{Bmatrix} + \begin{bmatrix} 1 & 0 & 0 \\ 0 & \cos\phi & \sin\phi \\ 0 & -\sin\phi & \cos\phi \end{bmatrix} \begin{Bmatrix} p \\ q \\ r \end{Bmatrix}_a \\
 &+ \begin{bmatrix} \cos\theta & 0 & -\sin\theta \\ 0 & 1 & 0 \\ \sin\theta & 0 & \cos\theta \end{bmatrix} \begin{Bmatrix} \ddot{\phi} \\ 0 \\ 0 \end{Bmatrix} + \dot{\phi} \begin{bmatrix} 0 & 0 & 0 \\ 0 & -\sin\phi & \cos\phi \\ 0 & -\cos\phi & -\sin\phi \end{bmatrix} \begin{Bmatrix} p \\ q \\ r \end{Bmatrix}_a \\
 &+ \begin{bmatrix} 1 & 0 & 0 \\ 0 & \cos\phi & \sin\phi \\ 0 & -\sin\phi & \cos\phi \end{bmatrix} \begin{Bmatrix} \dot{p} \\ \dot{q} \\ \dot{r} \end{Bmatrix}_a \quad (5-26)
 \end{aligned}$$

These equations represent a general form for defining angular velocities and accelerations of one axis system rotating relative to another axis system, which in turn is in motion.

5.5 RELATIVE MOTIONS AND TRANSFORMATIONS USED IN THE EQUATIONS OF MOTION

In this section are presented the inertial linear and angular velocities and accelerations of major components of the vehicle, including motion of the principal reference system, the fuselage, the swashplate, the control gyro, the rotor, and blade elements. Also included is the development of coordinate transformations that relate motion in one axis system to another. Motion of the principal reference axis system in relation to the earth is described. Motion of each component or reference axis system is then defined in terms of the degrees of freedom.

5.5.1 Hub Motion in Inertial Space

At each instant in time the hub axis (Section 5.2.2) is related to an inertial coordinate axis system. Inertial accelerations of the hub axis system are defined by the vector

$$\begin{Bmatrix} \ddot{x}_0 \\ \ddot{y}_0 \\ \ddot{z}_0 \\ \ddot{\phi}_0 \\ \ddot{\theta}_0 \\ \ddot{\psi}_0 \end{Bmatrix}_H^I \quad (5-27)$$

where the quantities represent the total inertial acceleration of the generalized coordinates of the vehicle as defined by motion of the principal coordinate axis system.

Orientation of this system relative to the earth is specified by Euler angles ϕ_E , θ_E , and ψ_E as seen in Figure 5-7. The sequence and definition of these angles is ψ_E (yaw), θ_E (pitch), ϕ_E (roll). Note that the

sequence of rotations is opposite to that given by Figure 5-16. The angular rates, p_H, q_H, r_H , of the hub or principal reference axis system with respect to the inertial coordinate system can be written as

$$\begin{aligned} \begin{Bmatrix} p \\ q \\ r \end{Bmatrix}_H &= \begin{Bmatrix} \dot{\phi}_E \\ 0 \\ 0 \end{Bmatrix} + \begin{bmatrix} 1 & 0 & 0 \\ 0 & \cos\phi_E & \sin\phi_E \\ 0 & -\sin\phi_E & \cos\phi_E \end{bmatrix} \begin{Bmatrix} 0 \\ \dot{\theta}_E \\ 0 \end{Bmatrix} \\ &+ \begin{bmatrix} \cos\theta_E & 0 & -\sin\theta_E \\ 0 & 1 & 0 \\ \sin\theta_E & 0 & \cos\theta_E \end{bmatrix} \begin{Bmatrix} 0 \\ 0 \\ \dot{\psi}_E \end{Bmatrix} \end{aligned} \quad (5-28)$$

This equation can be rewritten to solve for $\dot{\phi}_E, \dot{\theta}_E$, and $\dot{\psi}_E$ as

$$\begin{Bmatrix} \dot{\phi}_E \\ \dot{\theta}_E \\ \dot{\psi}_E \end{Bmatrix} = \begin{bmatrix} 1 & \sin\phi_E \tan\theta_E & \cos\phi_E \tan\theta_E \\ 0 & \cos\phi_E & -\sin\phi_E \\ 0 & \sin\phi_E \sec\theta_E & \cos\phi_E \sec\theta_E \end{bmatrix} \begin{Bmatrix} p \\ q \\ r \end{Bmatrix}_H \quad (5-29)$$

The Euler angles defining orientation of the principal reference axis system with respect to the earth is next obtained by integrating the rates with respect to time, or

$$\phi_E = \int_0^t \dot{\phi}_E dt \quad (5-30)$$

$$\theta_E = \int_0^t \dot{\theta}_E dt \quad (5-31)$$

$$\psi_E = \int_0^t \dot{\psi}_E dt \quad (5-32)$$

Angular velocities of the hub, with respect to the inertial axes reference system, p_H, q_H, r_H , are defined in terms of the degrees of freedom as

$$\begin{Bmatrix} p \\ q \\ r \end{Bmatrix}_H = \begin{Bmatrix} \dot{\phi}_0 \\ \dot{\theta}_0 \\ \dot{\psi}_0 \end{Bmatrix}_H^I = \int_0^t \begin{Bmatrix} \dot{p} \\ \dot{q} \\ \dot{r} \end{Bmatrix}_H dt \quad (5-33)$$

where

$$\begin{Bmatrix} \dot{p} \\ \dot{q} \\ \dot{r} \end{Bmatrix}_H = \begin{Bmatrix} \ddot{\phi}_0 \\ \ddot{\theta}_0 \\ \ddot{\psi}_0 \end{Bmatrix}_H^I \quad (5-34)$$

Linear velocities of the hub or principal axis system are now determined. The first three quantities of the hub axis acceleration vector represent the linear inertial acceleration of the hub. For a system in motion, the inertial acceleration, \ddot{a}_0^I , at the origin of the system is defined, based on the vector algebra of Section 5.4.1, as

$$\ddot{a}_0^I = \ddot{a}_0 + \vec{\omega} \times \vec{V}_0 \quad (5-35)$$

where \ddot{a}_0 is $\frac{d\vec{V}_0}{dt}$, the rate of change of velocity, V_0 , of the origin of the moving coordinate system and ω is the rotational velocity of the moving coordinate system, both relative to the earth. Now making the definition

$$\begin{Bmatrix} V_0 \end{Bmatrix}_H^I = \begin{Bmatrix} u \\ v \\ w \end{Bmatrix}_H \quad (5-36)$$

gives

$$\begin{Bmatrix} \ddot{X}_{OH} \\ \ddot{Y}_{OH} \\ \ddot{Z}_{OH} \end{Bmatrix}^I = \begin{Bmatrix} \dot{u} \\ \dot{v} \\ \dot{w} \end{Bmatrix}_H + \begin{bmatrix} 0 & -r & q \\ r & 0 & -p \\ -q & p & 0 \end{bmatrix} \begin{Bmatrix} u \\ v \\ w \end{Bmatrix}_H \quad (5-37)$$

From this equation, then, the rate of change of velocity of the moving coordinate reference system becomes

$$\begin{Bmatrix} \dot{u} \\ \dot{v} \\ \dot{w} \end{Bmatrix}_H = \begin{Bmatrix} \ddot{X}_{OH}^I - q_H w_H + r_H v_H \\ \ddot{Y}_{OH}^I - r_H u_H + p_H w_H \\ \ddot{Z}_{OH}^I - p_H v_H + q_H u_H \end{Bmatrix} \quad (5-38)$$

This set of accelerations and the time integral are transformed into rotor and fuselage sets and represent airflow acceleration and velocity incident on the helicopter.

A separate set of hub accelerations is carried through the analysis, based on the hub set, which contains the acceleration due to gravity. Ordinarily, gravity is treated as a force of mg on the right-hand side of the equations. However, the gravitational term can be introduced by defining

$$\begin{Bmatrix} \ddot{X}_{OH} \\ \ddot{Y}_{OH} \\ \ddot{Z}_{OH} \end{Bmatrix}_H = \begin{Bmatrix} \ddot{X}_{OH} \\ \ddot{Y}_{OH} \\ \ddot{Z}_{OH} \end{Bmatrix}_H^I - \begin{Bmatrix} g_X \\ g_Y \\ g_Z \end{Bmatrix}_H \quad (5-39)$$

where g_{XH} , g_{YH} , g_{ZH} are the three components of the gravity vector to be defined. The hub acceleration on the left may be defined as being in "earth-inertial" axes.

The logic behind this substitution is as follows. For a rigid body in motion, the equilibrium equations can be written as

$$\begin{aligned} m\ddot{X} &= m(\dot{u} + qw - rv) = F_X \\ m\ddot{Y} &= m(\dot{v} + ru - pw) = F_Y \\ m\ddot{Z} &= m(\dot{w} + pv - qu) = F_Z \end{aligned} \quad (5-40)$$

where

$$\begin{Bmatrix} F_X \\ F_Y \\ F_Z \end{Bmatrix} = \begin{Bmatrix} \bar{F}_X \\ \bar{F}_Y \\ \bar{F}_Z \end{Bmatrix} + \begin{Bmatrix} g_X \\ g_Y \\ g_Z \end{Bmatrix} m \quad (5-41)$$

\bar{F}_X , \bar{F}_Y , and \bar{F}_Z represent the external forces acting on the body, exclusive of gravitational forces.

Subtracting the gravitational vector from each side of the previous equations yields:

$$m(\ddot{X} - g_X) = m(\dot{u} + qw - rv - g_X) = \bar{F}_X \quad (5-42)$$

$$m(\ddot{Y} - g_Y) = m(\dot{v} + ru - pw - g_Y) = \bar{F}_Y \quad (5-43)$$

$$m(\ddot{Z} - g_Z) = m(\dot{w} + pv - qu - g_Z) = \bar{F}_Z \quad (5-44)$$

which by inspection gives

$$\ddot{X} - g_X = \dot{u} + qw - rv - g_X \quad (5-45)$$

$$\ddot{Y} - g_Y = \dot{v} + ru - pw - g_Y \quad (5-46)$$

$$\ddot{Z} - g_Z = \dot{w} + pv - qu - g_Z \quad (5-47)$$

Rearranging these equations yields:

$$\dot{u} = (\ddot{X} - g_X) - qw + rv + g_X \quad (5-48)$$

$$\dot{v} = (\ddot{Y} - g_Y) - ru + pw + g_Y \quad (5-49)$$

$$\dot{w} = (\ddot{Z} - g_Z) - pv + qu + g_Z \quad (5-50)$$

The first terms on the right side of the equation are identified with the proposed gravitational acceleration definition of equation 5-39.

Making the substitution:

$$\begin{Bmatrix} \dot{u} \\ \dot{v} \\ \dot{w} \end{Bmatrix}_H = \begin{Bmatrix} \ddot{X}_{OH} - q_H w_H + r_H v_H + g_{XH} \\ \ddot{Y}_{OH} - r_H u_H + p_H w_H + g_{YH} \\ \ddot{Z}_{OH} - p_H v_H + q_H u_H + g_{ZH} \end{Bmatrix} \quad (5-51)$$

In this equation, the accelerations \ddot{X}_{OH} , \ddot{Y}_{OH} , and \ddot{Z}_{OH} are the degree-of-freedom accelerations of the hub or principal reference axis system used in the REXOR analysis. These accelerations represent the inertial accelerations plus the equivalent accelerations of the reaction force to gravity. Thus, gravity is an equivalent acceleration applied to the reference coordinate axis system. Via coordinate system referencing, every mass element on the vehicle is therefore acted upon by this acceleration. This avoids including gravitational force as an external force individually applied to each mass element.

The gravitational vector at the hub is simply the gravity vector in earth axis transformed to the hub axis system through the Euler angle rotations

ϕ_E , θ_E , and ψ_E . Or

$$\begin{Bmatrix} g_X \\ g_Y \\ g_Z \end{Bmatrix} = [T_{E-H}] \begin{Bmatrix} 0 \\ 0 \\ g \end{Bmatrix} \quad (5-52)$$

where

$$[T_{E-H}] = \begin{bmatrix} 1 & 0 & 0 \\ 0 & \cos\phi_E & \sin\phi_E \\ 0 & -\sin\phi_E & \cos\phi_E \end{bmatrix} \begin{bmatrix} \cos\theta_E & 0 & -\sin\theta_E \\ 0 & 1 & 0 \\ \sin\theta_E & 0 & \cos\theta_E \end{bmatrix} \begin{bmatrix} \cos\psi_E & \sin\psi_E & 0 \\ -\sin\psi_E & \cos\psi_E & 0 \\ 0 & 0 & 1 \end{bmatrix} \quad (5-53)$$

The velocities of the principal axis system are obtained by integrating the rates of change of velocity with time, or

$$\begin{Bmatrix} \dot{x}_{OH} \\ \dot{y}_{OH} \\ \dot{z}_{OH} \end{Bmatrix}_H^I = \begin{Bmatrix} u \\ v \\ w \end{Bmatrix}_H^I = \int_0^t \begin{Bmatrix} \dot{u} \\ \dot{v} \\ \dot{w} \end{Bmatrix}_H^I dt \quad (5-54)$$

These velocities in earth coordinates can be written as

$$\begin{Bmatrix} \dot{x}_{OH} \\ \dot{y}_{OH} \\ \dot{z}_{OH} \end{Bmatrix}_E^I = [T_{H-E}] \begin{Bmatrix} \dot{x}_{OH} \\ \dot{y}_{OH} \\ \dot{z}_{OH} \end{Bmatrix}_H^I = [T_{E-H}]^T \begin{Bmatrix} \dot{x}_{OH} \\ \dot{y}_{OH} \\ \dot{z}_{OH} \end{Bmatrix}_H^I \quad (5-55)$$

which can be integrated to give the position of the system relative to the earth. Doing this yields

$$\begin{Bmatrix} x_{OH} \\ y_{OH} \\ z_{OH} \end{Bmatrix}_E = \int_0^t \begin{Bmatrix} \dot{x}_{OH} \\ \dot{y}_{OH} \\ \dot{z}_{OH} \end{Bmatrix}_E^I dt \quad (5-56)$$

5.5.2 Fuselage Motion in Inertial Space

As shown in Figure 5-3, the fuselage is rotated from the hub position by bending of the rotor shaft. The origin of the fuselage coordinate axis system is displaced from the hub axis system by the distances

$$\begin{Bmatrix} X_{OF} \\ Y_{OF} \\ Z_{OF} \end{Bmatrix}_H \quad \text{in hub coordinates} \quad (5-57)$$

or

$$\begin{Bmatrix} X_{OF} \\ Y_{OF} \\ Z_{OF} \end{Bmatrix}_F \quad \text{in fuselage coordinates} \quad (5-58)$$

As discussed earlier, X_{OF} and Y_{OF} are functions of shaft or pylon bending and hence are not independent degrees of freedom. The fuselage rotations relative to the hub are described by the Euler angles $-\theta_S$ and $-\phi_S$ taken in that order. The minus signs and reversed order are taken so the transform from fuselage to hub is ϕ_S and then θ_S .

From Figure 5-3, the location of the fuselage reference in hub coordinates is

$$\begin{Bmatrix} X_{OF} \\ Y_{OF} \\ Z_{OF} \end{Bmatrix}_H = \theta_S \begin{Bmatrix} \partial X_F / \partial \theta_S \\ 0 \\ 0 \end{Bmatrix}_H + \phi_S \begin{Bmatrix} 0 \\ \partial Y_F / \partial \phi_S \\ 0 \end{Bmatrix}_H + \begin{Bmatrix} 0 \\ 0 \\ Z_{OF} \end{Bmatrix}_H = \begin{Bmatrix} \theta_S \partial X_F / \partial \theta_S \\ \phi_S \partial Y_F / \partial \phi_S \\ Z_{OF} \end{Bmatrix}_H \quad (5-59)$$

Now, defining the transformation from hub to fuselage coordinates as

$$[T_{H-F}] = \begin{bmatrix} 1 & 0 & 0 \\ 0 & \cos\phi_S & -\sin\phi_S \\ 0 & \sin\phi_S & \cos\phi_S \end{bmatrix} \begin{bmatrix} \cos\theta_S & 0 & \sin\theta_S \\ 0 & 1 & 0 \\ -\sin\theta_S & 0 & \cos\theta_S \end{bmatrix} \quad (5-60)$$

The inertial velocities of the fuselage reference system in fuselage coordinates can be written as

$$\begin{aligned} \begin{Bmatrix} \dot{X}_{OF} \\ \dot{Y}_{OF} \\ \dot{Z}_{OF} \end{Bmatrix}_F^I &= [T_{H-F}] \left\{ \begin{Bmatrix} \dot{X}_{OH} \\ \dot{Y}_{OH} \\ \dot{Z}_{OH} \end{Bmatrix}_H^I + \begin{Bmatrix} \dot{\theta}_S \partial X_F / \partial \theta_S \\ \dot{\phi}_S \partial Y_F / \partial \phi_S \\ 0 \end{Bmatrix}_H \right. \\ &\quad \left. + \begin{bmatrix} 0 & -r & q \\ r & 0 & -p \\ -q & p & 0 \end{bmatrix}_H \begin{Bmatrix} \theta_S \partial X_F / \partial \theta_S \\ \phi_S \partial Y_F / \partial \phi_S \\ Z_{OF} \end{Bmatrix}_H \right\} \quad (5-61) \end{aligned}$$

Differentiating this expression once more with respect to time (Section 5.4.1) yields accelerations of the fuselage reference point in fuselage axes.

$$\begin{aligned} \begin{Bmatrix} \ddot{X}_{OF} \\ \ddot{Y}_{OF} \\ \ddot{Z}_{OF} \end{Bmatrix}_F^I &= [T_{H-F}] \left\{ \begin{Bmatrix} \ddot{X}_{OH} \\ \ddot{Y}_{OH} \\ \ddot{Z}_{OH} \end{Bmatrix}_H^I + \begin{Bmatrix} \ddot{\theta}_S \partial X_F / \partial \theta_S \\ \ddot{\phi}_S \partial Y_F / \partial \phi_S \\ 0 \end{Bmatrix}_H + \begin{bmatrix} 0 & -\dot{r} & \dot{q} \\ \dot{r} & 0 & -\dot{p} \\ -\dot{q} & \dot{p} & 0 \end{bmatrix}_H \begin{Bmatrix} \theta_S \partial X_F / \partial \theta_S \\ \phi_S \partial Y_F / \partial \phi_S \\ Z_{OF} \end{Bmatrix}_H \right. \\ &\quad + \begin{bmatrix} 0 & -r & q \\ r & 0 & p \\ -q & p & 0 \end{bmatrix}_H \begin{bmatrix} 0 & -r & q \\ r & 0 & p \\ -q & p & 0 \end{bmatrix}_H \begin{Bmatrix} \theta_S \partial X_F / \partial \theta_S \\ \phi_S \partial Y_F / \partial \phi_S \\ Z_{OF} \end{Bmatrix}_H \\ &\quad \left. + 2 \begin{bmatrix} 0 & -r & q \\ r & 0 & -p \\ -q & p & 0 \end{bmatrix}_H \begin{Bmatrix} \dot{\theta}_S \partial X_F / \partial \theta_S \\ \dot{\phi}_S \partial Y_F / \partial \phi_S \\ 0 \end{Bmatrix}_H \right\} \quad (5-62) \end{aligned}$$

These two equations define the linear velocities and accelerations of the fuselage reference point in fuselage axes in terms of the generalized coordinate velocities and accelerations of the hub or principal reference axis system, and in terms of the shaft or pylon bending generalized coordinate displacements, velocities, and accelerations.

Keeping in mind the order of rotation of θ_S and ϕ_S , and the rotation formulas developed, the angular velocities $(p, q, r)_F$, of the fuselage reference system can be written as:

$$\begin{aligned} \begin{Bmatrix} p \\ q \\ r \end{Bmatrix}_F &= \begin{Bmatrix} -\dot{\phi}_S \\ 0 \\ 0 \end{Bmatrix} + \begin{bmatrix} 1 & 0 & 0 \\ 0 & \cos\phi_S & -\sin\phi_S \\ 0 & \sin\phi_S & \cos\phi_S \end{bmatrix} \begin{Bmatrix} 0 \\ -\dot{\theta}_S \\ 0 \end{Bmatrix} \\ &+ \begin{bmatrix} \cos\theta_S & 0 & \sin\theta_S \\ 0 & 1 & 0 \\ -\sin\theta_S & 0 & \cos\theta_S \end{bmatrix} \begin{Bmatrix} p \\ q \\ r \end{Bmatrix}_H \end{aligned} \quad (5-63)$$

Likewise, the angular accelerations of the fuselage reference become

$$\begin{aligned} \begin{Bmatrix} \dot{p} \\ \dot{q} \\ \dot{r} \end{Bmatrix}_F &= \begin{Bmatrix} -\ddot{\phi}_S \\ 0 \\ 0 \end{Bmatrix} + \dot{\phi}_S \begin{bmatrix} 0 & 0 & 0 \\ 0 & -\sin\phi_S & -\cos\phi_S \\ 0 & \cos\phi_S & -\sin\phi_S \end{bmatrix} \begin{Bmatrix} 0 \\ -\dot{\theta}_S \\ 0 \end{Bmatrix} \\ &+ \begin{bmatrix} \cos\theta_S & 0 & \sin\theta_S \\ 0 & 1 & 0 \\ -\sin\theta_S & 0 & \cos\theta_S \end{bmatrix} \begin{Bmatrix} p \\ q \\ r \end{Bmatrix}_H + \begin{bmatrix} 1 & 0 & 0 \\ 0 & \cos\phi_S & -\sin\phi_S \\ 0 & \sin\phi_S & \cos\phi_S \end{bmatrix} \begin{Bmatrix} 0 \\ -\ddot{\theta}_S \\ 0 \end{Bmatrix} \\ &+ \theta_S \begin{bmatrix} -\sin\theta_S & 0 & \cos\theta_S \\ 0 & 0 & 0 \\ -\cos\theta_S & 0 & -\sin\theta_S \end{bmatrix} \begin{Bmatrix} p \\ q \\ r \end{Bmatrix}_H + \begin{bmatrix} \cos\theta_S & 0 & \sin\theta_S \\ 0 & 1 & 0 \\ -\sin\theta_S & 0 & \cos\theta_S \end{bmatrix} \begin{Bmatrix} \dot{p} \\ \dot{q} \\ \dot{r} \end{Bmatrix}_H \end{aligned} \quad (5-64)$$

The above equations define the fuselage reference axis system angular velocities and accelerations in terms of hub or principal reference axis system angular velocities and accelerations and shaft angular displacements.

5.5.3 Motion of Rotor Coordinate Axis

The rotor coordinate axis system is shown in Figure 5-5. Note that the rotor coordinate axis system is rotated 180 degrees about the Y axis relative to the hub axis system at the time when the rotor is at azimuth position zero. That is, X and Z change directions. The rotor coordinate system then rotates through the angle ψ_R from this position.

The sequence of rotation in going from hub to rotor coordinates consists of first a 180-degree θ rotation, followed by the ψ_R rotation.

Following the convention established in Section 5.4.2 for Euler angles:

$$\begin{aligned} [T_{H-R}] &= \begin{bmatrix} \cos\psi_R & \sin\psi_R & 0 \\ -\sin\psi_R & \cos\psi_R & 0 \\ 0 & 0 & 1 \end{bmatrix} \begin{bmatrix} \cos\pi & 0 & \sin\pi \\ 0 & 1 & 0 \\ -\sin\pi & 0 & \cos\pi \end{bmatrix} \\ &= \begin{bmatrix} \cos\psi_R & \sin\psi_R & 0 \\ -\sin\psi_R & \cos\psi_R & 0 \\ 0 & 0 & 1 \end{bmatrix} \begin{bmatrix} -1 & 0 & 0 \\ 0 & 1 & 0 \\ 0 & 0 & -1 \end{bmatrix} \quad (5-65) \end{aligned}$$

where the last matrix represents the 180-degree θ rotation. The next matrix is the rotor rotation, $\psi_R = \int_0^t \Omega_R dt$.

Since the origins of the rotor coordinate system and the principal reference axis system are coincident, the linear velocities and accelerations of the origin of the rotor coordinate system can be directly written as:

$$\begin{Bmatrix} \dot{X}_O \\ \dot{Y}_O \\ \dot{Z}_O \end{Bmatrix}_R = [T_{H-R}] \begin{Bmatrix} \dot{X}_{OH} \\ \dot{Y}_{OH} \\ \dot{Z}_{OH} \end{Bmatrix}_H \quad (5-66)$$

and

$$\begin{Bmatrix} \ddot{X}_0 \\ \ddot{Y}_0 \\ \ddot{Z}_0 \end{Bmatrix}_R^I = [T_{H-R}] \begin{Bmatrix} \ddot{X}_{OH} \\ \ddot{Y}_{OH} \\ \ddot{Z}_{OH} \end{Bmatrix}_H^I \quad (5-67)$$

Noting gravity has been treated as an equivalent acceleration in the hub generalized coordinate accelerations. This same equivalent acceleration is included in $(\ddot{X}_0, \ddot{Y}_0, \ddot{Z}_0)_R$, the rotor coordinate accelerations.

The angular velocities, p_R, q_R, r_R , and accelerations, $\dot{p}_R, \dot{q}_R, \dot{r}_R$ of the rotor coordinate system are determined; again noting the rotation order. The rotor coordinate system angular velocities are:

$$\begin{Bmatrix} p \\ q \\ r \end{Bmatrix}_R = \begin{Bmatrix} 0 \\ 0 \\ \dot{\psi}_R \end{Bmatrix}_H + \begin{bmatrix} \cos\psi_R & \sin\psi_R & 0 \\ -\sin\psi_R & \cos\psi_R & 0 \\ 0 & 0 & 1 \end{bmatrix} \begin{Bmatrix} -p \\ q \\ -r \end{Bmatrix}_H \quad (5-68)$$

Likewise, accelerations of the rotor coordinate system are:

$$\begin{Bmatrix} \dot{p} \\ \dot{q} \\ \dot{r} \end{Bmatrix}_R = \begin{Bmatrix} 0 \\ 0 \\ \ddot{\psi}_R \end{Bmatrix}_H + \dot{\psi}_R \begin{bmatrix} -\sin\psi_R & \cos\psi_R & 0 \\ -\cos\psi_R & -\sin\psi_R & 0 \\ 0 & 0 & 0 \end{bmatrix} \begin{Bmatrix} -p \\ q \\ -r \end{Bmatrix}_H + \begin{bmatrix} \cos\psi_R & \sin\psi_R & 0 \\ -\sin\psi_R & \cos\psi_R & 0 \\ 0 & 0 & 1 \end{bmatrix} \begin{Bmatrix} -\dot{p} \\ \dot{q} \\ -\dot{r} \end{Bmatrix}_H \quad (5-69)$$

The above equations then define the coordinate transformation from hub to rotor coordinates; and rotor axis system linear and angular velocities and accelerations in terms of velocities and accelerations of hub and the rotor degrees of freedom ψ_R .

5.5.4 Blade Coordinate Relative to Rotor Coordinates

Interim equations to describe teetering make use of Z_{OBL} , the blade undersling. These equations are approximations given in Section 6.7. It is assumed the blade axes and rotor axes origins coincide and $Z_{OBL} = 0$ in this section.

Referring to Figure 5-5, observe that each blade has its own coordinate axis system.

Since each blade has its own blade reference system, the X_{BLn} and Y_{BLn} axes are rotated with respect to the X_R and Y_R axes azimuthally by an angle ψ_{BLn} defined by the equation

$$\psi_{BLn} = \frac{-2\pi(n-1)}{b} \quad (5-70)$$

where b is the number of blades and n is the blade number. This equation states that the X_{BL1} and X_R , and the Y_{BL1} and the Y_R axes are coincident.

The transformations between the rotor coordinate axis system and the blade coordinate axis systems are defined by the equation

$$\begin{bmatrix} T_{R-BLn} \end{bmatrix} = \begin{bmatrix} \cos\psi_{BLn} & \sin\psi_{BLn} & 0 \\ -\sin\psi_{BLn} & \cos\psi_{BLn} & 0 \\ 0 & 0 & 1 \end{bmatrix} \quad (5-71)$$

Note that these equations define blade one as being straight aft at time zero.

In the blade reference axes, the velocities and accelerations of the origin of the blade reference axis system become:

$$\begin{Bmatrix} \dot{X}_{OBLn} \\ \dot{Y}_{OBLn} \\ \dot{Z}_{OBLn} \end{Bmatrix}_{BLn}^I = [T_{R-BLn}] \begin{Bmatrix} \dot{X}_0 \\ \dot{Y}_0 \\ \dot{Z}_0 \end{Bmatrix}_R^I \quad (5-72)$$

and

$$\begin{Bmatrix} \ddot{X}_{OBLn} \\ \ddot{Y}_{OBLn} \\ \ddot{Z}_{OBLn} \end{Bmatrix}_{BLn}^I = [T_{R-BLn}] \begin{Bmatrix} \ddot{X}_0 \\ \ddot{Y}_0 \\ \ddot{Z}_0 \end{Bmatrix}_R^I \quad (5-73)$$

Likewise, the angular velocities and accelerations of the blade reference axis systems become:

$$\begin{Bmatrix} p \\ q \\ r \end{Bmatrix}_{BLn} = [T_{R-BLn}] \begin{Bmatrix} p \\ q \\ r \end{Bmatrix}_R \quad (5-74)$$

and

$$\begin{Bmatrix} \dot{p} \\ \dot{q} \\ \dot{r} \end{Bmatrix}_{BLn} = [T_{R-BLn}] \begin{Bmatrix} \dot{p} \\ \dot{q} \\ \dot{r} \end{Bmatrix}_R \quad (5-75)$$

5.5.5 Blade Element Motion

The following blade motion description, due to the involved nature of the geometry, is rather lengthy. First, in this development, the motion of the blade with respect to the relative blade coordinates is given. This motion is the sum of static and modal deflections. Then the relation to freestream coordinates is computed. Partial derivatives are extracted from the transformations for use in the equations of motion of the blade in Section 6.6.

The blade element motions for the n th blade are defined relative to the blade (BLn) coordinate reference axes (Figure 5-5). The blade element relative motions are functions of the static shape, of blade feathering and torsional deflection, and of blade bending of the coupled inplane and flapping modes.

The static shape includes such items as blade twist, ϕ_{TW} , hub precone angle, β_0 , blade droop angle relative to the precone angle, γ , blade sweep angle, τ_0 , feathering axis precone, β_{FA} , the blade feathering angle, and the blade element center of gravity location.

The blade motions about this static shape include the effects of the three blade bending modes, A_{1n} , A_{2n} and A_{3n} , blade feathering, ϕ_F , and blade torsional deflection, ϕ_t .

The blade element motions are now defined. The blade static position in the blade reference axis system is first developed. The blade bending and feathering deflections are then introduced. Both deflections and slopes are developed and then these equations are differentiated with respect to time to obtain the blade element linear and angular velocities and accelerations.

The blade element linear motions are developed in blade (BLn) coordinates and the blade element angular velocities and accelerations are developed in blade element (BLE) coordinates. The coordinate transformation matrix $\begin{bmatrix} T_{BLn-BLE} \end{bmatrix}$ is also defined to permit the transformation of the inertial velocities and accelerations from one axis system to the other. The development of the blade relative motion equations now starts with the description of the shape of the blade.

5.5.5.1 Blade Static Shape

Blade elemental motion is defined as motion of the blade element reference axis system which has its origin at the blade element center of gravity. The blade aerodynamic reference axis is selected as the 1/4 chord. Likewise, the geometry and dynamics are referenced to the 1/4 chord, though any reference line could have been used. Starting with the straight untwisted blade with the blade 1/4 chord lying along the X_{BLn} axis as in Figure 5-18, the blade element cg and blade element coordinate axis system origin are defined by the coincident point defined by the vector

$$\begin{Bmatrix} X_{CG}(i) \\ Y_{CG}(i) \\ Z_{CG}(i) \end{Bmatrix}_{BLn} \quad (5-76)$$

in blade coordinates. The dimension $X_{CG}(i)_{BLn}$ is the undeformed spanwise location of the cg/blade element origin. The dimension $Y_{CG}(i)_{BLn}$ is the chordwise location of the cg/blade element axis system origin forward of the blade 1/4 chord and $Z_{CG}(i)_{BLn}$ is any vertical offset of the cg/blade element origin with respect to the reference chord plane of the blade.

Now, introducing blade twist by rotating about the X_{BLn} axis through the local blade twist angles, Figure 5-19, results in:

$$\begin{Bmatrix} X(i)_{BLE} \\ Y(i)_{BLE} \\ Z(i)_{BLE} \end{Bmatrix}_I = \begin{Bmatrix} X(i)_{BLE} \\ Y(i)_{BLE} \\ Z(i)_{BLE} \end{Bmatrix}_{BLn} = \begin{bmatrix} 1 & 0 & 0 \\ 0 & \cos\phi_{TW} & -\sin\phi_{TW} \\ 0 & \sin\phi_{TW} & \cos\phi_{TW} \end{bmatrix} \begin{Bmatrix} X_{CG} \\ Y_{CG} \\ Z_{CG} \end{Bmatrix}_{BLn} \quad (5-77)$$

The Roman numeral subscript I denotes the first of a sequence of static line transformations.

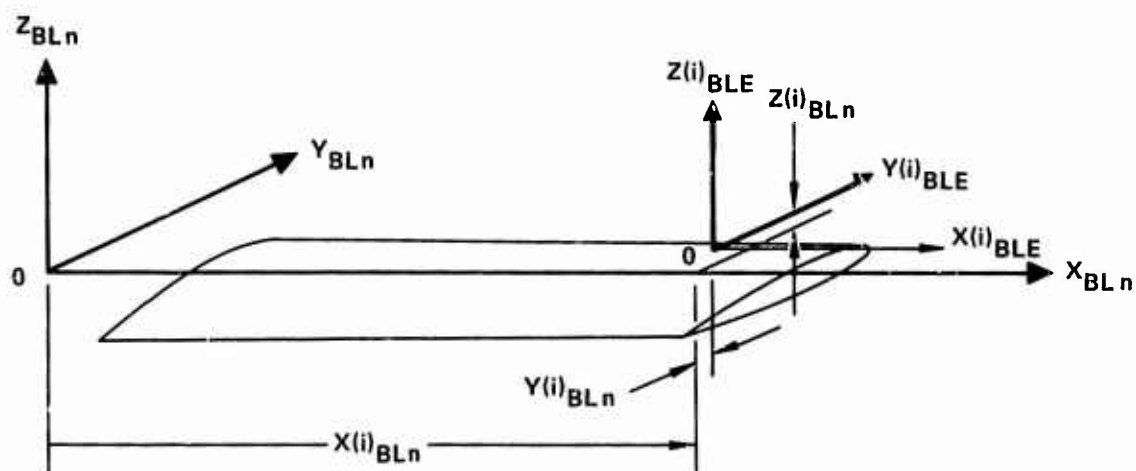


Figure 5-18. Blade Element CG/Origin Location in Blade Coordinates

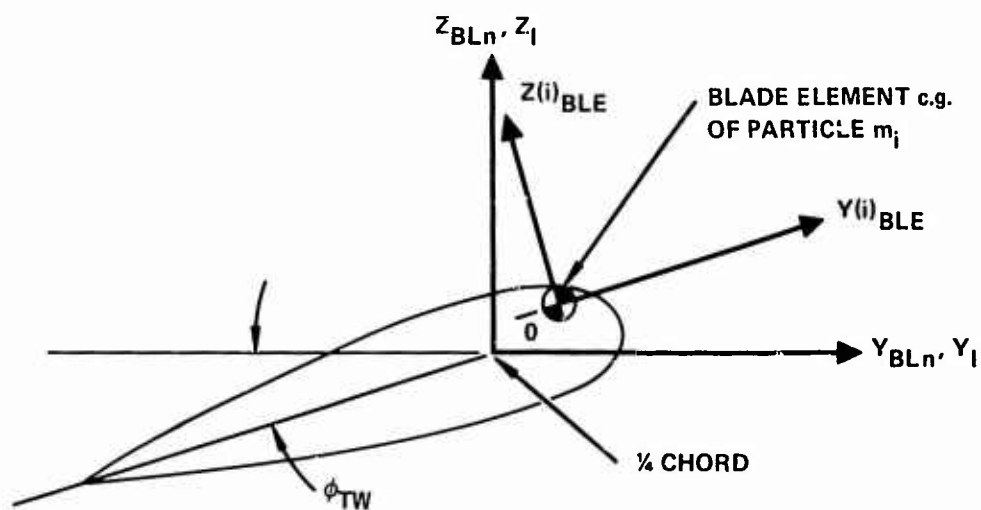


Figure 5-19. Effect of Blade Twist on Location of Blade Element CG/Axis System Origin

At this point the subscripting, BLE will be dropped to simplify the development. Rewriting the above equation, we have:

$$\begin{Bmatrix} X(i) \\ Y(i) \\ Z(i) \end{Bmatrix}_I = \begin{bmatrix} 1 & 0 & 0 \\ 0 & \cos\phi_{TW} & -\sin\phi_{TW} \\ 0 & \sin\phi_{TW} & \cos\phi_{TW} \end{bmatrix} \begin{Bmatrix} X_{CG} \\ Y_{CG} \\ Z_{CG} \end{Bmatrix} \quad (5-78)$$

Introducing blade coning, β_0 , results in the location of the blade as shown in Figure 5-20. This results in:

$$\begin{Bmatrix} X(i) \\ Y(i) \\ Z(i) \end{Bmatrix}_{II} = \begin{bmatrix} \cos\beta_0 & 0 & -\sin\beta_0 \\ 0 & 1 & 0 \\ \sin\beta_0 & 0 & \cos\beta_0 \end{bmatrix} \begin{Bmatrix} X(i) \\ Y(i) \\ Z(i) \end{Bmatrix}_I \quad (5-79)$$

The next item of static geometry that is considered is blade droop, γ , and then blade sweep, τ_0 . These rotations are shown in Figure 5-21. Note that since the blade sweep and droop angles are introduced at a distance X_{SW} out on the blade, it is first necessary to transfer axes to this location before making the rotations. Therefore, the blade displacements outboard of Station X_{SW} become:

$$\begin{Bmatrix} X(i) \\ Y(i) \\ Z(i) \end{Bmatrix}_{III} = \begin{bmatrix} \cos\tau_0 & -\sin\tau_0 & 0 \\ \sin\tau_0 & \cos\tau_0 & 0 \\ 0 & 0 & 1 \end{bmatrix} \begin{bmatrix} \cos\gamma & 0 & \sin\gamma \\ 0 & 1 & 0 \\ -\sin\gamma & 0 & \cos\gamma \end{bmatrix} \begin{Bmatrix} X(i) \\ Y(i) \\ Z(i) \end{Bmatrix}_{II} - \begin{Bmatrix} X_{SW}\cos\beta_0 \\ 0 \\ X_{SW}\sin\beta_0 \end{Bmatrix} \quad (5-80)$$

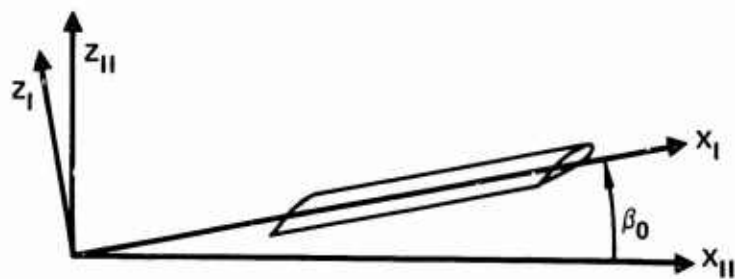


Figure 5-20. Blade Precone Angle, β_0

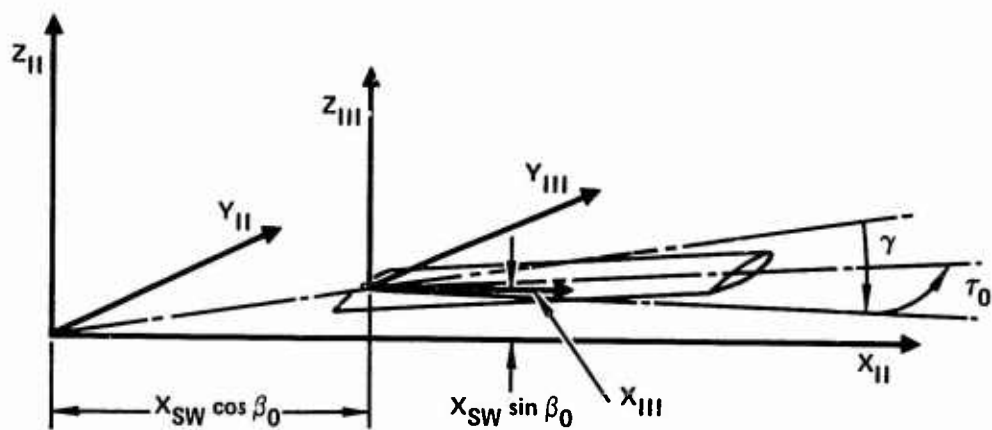


Figure 5-21. Blade Sweep, τ_0 , and Blade Droop, γ

At this same station, provisions are introduced to allow for offsets of the blade in both the vertical and horizontal directions by Z_{jog} and Y_{jog} , respectively. These offsets are shown in Figure 5-22. These offsets represent displacement of the blade 1/4 chord with respect to the blade precone line at blade station X_{SW} .

Introducing these offsets, then, and transferring back to the center of rotation through X_{SW} results in the description of the blade displacements outboard of station X_{SW} , including the effects of precone, sweep, droop, and offset of the blade from the precone line.

$$\begin{Bmatrix} X(i) \\ Y(i) \\ Z(i) \end{Bmatrix}_{IV} = \begin{Bmatrix} X(i) \\ Y(i) \\ Z(i) \end{Bmatrix}_{III} + \begin{Bmatrix} 0 \\ Y_{jog} \\ Z_{jog} \end{Bmatrix} + \begin{Bmatrix} X_{SW} \cos \beta_0 \\ 0 \\ X_{SW} \sin \beta_0 \end{Bmatrix} \quad (5-81)$$

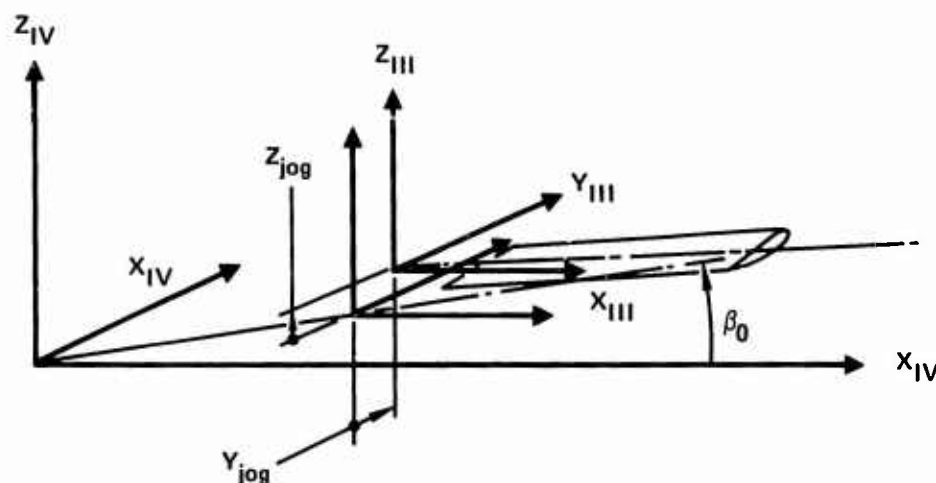


Figure 5-22. Introduction of Blade 1/4 Chord Offset, Y_{jog} and Z_{jog} With Respect to Precone Line

At this point, a reminder that the prior development represents the blade displacement inboard of Station X_{SW} and the above equation outboard of Station X_{SW} . Therefore, inboard of Station X_{SW} :

$$\begin{Bmatrix} X(i) \\ Y(i) \\ Z(i) \end{Bmatrix} = \begin{Bmatrix} X(i) \\ Y(i) \\ Z(i) \end{Bmatrix}_{II} \quad (5-82)$$

Outboard of Station X_{SW} :

$$\begin{Bmatrix} X(i) \\ Y(i) \\ Z(i) \end{Bmatrix} = \begin{Bmatrix} X(i) \\ Y(i) \\ Z(i) \end{Bmatrix}_{IV} \quad (5-83)$$

With this in mind, the remaining developing of including the effects of feathering axis static precone and blade reference feather angle in describing the static blade position continues. No distinction will be made in the following developments between inboard of

Station X_{SW} and outboard of Station X_{SW} .

Figure 5-23 shows how blade feathering is introduced. The axis system is translated to a point p which is located at the intersection of the precone line and the feathering axis. The location of this point is a distance l_p along the cone line, as shown in this figure. The blade is first rotated to the feather axis; then rotated about the reference feathering angle, ϕ_{REF} , the feathering angle for which the blade modes are defined. Doing this results in:

$$\begin{Bmatrix} X(i) \\ Y(i) \\ Z(i) \end{Bmatrix}_V = \begin{bmatrix} 1 & 0 & 0 \\ 0 & \cos\phi_{REF} & -\sin\phi_{REF} \\ 0 & \sin\phi_{REF} & \cos\phi_{REF} \end{bmatrix} \begin{bmatrix} \cos\beta_{FA} & 0 & \sin\beta_{FA} \\ 0 & 1 & 0 \\ -\sin\beta_{FA} & 0 & \cos\beta_{FA} \end{bmatrix} \begin{Bmatrix} X(i) \\ Y(i) \\ Z(i) \end{Bmatrix} - \begin{Bmatrix} l_p \cos\beta_0 \\ 0 \\ l_p \sin\beta_0 \end{Bmatrix} \quad (5-84)$$

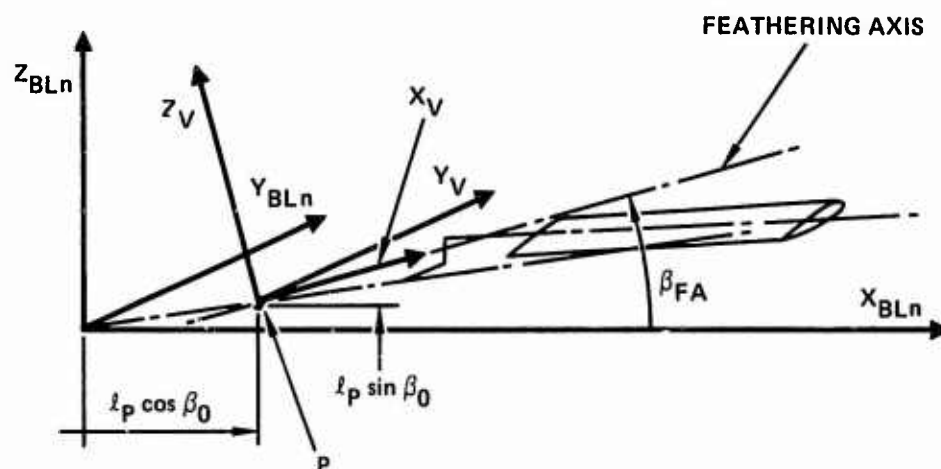


Figure 5-23. Point p and Feathering Axis Precone β_{FA}

This equation defines the location of the static shape of the blade in an axis system with the y-axis horizontal and the x-axis aligned with the blade static feathering axis. Transforming now back through the feathering axis precone angle and translating back to the rotor shaft centerline results in the static shape of the blade defined in blade coordinates, or

$$\begin{Bmatrix} X_S(i) \\ Y_S(i) \\ Z_S(i) \end{Bmatrix}_{BLn} = \begin{bmatrix} \cos\beta_{FA} & 0 & -\sin\beta_{FA} \\ 0 & 1 & 0 \\ \sin\beta_{FA} & 0 & \cos\beta_{FA} \end{bmatrix} \begin{Bmatrix} X(i) \\ Y(i) \\ Z(i) \end{Bmatrix}_V + \begin{Bmatrix} l_P \cos\beta_0 \\ 0 \\ l_P \sin\beta_0 \end{Bmatrix} \quad (5-85)$$

where subscript S refers to blade static or undeformed shape. Combining equations developed so far results, then, in the following two equations which represent the static shape of the blade for both inboard and outboard of blade station X_{SW} .

Inboard of Station X_{SW} :

$$\begin{aligned}
 r_{S_{BLn}} = \begin{Bmatrix} X_S \\ Y_S \\ Z_S \end{Bmatrix}_{BLn} &= \begin{bmatrix} \cos\beta_{FA} & 0 & -\sin\beta_{FA} \\ 0 & 1 & 0 \\ \sin\beta_{FA} & 0 & \cos\beta_{FA} \end{bmatrix} \begin{bmatrix} 1 & 0 & 0 \\ 0 & \cos\phi_{REF} & -\sin\phi_{REF} \\ 0 & \sin\phi_{REF} & \cos\phi_{REF} \end{bmatrix} \\
 &\cdot \begin{bmatrix} \cos\beta_{FA} & 0 & \sin\beta_{FA} \\ 0 & 1 & 0 \\ -\sin\beta_{FA} & 0 & \cos\beta_{FA} \end{bmatrix} \left\{ \begin{bmatrix} \cos\beta_0 & 0 & -\sin\beta_0 \\ 0 & 1 & 0 \\ \sin\beta_0 & 0 & \cos\beta_0 \end{bmatrix} \right. \\
 &\cdot \begin{bmatrix} 1 & 0 & 0 \\ 0 & \cos\phi_{TW} & -\sin\phi_{TW} \\ 0 & \sin\phi_{TW} & \cos\phi_{TW} \end{bmatrix} \left\{ \begin{matrix} X_{CG} \\ Y_{CG} \\ Z_{CG} \end{matrix} \right\} - \left\{ \begin{matrix} \ell_p \cos\beta_0 \\ 0 \\ \ell_p \sin\beta_0 \end{matrix} \right\} \\
 &+ \left\{ \begin{matrix} \ell_p \cos\beta_0 \\ 0 \\ \ell_p \sin\beta_0 \end{matrix} \right\}
 \end{aligned}
 \tag{5-86}$$

Outboard of Station X_{SW} :

$$\begin{aligned}
 r_{S_{BLn}} = \begin{Bmatrix} X_S \\ Y_S \\ Z_S \end{Bmatrix} &= \begin{bmatrix} \cos\beta_{FA} & 0 & -\sin\beta_{FA} \\ 0 & 1 & 0 \\ \sin\beta_{FA} & 0 & \cos\beta_{FA} \end{bmatrix} \begin{bmatrix} 1 & 0 & 0 \\ 0 & \cos\phi_{REF} & -\sin\phi_{REF} \\ 0 & \sin\phi_{REF} & \cos\phi_{REF} \end{bmatrix} \\
 &\cdot \begin{bmatrix} \cos\beta_{FA} & 0 & \sin\beta_{FA} \\ 0 & 1 & 0 \\ -\sin\beta_{FA} & 0 & \cos\beta_{FA} \end{bmatrix} \left\{ \begin{bmatrix} \cos\tau_0 & -\sin\tau_0 & 0 \\ \sin\tau_0 & \cos\tau_0 & 0 \\ 0 & 0 & 1 \end{bmatrix} \begin{bmatrix} \cos\gamma & 0 & \sin\gamma \\ 0 & 1 & 0 \\ -\sin\gamma & 0 & \cos\gamma \end{bmatrix} \right. \\
 &\cdot \left. \begin{bmatrix} \cos\beta_0 & 0 & -\sin\beta_0 \\ 0 & 1 & 0 \\ \sin\beta_0 & 0 & \cos\beta_0 \end{bmatrix} \begin{bmatrix} 1 & 0 & 0 \\ 0 & \cos\phi_{TW} & -\sin\phi_{TW} \\ 0 & \sin\phi_{TW} & \cos\phi_{TW} \end{bmatrix} \begin{Bmatrix} X_{CG} \\ Y_{CG} \\ Z_{CG} \end{Bmatrix} \right. \\
 &- \begin{Bmatrix} X_{SW}\cos\beta_0 \\ 0 \\ X_{SW}\sin\beta_0 \end{Bmatrix} \left. + \begin{Bmatrix} 0 \\ Y_{jog} \\ Z_{jog} \end{Bmatrix} + \begin{Bmatrix} X_{SW}\cos\beta_0 \\ 0 \\ X_{SW}\sin\beta_0 \end{Bmatrix} - \begin{Bmatrix} l_p\cos\beta_0 \\ 0 \\ l_p\sin\beta_0 \end{Bmatrix} \right. \\
 &+ \begin{Bmatrix} l_p\cos\beta_0 \\ 0 \\ l_p\sin\beta_0 \end{Bmatrix} \tag{5-87}
 \end{aligned}$$

These two equations then define completely the static shape of the blade. The development will now proceed to include the blade bending or elastic deformation. However, before proceeding with this, the static location of the blade feathering bearing is defined since these will be used in the development that follows.

Referring to Figure 5-24, it can be seen that the static position of the inboard feather bearing location can be written as:

$$\begin{Bmatrix} x_{S_{IB}} \\ y_{S_{IB}} \\ z_{S_{IB}} \end{Bmatrix}_{BLn} = \begin{Bmatrix} \ell_{IB} \cos \beta_0 \\ 0 \\ \ell_{IB} \sin \beta_0 - (\ell_p - \ell_{IB}) (\tan(\beta_{FA} - \beta_0)) \cos \beta_0 \end{Bmatrix} \quad (5-88)$$

The static location of the outboard feather bearing is:

$$\begin{Bmatrix} x_{S_{OB}} \\ y_{S_{OB}} \\ z_{S_{OB}} \end{Bmatrix}_{BLn} = \begin{Bmatrix} \ell_{OB} \cos \beta_0 \\ 0 \\ \ell_{OB} \sin \beta_0 + (\ell_{OB} - \ell_p) (\tan(\beta_{FA} - \beta_0)) \cos \beta_0 \end{Bmatrix} \quad (5-89)$$

With these definitions, the analysis will now proceed to include the effects of blade bending, blade feathering, and torsional deflection.

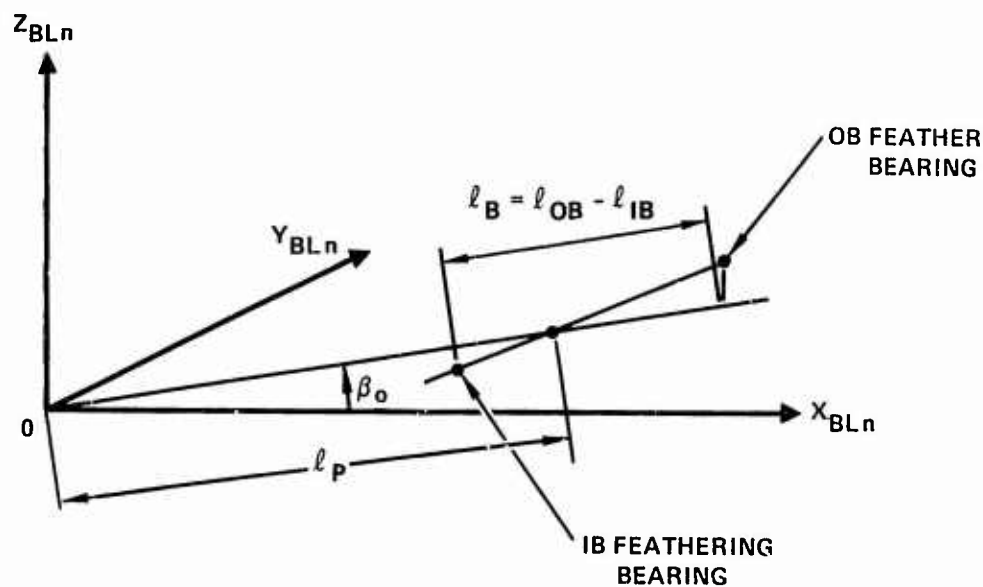


Figure 5-24. Static Feather Bearing Geometry

5.5.5.2 Blade Shape - Elastic Deformation

In the foregoing development, the analysis has proceeded in a completely rigorous fashion. At this point, though, a departure from a completely rigorous simulation of the elemental blade motions will be made. It will be assumed, as far as blade elastic deformation is concerned, that the cosine of angles, like precone less droop, blade sweep, elastic flapping, and elastic inplane slopes, but not blade feathering is approximately equal to 1, and therefore, the blade elastic deflections, y and z , in blade coordinates, will be assumed to be equal to those in the static blade element coordinates. This assumption is a reasonably valid assumption and is completely consistent with standard practice in the mathematical representation of blade element motions.

Additionally, as far as the effect on structural axis reorientation due to blade ϕ rotation, the effect due to blade elastic twist is considered to be small compared to that due to blade cyclic and collective feathering. Also it will be assumed that the contributions to blade Y and Z motion are small due to blade torsional motion, other than that due to local center of gravity offset.

With these assumptions in mind, blade elastic bending will now be introduced. The contribution to elastic blade bending is simply

$$\begin{Bmatrix} 0 \\ Y_{BEND} \\ Z_{BEND} \end{Bmatrix}_{BLn} = \begin{bmatrix} 0 & 0 & 0 \\ Y_1 & Y_2 & Y_3 \\ Z_1 & Z_2 & Z_3 \end{bmatrix} \begin{Bmatrix} A_{1n} \\ A_{2n} \\ A_{3n} \end{Bmatrix} \quad (5-90)$$

Note that X or spanwise motions are not included in this equation. Blade spanwise motion will be determined separately by utilizing blade slope data to determine the change in the projected blade length upon the blade X axis. With this in mind, the total Y and Z blade motions including blade bending, but not yet including blade feathering or blade elastic twist, is strictly the sum of the previous static line expressions and the modal deflection. Blade torsional deflection is treated as an independent degree of freedom, and therefore is not included as part of these blade modes. Combining the previous static deflection with the modal deflections gives:

$$\begin{Bmatrix} X_{(B+S)} \\ Y_{(B+S)} \\ Z_{(B+S)} \end{Bmatrix}_{BLn} = \begin{Bmatrix} X_S \\ Y_S \\ Z_S \end{Bmatrix}_{BLn} + \begin{Bmatrix} 0 \\ Y_{BEND} \\ Z_{BEND} \end{Bmatrix}_{BLn} \quad (5-91)$$

5.5.5.3 Blade Feathering

Blade feathering is relative to the reference feathering angle ϕ_{REF} . The feather angle, then, as far as blade motion is concerned, is due to the difference in the total feather angle ϕ_F and the reference feather angle ϕ_{REF} .

The blade feathering motion is introduced similarly to the way the blade reference feathering angle was introduced, except that the feather axis slopes are due to the static position as well as due to elastic deformation in both the flapwise and inplane deflection.

If we let Z'_{FA} and Y'_{FA} represent the instantaneous vertical and inplane slopes of the feathering axis, then transferring to the inboard feathering bearing, making the rotations through Z'_{FA} and Y'_{FA} to the feathering axis, rotating through the delta feather angle $-(\phi_F - \phi_{REF})$ or $-\Delta\phi_F$, rotating back through $-Y'_{FA}$ and $-Z'_{FA}$, and then transferring back to the BLn axis system results in the definition of the displacements in blade axis coordinates.

However, before proceeding with this, the feathering axis slopes Y'_{FA} and Z'_{FA} are defined. The slopes are simply defined as the difference in the total static and elastic deflection of the outboard and inboard feather bearings divided by the spanwise distance between the bearings. Then from Figure 5-24 and the bearing static location equation:

$$Y'_{FA} \approx \sin^{-1} \left(\frac{Y_{OB} - Y_{IB}}{l_B} \right) \quad (5-92)$$

and

$$Z'_{FA} \approx \sin^{-1} \left(\frac{Z_{OB} - Z_{IB}}{l_B} \right) \quad (5-93)$$

where in terms of the static and modal deflections

$$\begin{Bmatrix} X_{IB} \\ Y_{IB} \\ Z_{IB} \end{Bmatrix} = \begin{Bmatrix} X_{S_{IB}} \\ Y_{S_{IB}} \\ Z_{S_{IB}} \end{Bmatrix} + \begin{bmatrix} 0 & 0 & 0 \\ Y_{IB_1} & Y_{IB_2} & Y_{IB_3} \\ Z_{IB_1} & Z_{IB_2} & Z_{IB_3} \end{bmatrix} \begin{Bmatrix} A_{1n} \\ A_{2n} \\ A_{3n} \end{Bmatrix} \quad (5-94)$$

and

$$\begin{Bmatrix} - \\ Y_{OB} \\ Z_{OB} \end{Bmatrix} = \begin{Bmatrix} - \\ Y_{S_{OB}} \\ Z_{S_{OB}} \end{Bmatrix} + \begin{bmatrix} 0 & 0 & 0 \\ Y_{OB_1} & Y_{OB_2} & Y_{OB_3} \\ Z_{OB_1} & Z_{OB_2} & Z_{OB_3} \end{bmatrix} \begin{Bmatrix} A_{1n} \\ A_{2n} \\ A_{3n} \end{Bmatrix} \quad (5-95)$$

In the development that follows, the time derivatives of Y'_{FA} and Z'_{FA} are required, so therefore, they are now defined. Taking the first and second time derivatives of the slope equations yields:

$$\dot{Y}'_{FA} \approx (\dot{Y}_{OB} - \dot{Y}_{IB}) / \cos(Y'_{FA}) l_B \quad (5-96)$$

$$\dot{Z}'_{FA} \approx (\dot{Z}_{OB} - \dot{Z}_{IB}) / \cos(Z'_{FA}) l_B \quad (5-97)$$

and

$$\ddot{Y}'_{FA} \approx (\ddot{Y}_{OB} - \ddot{Y}_{IB}) / \cos(Y'_{FA}) l_B + \sin(Y'_{FA}) \dot{Y}'_{FA}^2 / \cos(Y'_{FA}) \quad (5-98)$$

$$\ddot{Z}'_{FA} \approx (\ddot{Z}_{OB} - \ddot{Z}_{IB}) / \cos(Z'_{FA}) l_B + \sin(Z'_{FA}) \dot{Z}'_{FA}^2 / \cos(Z'_{FA}) \quad (5-99)$$

where

$$\begin{Bmatrix} \dot{Y}_{IB} \\ \dot{Z}_{IB} \end{Bmatrix} = \begin{bmatrix} Y_{IB_1} & Y_{IB_2} & Y_{IB_3} \\ Z_{IB_1} & Z_{IB_2} & Z_{IB_3} \end{bmatrix} \begin{Bmatrix} \dot{A}_{1n} \\ \dot{A}_{2n} \\ \dot{A}_{3n} \end{Bmatrix} \quad (5-100)$$

$$\begin{Bmatrix} \dot{Y}_{OB} \\ \dot{Z}_{OB} \end{Bmatrix} = \begin{bmatrix} Y_{OB_1} & Y_{OB_2} & Y_{OB_3} \\ Z_{OB_1} & Z_{OB_2} & Z_{OB_3} \end{bmatrix} \begin{Bmatrix} \dot{A}_{1n} \\ \dot{A}_{2n} \\ \dot{A}_{3n} \end{Bmatrix} \quad (5-101)$$

and where

$$\begin{Bmatrix} \ddot{Y}_{IB} \\ \ddot{Z}_{IB} \end{Bmatrix} = \begin{bmatrix} Y_{IB_1} & Y_{IB_2} & Y_{IB_3} \\ Z_{IB_1} & Z_{IB_2} & Z_{IB_3} \end{bmatrix} \begin{Bmatrix} \ddot{A}_{1n} \\ \ddot{A}_{2n} \\ \ddot{A}_{3n} \end{Bmatrix} \quad (5-102)$$

$$\begin{Bmatrix} \ddot{Y}_{OB} \\ \ddot{Z}_{OB} \end{Bmatrix} = \begin{bmatrix} Y_{OB_1} & Y_{OB_2} & Y_{OB_3} \\ Z_{OB_1} & Z_{OB_2} & Z_{OB_3} \end{bmatrix} \begin{Bmatrix} \ddot{A}_{1n} \\ \ddot{A}_{2n} \\ \ddot{A}_{3n} \end{Bmatrix} \quad (5-103)$$

Transferring the blade displacements as indicated above to the inboard feather bearing, transforming to the feathering axis, and

performing the feathering rotation as discussed earlier, yields the following equation which defines the blade displacements in blade axis coordinates:

$$\begin{aligned}
 \begin{Bmatrix} X_{(F+B+S)} \\ Y_{(F+B+S)} \\ Z_{(F+B+S)} \end{Bmatrix}_{BLn} &= \begin{bmatrix} \cos Z'_{FA} & 0 & -\sin Z'_{FA} \\ 0 & 1 & 0 \\ \sin Z'_{FA} & 0 & \cos Z'_{FA} \end{bmatrix} \begin{bmatrix} \cos Y'_{FA} & -\sin Y'_{FA} & 0 \\ \sin Y'_{FA} & \cos Y'_{FA} & 0 \\ 0 & 0 & 1 \end{bmatrix} \\
 &\cdot \begin{bmatrix} 1 & 0 & 0 \\ 0 & \cos \Delta \phi_F & -\sin \Delta \phi_F \\ 0 & \sin \Delta \phi_F & \cos \Delta \phi_F \end{bmatrix} \begin{bmatrix} \cos Y'_{FA} & \sin Y'_{FA} & 0 \\ -\sin Y'_{FA} & \cos Y'_{FA} & 0 \\ 0 & 0 & 1 \end{bmatrix} \\
 &\cdot \begin{bmatrix} \cos Z'_{FA} & 0 & \sin Z'_{FA} \\ 0 & 1 & 0 \\ -\sin Z'_{FA} & 0 & \cos Z'_{FA} \end{bmatrix} \begin{Bmatrix} X_{(B+S)} \\ Y_{(B+S)} \\ Z_{(B+S)} \end{Bmatrix} \\
 &- \begin{Bmatrix} X_{IB} \\ Y_{IB} \\ Z_{IB} \end{Bmatrix} + \begin{Bmatrix} X_{IB} \\ Y_{IB} \\ Z_{IB} \end{Bmatrix} \quad (5-104)
 \end{aligned}$$

This equation then gives the blade displacement in blade coordinates, including the effects of the static shape, blade bending, and blade static twist. The effect of blade elastic twist is now considered.

5.5.5.4 Blade Elastic Twist

Blade motion due to blade elastic twist is accounted for by going back to the static twist equation. Blade elastic twist, ϕ_T is assumed to be directly superpositionable with blade static or blade pretwist, ϕ_{TW} , except that the static pretwist takes place about the $1/4$ chord, and the blade elastic twist takes place about the

blade element shear center. This is shown in Figure 5-25. From this figure it can be seen that previous static twist equation can be rewritten as:

$$\begin{Bmatrix} X_{BLE} \\ Y_{BLE} \\ Z_{BLE} \end{Bmatrix}_I = \begin{bmatrix} 1 & 0 & 0 \\ 0 & \cos\phi_T & -\sin\phi_T \\ 0 & \sin\phi_T & \cos\phi_T \end{bmatrix} \begin{bmatrix} 1 & 0 & 0 \\ 0 & \cos\phi_{TW} & -\sin\phi_{TW} \\ 0 & \sin\phi_{TW} & \cos\phi_{TW} \end{bmatrix} \begin{Bmatrix} X_{CG} \\ Y_{CG} \\ Z_{CG} \end{Bmatrix} - \begin{Bmatrix} 0 \\ Y_{SC} \\ 0 \end{Bmatrix} + \begin{bmatrix} 1 & 0 & 0 \\ 0 & \cos\phi_{TW} & -\sin\phi_{TW} \\ 0 & \sin\phi_{TW} & \cos\phi_{TW} \end{bmatrix} \begin{Bmatrix} 0 \\ Y_{SC} \\ 0 \end{Bmatrix} \quad (5-105)$$

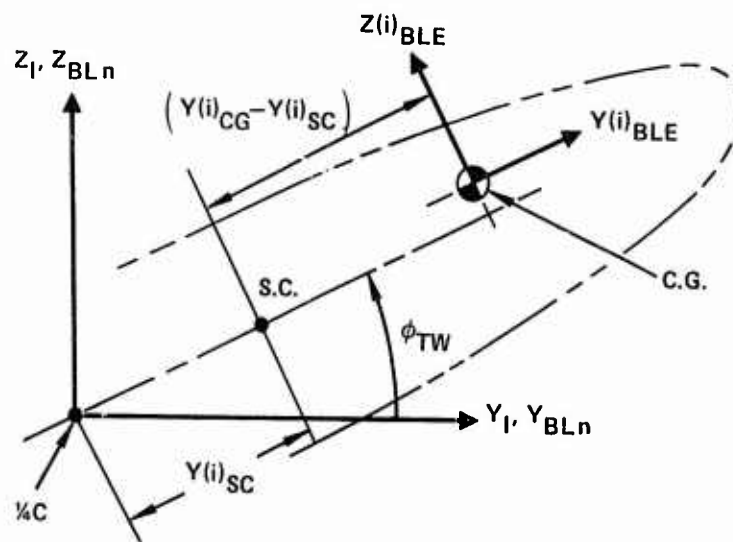
If we let $\phi_T = (\phi_T + \phi_{TW})$ then this equation becomes

$$\begin{Bmatrix} X_{BLE} \\ Y_{BLE} \\ Z_{BLE} \end{Bmatrix}_I = \begin{bmatrix} 1 & 0 & 0 \\ 0 & \cos\phi_T & -\sin\phi_T \\ 0 & \sin\phi_T & \cos\phi_T \end{bmatrix} \left\{ \begin{Bmatrix} X_{CG} \\ Y_{CG} \\ Z_{CG} \end{Bmatrix} - \begin{Bmatrix} 0 \\ Y_{SC} \\ 0 \end{Bmatrix} + \begin{Bmatrix} 0 \\ Y_{SC} \cos\phi_{TW} \\ Y_{SC} \sin\phi_{TW} \end{Bmatrix} \right\} \\ = \begin{bmatrix} 1 & 0 & 0 \\ 0 & \cos\phi_T & -\sin\phi_T \\ 0 & \sin\phi_T & \cos\phi_T \end{bmatrix} \begin{Bmatrix} X_{CG} \\ Y_{CG} \\ Z_{CG} \end{Bmatrix} + Y_{SC} \begin{Bmatrix} 0 \\ \cos\phi_{TW} - \cos\phi_T \\ \sin\phi_{TW} - \sin\phi_T \end{Bmatrix} \quad (5-106)$$

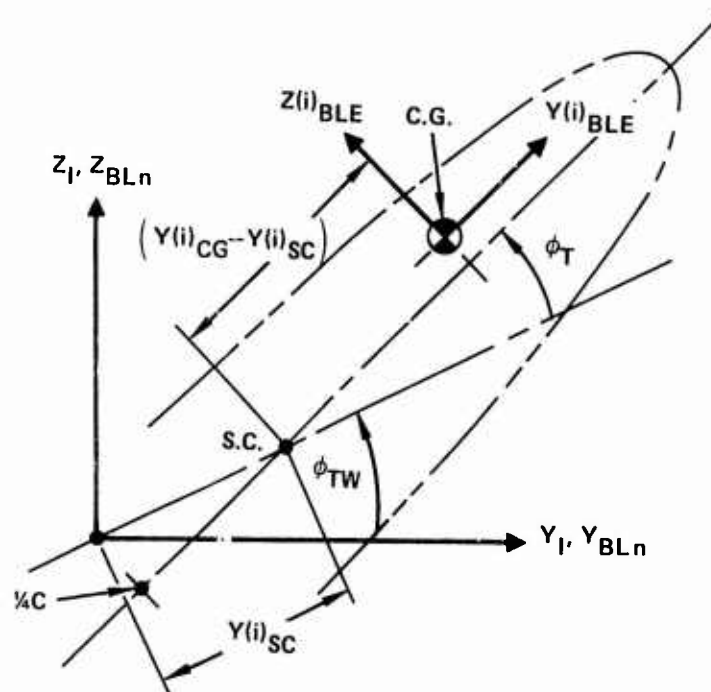
5.5.5.5 Final Blade Element Y,Z Displacement Equation

Substituting the above equation in the previous development sequence yields the blade displacement equation which includes the effect of the static shape of blade bending, of blade feathering, and of blade elastic twist.

However, before proceeding with these substitutions, the following column vector is defined to simplify the notation.



a) BLADE PRETWIST, $\phi_{TW}^{(i)}$, ABOUT BLADE REFERENCE AXIS



b) BLADE ELASTIC TWIST, $\phi_T^{(i)}$, ABOUT BLADE SHEAR CENTER

Figure 5-25. Blade Static Pretwist, ϕ_{TW} and Elastic Twist, ϕ_T

$$\begin{Bmatrix} r_a \end{Bmatrix} = \begin{Bmatrix} X_a \\ Y_a \\ Z_a \end{Bmatrix} \quad (5-107)$$

The total blade element displacement equation becomes:

$$\begin{aligned} \begin{Bmatrix} r_{BLE} \end{Bmatrix}_{BLn} &= \begin{bmatrix} T_{Z', FA} \\ T_{Y', FA} \\ T_{\Delta\phi_F} \end{bmatrix}^T \begin{bmatrix} T_{Y', FA} \\ T_{Z', FA} \end{bmatrix} \left\{ \left[\frac{\partial r}{\partial A_n} \right] \begin{Bmatrix} A_{jn} \end{Bmatrix} \right\} \\ &+ \left\{ \begin{bmatrix} T_{\beta_{FA}} \\ T_{\phi_{REF}} \end{bmatrix}^T \begin{bmatrix} T_{\beta_{FA}} \end{bmatrix} \right\} \left\{ \begin{bmatrix} T_{\tau_O} \\ T_Y \end{bmatrix}^T \right\} \\ &\cdot \left\{ \begin{bmatrix} T_{\beta_O} \end{bmatrix}^T \left\{ \begin{bmatrix} T_{\phi_T} \end{bmatrix}^T \begin{Bmatrix} r_{CG} \end{Bmatrix} + \left\{ \begin{bmatrix} T_{\phi_{TW}} \end{bmatrix}^T - \begin{bmatrix} T_{\phi_T} \end{bmatrix}^T \right\} \begin{Bmatrix} r_{SC} \end{Bmatrix} \right. \right. \\ &- \left. \begin{bmatrix} T_{\beta_O} \end{bmatrix}^T \begin{Bmatrix} r_{SW} \end{Bmatrix} \right\} + \left\{ \begin{Bmatrix} r_{Jog} \end{Bmatrix} + \begin{bmatrix} T_{\beta_O} \end{bmatrix}^T \begin{Bmatrix} r_{SW} \end{Bmatrix} \right. \\ &- \left. \begin{bmatrix} T_{\beta_O} \end{bmatrix}^T \begin{Bmatrix} r_p \end{Bmatrix} \right\} \right\} + \left\{ \begin{bmatrix} T_{\beta_O} \end{bmatrix}^T \begin{Bmatrix} r_p \end{Bmatrix} \right. \\ &- \left. \left. \begin{Bmatrix} r_{IB} \end{Bmatrix} \right\} \right\} + \begin{Bmatrix} r_{IB} \end{Bmatrix} \end{aligned} \quad (5-108)$$

where:

$$\left[\frac{\partial r}{\partial A_n} \right] \begin{Bmatrix} A_{jn} \end{Bmatrix} = \begin{bmatrix} 0 & 0 & 0 \\ Y_{1n} & Y_{2n} & Y_{3n} \\ Z_{1n} & Z_{2n} & Z_{3n} \end{bmatrix} \begin{Bmatrix} A_{1n} \\ A_{2n} \\ A_{3n} \end{Bmatrix} \quad (5-109)$$

Note that for convenience of using the condensed matrix notation discussed above, the most general vectors for such terms as ℓ_p , X_{SW} , Z_{jog} , and Y_{SC} have been used. As can be seen in this equation, these have all been treated as full vectors. Making the appropriate substitutions of course will result in the expressions previously obtained.

It is noted that the equation is written for the relative displacement of points on the blade outboard of Station X_{SW} . Inboard of that station, the displacements are determined from the previous inboard equation or simply by zeroing out such terms as $\{r_{jog}\}$ and $\{r_{SW}\}$ and substituting unit diagonal transformations for $\begin{bmatrix} T_{\tau_0} \end{bmatrix}$ and $\begin{bmatrix} T_Y \end{bmatrix}$ in the full equation. Following either approach yields the blade displacement equation for points inboard of Station X_{SW} ; or

$$\begin{aligned} \left\{ r_{BLE} \right\}_{BLn} = & \left[\begin{bmatrix} T_{Z', FA} \end{bmatrix}^T \begin{bmatrix} T_{Y', FA} \end{bmatrix}^T \begin{bmatrix} T_{\Delta\phi_F} \end{bmatrix}^T \begin{bmatrix} T_{Y', FA} \end{bmatrix} \begin{bmatrix} T_{Z', FA} \end{bmatrix} \right] \left\{ \left[\frac{\partial r}{\partial A_n} \right] \{ A_{jn} \} \right\} \\ & + \left\{ \left[\begin{bmatrix} T_{\beta_{FA}} \end{bmatrix}^T \begin{bmatrix} T_{\phi_{REF}} \end{bmatrix}^T \begin{bmatrix} T_{\beta_{FA}} \end{bmatrix} \right] \left[\begin{bmatrix} T_{\beta_0} \end{bmatrix} \right]^T \left[\begin{bmatrix} T_{\phi_T} \end{bmatrix} \right]^T \{ r_{CG} \} \right. \\ & + \left\{ \left[\begin{bmatrix} T_{\phi_{TW}} \end{bmatrix} \right]^T - \left[\begin{bmatrix} T_{\phi_T} \end{bmatrix} \right]^T \right\} \{ r_{SC} \} \left. - \left[\begin{bmatrix} T_{\beta_0} \end{bmatrix} \right]^T \{ r_p \} \right. \\ & \left. + \left[\begin{bmatrix} T_{\beta_0} \end{bmatrix} \right]^T \{ r_p \} \right\} - \{ r_{IB} \} + \{ r_{IB} \} \quad (5-110) \end{aligned}$$

The i th station blade displacements, Y and Z , in blade coordinates for points on the blade both outboard and inboard of station X_{SW} are then defined.

5.5.5.6 Blade Element Y and Z Relative Velocities and Accelerations

The blade element coordinate axis system linear Y and Z velocities relative to the blade reference axis system can be found by differentiating the position equation with respect to time. Note that no distinction will be made at this point between outboard or inboard of station X_{SW} , but using the equation for displacements outboard of

this station and as discussed earlier, zeroing out certain terms, results in the equations for velocities or accelerations of points inboard of that station.

$$\begin{aligned}
 \left\{ \dot{r}_{BLE} \right\}_{BLn} = & \left[\dot{Z}'_{FA} \left[\left[\dot{T}_{Z,FA} \right]^T \left[T_{Y,FA} \right]^T \left[T_{\Delta\phi_F} \right]^T \left[T_{Y,FA} \right] \left[T_{Z,FA} \right] \right. \right. \\
 & + \left. \left[T_{Z,FA} \right]^T \left[T_{Y,FA} \right]^T \left[T_{\Delta\phi_F} \right]^T \left[T_{Y,FA} \right] \left[\dot{T}_{Z,FA} \right] \right] \\
 & + \dot{Y}'_{FA} \left[\left[T_{Z,FA} \right]^T \left[\dot{T}_{Y,FA} \right]^T \left[T_{\Delta\phi_F} \right]^T \left[T_{Y,FA} \right] \left[T_{Z,FA} \right] \right. \\
 & + \left. \left[T_{Z,FA} \right]^T \left[T_{Y,FA} \right]^T \left[T_{\Delta\phi_F} \right]^T \left[\dot{T}_{Y,FA} \right] \left[T_{Z,FA} \right] \right] \\
 & + \dot{\phi}_F \left[\left[T_{Z,FA} \right]^T \left[T_{Y,FA} \right] \left[\dot{T}_{\Delta\phi_F} \right] \left[T_{Y,FA} \right] \left[T_{Z,FA} \right] \right] \\
 & \cdot \left\{ \left[\frac{\partial r}{\partial A_n} \right] \left\{ A_{jn} \right\} \right\} + \left\{ \left[\left[T_{\beta_{FA}} \right]^T \left[T_{\phi_{REF}} \right]^T \left[T_{\beta_{FA}} \right] \right] \right. \\
 & \cdot \left\{ \left[\left[T_{\tau_O} \right]^T \left[T_Y \right]^T \right] \left\{ \left[T_{\beta_O} \right]^T \left\{ \left[T_{\phi_T} \right]^T \left\{ r_{CG} \right\} \right. \right. \right. \\
 & + \left. \left. \left\{ \left[T_{\phi_{TW}} \right]^T - \left[T_{\phi_T} \right]^T \right\} \left\{ r_{SC} \right\} \right\} - \left[T_{\beta_O} \right]^T \left\{ r_{SW} \right\} \right\} + \left\{ r_{Jog} \right\} \\
 & + \left. \left. \left. \left[T_{\epsilon_O} \right]^T \left\{ r_{SW} \right\} - \left[T_{\beta_O} \right]^T \left\{ r_P \right\} \right\} \right\} + \left\{ \left[T_{\beta_O} \right]^T \left\{ r_P \right\} \right. \right. \\
 & - \left. \left. \left. \left\{ r_{IB} \right\} \right\} \right\} \right\} + \left[\left[T_{Z,FA} \right]^T \left[T_{Y,FA} \right]^T \left[T_{\Delta\phi_F} \right]^T \left[T_{Y,FA} \right] \left[T_{Z,FA} \right] \right] \\
 & \cdot \left\{ \left\{ \left[\frac{\partial r}{\partial A_n} \right] \left\{ \dot{A}_{jn} \right\} \right\} + \left[\left[T_{\beta_{FA}} \right]^T \left[T_{\phi_{REF}} \right]^T \left[T_{\beta_{FA}} \right] \right] \left[\left[T_{\tau_O} \right]^T \left[T_Y \right]^T \right] \right. \\
 & \cdot \left. \left[T_{\beta_O} \right]^T \dot{\phi}_T \left[\dot{T}_{\phi_T} \right]^T \left\{ \left\{ r_{CG} \right\} - \left\{ r_{SC} \right\} \right\} \right\} - \left\{ \dot{r}_{IB} \right\} \right\} + \left\{ \dot{r}_{IB} \right\} \quad (5-111)
 \end{aligned}$$

Note in the above equation that the $\begin{bmatrix} \dot{T} \\ \dot{\zeta} \end{bmatrix}$ matrices are not time derivatives of the $\begin{bmatrix} T \\ \zeta \end{bmatrix}$ matrices but are derivatives of the transformation matrices with respect to the transformation angle ζ . This is arrived at by making the substitution that:

$$\frac{d}{dt} \begin{bmatrix} T \\ \zeta \end{bmatrix} = \frac{d\zeta}{dt} \begin{bmatrix} \frac{dT}{d\zeta} \\ 1 \end{bmatrix} = \dot{\zeta} \begin{bmatrix} \dot{T} \\ \dot{\zeta} \end{bmatrix} \quad (5-112)$$

and

$$\frac{d^2}{dt^2} \begin{bmatrix} T \\ \zeta \end{bmatrix} = \ddot{\zeta} \begin{bmatrix} \dot{T} \\ \dot{\zeta} \end{bmatrix} + \dot{\zeta}^2 \begin{bmatrix} \ddot{T} \\ \ddot{\zeta} \end{bmatrix} \quad (5-113)$$

Taking the time derivative again of Equation 5-111 yields the blade element Y and Z linear accelerations relative to the blade reference axis system.

$$\begin{aligned} \left\{ \ddot{r}_{BLE} \right\}_{BLn} = & \ddot{Z}'_{FA} \begin{bmatrix} \dot{T}_{Z,FA} \\ \dot{T}_{Y,FA} \end{bmatrix}^T \begin{bmatrix} T_{Y,FA} \\ T_{\Delta\phi_F} \end{bmatrix}^T \begin{bmatrix} T_{Y,FA} \\ T_{Z,FA} \end{bmatrix} \\ & + \begin{bmatrix} T_{Z,FA} \\ T_{Y,FA} \end{bmatrix}^T \begin{bmatrix} T_{Y,FA} \\ T_{\Delta\phi_F} \end{bmatrix}^T \begin{bmatrix} T_{Y,FA} \\ \dot{T}_{Z,FA} \end{bmatrix} \\ & + \ddot{Y}'_{FA} \begin{bmatrix} T_{Z,FA} \\ \dot{T}_{Y,FA} \end{bmatrix}^T \begin{bmatrix} T_{\Delta\phi_F} \\ T_{Y,FA} \end{bmatrix}^T \begin{bmatrix} T_{Y,FA} \\ T_{Z,FA} \end{bmatrix} \\ & + \begin{bmatrix} T_{Z,FA} \\ T_{Y,FA} \end{bmatrix}^T \begin{bmatrix} T_{Y,FA} \\ T_{\Delta\phi_F} \end{bmatrix}^T \begin{bmatrix} \dot{T}_{Y,FA} \\ T_{Z,FA} \end{bmatrix} \\ & + \ddot{\phi}_F \begin{bmatrix} T_{Z,FA} \\ T_{Y,FA} \end{bmatrix}^T \begin{bmatrix} \dot{T}_{\Delta\phi_F} \\ T_{Y,FA} \end{bmatrix}^T \begin{bmatrix} T_{Y,FA} \\ T_{Z,FA} \end{bmatrix} \\ & + \left(\dot{Z}'_{FA} \right)^2 \begin{bmatrix} \ddot{T}_{Z,FA} \\ T_{Y,FA} \end{bmatrix}^T \begin{bmatrix} T_{\Delta\phi_F} \\ T_{Y,FA} \end{bmatrix}^T \begin{bmatrix} T_{Y,FA} \\ T_{Z,FA} \end{bmatrix} \\ & + 2 \begin{bmatrix} \dot{T}_{Z,FA} \\ T_{Y,FA} \end{bmatrix}^T \begin{bmatrix} T_{\Delta\phi_F} \\ T_{Y,FA} \end{bmatrix}^T \begin{bmatrix} T_{Y,FA} \\ \dot{T}_{Z,FA} \end{bmatrix} \end{aligned}$$

$$\begin{aligned}
& + \begin{bmatrix} T_{Z,FA} \end{bmatrix}^T \begin{bmatrix} T_{Y,FA} \end{bmatrix}^T \begin{bmatrix} T_{\Delta\phi_F} \end{bmatrix}^T \begin{bmatrix} T_{Y,FA} \end{bmatrix} \begin{bmatrix} \ddot{T}_{Z,FA} \end{bmatrix} \\
& + \left(\dot{Y}_{FA} \right)^2 \left[\begin{bmatrix} T_{Z,FA} \end{bmatrix}^T \begin{bmatrix} \ddot{T}_{Y,FA} \end{bmatrix}^T \begin{bmatrix} T_{\Delta\phi_F} \end{bmatrix}^T \begin{bmatrix} T_{Y,FA} \end{bmatrix} \begin{bmatrix} T_{Z,FA} \end{bmatrix} \right. \\
& + 2 \begin{bmatrix} T_{Z,FA} \end{bmatrix}^T \begin{bmatrix} \dot{T}_{Y,FA} \end{bmatrix}^T \begin{bmatrix} T_{\Delta\phi_F} \end{bmatrix}^T \begin{bmatrix} \dot{T}_{Y,FA} \end{bmatrix} \begin{bmatrix} T_{Z,FA} \end{bmatrix} \\
& + \begin{bmatrix} T_{Z,FA} \end{bmatrix}^T \begin{bmatrix} T_{Y,FA} \end{bmatrix}^T \begin{bmatrix} T_{\Delta\phi_F} \end{bmatrix}^T \begin{bmatrix} \ddot{T}_{Y,FA} \end{bmatrix} \begin{bmatrix} T_{Z,FA} \end{bmatrix} \\
& + \left(\dot{\phi}_F \right)^2 \left[\begin{bmatrix} T_{Z,FA} \end{bmatrix}^T \begin{bmatrix} T_{Y,FA} \end{bmatrix}^T \begin{bmatrix} \ddot{T}_{\Delta\phi_F} \end{bmatrix}^T \begin{bmatrix} T_{Y,FA} \end{bmatrix} \begin{bmatrix} T_{Z,FA} \end{bmatrix} \right] \\
& + 2 \left(\dot{Z}_{FA} \right) \left(\dot{Y}_{FA} \right) \left[\begin{bmatrix} \dot{T}_{Z,FA} \end{bmatrix}^T \begin{bmatrix} \dot{T}_{Y,FA} \end{bmatrix}^T \begin{bmatrix} T_{\Delta\phi_F} \end{bmatrix}^T \begin{bmatrix} T_{Y,FA} \end{bmatrix} \begin{bmatrix} T_{Z,FA} \end{bmatrix} \right. \\
& + \begin{bmatrix} \dot{T}_{Z,FA} \end{bmatrix}^T \begin{bmatrix} T_{Y,FA} \end{bmatrix}^T \begin{bmatrix} T_{\Delta\phi_F} \end{bmatrix}^T \begin{bmatrix} \dot{T}_{Y,FA} \end{bmatrix} \begin{bmatrix} \dot{T}_{Z,FA} \end{bmatrix} \\
& + \begin{bmatrix} T_{Z,FA} \end{bmatrix}^T \begin{bmatrix} \dot{T}_{Y,FA} \end{bmatrix}^T \begin{bmatrix} T_{\Delta\phi_F} \end{bmatrix}^T \begin{bmatrix} T_{Y,FA} \end{bmatrix} \begin{bmatrix} \dot{T}_{Z,FA} \end{bmatrix} \\
& + \begin{bmatrix} T_{Z,FA} \end{bmatrix}^T \begin{bmatrix} T_{Y,FA} \end{bmatrix}^T \begin{bmatrix} T_{\Delta\phi_F} \end{bmatrix}^T \begin{bmatrix} \dot{T}_{Y,FA} \end{bmatrix} \begin{bmatrix} \dot{T}_{Z,FA} \end{bmatrix} \\
& + 2 \left(\dot{Z}_{FA} \right) \left(\dot{\phi}_F \right) \left[\begin{bmatrix} \dot{T}_{Z,FA} \end{bmatrix}^T \begin{bmatrix} T_{Y,FA} \end{bmatrix}^T \begin{bmatrix} \dot{T}_{\Delta\phi_F} \end{bmatrix}^T \begin{bmatrix} T_{Y,FA} \end{bmatrix} \begin{bmatrix} T_{Z,FA} \end{bmatrix} \right. \\
& + \begin{bmatrix} T_{Z,FA} \end{bmatrix}^T \begin{bmatrix} T_{Y,FA} \end{bmatrix}^T \begin{bmatrix} \dot{T}_{\Delta\phi_F} \end{bmatrix}^T \begin{bmatrix} T_{Y,FA} \end{bmatrix} \begin{bmatrix} \dot{T}_{Z,FA} \end{bmatrix} \\
& + 2 \left(\dot{Y}_{FA} \right) \left(\dot{\phi}_F \right) \left[\begin{bmatrix} T_{Z,FA} \end{bmatrix}^T \begin{bmatrix} \dot{T}_{Y,FA} \end{bmatrix}^T \begin{bmatrix} \dot{T}_{\Delta\phi_F} \end{bmatrix}^T \begin{bmatrix} T_{Y,FA} \end{bmatrix} \begin{bmatrix} T_{Z,FA} \end{bmatrix} \right. \\
& + \left. \left. \begin{bmatrix} T_{Z,FA} \end{bmatrix}^T \begin{bmatrix} T_{Y,FA} \end{bmatrix}^T \begin{bmatrix} \dot{T}_{\Delta\phi_F} \end{bmatrix}^T \begin{bmatrix} \dot{T}_{Y,FA} \end{bmatrix} \begin{bmatrix} T_{Z,FA} \end{bmatrix} \right] \left\{ \left[\frac{\partial \mathbf{r}}{\partial A_n} \right] \{ A_{jn} \} \right\}
\end{aligned}$$

$$\begin{aligned}
& + \left\{ \left[\begin{bmatrix} T_{\beta_{FA}} \end{bmatrix}^T \begin{bmatrix} T_{\phi_{REF}} \end{bmatrix}^T \begin{bmatrix} T_{\beta_{FA}} \end{bmatrix} \right] \left\{ \left[\begin{bmatrix} T_{\tau_0} \end{bmatrix}^T \begin{bmatrix} T_Y \end{bmatrix}^T \right] \left\{ \begin{bmatrix} T_{\beta_0} \end{bmatrix}^T \left\{ \begin{bmatrix} T_{\phi_T} \end{bmatrix}^T \right. \right. \right. \\
& \cdot \left. \left. \left. \begin{bmatrix} r_{CG} \end{bmatrix} \right\} + \left\{ \begin{bmatrix} T_{\phi_{TW}} \end{bmatrix}^T - \begin{bmatrix} T_{\phi_T} \end{bmatrix}^T \right\} \left\{ \begin{bmatrix} r_{SC} \end{bmatrix} \right\} \right\} - \begin{bmatrix} T_{\beta_0} \end{bmatrix}^T \left\{ \begin{bmatrix} r_{SW} \end{bmatrix} \right\} + \left\{ \begin{bmatrix} r_{Jog} \end{bmatrix} \right. \right. \\
& + \left. \left. \begin{bmatrix} T_{\beta_0} \end{bmatrix}^T \left\{ \begin{bmatrix} r_{SW} \end{bmatrix} \right\} - \begin{bmatrix} T_{\beta_0} \end{bmatrix}^T \left\{ \begin{bmatrix} r_P \end{bmatrix} \right\} \right\} \right\} + \left\{ \begin{bmatrix} T_{\beta_0} \end{bmatrix}^T \left\{ \begin{bmatrix} r_P \end{bmatrix} \right\} - \left\{ \begin{bmatrix} r_{IB} \end{bmatrix} \right\} \right\} \right\} \\
& + 2 \left[\dot{Z}'_{FA} \left[\begin{bmatrix} \dot{T}_{Z'_{FA}} \end{bmatrix}^T \begin{bmatrix} T_{Y'_{FA}} \end{bmatrix}^T \begin{bmatrix} T_{\Delta\phi_F} \end{bmatrix}^T \begin{bmatrix} T_{Y'_{FA}} \end{bmatrix} \begin{bmatrix} T_{Z'_{FA}} \end{bmatrix} \right. \right. \\
& + \left. \left. \begin{bmatrix} T_{Z'_{FA}} \end{bmatrix}^T \begin{bmatrix} T_{Y'_{FA}} \end{bmatrix}^T \begin{bmatrix} T_{\Delta\phi_F} \end{bmatrix}^T \begin{bmatrix} T_{Y'_{FA}} \end{bmatrix} \begin{bmatrix} \dot{T}_{Z'_{FA}} \end{bmatrix} \right] \\
& + \dot{Y}'_{FA} \left[\begin{bmatrix} T_{Z'_{FA}} \end{bmatrix}^T \begin{bmatrix} \dot{T}_{Y'_{FA}} \end{bmatrix}^T \begin{bmatrix} T_{\Delta\phi_F} \end{bmatrix}^T \begin{bmatrix} T_{Y'_{FA}} \end{bmatrix} \begin{bmatrix} T_{Z'_{FA}} \end{bmatrix} \right. \\
& + \left. \left. \begin{bmatrix} T_{Z'_{FA}} \end{bmatrix}^T \begin{bmatrix} T_{Y'_{FA}} \end{bmatrix}^T \begin{bmatrix} T_{\Delta\phi_F} \end{bmatrix}^T \begin{bmatrix} \dot{T}_{Y'_{FA}} \end{bmatrix} \begin{bmatrix} T_{Z'_{FA}} \end{bmatrix} \right] \\
& + \dot{\phi}_F \left[\begin{bmatrix} T_{Z'_{FA}} \end{bmatrix}^T \begin{bmatrix} T_{Y'_{FA}} \end{bmatrix}^T \begin{bmatrix} \dot{T}_{\Delta\phi_F} \end{bmatrix}^T \begin{bmatrix} T_{Y'_{FA}} \end{bmatrix} \begin{bmatrix} T_{Z'_{FA}} \end{bmatrix} \right] \\
& \cdot \left\{ \left(\left[\frac{\partial r}{\partial A_n} \right] \left\{ \dot{A}_{Jn} \right\} \right) + \left[\begin{bmatrix} T_{\beta_{FA}} \end{bmatrix}^T \begin{bmatrix} T_{\phi_{REF}} \end{bmatrix}^T \begin{bmatrix} T_{\beta_{FA}} \end{bmatrix} \right] \left[\begin{bmatrix} T_{\tau_0} \end{bmatrix}^T \begin{bmatrix} T_Y \end{bmatrix}^T \right] \right. \\
& \cdot \left. \begin{bmatrix} T_{\beta_0} \end{bmatrix}^T \left\{ \dot{\phi}_T \begin{bmatrix} \dot{T}_{\phi_T} \end{bmatrix}^T \left\{ \left\{ \begin{bmatrix} r_{CG} \end{bmatrix} \right\} - \left\{ \begin{bmatrix} r_{SC} \end{bmatrix} \right\} \right\} \right\} - \left\{ \dot{r}_{IB} \right\} \right\} \\
& + \left[\begin{bmatrix} T_{Z'_{FA}} \end{bmatrix}^T \begin{bmatrix} T_{Y'_{FA}} \end{bmatrix}^T \begin{bmatrix} T_{\Delta\phi_F} \end{bmatrix}^T \begin{bmatrix} T_{Y'_{FA}} \end{bmatrix} \begin{bmatrix} T_{Z'_{FA}} \end{bmatrix} \right] \left\{ \left(\left[\frac{\partial r}{\partial A_n} \right] \left\{ \ddot{A}_{Jn} \right\} \right) \right. \\
& + \left. \left[\begin{bmatrix} T_{\beta_{FA}} \end{bmatrix}^T \begin{bmatrix} T_{\phi_{REF}} \end{bmatrix}^T \begin{bmatrix} T_{\beta_{FA}} \end{bmatrix} \right] \left[\begin{bmatrix} T_{\tau_0} \end{bmatrix}^T \begin{bmatrix} T_Y \end{bmatrix}^T \right] \begin{bmatrix} T_{\beta_0} \end{bmatrix}^T \right. \\
& \cdot \left. \left\{ \ddot{\phi}_T \begin{bmatrix} \dot{T}_{\phi_T} \end{bmatrix}^T \left\{ \left\{ \begin{bmatrix} r_{CG} \end{bmatrix} \right\} - \left\{ \begin{bmatrix} r_{SC} \end{bmatrix} \right\} \right\} \right\} - \left\{ \ddot{r}_{IB} \right\} \right\} + \left\{ \ddot{r}_{IB} \right\} \quad (5-114)
\end{aligned}$$

These equations define the blade element relative displacement velocities and accelerations, respectively, required by the blade inertial velocity equations developed shortly. Note that in the preceding development these equations are written for the nth blade,

and with the exception of the $\left[\frac{\partial r}{\partial A_n} \right]$, $[T_{\beta_{FA}}]$, $[T_{\phi_{REF}}]$, $[T_{\tau_O}]$, $[T_Y]$, $[T_{\beta_O}]$, $[T_{\phi_{TW}}]$, $\{r_{SC}\}$, $\{r_{SW}\}$, $\{r_{jog}\}$, $\{r_p\}$, and $\{r_{CG}\}$ matrices, the terms are all blade dependent. Remember, also, that inboard of $\{r_{SW}\}$ the $[T_{\tau_O}]$ and $[T_Y]$ matrices are unit diagonal.

5.5.5.7 Blade Element Slopes

The blade element Y' and Z' slopes are determined by differentiating the deflection equation with respect to the nth blade radial distance, X_{BLn} . These formulations are used for quasi-static torsion formulation and output. Performing the required differentiation for points along the blade reference line:

$$\frac{\partial}{\partial X_{BLn}} \begin{Bmatrix} - \\ Y_{BLE} \\ Z_{BLE} \end{Bmatrix}_{BLn} = \begin{Bmatrix} - \\ Y'_{BLE} \\ Z'_{BLE} \end{Bmatrix}_{BLn} = \{r'_{BLE}\}_{BLn} \quad (5-115)$$

$$\begin{aligned} \{r'_{BLE}\}_{BLn} &= \begin{bmatrix} [T_{Z'_{FA}}]^T & [T_{Y'_{FA}}]^T & [T_{\Delta\phi_F}]^T & [T_{Y'_{FA}}] & [T_{Z'_{FA}}] \end{bmatrix} \left\{ \left[\frac{\partial r'}{\partial A_n} \right] \{A_{jn}\} \right\} \\ &+ \begin{bmatrix} [T_{\beta_{FA}}]^T & [T_{\phi_{REF}}]^T & [T_{\beta_{FA}}] & [T_{\tau_O}]^T & [T_Y]^T & [T_{\beta_O}]^T \end{bmatrix} \end{aligned} \quad (5-116)$$

5.5.5.8 Transformation from Blade-to-Blade Element Coordinates

In this section, the transformation matrix from blade (root) to i th blade element motions will be developed. Each blade will have its own transformation matrix for each i th blade station. The transformation matrix will initially be developed as the transform from blade element to blade coordinates, $\begin{bmatrix} T_{BLE-BLn} \end{bmatrix}$.

The transformation matrix, $\begin{bmatrix} T_{BLE-BLn} \end{bmatrix}$, can be developed by referring to the development of the deflection equations. The first rotation from blade element to blade coordinates is through the combined twist angle, $-\phi_T$; the second rotation is through the negative of the precone, β_0 ; the third through the negative of the sweep and droop angles, τ_0, γ ; the fourth through the feathering axis angle, β_{FA} ; the fifth through the negative of the reference feathering angles ϕ_{REF} ; and the sixth back through the negative of the feathering axis precone angle, β_{FA} .

These rotations then define the transformation from blade element to blade coordinates, including the effects of the static shape of the blade, pretwist, precone, sweep, droop, etc. Also included is the effect of blade elastic twist. Again note that for stations inboard of Station X_{SW} , the sweep and droop angles, τ_0 and γ , respectively, must be set to zero in the formulation of the transformation matrix as in the definition of the blade displacements and blade slopes. This portion of the transformation matrix which includes the static blade shape and combined twist is defined as follows:

$$\begin{bmatrix} T_{BLE-BLn} \end{bmatrix}_S = \begin{bmatrix} \begin{bmatrix} T_{\beta_{FA}} \end{bmatrix}^T \begin{bmatrix} T_{\phi_{REF}} \end{bmatrix}^T \begin{bmatrix} T_{\beta_{FA}} \end{bmatrix} \end{bmatrix} \begin{bmatrix} \begin{bmatrix} T_{\tau_0} \end{bmatrix}^T \begin{bmatrix} T_{\gamma} \end{bmatrix}^T \begin{bmatrix} T_{\beta_0} \end{bmatrix}^T \begin{bmatrix} T_{\phi_T} \end{bmatrix}^T \end{bmatrix} \quad (5-117)$$

The next two rotations from blade element to blade coordinates are due to the elastic blade bending slopes. Since Y'_{BEND} and Z'_{BEND} are motions of the blade elements with respect to the blade, then to transform from blade element to blade coordinates requires negative rotations of Y'_{BEND} and Z'_{BEND} to be included. Finally, the blade

feathering rotation from the reference feather angle must be included. The final transformation then, from blade element to blade coordinates, is defined by the following equation:

$$\begin{aligned} \left[T_{BLE-BLn} \right] &= \left[T_{Z', FA} \right]^T \left[T_{Y', FA} \right]^T \left[T_{\Delta\phi_F} \right]^T \left[T_{\tau', FA} \right] \left[T_{Z', FA} \right] \left[T_{Z', BEND} \right]^T \left[T_{Y', BEND} \right]^T \\ &\cdot \left[T_{\beta_{FA}} \right]^T \left[T_{\phi_{REF}} \right]^T \left[T_{\beta_{FA}} \right] \left[T_{\tau_0} \right]^T \left[T_Y \right]^T \left[T_{\beta_0} \right]^T \left[T_{\phi_T} \right]^T \end{aligned} \quad (5-118)$$

where

$$\left[T_{Z', BEND} \right] = \begin{bmatrix} \cos(Z'_{BEND}) & 0 & \sin(Z'_{BEND}) \\ 0 & 1 & 0 \\ -\sin(Z'_{BEND}) & 0 & \cos(Z'_{BEND}) \end{bmatrix} \quad (5-119)$$

and

$$\left[T_{Y', BEND} \right] = \begin{bmatrix} \cos(Y'_{BEND}) & \sin(Y'_{BEND}) & 0 \\ -\sin(Y'_{BEND}) & \cos(Y'_{BEND}) & 0 \\ 0 & 0 & 1 \end{bmatrix} \quad (5-120)$$

and again where

$$\left[T_{\tau_0} \right]^T \left[T_Y \right]^T = \left[I \right] \quad (5-121)$$

inboard of Station X_{SW} .

Also:

$$\begin{Bmatrix} Y'_{BEND} \\ Z'_{BEND} \end{Bmatrix} = \begin{bmatrix} Y_1' & Y_2' & Y_3' \\ Z_1' & Z_2' & Z_3' \end{bmatrix} \begin{Bmatrix} A_{1n} \\ A_{2n} \\ A_{3n} \end{Bmatrix} \quad (5-122)$$

The inverse or transpose of this equation yields the transformation from blade to blade element coordinates, or:

$$\begin{aligned} [T_{BLn-BLE}] &= [T_{BLE-BLn}]^T \\ &= [T_{\phi_T}] [T_{\beta_0}] [T_Y] [T_{\tau_0}] [T_{\beta_{FA}}]^T [T_{\phi_{REF}}] [T_{\beta_{FA}}] \\ &\quad \cdot [T_{Y'_{BEND}}] [T_{Z'_{BEND}}] [T_{Z'_{FA}}]^T [T_{Y'_{FA}}]^T [T_{\Delta\phi_F}] [T_{Y'_{FA}}] [T_{Z'_{FA}}] \end{aligned} \quad (5-123)$$

again where

$$\begin{bmatrix} T_Y \\ T_{\tau_0} \end{bmatrix} = [I] \quad (5-124)$$

inboard of station X_{SW} .

5.5.5.9 Blade Element Angular Velocities and Accelerations

From the foregoing discussion, the blade element angular velocity vector can be determined. Starting with the angular velocities $(p, q, r)_{BLn}$ of the blade reference axis system and systematically and progressively transforming these velocities through each axis rotation and adding the respective angular velocity associated with

each of the indicated angular rotations, results in the following equation for the blade element angular velocities.

$$\begin{aligned} \left\{ \begin{matrix} p \\ q \\ r \end{matrix} \right\}_{BLE} &= \left\{ \begin{matrix} \dot{\phi}_T \\ 0 \\ 0 \end{matrix} \right\} + [T_{\phi_T}] [T_{\beta_O}] [T_Y] [T_{\tau_O}] [T_{\beta_{FA}}]^T [T_{\phi_{REF}}] [T_{\beta_{FA}}] \left\{ \begin{matrix} 0 \\ 0 \\ \dot{Y}'_{BEND} \end{matrix} \right\} \\ &+ [T_{Y'_{BEND}}] \left\{ \begin{matrix} 0 \\ -\dot{Z}'_{BEND} \\ 0 \end{matrix} \right\} + [T_{Z'_{BEND}}] \left\{ \begin{matrix} 0 \\ \dot{Z}'_{FA} \\ 0 \end{matrix} \right\} \\ &+ [T_{Z'_{FA}}]^T \left\{ \begin{matrix} 0 \\ 0 \\ -\dot{Y}'_{FA} \end{matrix} \right\} + [T_{Y'_{FA}}]^T \left\{ \begin{matrix} \dot{\phi}_F \\ 0 \\ 0 \end{matrix} \right\} + [T_{\Delta\phi_F}] \left\{ \begin{matrix} 0 \\ 0 \\ Y'_{FA} \end{matrix} \right\} \\ &+ [T_{Y'_{FA}}] \left\{ \begin{matrix} 0 \\ -\dot{Z}'_{FA} \\ 0 \end{matrix} \right\} + [T_{Z'_{FA}}] \left\{ \begin{matrix} p \\ q \\ r \end{matrix} \right\}_{BLn} \Bigg\} \quad (5-125) \end{aligned}$$

Note that in this equation, starting on the right-hand side with the quantities in the innermost brackets, the blade reference system angular velocities are first transformed through the increment of feathering axis flapping slope due to bending, Z'_{FA} , and then the feathering axis flapping angular velocity, $-Z'_{FA}$, is added. Minus is used since Z' is a negative θ rotation. Next, the resultant W vector is transformed through Y'_{FA} and Y'_{FA} is added. This is then transformed through the delta feathering angle, $\Delta\phi_F$, and the

feathering angular velocity, $\dot{\phi}_F$, is added. This is then transformed back through the increments of feathering axis slopes due to blade bending, giving the vector:

$$\begin{aligned} & \begin{Bmatrix} 0 \\ \dot{Z}'_{FA} \\ 0 \end{Bmatrix} + [T_{Z'_{FA}}]^T \begin{Bmatrix} 0 \\ 0 \\ -\dot{Y}'_{FA} \end{Bmatrix} + [T_{Y'_{FA}}]^T \begin{Bmatrix} \dot{\phi}_F \\ 0 \\ 0 \end{Bmatrix} + [T_{\Delta\phi_F}] \begin{Bmatrix} 0 \\ 0 \\ \dot{Y}'_{FA} \end{Bmatrix} \\ & + [T_{Y'_{FA}}] \begin{Bmatrix} 0 \\ -\dot{Z}'_{FA} \\ 0 \end{Bmatrix} + [T_{Z'_{FA}}] \begin{Bmatrix} p \\ q \\ r \end{Bmatrix}_{BLn} \cdot \cdot \cdot \end{aligned} \quad (5-126)$$

which represents the blade element angular velocities due to combined blade feathering and blade reference axis system angular velocities.

Next, the effects of blade bending at each blade station are introduced. The above vector is first transformed through the local blade element flapwise bending slope, Z'_{BEND} , and then the angular velocity, $-Z'_{BEND}$, is added. This result is transformed through the blade element inplane bending slope, Y'_{BEND} , and the inplane angular velocity due to blade bending, Y'_{BEND} , is added, resulting in the total vector less the initial transformation string. This vector then represents the blade element angular velocities due to the combined effects of the blade reference axis system angular velocities of the blade feathering angle and of the blade angular velocities due to blade elastic bending. The remaining transformations then include the static effects of the blade feathering axis precone, β_{FA} , the blade reference feathering angle, ϕ_{REF} , blade sweep, τ_0 , blade droop, γ , and blade or hub precone, β_0 , and the combined effect of blade static and elastic twist, represented by ϕ_T . Finally, the blade elastic twist angular velocity, $\dot{\phi}_T$, is

added, giving the total blade element angular velocities, $\begin{Bmatrix} p \\ q \\ r \end{Bmatrix}_{BLE}$.

Also note, as indicated before, the matrix $\begin{bmatrix} T_Y \end{bmatrix} \begin{bmatrix} T_{\tau_0} \end{bmatrix}$ has the value calculated if X is greater than X_{SW} and has the value of unity if X is inboard of station X_{SW} .

At this point it has been assumed that the contributions of \dot{Y}'_{FA}

and \dot{Z}'_{FA} are small compared to the other contributions to $\begin{Bmatrix} p \\ q \\ r \end{Bmatrix}_{BLE}$.

This assumption is supported by referring to the final form of the above development. First of all, both of these vectors are small

compared to $\begin{Bmatrix} p \\ q \\ r \end{Bmatrix}_{BLn}$, which is fundamentally the rotational speed

of the rotor. Also, both of the feathering axis flapping and inplane angular velocities are first added and then transformed through the delta feathering angle and then subtracted, meaning that fundamentally the principal magnitude or component contributions due to \dot{Y}'_{FA} and \dot{Z}'_{FA} are self-cancelling.

With the above assumption:

$$\begin{aligned} \begin{Bmatrix} p \\ q \\ r \end{Bmatrix}_{BLE} &= \begin{Bmatrix} \dot{\phi}_T \\ 0 \\ 0 \end{Bmatrix} + \begin{bmatrix} T_{\phi_T} \end{bmatrix} \begin{bmatrix} R \end{bmatrix}^T \begin{Bmatrix} 0 \\ 0 \\ \dot{Y}'_{BEND} \end{Bmatrix} + \begin{bmatrix} T_{Y', BEND} \end{bmatrix} \begin{Bmatrix} 0 \\ -\dot{Z}'_{BEND} \\ 0 \end{Bmatrix} \\ &+ \begin{bmatrix} T_{Z', BEND} \end{bmatrix} \left\{ \begin{bmatrix} T_{Z', FA} \end{bmatrix}^T \begin{bmatrix} T_{Y', FA} \end{bmatrix}^T \begin{Bmatrix} \dot{\phi}_F \\ 0 \\ 0 \end{Bmatrix} \right. \\ &\left. + \begin{bmatrix} T_{\Delta\phi_F} \end{bmatrix} \left\{ \begin{bmatrix} T_{Y', FA} \end{bmatrix} \begin{bmatrix} T_{Z', FA} \end{bmatrix} \begin{Bmatrix} p \\ q \\ r \end{Bmatrix}_{BLn} \right\} \right\} \end{aligned} \quad (5-127)$$

where:

$$\begin{bmatrix} R \end{bmatrix}^T = \begin{bmatrix} T_{\beta_0} \end{bmatrix} \begin{bmatrix} T_Y \end{bmatrix} \begin{bmatrix} T_{\tau_0} \end{bmatrix} \begin{bmatrix} T_{\beta_{FA}} \end{bmatrix}^T \begin{bmatrix} T_{\phi_{REF}} \end{bmatrix} \begin{bmatrix} T_{\beta_{FA}} \end{bmatrix} \quad (5-128)$$

and:

$$\begin{Bmatrix} \dot{Y}'_{BEND} \\ \dot{Z}'_{BEND} \end{Bmatrix} = \begin{bmatrix} Y_1' & Y_2' & Y_3' \\ Z_1' & Z_2' & Z_3' \end{bmatrix} \begin{Bmatrix} \dot{A}_{1n} \\ \dot{A}_{2n} \\ \dot{A}_{3n} \end{Bmatrix} \quad (5-129)$$

The blade element angular accelerations can now be determined by differentiating this equation with respect to time. Again, as in the case of the angular velocities, the contributions due to time derivatives of the feathering axis flapping and inplane slope changes due to bending are neglected. With this assumption, the time derivative is:

$$\begin{aligned} \begin{Bmatrix} \dot{p} \\ \dot{q} \\ \dot{r} \end{Bmatrix}_{BLE} &= \begin{Bmatrix} \ddot{\phi}_T \\ 0 \\ 0 \end{Bmatrix} + \dot{\phi}_T \begin{bmatrix} \dot{T}_{\phi_T} \end{bmatrix} \begin{bmatrix} R \end{bmatrix}^T \begin{Bmatrix} 0 \\ 0 \\ \dot{Y}'_{BEND} \end{Bmatrix} + \begin{bmatrix} T_{Y', BEND} \end{bmatrix} \begin{Bmatrix} 0 \\ -\dot{Z}'_{BEND} \\ 0 \end{Bmatrix} \\ &+ \begin{bmatrix} T_{Z', BEND} \end{bmatrix} \left\{ \begin{bmatrix} T_{Z', FA} \end{bmatrix}^T \begin{bmatrix} T_{Y', FA} \end{bmatrix}^T \begin{Bmatrix} \ddot{\phi}_F \\ 0 \\ 0 \end{Bmatrix} + \begin{bmatrix} T_{\Delta\phi_F} \end{bmatrix} \begin{bmatrix} T_{Y', FA} \end{bmatrix} \begin{bmatrix} T_{Z', FA} \end{bmatrix} \right. \\ &\cdot \left. \begin{Bmatrix} p \\ q \\ r \end{Bmatrix}_{BLn} \right\} + \begin{bmatrix} T_{\phi_T} \end{bmatrix} \begin{bmatrix} R \end{bmatrix}^T \begin{Bmatrix} 0 \\ 0 \\ \ddot{Y}'_{BEND} \end{Bmatrix} + \dot{Y}'_{BEND} \begin{bmatrix} \dot{T}_{Y', BEND} \end{bmatrix} \\ &\cdot \left\{ \begin{Bmatrix} 0 \\ -\dot{Z}'_{BEND} \\ 0 \end{Bmatrix} + \begin{bmatrix} T_{Z', BEND} \end{bmatrix} \begin{bmatrix} T_{Z', FA} \end{bmatrix}^T \begin{bmatrix} T_{Y', FA} \end{bmatrix}^T \begin{Bmatrix} \dot{\phi}_F \\ 0 \\ 0 \end{Bmatrix} \right\} \end{aligned}$$

$$\begin{aligned}
& + \left[T_{\Delta\phi_F} \right] \left\{ \left[T_{Y', FA} \right] \left[T_{Z', FA} \right] \begin{Bmatrix} p \\ q \\ r \end{Bmatrix}_{BLn} \right\} \left\{ \right\} \left\{ \right\} \left\{ \right\} + \left[T_{Y', BEND} \right] \left\{ \begin{Bmatrix} 0 \\ -\ddot{Z}'_{BEND} \\ 0 \end{Bmatrix} \right\} \\
& + \dot{Z}'_{BEND} \left[\dot{T}_{Z', BEND} \right] \left\{ \left[T_{Z', FA} \right]^T \left[T_{Y', FA} \right]^T \begin{Bmatrix} \dot{\phi}_F \\ 0 \\ 0 \end{Bmatrix} \right\} \\
& + \left[T_{\Delta\phi_F} \right] \left\{ \left[T_{Y', FA} \right] \left[T_{Z', FA} \right] \begin{Bmatrix} p \\ q \\ r \end{Bmatrix}_{BLn} \right\} \left\{ \right\} \left\{ \right\} \\
& + \left[T_{Z', BEND} \right] \left\{ \left[T_{Z', FA} \right]^T \left[T_{Y', FA} \right]^T \begin{Bmatrix} \ddot{\phi}_F \\ 0 \\ 0 \end{Bmatrix} \right\} \\
& + \dot{\phi}_F \left[\dot{T}_{\Delta\phi_F} \right] \left\{ \left[T_{Y', FA} \right] \left[T_{Z', FA} \right] \begin{Bmatrix} p \\ q \\ r \end{Bmatrix}_{BLn} \right\} \\
& + \left[T_{\Delta\phi_F} \right] \left\{ \left[T_{Y', FA} \right] \left[T_{Z', FA} \right] \begin{Bmatrix} \dot{p} \\ \dot{q} \\ \dot{r} \end{Bmatrix}_{BLn} \right\} \left\{ \right\} \left\{ \right\} \left\{ \right\} \left\{ \right\}
\end{aligned} \tag{5-130}$$

where:

$$\begin{Bmatrix} \ddot{Y}'_{BEND} \\ \ddot{Z}'_{BEND} \end{Bmatrix} = \begin{bmatrix} Y_1' & Y_2' & Y_3' \\ Z_1' & Z_2' & Z_3' \end{bmatrix} \begin{Bmatrix} \ddot{A}_{1n} \\ \ddot{A}_{2n} \\ \ddot{A}_{3n} \end{Bmatrix} \tag{5-131}$$

5.5.5.10 Blade Element X Motions

In the previous development, the equations did not account for the blade element displacement, velocity, and acceleration in the spanwise direction. The method used to define these is one of finding the neutral axis as the axis of no stretch and determining the projection of this axis onto the X-axis as the blade bends. This projection, then, is the spanwise or X location of the neutral axis in blade coordinates. The rate of change of this projection is the spanwise relative velocity and the second rate of change is the spanwise relative acceleration of the blade element neutral axis location or point. The motions are then transformed to the center of gravity to obtain the spanwise motion of the origin of the blade element reference axis.

In Figure 5-26, the deflected neutral axis is shown as a function of blade radius. The (i-1) and ith station are shown. It can be seen from this figure that as $X_{NA}(i-1)$ approaches $X_{NA}(i)$, then the delta length of the blade $(S_{NA}(i) - S_{NA}(i-1))$, can be written as:

$$\begin{aligned} (S_{NA}(i) - S_{NA}(i-1))^2 &= (X_{NA}(i) - X_{NA}(i-1))_{BLn}^2 + (Y_{NA}(i) - Y_{NA}(i-1))_{BLn}^2 \\ &\quad + (Z_{NA}(i) - Z_{NA}(i-1))_{BLn}^2 \end{aligned} \quad (5-132)$$

Rearranging this equation and summing from the blade root to the kth blade station yields:

$$\begin{aligned} X_{NA}(k) &= \sum_{i=1}^k (X_{NA}(i) - X_{NA}(i-1))_{BLn} = \sum_{i=1}^k \left[(S_{NA}(i) - S_{NA}(i-1))^2 \right. \\ &\quad \left. - (Y_{NA}(i) - Y_{NA}(i-1))_{BLn}^2 - (Z_{NA}(i) - Z_{NA}(i-1))_{BLn}^2 \right]^{1/2} \end{aligned} \quad (5-133)$$

where for $i=1$,

$$S_{NA}(1) = Y_{NA}(1) = Z_{NA}(1) = X_{NA}(1) = 0 \quad (5-134)$$

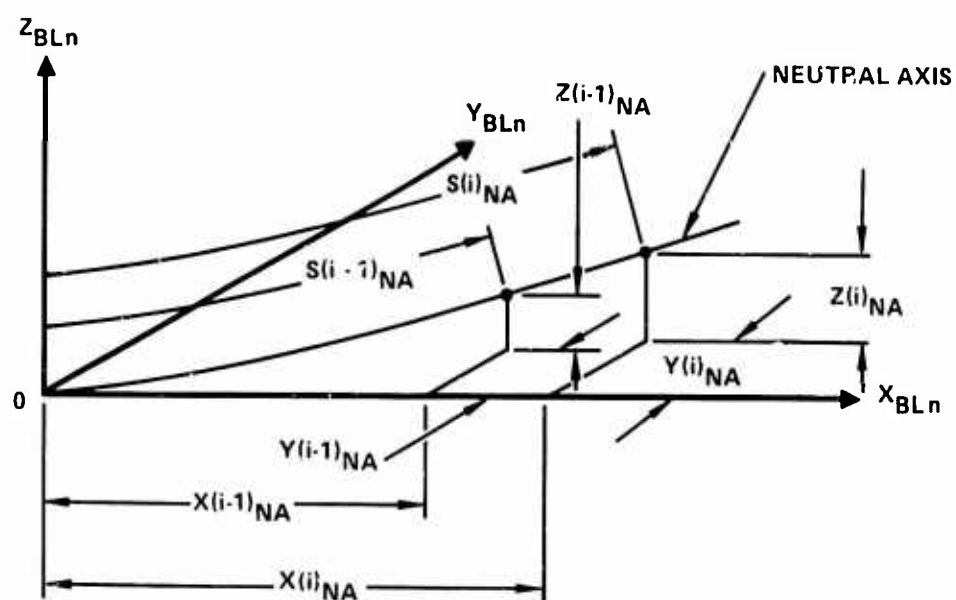


Figure 5-26. Neutral Axis vs Blade Radius

Likewise,

$$X_{NA_BLn}^{(1)} = \dot{X}_{NA_BLn}^{(1)} = \ddot{X}_{NA_BLn}^{(1)} = 0 \quad (5-135)$$

$S_{NA}(i)$ is simply the blade length to the i th station measured along the neutral axis and $Y_{NA_BLn}(i)$ and $Z_{NA_BLn}(i)$ are the Y and Z locations

of the neutral axis in the blade coordinate axis system for the n th blade. These displacements, along with their derivatives, will be defined later. First, however, by taking the first and second time derivative of X equation, the spanwise velocities and accelerations of the blade element neutral axis point are determined and are given by the following two equations.

$$\dot{X}_{NA_BLn}^{(k)} = \sum_{i=1}^k \left[\frac{-\left(Y_{NA}(i) - Y_{NA}(i-1)\right)_{BLn} \left(\dot{Y}_{NA}(i) - \dot{Y}_{NA}(i-1)\right)_{BLn}}{\left(X_{NA}(i) - X_{NA}(i-1)\right)_{BLn}} - \frac{\left(Z_{NA}(i) - Z_{NA}(i-1)\right)_{BLn} \left(\dot{Z}_{NA}(i) - \dot{Z}_{NA}(i-1)\right)_{BLn}}{\left(X_{NA}(i) - X_{NA}(i-1)\right)_{BLn}} \right] \quad (5-136)$$

$$\begin{aligned}
\ddot{X}_{NA}^{(k)} = \sum_{i=1}^k & \left[\frac{-\left(\dot{Y}_{NA}(i) - \dot{Y}_{NA}(i-1)\right)_{BLn}^2 - \left(\dot{Z}_{NA}(i) - \dot{Z}_{NA}(i-1)\right)_{BLn}^2}{\left(X_{NA}(i) - X_{NA}(i-1)\right)_{BLn}} \right. \\
& - \frac{\left(Y_{NA}(i) - Y_{NA}(i-1)\right)_{BLn} \left(\ddot{Y}_{NA}(i) - \ddot{Y}_{NA}(i-1)\right)_{BLn}}{\left(X_{NA}(i) - X_{NA}(i-1)\right)_{BLn}} \\
& - \frac{\left(Z_{NA}(i) - Z_{NA}(i-1)\right)_{BLn} \left(\ddot{Z}_{NA}(i) - \ddot{Z}_{NA}(i-1)\right)_{BLn}}{\left(X_{NA}(i) - X_{NA}(i-1)\right)_{BLn}} \\
& - \frac{\left[\left(Y_{NA}(i) - Y_{NA}(i-1)\right)_{BLn} \left(\dot{Y}_{NA}(i) - \dot{Y}_{NA}(i-1)\right)_{BLn} \right.}{\left(X_{NA}(i) - X_{NA}(i-1)\right)_{BLn}^3} \\
& \left. \left. + \left(Z_{NA}(i) - Z_{NA}(i-1)\right)_{BLn} \left(\dot{Z}_{NA}(i) - \dot{Z}_{NA}(i-1)\right)_{BLn} \right]^2}{\left(X_{NA}(i) - X_{NA}(i-1)\right)_{BLn}^3} \right] \quad (5-137)
\end{aligned}$$

If $Y_{ONA}(i)$ is the distance along the i th blade element chord line from the blade element reference axis origin or center of gravity to the blade element neutral axis, then the blade element neutral axis motions can be written in terms of the blade element motions as:

$$\begin{Bmatrix} \Delta X_{NA}(i) \\ Y_{NA}(i) \\ Z_{NA}(i) \end{Bmatrix}_{BLn} = \begin{Bmatrix} 0 \\ Y_{BLE}(i) \\ Z_{BLE}(i) \end{Bmatrix}_{BLn} + \begin{bmatrix} T_{BLE-BLn} \end{bmatrix} \begin{Bmatrix} 0 \\ Y_{ONA}(i) \\ 0 \end{Bmatrix}_{BLE} \quad (5-138)$$

Referring to Section 5.5, the time derivative of the above equation is:

$$\begin{Bmatrix} \Delta \dot{X}_{NA}(i) \\ \dot{Y}_{NA}(i) \\ \dot{Z}_{NA}(i) \end{Bmatrix}_{BLn} = \begin{Bmatrix} 0 \\ \dot{Y}_{BLE}(i) \\ \dot{Z}_{BLE}(i) \end{Bmatrix}_{BLn} + \begin{bmatrix} T_{BLE-BLn} \end{bmatrix} \begin{Bmatrix} -r_{BLE}^{Y_{ONA}} \\ 0 \\ p_{BLE}^{Y_{ONA}} \end{Bmatrix}_{BLE(i)} \quad (5-139)$$

and likewise, the second time derivative is:

$$\begin{Bmatrix} \Delta \ddot{X}_{NA}(i) \\ \ddot{Y}_{NA}(i) \\ \ddot{Z}_{NA}(i) \end{Bmatrix}_{BLn} = \begin{Bmatrix} 0 \\ \ddot{Y}_{NA}(i) \\ \ddot{Z}_{NA}(i) \end{Bmatrix}_{BLn} + \begin{bmatrix} T_{BLE-BLn} \end{bmatrix} \begin{Bmatrix} (p_{BLE} q_{BLE} - \dot{r}_{BLE})^{Y_{ONA}} \\ (-r_{BLE}^2 - p_{BLE}^2)^{Y_{ONA}} \\ (q_{BLE} r_{BLE} + p_{BLE})^{Y_{ONA}} \end{Bmatrix}_{BLE(i)} \quad (5-140)$$

These three equations, then, define the Y and Z displacements, velocities, and accelerations of the neutral axis point used in the X equations and time derivatives. Also, the increments of spanwise motions due to the offset between the center of gravity and neutral axis are defined by these same three equations. This increment represents the motion of the neutral axis relative to the blade reference axis origin, therefore, the span motion at the center of gravity is determined by subtracting $\Delta X_{NA_{BLn}}(i)$ from the spanwise motion of the neutral axis, or:

$$X_{BLE_{BLn}}(i) = X_{NA_{BLn}}(i) - \Delta X_{NA_{BLn}}(i) \quad (5-141)$$

$$\dot{X}_{BLE_{BLn}}(i) = \dot{X}_{NA_{BLn}}(i) - \dot{\Delta X}_{NA_{BLn}}(i) \quad (5-142)$$

$$\ddot{X}_{BLE_{BLn}}(i) = \ddot{X}_{NA_{BLn}}(i) - \ddot{\Delta X}_{NA_{BLn}}(i) \quad (5-143)$$

These equations, then, along with the previous expressions for X and Z, define the blade element relative displacement, velocity, and acceleration vectors required for the total inertial vectors which follow.

5.5.5.11 Blade Motion in Absolute Coordinates

To this point the blade element motion has been defined in terms of the blade axis or relative coordinates. The elements defined are:

$$\text{blade element relative displacements} \quad \left\{ \begin{array}{c} X_{BLE}^{(i)} \\ Y_{BLE}^{(i)} \\ Z_{BLE}^{(i)} \end{array} \right\}_{BLn} \quad (5-144)$$

$$\text{blade element relative velocities} \quad \left\{ \begin{array}{c} \dot{X}_{BLE}^{(i)} \\ \dot{Y}_{BLE}^{(i)} \\ \dot{Z}_{BLE}^{(i)} \end{array} \right\}_{BLn} \quad (5-145)$$

$$\text{and blade element relative accelerations} \quad \left\{ \begin{array}{c} \ddot{X}_{BLE}^{(i)} \\ \ddot{Y}_{BLE}^{(i)} \\ \ddot{Z}_{BLE}^{(i)} \end{array} \right\}_{BLn} \quad (5-146)$$

Using the method of Section 5.4.1, expressions in freestream (absolute) coordinates can be written for use in the equations of motion. The blade element velocity becomes:

$$\left\{ \begin{array}{c} X_{BLE}^{(i)} \\ Y_{BLE}^{(i)} \\ Z_{BLE}^{(i)} \end{array} \right\}_{BLn}^I = \left\{ \begin{array}{c} X_{OBLn} \\ Y_{OBLn} \\ Z_{OBLn} \end{array} \right\}_{BLn}^I + \left\{ \begin{array}{c} X_{BLE}^{(i)} \\ Y_{BLE}^{(i)} \\ Z_{BLE}^{(i)} \end{array} \right\}_{BLn} + \begin{bmatrix} 0 & -r & q \\ r & 0 & -p \\ -q & p & 0 \end{bmatrix} \left\{ \begin{array}{c} X_{BLE}^{(i)} \\ Y_{BLE}^{(i)} \\ Z_{BLE}^{(i)} \end{array} \right\}_{BLn} \quad (5-147)$$

The blade element accelerations are:

$$\begin{aligned}
 \begin{Bmatrix} \ddot{x}_{BLE(i)} \\ \ddot{y}_{BLE(i)} \\ \ddot{z}_{BLE(i)} \end{Bmatrix}_{BLn}^I &= \begin{Bmatrix} \ddot{x}_{OBLn} \\ \ddot{y}_{OBLn} \\ \ddot{z}_{OBLn} \end{Bmatrix}_{BLn}^I + \begin{Bmatrix} \ddot{x}_{BLE(i)} \\ \ddot{y}_{BLE(i)} \\ \ddot{z}_{BLE(i)} \end{Bmatrix}_{BLn} \\
 &+ \begin{bmatrix} 0 & -\dot{r} & \dot{q} \\ \dot{r} & 0 & -\dot{p} \\ -\dot{q} & \dot{p} & 0 \end{bmatrix}_{BLn} \begin{Bmatrix} x_{BLE(i)} \\ y_{BLE(i)} \\ z_{BLE(i)} \end{Bmatrix}_{BLn} \\
 &+ \begin{bmatrix} 0 & -r & q \\ r & 0 & -p \\ -q & p & 0 \end{bmatrix}_{BLn} \begin{bmatrix} 0 & -\dot{r} & \dot{q} \\ r & 0 & -\dot{p} \\ -q & p & 0 \end{bmatrix}_{BLn} \begin{Bmatrix} x_{BLE(i)} \\ y_{BLE(i)} \\ z_{BLE(i)} \end{Bmatrix}_{BLn} \\
 &+ 2 \begin{bmatrix} 0 & -r & q \\ r & 0 & -p \\ -q & p & 0 \end{bmatrix}_{BLn} \begin{Bmatrix} \dot{x}_{BLE} \\ \dot{y}_{BLE} \\ \dot{z}_{BLE} \end{Bmatrix}_{BLn} \quad (5-148)
 \end{aligned}$$

where

$$\begin{Bmatrix} \ddot{x}_0 \\ \ddot{y}_0 \\ \ddot{z}_0 \end{Bmatrix}_{BLn} , \quad \begin{Bmatrix} \dot{x}_0 \\ \dot{y}_0 \\ \dot{z}_0 \end{Bmatrix}_{BLn} , \quad (5-149)$$

and matching rotation terms are defined in Section 5.5.4 in terms of rotor axis terms which are in turn related to the principal (hub) reference axis.

5.5.6 Swashplate Motion

As shown in Figure 5-9, the swashplate reference axis system is defined with the Z-axis down. The motion of the swashplate reference system is defined by three generalized coordinate displacements, Z_{SP} , ϕ_{SP} , and θ_{SP} , which move relative to the hub or principal reference axis system.

The rotations ϕ_{SP} and θ_{SP} are taken in the same order as shown in Figure 5-17 and therefore, from Section 5.4.3 the angular velocities are:

$$\begin{aligned} \begin{Bmatrix} p \\ q \\ r \end{Bmatrix}_{SP_R} &= \begin{Bmatrix} 0 \\ 0 \\ \dot{\psi}_{SP} \end{Bmatrix} + \begin{bmatrix} \cos\psi & \sin\psi & 0 \\ -\sin\psi & \cos\psi & 0 \\ 0 & 0 & 1 \end{bmatrix} \begin{Bmatrix} 0 \\ \dot{\theta}_{SP} \\ 0 \end{Bmatrix} \\ &+ \begin{bmatrix} \cos\theta_{SP} & 0 & -\sin\theta_{SP} \\ 0 & 1 & 0 \\ \sin\theta_{SP} & 0 & \cos\theta_{SP} \end{bmatrix} \begin{Bmatrix} \dot{\phi}_{SP} \\ 0 \\ 0 \end{Bmatrix} \\ &+ \begin{bmatrix} 1 & 0 & 0 \\ 0 & \cos\phi_{SP} & \sin\phi_{SP} \\ 0 & -\sin\phi_{SP} & \cos\phi_{SP} \end{bmatrix} \begin{Bmatrix} p \\ q \\ r \end{Bmatrix}_H \end{aligned} \quad (5-150)$$

Where $\dot{\psi}_{SP}$ is the rotational speed of the swashplate, and

$$\dot{\psi}_{SP} = -\dot{\psi}_R \quad (5-151)$$

where $\dot{\psi}_R$ is the rotational speed of the rotor.

As indicated before, the swashplate axes do not rotate at the rotational speed $\dot{\psi}_{SP}$. However, the total angular velocities reflect the rotational

rate $\dot{\psi}_{SP}$. Therefore, the total angular rates of the swashplate in swashplate axes are obtained with $\psi = 0$. This gives

$$\begin{aligned} \begin{Bmatrix} p \\ q \\ r \end{Bmatrix}_{SP_R} &= \begin{Bmatrix} 0 \\ 0 \\ \dot{\psi}_{SP} \end{Bmatrix} + \begin{Bmatrix} 0 \\ \dot{\theta}_{SP} \\ 0 \end{Bmatrix} + \begin{bmatrix} \cos\theta_{SP} & 0 & -\sin\theta_{SP} \\ 0 & 1 & 0 \\ \sin\theta_{SP} & 0 & \cos\theta_{SP} \end{bmatrix} \begin{Bmatrix} \dot{\phi}_{SP} \\ 0 \\ 0 \end{Bmatrix} \\ &+ \begin{bmatrix} 1 & 0 & 0 \\ 0 & \cos\phi_{SP} & \sin\phi_{SP} \\ 0 & -\sin\phi_{SP} & \cos\phi_{SP} \end{bmatrix} \begin{Bmatrix} p \\ q \\ r \end{Bmatrix}_H \end{aligned} \quad (5-152)$$

Nonrotating swashplate angular velocities, subscripted SP_{NR} , are obtained by deleting $\dot{\psi}_{SP}$ above.

The swashplate angular accelerations can be similarly determined by evaluating the general expression at $\psi = \psi_{SP} = 0$. This yields:

$$\begin{aligned} \begin{Bmatrix} \dot{p} \\ \dot{q} \\ \dot{r} \end{Bmatrix}_{SP_R} &= \begin{Bmatrix} 0 \\ \ddot{\theta}_{SP} \\ 0 \end{Bmatrix} + \begin{Bmatrix} \dot{\psi}_{SP} q_{SP} \\ -\dot{\psi}_{SP} p_{SP} \\ \ddot{\psi}_{SP} \end{Bmatrix} + \dot{\theta}_{SP} \begin{bmatrix} -\sin\theta_{SP} & 0 & -\cos\theta_{SP} \\ 0 & 0 & 0 \\ \cos\theta_{SP} & 0 & -\sin\theta_{SP} \end{bmatrix} \begin{Bmatrix} \dot{\phi}_{SP} \\ 0 \\ 0 \end{Bmatrix} \\ &+ \begin{bmatrix} 1 & 0 & 0 \\ 0 & \cos\phi_{SP} & \sin\phi_{SP} \\ 0 & -\sin\phi_{SP} & \cos\phi_{SP} \end{bmatrix} \begin{Bmatrix} p \\ q \\ r \end{Bmatrix}_H + \begin{bmatrix} \cos\theta_{SP} & 0 & -\sin\theta_{SP} \\ 0 & 1 & 0 \\ \sin\theta_{SP} & 0 & \cos\theta_{SP} \end{bmatrix} \begin{Bmatrix} \ddot{\phi}_{SP} \\ 0 \\ 0 \end{Bmatrix} \\ &+ \dot{\phi}_{SP} \begin{bmatrix} 0 & 0 & 0 \\ 0 & -\sin\phi_{SP} & \cos\phi_{SP} \\ 0 & -\cos\phi_{SP} & -\sin\phi_{SP} \end{bmatrix} \begin{Bmatrix} p \\ q \\ r \end{Bmatrix}_H + \begin{bmatrix} 1 & 0 & 0 \\ 0 & \cos\phi_{SP} & \sin\phi_{SP} \\ 0 & -\sin\phi_{SP} & \cos\phi_{SP} \end{bmatrix} \begin{Bmatrix} \dot{p} \\ \dot{q} \\ \dot{r} \end{Bmatrix}_H \end{aligned} \quad (5-153)$$

The vertical velocities and accelerations of the swashplate are simply defined as:

$$\dot{Z}_{OSP}^I = \dot{Z}_{SP} + \dot{Z}_{OH}^I \quad (5-154)$$

and

$$\ddot{Z}_{OSP}^I = \ddot{Z}_{SP} + \ddot{Z}_{OH}^I \quad (5-155)$$

It is noted in these equations that the Z-axis motion is assumed to remain parallel to the hub Z axis.

The swashplate angular displacements are obtained by integrating the angular velocities, or:

$$\phi_{SP} = \int_0^t \dot{\phi}_{SP} dt \quad (5-156)$$

and

$$\theta_{SP} = \int_0^t \dot{\theta}_{SP} dt \quad (5-157)$$

Likewise, the vertical displacement of the swashplate relative to the hub or principal reference axis system is:

$$Z_{SP} = \int_0^t \dot{Z}_{SP} dt + Z_{OSP} \quad (5-158)$$

Where Z_{OSP} is the location of the swashplate reference point with respect to hub or principle axis reference points along the Z-axis.

It is noted that in a feathering moment feedback-gyro control system, the swashplate is used for the control gyro.

5.5.7 Direct Feedback Control System Gyro Motion

As indicated before, the equations of motion incorporate a description of a control gyro that is used in a direct flapping moment feedback control system (DFCS), which is an option in the program. The gyro motion is defined by the Euler angle rotations ϕ_G and θ_G relative to the fuselage reference axis system as shown in Figure 5-9. The order of rotation has been selected to be first ϕ_G and then θ_G , so therefore, the transformation from the fuselage reference axis system to the gyro system is:

$$\begin{bmatrix} T_{F-G} \end{bmatrix} = \begin{bmatrix} \cos\theta_G & 0 & -\sin\theta_G \\ 0 & 1 & 0 \\ \sin\theta_G & 0 & \cos\theta_G \end{bmatrix} \begin{bmatrix} 1 & 0 & 0 \\ 0 & \cos\phi_G & \sin\phi_G \\ 0 & -\sin\phi_G & \cos\phi_G \end{bmatrix} \quad (5-159)$$

In the same manner as the swashplate equations, the angular velocities are written with $\psi = \psi_G = 0$.

$$\begin{aligned} \begin{Bmatrix} p \\ q \\ r \end{Bmatrix}_G &= \begin{Bmatrix} 0 \\ 0 \\ \dot{\psi}_G \end{Bmatrix} + \begin{Bmatrix} 0 \\ \dot{\theta}_G \\ 0 \end{Bmatrix} + \begin{bmatrix} \cos\theta_G & 0 & -\sin\theta_G \\ 0 & 1 & 0 \\ \sin\theta_G & 0 & \cos\theta_G \end{bmatrix} \begin{Bmatrix} \dot{\phi}_G \\ 0 \\ 0 \end{Bmatrix} \\ &+ \begin{bmatrix} 1 & 0 & 0 \\ 0 & \cos\phi_G & \sin\phi_G \\ 0 & \sin\phi_G & \cos\phi_G \end{bmatrix} \begin{Bmatrix} p \\ q \\ r \end{Bmatrix}_F \end{aligned} \quad (5-160)$$

The p and q terms of this equation give the angular velocities of the nonrotating portion on the gyro, i.e., its gimbal frame.

The angular accelerations rotating gyro mass or inertia are likewise evaluated from Section 5.4.3 by setting $\psi = \psi_G = 0$.

$$\begin{aligned}
 \begin{Bmatrix} \dot{p} \\ \dot{q} \\ \dot{r} \end{Bmatrix}_{G_R} &= \begin{Bmatrix} \dot{\psi}_G q_G \\ -\dot{\psi}_G p_G \\ \ddot{\psi}_G \end{Bmatrix} + \begin{Bmatrix} 0 \\ \ddot{\theta}_G \\ 0 \end{Bmatrix} + \dot{\theta}_G \begin{bmatrix} -\sin\theta_G & 0 & -\cos\theta_G \\ 0 & 0 & 0 \\ \cos\theta_G & 0 & -\sin\theta_G \end{bmatrix} \begin{Bmatrix} \dot{\phi}_G \\ 0 \\ 0 \end{Bmatrix} \\
 &+ \begin{bmatrix} 1 & 0 & 0 \\ 0 & \cos\phi_G & -\sin\phi_G \\ 0 & \sin\phi_G & \cos\phi_G \end{bmatrix} \begin{Bmatrix} p \\ q \\ r \end{Bmatrix}_F + \begin{bmatrix} \cos\theta_G & 0 & -\sin\theta_G \\ 0 & 1 & 0 \\ \sin\theta_G & 0 & \cos\theta_G \end{bmatrix} \begin{Bmatrix} \ddot{\phi}_G \\ 0 \\ 0 \end{Bmatrix} \\
 &+ \dot{\phi}_G \begin{bmatrix} 0 & 0 & 0 \\ 0 & -\sin\phi_G & -\cos\phi_G \\ 0 & \cos\phi_G & -\sin\phi_G \end{bmatrix} \begin{Bmatrix} p \\ q \\ r \end{Bmatrix}_F + \begin{bmatrix} 1 & 0 & 0 \\ 0 & \cos\phi_G & -\sin\phi_G \\ 0 & \sin\phi_G & \cos\phi_G \end{bmatrix} \begin{Bmatrix} \dot{p} \\ \dot{q} \\ \dot{r} \end{Bmatrix}_F
 \end{aligned}
 \tag{5-161}$$

The accelerations, then, of the nonrotating part, subscripted G_{NR} , are simply obtained by deleting the first term of the previous equation.

Or:

$$\begin{Bmatrix} \dot{p} \\ \dot{q} \\ \dot{r} \end{Bmatrix}_{G_{NR}} = \begin{Bmatrix} \dot{p} \\ \dot{q} \\ \dot{r} \end{Bmatrix}_{G_R} - \begin{Bmatrix} \dot{\psi}_G q_G \\ -\dot{\psi}_G p_G \\ \ddot{\psi}_G \end{Bmatrix}
 \tag{5-162}$$

5.5.8 Blade Feathering Motion

The feathering occurring at the feather bearings, Figure 5-14, is taken to be the sum of the motions of the following dynamic and kinematic elements:

- Swashplate - collective command
- Swashplate - cyclic command

- Blade bending to feathering couplings
- Elastic pitch horn and associated components

The total feathering response is:

$$\begin{aligned}\phi_{Fn} = & \theta_0 - A_{1S} \cos(\psi_{BLn} + \psi_R) - B_{1S} \sin(\psi_{BLn} + \psi_R) - C_1 \frac{\partial Y'_{FA}}{\partial A_1} A_{1n} \\ & - C_2 \frac{\partial Z'_{FA}}{\partial A_2} A_{2n} - C_3 \frac{\partial Z'_{FA}}{\partial A_3} A_{3n} + \frac{\partial \phi_F}{\partial \beta_{PH}} \beta_{PHn}\end{aligned}\quad (5-163)$$

Velocities and accelerations are formed by differentiation. The desired relations are:

$$\begin{aligned}\dot{\phi}_{Fn} = & \dot{\theta}_0 - \dot{A}_{1S} \cos(\psi_{BLn} + \psi_R) - \dot{B}_{1S} \sin(\psi_{BLn} + \psi_R) \\ & + \left[A_{1S} \sin(\psi_{BLn} + \psi_R) - B_{1S} \cos(\psi_{BLn} + \psi_R) \right] \dot{\psi}_R \\ & - C_1 \frac{\partial Y'_{FA}}{\partial A_1} \dot{A}_{1n} - C_2 \frac{\partial Z'_{FA}}{\partial A_2} \dot{A}_{2n} - C_3 \frac{\partial Z'_{FA}}{\partial A_3} \dot{A}_{3n} + \frac{\partial \phi_F}{\partial \beta_{PH}} \dot{\beta}_{PHn}\end{aligned}\quad (5-164)$$

and for accelerations:

$$\begin{aligned}\ddot{\phi}_{Fn} = & \ddot{\theta}_0 - \ddot{A}_{1S} \cos(\psi_{BLn} + \psi_R) - \ddot{B}_{1S} \sin(\psi_{BLn} + \psi_R) \\ & + 2 \left[\dot{A}_{1S} \sin(\psi_{BLn} + \psi_R) - \dot{B}_{1S} \cos(\psi_{BLn} + \psi_R) \right] \dot{\psi}_R \\ & + \left[A_{1S} \cos(\psi_{BLn} + \psi_R) + B_{1S} \sin(\psi_{BLn} + \psi_R) \right] \dot{\psi}_R^2 \\ & + \left[A_{1S} \cos(\psi_{BLn} + \psi_R) - B_{1S} \sin(\psi_{BLn} + \psi_R) \right] \ddot{\psi} - C_1 \frac{\partial Y'_{FA}}{\partial A_1} \ddot{A}_{1n} \\ & - C_2 \frac{\partial Z'_{FA}}{\partial A_2} \ddot{A}_{2n} - C_3 \frac{\partial Z'_{FA}}{\partial A_3} \ddot{A}_{3n} + \frac{\partial \phi_F}{\partial \beta_{PH}} \ddot{\beta}_{PHn}\end{aligned}\quad (5-165)$$

The commanded cyclic blade angles are:

$$\begin{Bmatrix} A_{1S} \\ B_{1S} \end{Bmatrix} = \left(\frac{d}{e}\right) \begin{bmatrix} \sin\psi_{PH} & \cos\psi_{PH} \\ \cos\psi_{PH} & -\sin\psi_{PH} \end{bmatrix} \begin{Bmatrix} \phi_{SP} \\ \theta_{SP} \end{Bmatrix} \quad (5-166)$$

where the angle ψ_{PH} is the pitch horn-swashplate connection lead to feather axis. See Figure 5-27. This angle is computed as a static value. It should be noted that some hub configurations carry the pitch horn toward the blade trailing edge. These configurations are entered in REXOR by forming the supplement of ψ_{PH} .

$$\psi_{PH} = 180 - \psi_{PH} \text{ (degrees)} \quad (5-167)$$

This angle gives the correct modeling of the sense of rotation reversal with the trailing pitch horn geometry.

The velocities and accelerations of the command cyclic are obtained by differentiation.

$$\begin{aligned} \begin{Bmatrix} \dot{A}_{1S} \\ \dot{B}_{1S} \end{Bmatrix} &= \left(\frac{d}{e}\right) \begin{bmatrix} \sin\psi_{PH} & \cos\psi_{PH} \\ \cos\psi_{PH} & -\sin\psi_{PH} \end{bmatrix} \begin{Bmatrix} \dot{\phi}_{SP} \\ \dot{\theta}_{SP} \end{Bmatrix} \\ &+ \left(\frac{d}{e}\right)_1 \dot{\theta}_0 \begin{bmatrix} \sin\psi_{PH} & \cos\psi_{PH} \\ \cos\psi_{PH} & -\sin\psi_{PH} \end{bmatrix} \begin{Bmatrix} \phi_{SP} \\ \theta_{SP} \end{Bmatrix} \end{aligned} \quad (5-168)$$

and

$$\begin{aligned} \begin{Bmatrix} \ddot{A}_{1S} \\ \ddot{B}_{1S} \end{Bmatrix} &= \left(\frac{d}{e}\right) \begin{bmatrix} \sin\psi_{PH} & \cos\psi_{PH} \\ \cos\psi_{PH} & -\sin\psi_{PH} \end{bmatrix} \begin{Bmatrix} \ddot{\phi}_{SP} \\ \ddot{\theta}_{SP} \end{Bmatrix} \\ &+ 2\left(\frac{d}{e}\right)_1 \dot{\theta}_0 \begin{bmatrix} \sin\psi_{PH} & \cos\psi_{PH} \\ \cos\psi_{PH} & -\sin\psi_{PH} \end{bmatrix} \begin{Bmatrix} \dot{\phi}_{SP} \\ \dot{\theta}_{SP} \end{Bmatrix} \\ &+ \left(\frac{d}{e}\right)_1 \ddot{\theta}_0 \begin{bmatrix} \sin\psi_{PH} & \cos\psi_{PH} \\ \cos\psi_{PH} & -\sin\psi_{PH} \end{bmatrix} \begin{Bmatrix} \phi_{SP} \\ \theta_{SP} \end{Bmatrix} \end{aligned} \quad (5-169)$$

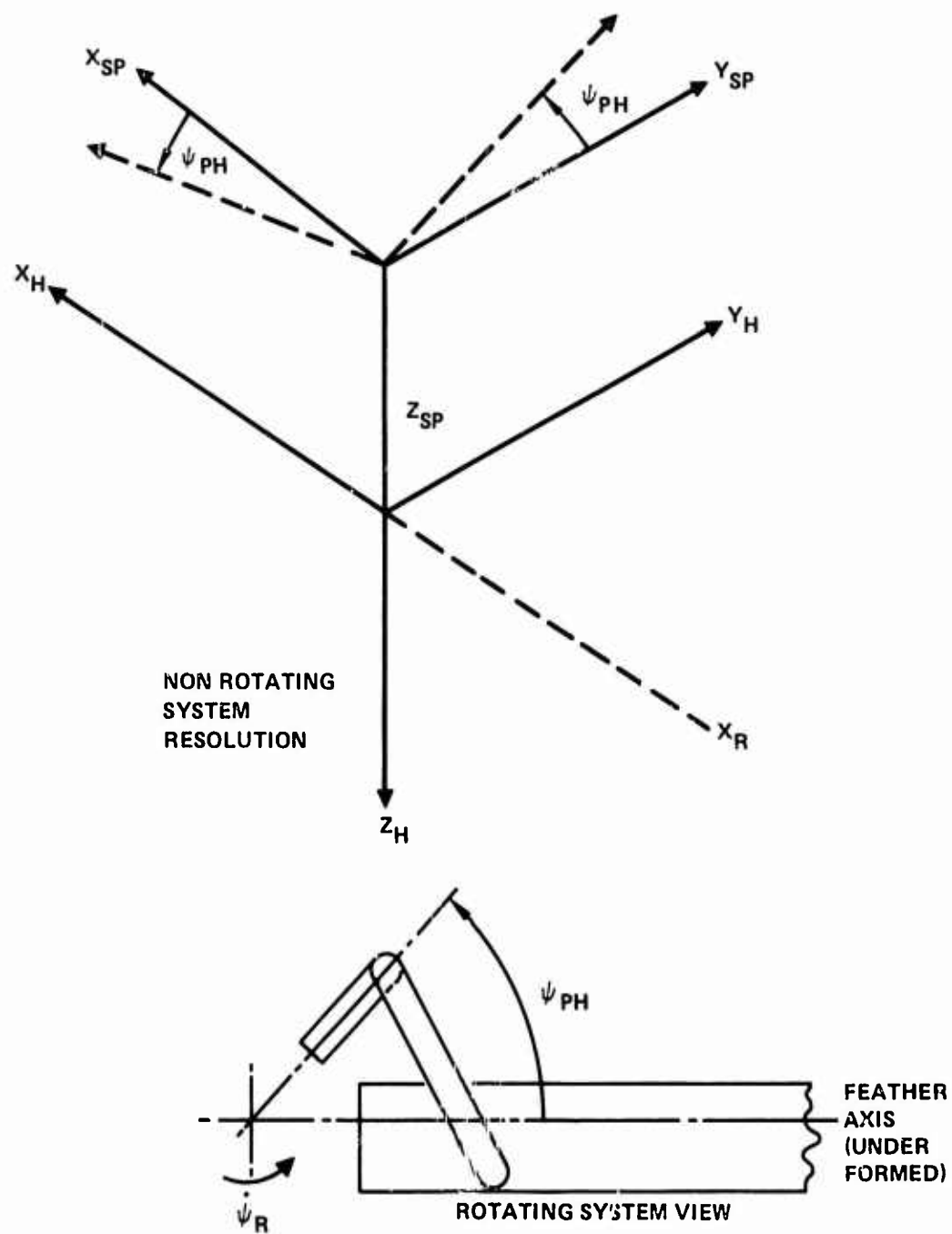


Figure 5-27. Pitch Horn Blade Feathering Phase Angle

The overall coupling (swashplate to feathering) gear ratio, d/e , is expressed as a static term plus a first-order collective correction.

$$\left(\frac{d}{e}\right) = \left(\frac{d}{e}\right)_0 + \left(\frac{d}{e}\right)_1 \theta_0 \quad (5-170)$$

The commanded collective is:

$$\theta_0 = -Z_{SP}/e \quad (5-171)$$

The swashplate vertical motion, Z_{SP} , is developed in Section 5.5.6. The value e is the static effective crank (pitch horn) arm about the blade feather axis. This crank length is inputted as a negative number for a trailing pitch horn geometry to give the proper sense of collective for swashplate vertical translation.

Taking time derivatives:

$$\dot{\theta}_0 = -\dot{Z}_{SP}/e \quad (5-172)$$

and:

$$\ddot{\theta}_0 = -\ddot{Z}_{SP}/e \quad (5-173)$$

The blade bending to feathering coupling factors are C_1 , C_2 , and C_3 for the first, second, and third blade models. The blade bending modes are described without a torsion component; this allows freedom in varying the blade sweep, droop, jog, or other geometric parameters without new input data for the blade mode shape. The torsion either is calculated separately along the blade proper or as a blade root component by pitch horn bending. The $C_1 \dots C_3$ factors are intended to add a feathering component to the blade mode which would exist even with no torsion or feathering moments. As such, they are in effect the δ_3 , α_2 , etc., coupling usually described in the literature. These couplings are usually determined as a function of the distance from the flap or inplane mechanical or vertical hinge to a pitch horn projection.

The factor C_1 is defined positive as nose up feathering (radians) per radian aft inplane deflection of the feather axis slope. The factors C_2 and C_3 are defined positive as nose up feathering (radians) per radian of up flapping feather axis slope for the first and second flap modes, respectively. These factors require the inplane feathering axis slope

$\frac{\partial Y'_{FA}}{\partial A_1}$ for mode one and the out-of-plane slopes $\frac{\partial Z'_{FA}}{\partial A_2}$ and $\frac{\partial Z'_{FA}}{\partial A_3}$ for

the other two modes. The slopes are defined as

$$\frac{\partial Y'_{FA}}{\partial A_1} \approx \left(\frac{\partial Y_{OB}}{\partial A_1} - \frac{\partial Y_{IB}}{\partial A_1} \right) / \cos(Y'_{FA}) l_B \quad (5-174)$$

$$\frac{\partial Z'_{FA}}{\partial A_2} \approx \left(\frac{\partial Z_{OB}}{\partial A_2} - \frac{\partial Z_{IB}}{\partial A_2} \right) / \cos(Z'_{FA}) l_B \quad (5-175)$$

and

$$\frac{\partial Z'_{FA}}{\partial A_3} \approx \left(\frac{\partial Z_{OB}}{\partial A_3} - \frac{\partial Z_{IB}}{\partial A_3} \right) / \cos(Z'_{FA}) l_B \quad (5-176)$$

The mode partial $\frac{\partial Y_{OB}}{\partial A_1}$, etc., describe the inplane or outplane component

displacement at the inboard or outboard bearing location due to mode A_{1n} , A_{2n} , A_{3n} . The length l_B is the distance between bearings. These partials are the same type as described in Section 5.5.5 where the blade motion is built up from the bending, feathering, and twist components.

6. EQUATIONS OF MOTION

6.1 INTRODUCTION

With the coordinate systems and transformation between systems well in hand, the development can proceed to the equations of motion. The development yields a set of second-order differential equations with time varying coefficients. These equations are formulated using the energy approach in a form credited to Lagrange. The solution to the system of equations is in the time domain by numerical integration. The result is a time history of the displacements, velocities, accelerations, and loads of the components of the helicopter modeled. Extra attention is given the main rotor where the blade geometry is modeled in detail, and the program treats each blade separately.

Following the development of the equation methodology used, the math modeling of the vehicle component parts is carried out.

6.2 ENERGY APPROACH TO DEVELOPMENT OF EQUATIONS OF MOTION

There are two basic approaches to developing the equations of motion for a physical system. These are:

- Vector summation of forces
- Energy approach.

Given an equal set of conditions, limitations, and assumptions, both procedures should result in equivalent sets of equations. The difference is in the ease of arriving at a complete set of equations. Note that force is a vector, whereas energy is a scalar quantity. Therefore, in dealing in terms of energy, less information regarding direction needs to be handled. Also the systematic nature of the energy approach reduces the risk of error. As stated by Lagrange (Mecanique Analytique, 1788), "The methods which I present here do not require either constructions or reasonings of geometrical or mechanical nature, but only algebraic operations proceeding after a regular and uniform plan".

The starting point of this development is Lagrange's equation. It may be derived by postulating Newton's second law, or from Hamilton's principle. Lagrange's equation may be written in the following form:

$$\frac{d}{dt} \left(\frac{\partial T}{\partial \dot{q}_r} \right) - \frac{\partial T}{\partial q_r} + \frac{\partial B}{\partial \dot{q}_r} + \frac{\partial U}{\partial q_r} = Q_r \quad (6-1)$$

where

T is kinetic energy

q is a generalized coordinate

B is dissipation function

U is potential energy function

Q_r is the generalized force, derived from the virtual work, δW , and is defined by the equation

$$Q_r = \frac{\partial \delta W}{\partial q_r} \quad (6-2)$$

Equation 6-1 will now be developed into the form as applied in REXOR. This form bears a close resemblance to a force balance equation, but is derived from energy considerations. For clarity, the development is first shown for a set of discrete mass particles, then, in the section that follows, is extended to the distributed elemental masses of the REXOR modeling and to the iterative solution scheme used.

In a conventional manner the equation is formulated in terms of generalized coordinates. These coordinates are a function of time, and completely define the system. They are generally not directly identifiable as a physical quantity.

The physical parameters or elemental coordinates are defined to be functions of the generalized coordinates and in turn a function of time. Consider a system to be composed of particles whose physical coordinates are a function of n generalized coordinates. For the ith particle:

$$x_i = x_i(q_1, q_2, \dots, q_n; t) \quad (6-3)$$

$$y_i = y_i(q_1, q_2, \dots, q_n; t) \quad (6-4)$$

$$z_i = z_i(q_1, q_2, \dots, q_n; t) \quad (6-5)$$

Note: a Cartesian coordinate set is selected, and used in REXOR. However, the argument is true for an arbitrary coordinate set.

The functional relationship of the physical or constrained coordinates and generalized coordinates yields:

$$\delta x_i = \frac{\partial x_i}{\partial q_1} \delta q_1 + \frac{\partial x_i}{\partial q_2} \delta q_2 + \dots + \frac{\partial x_i}{\partial q_n} \delta q_n \quad (6-6)$$

$$\delta y_i = \frac{\partial y_i}{\partial q_1} \delta q_1 + \frac{\partial y_i}{\partial q_2} \delta q_2 + \dots + \frac{\partial y_i}{\partial q_n} \delta q_n \quad (6-7)$$

$$\delta z_i = \frac{\partial z_i}{\partial q_1} \delta q_1 + \frac{\partial z_i}{\partial q_2} \delta q_2 + \dots + \frac{\partial z_i}{\partial q_n} \delta q_n \quad (6-8)$$

The time dependence is implicit in the increments of the generalized coordinates. The equation is strictly true for infinitesimal increments. In REXOR the generalized coordinates are distinct from physical coordinates in the main rotor blade descriptions. Here the generalized coordinates are blade modal variables. The modal variables represent tangible deflections of the blade from a reference position, and as such are small but not infinitesimal variables.

As the variables are a function of time:

$$\dot{x}_i = \frac{\partial x_i}{\partial q_1} \dot{q}_1 + \frac{\partial x_i}{\partial q_2} \dot{q}_2 + \dots + \frac{\partial x_i}{\partial q_n} \dot{q}_n \quad (6-9)$$

$$\dot{y}_i = \frac{\partial y_i}{\partial q_1} \dot{q}_1 + \frac{\partial y_i}{\partial q_2} \dot{q}_2 + \dots + \frac{\partial y_i}{\partial q_n} \dot{q}_n \quad (6-10)$$

$$\dot{z}_i = \frac{\partial z_i}{\partial q_1} \dot{q}_1 + \frac{\partial z_i}{\partial q_2} \dot{q}_2 + \dots + \frac{\partial z_i}{\partial q_n} \dot{q}_n \quad (6-11)$$

In terms of the ith particle the kinetic energy for the system may be identified as:

$$T = \sum_{i=1}^N \frac{1}{2} m_i \left(\dot{x}_i^2 + \dot{y}_i^2 + \dot{z}_i^2 \right) \quad (6-12)$$

Toward the particular formulation of Lagrange's equation used in REXOR, the first two terms of the previously stated form, Equation 6-1, are developed:

$$\frac{d}{dt} \left(\frac{\partial T}{\partial \dot{q}_r} \right) - \frac{\partial T}{\partial q_r} \quad (6-13)$$

Performing these operations for the i th particle case and the r th generalized coordinate and summing over the system yields:

$$\begin{aligned} \frac{d}{dt} \left(\frac{\partial T}{\partial \dot{q}_r} \right) - \frac{\partial T}{\partial q_r} = \sum_{i=1}^N \left(\frac{1}{2} m_i \frac{d}{dt} \frac{\partial}{\partial \dot{q}_r} \left(\dot{x}_i^2 + \dot{y}_i^2 + \dot{z}_i^2 \right) \right) \\ - \frac{1}{2} m_i \frac{\partial}{\partial q_r} \left(\dot{x}_i^2 + \dot{y}_i^2 + \dot{z}_i^2 \right) \end{aligned} \quad (6-14)$$

A useful math operation of cancellation of the dots is developed prior to proceeding. Recall:

$$\delta x_i = \frac{\partial x_i}{\partial q_1} \delta q_1 + \frac{\partial x_i}{\partial q_2} \delta q_2 + \dots + \frac{\partial x_i}{\partial q_n} \delta q_n \quad (6-15)$$

Then also

$$\dot{x}_i = \frac{\partial x_i}{\partial q_1} \dot{q}_1 + \frac{\partial x_i}{\partial q_2} \dot{q}_2 + \dots + \frac{\partial x_i}{\partial q_n} \dot{q}_n \quad (6-16)$$

or

$$\frac{\partial \dot{x}_i}{\partial \dot{q}_r} = \frac{\partial x_i}{\partial q_r} \quad (6-17)$$

This is also true for y and z and for the double dot terms in x , y and z .

An operation to reverse the order of spacial and temporal differentiation is required. To show this the time derivative of a partial is taken as

$$\frac{d}{dt} \left(\frac{\partial x_i}{\partial q_r} \right) = \frac{\partial}{\partial q_1} \left(\frac{\partial x_i}{\partial q_r} \right) \dot{q}_1 + \frac{\partial}{\partial q_2} \left(\frac{\partial x_i}{\partial q_r} \right) \dot{q}_2 + \dots + \frac{\partial}{\partial q_n} \left(\frac{\partial x_i}{\partial q_r} \right) \dot{q}_n \quad (6-18)$$

Next the spacial derivative of \dot{x}_i is given as

$$\frac{\partial \dot{x}_i}{\partial \dot{q}_r} = \frac{\partial}{\partial \dot{q}_r} \left(\frac{\partial x_i}{\partial q_1} \dot{q}_1 + \frac{\partial x_i}{\partial q_2} \dot{q}_2 + \dots + \frac{\partial x_i}{\partial q_n} \dot{q}_n \right) \quad (6-19)$$

Now since

$$x_i = x_i(q_1, q_2, \dots, q_n) \quad (6-20)$$

the order of spacial differentiation is reversible

$$\frac{\partial^2 x_i}{\partial \dot{q}_r \partial \dot{q}_s} = \frac{\partial^2 x_i}{\partial \dot{q}_s \partial \dot{q}_r} \quad (6-21)$$

and hence

$$\frac{d}{dt} \left(\frac{\partial x_i}{\partial \dot{q}_r} \right) = \frac{\partial \dot{x}_i}{\partial \dot{q}_r} \quad (6-22)$$

Similar relations exist for y_i and z_i .

Proceeding on with the kinetic energy terms:

$$\begin{aligned} \frac{d}{dt} \left(\frac{\partial T}{\partial \dot{q}_r} \right) - \frac{\partial T}{\partial q_r} = & \sum_{i=1}^N m_i \left[\ddot{x}_i \frac{\partial \dot{x}_i}{\partial \dot{q}_r} + \ddot{y}_i \frac{\partial \dot{y}_i}{\partial \dot{q}_r} + \ddot{z}_i \frac{\partial \dot{z}_i}{\partial \dot{q}_r} + \dot{x}_i \frac{d}{dt} \left(\frac{\partial \dot{x}_i}{\partial \dot{q}_r} \right) + \dot{y}_i \frac{d}{dt} \left(\frac{\partial \dot{y}_i}{\partial \dot{q}_r} \right) \right. \\ & \left. + \dot{z}_i \frac{d}{dt} \left(\frac{\partial \dot{z}_i}{\partial \dot{q}_r} \right) - \dot{x}_i \frac{\partial \dot{x}_i}{\partial q_r} - \dot{y}_i \frac{\partial \dot{y}_i}{\partial q_r} - \dot{z}_i \frac{\partial \dot{z}_i}{\partial q_r} \right] \quad (6-23) \end{aligned}$$

Using the relationship for cancelling dots in partials, reversing the order of differentiation and cancelling terms gives

$$\frac{d}{dt} \left(\frac{\partial T}{\partial \dot{q}_r} \right) - \frac{\partial T}{\partial q_r} = \sum_{i=1}^N m_i \left[\ddot{x}_i \frac{\partial \dot{x}_i}{\partial \dot{q}_r} + \ddot{y}_i \frac{\partial \dot{y}_i}{\partial \dot{q}_r} + \ddot{z}_i \frac{\partial \dot{z}_i}{\partial \dot{q}_r} \right] \quad (6-24)$$

Then from Equation 6-1, Lagrange's Equation in constrained coordinates with point masses becomes

$$\sum_{i=1}^N m_i \left[\ddot{x}_i \frac{\partial x_i}{\partial q_r} + \ddot{y}_i \frac{\partial y_i}{\partial q_r} + \ddot{z}_i \frac{\partial z_i}{\partial q_r} \right] + \frac{\partial B}{\partial \dot{q}_r} + \frac{\partial U}{\partial q_r} = Q_r \quad (6-25)$$

Also, in the same vein of defining the generalized coordinates, the relationship between the elemental and generalized forces can be developed. This relationship is developed from the definition of virtual work on a particle as the scalar product of the applied force and an infinitesimal displacement. Therefore for the total system of N elements,

$$\delta W = \sum_{i=1}^N \left[F_{x_i} \delta x_i + F_{y_i} \delta y_i + F_{z_i} \delta z_i \right] \quad (6-26)$$

Using the definition of Q_r from Equation 6-2 gives:

$$Q_r = \sum_{i=1}^N \left(F_{x_i} \frac{\partial x_i}{\partial q_r} + F_{y_i} \frac{\partial y_i}{\partial q_r} + F_{z_i} \frac{\partial z_i}{\partial q_r} \right) \quad (6-27)$$

Substituting Equation 6-27 into Equation 6-25 yields the final form of the Lagrange energy equation in constrained coordinates for point masses, which is in the form from which the REXOR Equations of motion are developed. Making this substitution and rearranging the equation yields

$$\begin{aligned} \sum_{i=1}^N \left[\left(m_i \ddot{x}_i - F_{x_i} \right) \frac{\partial x_i}{\partial q_r} + \left(m_i \ddot{y}_i - F_{y_i} \right) \frac{\partial y_i}{\partial q_r} + \left(m_i \ddot{z}_i - F_{z_i} \right) \frac{\partial z_i}{\partial q_r} \right] \\ + \frac{\partial B}{\partial \dot{q}_r} + \frac{\partial U}{\partial q_r} = 0 \end{aligned} \quad (6-28)$$

The above equation is the basis for the entire derivation of the equations of motion of REXOR. Note that this equation is written for discrete element masses and discrete forces. Also, at any instant in time all of the ingredients required to define the elemental accelerations, $\ddot{x}_i, \ddot{y}_i, \ddot{z}_i$, are not known. Specifically, the generalized coordinate displacements and velocities, q_r and \dot{q}_r , are known at any instant in time but the generalized coordinate accelerations, \ddot{q}_r , remain to be determined at the time the elemental accelerations are computed.

The following section presents the manner in which the foregoing equation set is adapted to the REXOR numerical solution to solve the equilibrium equations or equations of motions for the generalized coordinate accelerations. This development is first presented in the simpler form, for clarity, for discrete mass elements and forces and then in expanded form to include elemental distributed masses and applied moments.

6.3 ITERATIVE CONCEPT AND EQUATION SET SOLUTION METHOD

Given a set of equations as developed in the previous section, the next step is to establish a method of solution. The solution process is defined as solving the equation set for the accelerations, integrating the accelerations for updated velocity, and position; then substituting the integrands back into the equations to determine new values of accelerations.

The first step of the process is to define explicitly the accelerations from the equation set. In the process of implementing the REXOR equations, it is desirable to handle the accelerations as an estimated plus a corrective term. In generalized coordinates then we can write

$$\begin{Bmatrix} \ddot{q}_1 \\ . \\ . \\ . \\ \ddot{q}_n \end{Bmatrix}_{\text{NEW}} = \begin{Bmatrix} \ddot{q}_1 \\ . \\ . \\ . \\ \ddot{q}_n \end{Bmatrix}_{\text{CORR.}} + \begin{Bmatrix} \ddot{q}_1 \\ . \\ . \\ . \\ \ddot{q}_n \end{Bmatrix}_{\text{OLD}} \quad (6-29)$$

This operation proceeds on a sequential time basis. For each increment advance in time, the previous 'NEW' becomes the 'OLD'. In REXOR, the time increment corresponds with a step azimuthal advance of the main rotor

blades. However, this need not be the case. The 'NEW' accelerations must be used in the numerical integration process to define the generalized coordinate velocities and displacements. But if some form of a predictor on accelerations is used then the 'OLD' would be this predicted value and in this case it would be an estimated, 'EST', value.

Using the notation 'OLD' and 'EST' interchangeably the linear elemental accelerations can be written at time t as

$$\begin{Bmatrix} \ddot{x}_i \\ \ddot{y}_i \\ \ddot{z}_i \end{Bmatrix}_t^I = \begin{Bmatrix} \ddot{x}_i \\ \ddot{y}_i \\ \ddot{z}_i \end{Bmatrix}_{\text{CORR}} + \begin{Bmatrix} \ddot{x}_i \\ \ddot{y}_i \\ \ddot{z}_i \end{Bmatrix}_{\text{EST}}^I \quad (6-30)$$

where the estimated accelerations are determined using the generalized displacements and velocities, q_r and \dot{q}_r , at time t , and the generalized coordinate accelerations \ddot{q}_r , either estimated or from one previous time step in the numerical integration process.

Then, at any given instant in time where the 'EST' elemental accelerations are thusly determined, it can easily be shown that the corrective elemental accelerations, $(\ddot{x}, \ddot{y}, \ddot{z})_{\text{CORR}}$, are a function only of the generalized coordinate corrective accelerations.

Or

$$\begin{Bmatrix} \ddot{x}_i \\ \ddot{y}_i \\ \ddot{z}_i \end{Bmatrix}_{\text{CORR}} = \begin{Bmatrix} \frac{\partial x_i}{\partial q_1} \ddot{q}_{1\text{CORR}} + \dots + \frac{\partial x_i}{\partial q_n} \ddot{q}_{n\text{CORR}} \\ \frac{\partial y_i}{\partial q_1} \ddot{q}_{1\text{CORR}} + \dots + \frac{\partial y_i}{\partial q_n} \ddot{q}_{n\text{CORR}} \\ \frac{\partial z_i}{\partial q_1} \ddot{q}_{1\text{CORR}} + \dots + \frac{\partial z_i}{\partial q_n} \ddot{q}_{n\text{CORR}} \end{Bmatrix} \quad (6-31)$$

or

$$\begin{Bmatrix} \ddot{x}_i \\ \ddot{y}_i \\ \ddot{z}_i \end{Bmatrix}_{\text{CORR}} = \sum_{k=1}^n \begin{Bmatrix} \frac{\partial x_i}{\partial q_k} \ddot{q}_{k\text{CORR}} \\ \frac{\partial y_i}{\partial q_k} \ddot{q}_{k\text{CORR}} \\ \frac{\partial z_i}{\partial q_k} \ddot{q}_{k\text{CORR}} \end{Bmatrix} \quad (6-32)$$

Now making the substitution of Equations 6-27 and 6-31 into Equation 6-25 from the previous section and rearranging terms yields the Lagrange equation for the q_r coordinate in terms of the estimated elemental accelerations and the corrective generalized coordinate accelerations.

$$\begin{aligned} & \sum_{i=1}^N \left[\left(m_i \ddot{x}_{i\text{EST}} - F_{x_i} \right) \frac{\partial x_i}{\partial q_r} + \left(m_i \ddot{y}_{i\text{EST}} - F_{y_i} \right) \frac{\partial y_i}{\partial q_r} + \left(m_i \ddot{z}_{i\text{EST}} - F_{z_i} \right) \frac{\partial z_i}{\partial q_r} \right] \\ & + \sum_{i=1}^N m_i \left[\frac{\partial x_i}{\partial q_r} \sum_{k=1}^n \frac{\partial x_i}{\partial q_k} \ddot{q}_{k\text{CORR.}} + \frac{\partial y_i}{\partial q_r} \sum_{k=1}^n \frac{\partial y_i}{\partial q_k} \ddot{q}_{k\text{CORR.}} + \frac{\partial z_i}{\partial q_r} \sum_{k=1}^n \frac{\partial z_i}{\partial q_k} \ddot{q}_{k\text{CORR.}} \right] \\ & + \frac{\partial B}{\partial \dot{q}_r} + \frac{\partial U}{\partial q_r} = 0 \end{aligned} \quad (6-33)$$

The equations of motion for the system can now be combined and presented in matrix form.

$$\begin{aligned}
 & \left[\begin{array}{c} M_{rk} \\ \text{MASS} \\ \text{MATRIX} \end{array} \right] \left\{ \begin{array}{c} \ddot{q}_1 \\ \cdot \\ \cdot \\ \ddot{q}_n \end{array} \right\} + \left[\begin{array}{c} \sum_{i=1}^N \left[\left(m_i \ddot{x}_{i \text{ EST}} - F_{x_i} \right) \frac{\partial x_i}{\partial q_1} + \left(\quad \right) \frac{\partial y_i}{\partial q_1} + \left(\quad \right) \frac{\partial z_i}{\partial q_1} \right] \\ \cdot \\ \cdot \\ \sum_{i=1}^N \left[\left(m_i \ddot{x}_{i \text{ EST}} - F_{x_i} \right) \frac{\partial x_i}{\partial q_n} + \left(\quad \right) \frac{\partial y_i}{\partial q_n} + \left(\quad \right) \frac{\partial z_i}{\partial q_n} \right] \end{array} \right] + \\
 & + \left[\begin{array}{c} C_{rk} \\ \text{DAMPING} \\ \text{MATRIX} \end{array} \right] \left\{ \begin{array}{c} \dot{q}_1 \\ \cdot \\ \cdot \\ \dot{q}_n \end{array} \right\} + \left[\begin{array}{c} K_{rk} \\ \text{STIFFNESS} \\ \text{MATRIX} \end{array} \right] \left\{ \begin{array}{c} q_1 \\ \cdot \\ \cdot \\ q_n \end{array} \right\} = 0 \quad (6-34)
 \end{aligned}$$

where the matrices, M_{rk} , C_{rk} and K_{rk} will be defined in the following discussion. However before proceeding with this, Equation 6-34 is now rearranged into the form actually used in the numerical process in REXOR. The equation is solved in terms of the corrective accelerations.

The correction terms come from an inversion (or simultaneous equation, Cholesky method) operation on the model equation set.

$$\begin{aligned}
 \begin{Bmatrix} \ddot{q}_1 \\ \vdots \\ \ddot{q}_n \end{Bmatrix}_{\text{CORR.}} &= - \begin{bmatrix} & & \\ & M_{rk} & \\ & \text{MASS} & \\ & \text{MATRIX} & \end{bmatrix}^{-1} \left\{ \begin{aligned} & \sum_{i=1}^N \left[\left(m_i \ddot{x}_{i\text{EST}} - F_{x_i} \right) \frac{\partial x_i}{\partial q_1} + \dots \right. \\ & \quad \vdots \\ & \sum_{i=1}^N \left[\left(m_i \ddot{x}_{i\text{EST}} - F_{x_i} \right) \frac{\partial x_i}{\partial q_n} + \dots \right. \\ & + \begin{bmatrix} & \\ & C_{rk} \\ & \text{DAMPING} \\ & \text{MATRIX} \end{bmatrix} \begin{Bmatrix} \dot{q}_1 \\ \vdots \\ \dot{q}_n \end{Bmatrix} + \begin{bmatrix} & \\ & K_{rk} \\ & \text{STIFFNESS} \\ & \text{MATRIX} \end{bmatrix} \begin{Bmatrix} q_1 \\ \vdots \\ q_n \end{Bmatrix} \end{aligned} \right\} \quad (6-35)
 \end{aligned}$$

As indicated before estimated accelerations in physical coordinates come from the 'EST' or 'OLD' generalized coordinate accelerations and the current generalized coordinate velocities and displacements. The integration part of the solution operation supplies the (\dot{q}) and (q) data.

$$\dot{q} = \int \ddot{q}_{\text{NEW}} dt \quad ; \quad q = \int \dot{q} dt \quad (6-36)$$

The whole package operates in a cyclical fashion, as shown in Figure 6-1. Arranging the solution sequence as such gives it some important attributes and advantages.

First, to determine the corrective acceleration, the inverted mass matrix premultiplies the difference of applied and estimated reactive forces represented by the quantity in the large brackets on the right-hand side

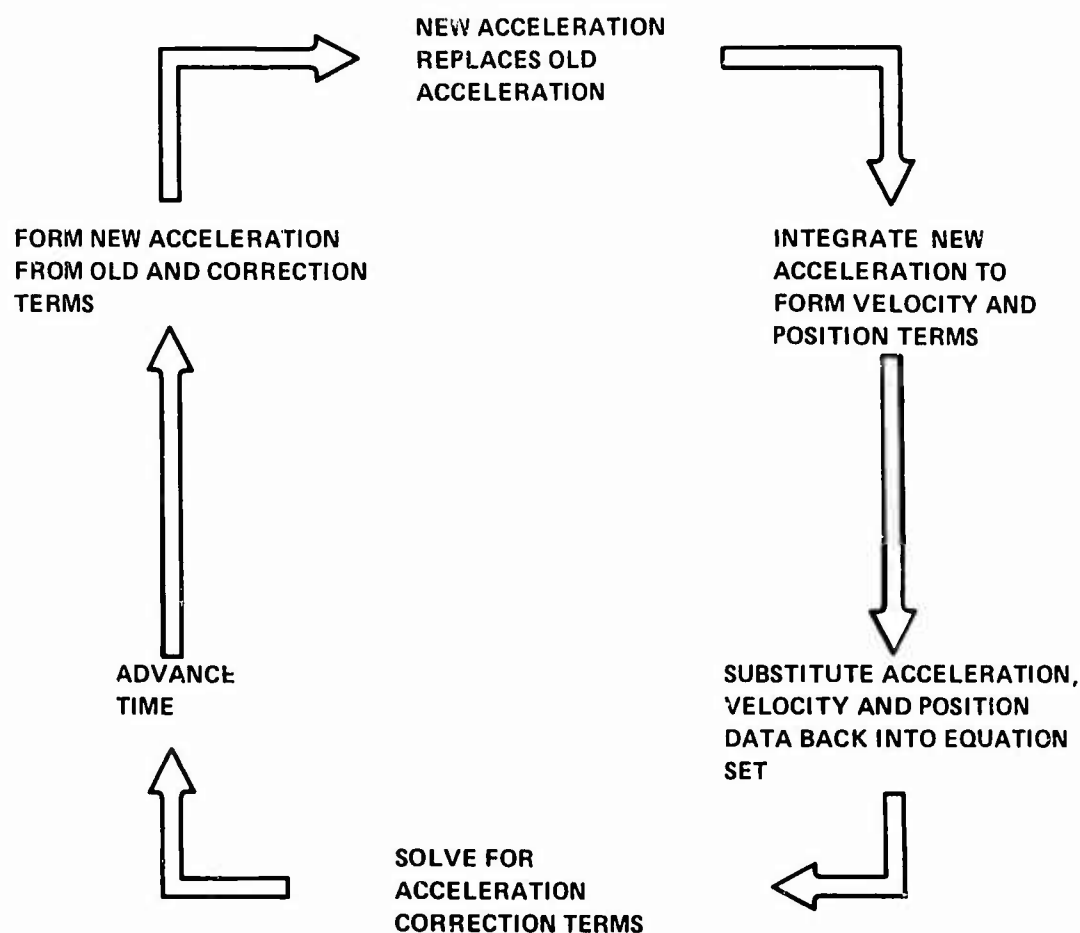


Figure 6-1. Equation Solution Loop

of Equation 6-35. With the usual, small, integration steps these differences will be relatively small. Therefore, inaccuracies in the mass matrix or its inversion process only slightly affect the total acceleration determination. This means approximations and simplifications to the mass matrix are acceptable. In some instances, a diagonal mass matrix will give convergence to the required solution.

Second, as will be shown in the Section 6.4, (blade equations section), carrying the running acceleration in elemental coordinates allows for the simple separation of the centrifugal and structural stiffness of the rotor blades which has important advantages which have been discussed. Also, the aerodynamic loading terms, already by nature in physical coordinates, are easily accounted for.

In the actual application of Equation 6-35 to REXOR, distributed elemental rigid body masses are associated with each coordinate point and applied moments in addition to forces at each coordinate point are accounted for.

Referring back to Equation 6-27 the generalized force, Q_r , from virtual work can be simply written in the following form to account for applied moments at each of the i th grid points as

$$Q_r = \sum_{i=1}^N \left[F_{x_i} \frac{\partial x_i}{\partial q_r} + F_{y_i} \frac{\partial y_i}{\partial q_r} + F_{z_i} \frac{\partial z_i}{\partial q_r} + M_{\phi_i} \frac{\partial \phi_i}{\partial q_r} + M_{\theta_i} \frac{\partial \theta_i}{\partial q_r} + M_{\psi_i} \frac{\partial \psi_i}{\partial q_r} \right] \quad (6-37)$$

The terms of Equation 6-24 in Equation 6-28 can be developed for the distributed masses by going back to the elemental acceleration equation, Equation 5-11 of Section 5.4.1 which is repeated here, in a rearranged form, for clarity of this development.

$$\begin{aligned} \begin{pmatrix} \ddot{x} \\ \ddot{y} \\ \ddot{z} \end{pmatrix}_a^I &= \begin{pmatrix} \ddot{x}_0 \\ \ddot{y}_0 \\ \ddot{z}_0 \end{pmatrix}_a^I + \begin{pmatrix} \ddot{x} \\ \ddot{y} \\ \ddot{z} \end{pmatrix}_a + \begin{bmatrix} (-r^2 - q^2) & pq & pr \\ pq & (-r^2 - p^2) & qr \\ pr & qr & (-p^2 - q^2) \end{bmatrix} \begin{pmatrix} x \\ y \\ z \end{pmatrix}_a \\ &+ 2 \begin{bmatrix} 0 & -r & q \\ r & 0 & -p \\ -q & p & 0 \end{bmatrix} \begin{pmatrix} \dot{x} \\ \dot{y} \\ \dot{z} \end{pmatrix}_a + \begin{bmatrix} 0 & z & -y \\ -z & 0 & x \\ y & -x & 0 \end{bmatrix} \begin{pmatrix} \dot{p} \\ \dot{q} \\ \dot{r} \end{pmatrix}_a \end{aligned} \quad (6-38)$$

For distributed masses of a rigid body with coordinate point and system embedded in the body:

$$\dot{x} = \dot{y} = \dot{z} = 0 \quad (6-39)$$

and Equation 6-38 becomes:

$$\begin{Bmatrix} \ddot{x} \\ \ddot{y} \\ \ddot{z} \end{Bmatrix}_a^I = \begin{Bmatrix} \ddot{x}_0 \\ \ddot{y}_0 \\ \ddot{z}_0 \end{Bmatrix}_a^I + \begin{bmatrix} -x(r^2+q^2) + ypq + zpr \\ xpq - y(r^2+p^2) + zqr \\ xpr + yqr - z(p^2+q^2) \end{bmatrix} + \begin{bmatrix} z\dot{q} - y\dot{r} \\ -z\dot{p} + x\dot{r} \\ y\dot{p} - x\dot{q} \end{bmatrix} \quad (6-40)$$

Now, remembering that for a point mass,

$$\frac{\partial x}{\partial q_r} = \frac{\partial \ddot{x}}{\partial \ddot{q}_r} \quad (6-41)$$

$$\frac{\partial y}{\partial q_r} = \frac{\partial \ddot{y}}{\partial \ddot{q}_r} \quad (6-42)$$

$$\frac{\partial z}{\partial q_r} = \frac{\partial \ddot{z}}{\partial \ddot{q}_r} \quad (6-43)$$

$$\frac{\partial \phi}{\partial q_r} = \frac{\partial \dot{p}}{\partial \dot{q}_r} \quad (6-44)$$

$$\frac{\partial \theta}{\partial q_r} = \frac{\partial \dot{q}}{\partial \dot{q}_r} \quad (6-45)$$

and

$$\frac{\partial \psi}{\partial q_r} = \frac{\partial \dot{r}}{\partial \dot{q}_r} \quad (6-46)$$

The total partial derivatives relating the motion of the coordinate point and set imbedded within each elemental body and the motion of the generalized coordinate becomes

$$\frac{\partial x}{\partial q_r} = \frac{\partial x_0}{\partial q_r} - y \frac{\partial \psi}{\partial q_r} + z \frac{\partial \theta}{\partial q_r} \quad (6-47)$$

$$\frac{\partial y}{\partial q_r} = \frac{\partial y_0}{\partial q_r} + x \frac{\partial \psi}{\partial q_r} - z \frac{\partial \phi}{\partial q_r} \quad (6-48)$$

$$\frac{\partial z}{\partial q_r} = \frac{\partial z_0}{\partial q_r} - x \frac{\partial \theta}{\partial q_r} + y \frac{\partial \phi}{\partial q_r} \quad (6-49)$$

where on the right side of these equations, x , y , and z represent the location of the distributed masses within the rigid body elemental mass, and x_0 , y_0 and z_0 represent the motion of the mass element reference point.

For each j th coordinate of the system, the elements of Equation 6-24 can be written by substitution of Equations 6-40, 6-47, 6-48 and 6-49. This gives

$$\begin{aligned}
& \left[\sum_{i=1}^N m_i \begin{pmatrix} \ddot{x}_i \\ \ddot{y}_i \\ \ddot{z}_i \end{pmatrix}_{EST} \cdot \frac{\partial}{\partial q_r} \begin{pmatrix} x_i \\ y_i \\ z_i \end{pmatrix} \right]_j \\
&= \sum_{i=1}^N m_i \left[\begin{aligned}
& \ddot{x}_0 \frac{\partial x_0}{\partial q_r} - \ddot{x}_0 y_i \frac{\partial \psi}{\partial q_r} + \ddot{x}_0 z_i \frac{\partial \theta}{\partial q_r} - x_i (r^2 + q^2) \frac{\partial x_0}{\partial q_r} + x_i y_i (r^2 + q^2) \frac{\partial \psi}{\partial q_r} \\
& \ddot{y}_0 \frac{\partial y_0}{\partial q_r} + \ddot{y}_0 x_i \frac{\partial \psi}{\partial q_r} - \ddot{y}_0 z_i \frac{\partial \phi}{\partial q_r} + x_i p q \frac{\partial y_0}{\partial q_r} + x_i^2 p q \frac{\partial \psi}{\partial q_r} - x_i y_i p q \frac{\partial \phi}{\partial q_r} \\
& \ddot{z}_0 \frac{\partial z_0}{\partial q_r} - \ddot{z}_0 x_i \frac{\partial \theta}{\partial q_r} + \ddot{z}_0 y_i \frac{\partial \phi}{\partial q_r} + x_i p r \frac{\partial z_0}{\partial q_r} - x_i^2 p r \frac{\partial \theta}{\partial q_r} + x_i y_i p r \frac{\partial \phi}{\partial q_r} \\
& - x_i z_i (r^2 + q^2) \frac{\partial \theta}{\partial q_r} + y_i p q \frac{\partial x_0}{\partial q_r} - y_i^2 p q \frac{\partial \psi}{\partial q_r} + y_i z_i p q \frac{\partial \theta}{\partial q_r} + z_i p r \frac{\partial x_0}{\partial q_r} \\
& + - y_i (r^2 + p^2) \frac{\partial y_0}{\partial q_r} - x_i y_i (r^2 + p^2) \frac{\partial \psi}{\partial q_r} + y_i z_i (r^2 + p^2) \frac{\partial \phi}{\partial q_r} + z_i q r \frac{\partial y_0}{\partial q_r} \\
& + y_i q r \frac{\partial z_0}{\partial q_r} - x_i y_i q r \frac{\partial \theta}{\partial q_r} + y_i^2 q r \frac{\partial \phi}{\partial q_r} - z_i (p^2 + q^2) \frac{\partial z_0}{\partial q_r} \\
& - z_i y_i p r \frac{\partial \psi}{\partial q_r} + z_i^2 p r \frac{\partial \theta}{\partial q_r} + z_i \dot{q} \frac{\partial x_0}{\partial q_r} - y_i z_i \dot{q} \frac{\partial \psi}{\partial q_r} + z_i^2 \dot{q} \frac{\partial \theta}{\partial q_r} \\
& + x_i z_i q r \frac{\partial \psi}{\partial q_r} - z_i^2 q r \frac{\partial \phi}{\partial q_r} - z_i \dot{p} \frac{\partial y_0}{\partial q_r} - x_i z_i \dot{p} \frac{\partial \psi}{\partial q_r} - z_i^2 \dot{p} \frac{\partial \phi}{\partial q_r} \\
& + x_i z_i (p^2 + q^2) \frac{\partial \theta}{\partial q_r} - y_i z_i (p^2 + q^2) \frac{\partial \phi}{\partial q_r} + y_i \dot{p} \frac{\partial z_0}{\partial q_r} - x_i y_i \dot{p} \frac{\partial \theta}{\partial q_r} \\
& - y_i \dot{r} \frac{\partial x_0}{\partial q_r} + y_i^2 \dot{r} \frac{\partial \psi}{\partial q_r} - z_i y_i \dot{r} \frac{\partial \theta}{\partial q_r} \\
& + x_i \dot{r} \frac{\partial y_0}{\partial q_r} + x_i^2 \dot{r} \frac{\partial \psi}{\partial q_r} + x_i z_i \dot{r} \frac{\partial \phi}{\partial q_r} \\
& + y_i^2 \dot{p} \frac{\partial \phi}{\partial q_r} - x_i \dot{q} \frac{\partial z_0}{\partial q_r} + x_i^2 \dot{q} \frac{\partial \theta}{\partial q_r} - x_i y_i \dot{q} \frac{\partial \phi}{\partial q_r}
\end{aligned} \right]_j
\end{aligned}
\tag{6-50}$$

Expanding and identifying mass moment and moment of inertia terms:

$$\left[\sum_{i=1}^N m_i \begin{pmatrix} \ddot{x}_i \\ \ddot{y}_i \\ \ddot{z}_i \end{pmatrix} \cdot \frac{\partial}{\partial q_r} \begin{pmatrix} x_i \\ y_i \\ z_i \end{pmatrix} \right]_{EST} = \left[\begin{aligned} & \left[\begin{aligned} & M\ddot{x} \frac{\partial x_0}{\partial q_r} - M\ddot{y} \frac{\partial y_0}{\partial q_r} + M\ddot{z} \frac{\partial z_0}{\partial q_r} - M\ddot{\theta} \frac{\partial \theta}{\partial q_r} + I_{XY}(r^2+q^2) \frac{\partial \psi}{\partial q_r} \\ & M\ddot{y} \frac{\partial y_0}{\partial q_r} + M\ddot{x} \frac{\partial x_0}{\partial q_r} - M\ddot{z} \frac{\partial z_0}{\partial q_r} + M\ddot{\theta} \frac{\partial \theta}{\partial q_r} + I_{XZ}(r^2+q^2) \frac{\partial \psi}{\partial q_r} - I_{YZ}(r^2+q^2) \frac{\partial \phi}{\partial q_r} \\ & M\ddot{z} \frac{\partial z_0}{\partial q_r} - M\ddot{x} \frac{\partial x_0}{\partial q_r} + M\ddot{y} \frac{\partial y_0}{\partial q_r} + M\ddot{\theta} \frac{\partial \theta}{\partial q_r} - I_{XZ}(r^2+q^2) \frac{\partial \psi}{\partial q_r} + I_{YZ}(r^2+q^2) \frac{\partial \phi}{\partial q_r} \end{aligned} \right] \\ & + \left[\begin{aligned} & - I_{XZ}(r^2+q^2) \frac{\partial \theta}{\partial q_r} + M\ddot{y} \frac{\partial x_0}{\partial q_r} - I_{YX} \frac{\partial \psi}{\partial q_r} + I_{YZ} \frac{\partial \theta}{\partial q_r} + M\ddot{z} \frac{\partial x_0}{\partial q_r} \\ & - M\ddot{y}(r^2+p^2) \frac{\partial y_0}{\partial q_r} - I_{XY}(r^2+p^2) \frac{\partial \psi}{\partial q_r} + I_{YZ}(r^2+p^2) \frac{\partial \phi}{\partial q_r} + M\ddot{z} \frac{\partial y_0}{\partial q_r} \\ & + M\ddot{y} \frac{\partial z_0}{\partial q_r} - I_{XY} \frac{\partial \theta}{\partial q_r} + I_{YX} \frac{\partial \phi}{\partial q_r} - M\ddot{z}(p^2+q^2) \frac{\partial z_0}{\partial q_r} + I_{XZ}(p^2+q^2) \frac{\partial \theta}{\partial q_r} \end{aligned} \right] \\ & + \left[\begin{aligned} & - I_{ZY} \frac{\partial \psi}{\partial q_r} + I_{ZP} \frac{\partial \theta}{\partial q_r} + M\ddot{z} \frac{\partial x_0}{\partial q_r} - I_{YZ} \frac{\partial \psi}{\partial q_r} + I_{ZP} \frac{\partial \theta}{\partial q_r} - M\ddot{y} \frac{\partial x_0}{\partial q_r} \\ & + I_{XZ} \frac{\partial \psi}{\partial q_r} - I_{ZP} \frac{\partial \phi}{\partial q_r} - M\ddot{z} \frac{\partial y_0}{\partial q_r} - I_{XZ} \frac{\partial \psi}{\partial q_r} + I_{ZP} \frac{\partial \phi}{\partial q_r} + M\ddot{x} \frac{\partial y_0}{\partial q_r} \\ & - I_{YZ}(p^2+q^2) \frac{\partial \phi}{\partial q_r} + M\ddot{y} \frac{\partial z_0}{\partial q_r} - I_{XY} \frac{\partial \theta}{\partial q_r} + I_{YX} \frac{\partial \phi}{\partial q_r} - M\ddot{x} \frac{\partial z_0}{\partial q_r} + I_{XZ} \frac{\partial \theta}{\partial q_r} \end{aligned} \right] \\ & + \left[\begin{aligned} & + I_{YX} \frac{\partial \psi}{\partial q_r} - I_{YZ} \frac{\partial \theta}{\partial q_r} \\ & + I_{XZ} \frac{\partial \psi}{\partial q_r} - I_{XZ} \frac{\partial \phi}{\partial q_r} \\ & - I_{XY} \frac{\partial \phi}{\partial q_r} \end{aligned} \right] \end{aligned} \right]_j \quad (6-51)$$

and finally collecting and grouping terms yields the final and complete definition of the terms of Equation 6-35 for the estimated elemental accelerations.

$$\begin{aligned}
 & \left[\sum_{i=1}^N m_i \begin{pmatrix} \ddot{x} \\ \ddot{y} \\ \ddot{z} \end{pmatrix}_{\text{EST}} \cdot \frac{\partial}{\partial q_r} \begin{pmatrix} x \\ y \\ z \end{pmatrix} \right]_j = \\
 & \left[M \begin{pmatrix} \ddot{x} \\ \ddot{y} \\ \ddot{z} \end{pmatrix} + M\bar{x} \begin{pmatrix} -(r^2+q^2) \\ pq+\dot{r} \\ pr-\dot{q} \end{pmatrix} + M\bar{y} \begin{pmatrix} pq-\dot{r} \\ -(r^2+p^2) \\ qr+\dot{p} \end{pmatrix} + M\bar{z} \begin{pmatrix} pr+\dot{q} \\ qr-\dot{p} \\ -(p^2+q^2) \end{pmatrix} \right] \frac{\partial}{\partial q_r} \begin{pmatrix} x_0 \\ y_0 \\ z_0 \end{pmatrix} \\
 & + M \left[\frac{\partial \phi}{\partial q_r} \begin{pmatrix} 0 \\ -\bar{z}\dot{y} \\ \bar{y}\dot{z} \end{pmatrix} + \frac{\partial \theta}{\partial q_r} \begin{pmatrix} \bar{z}\ddot{x} \\ 0 \\ -\bar{x}\ddot{z} \end{pmatrix} + \frac{\partial \psi}{\partial q_r} \begin{pmatrix} -\bar{y}\ddot{x} \\ \bar{x}\ddot{y} \\ 0 \end{pmatrix} \right] \\
 & + \left[\begin{array}{ccc} I_X(0) & +I_Y\left(-\frac{\partial \psi}{\partial q_r}(pq-\dot{r})\right) & +I_Z\left(\frac{\partial \theta}{\partial q_r}(pr+\dot{q})\right) \\ I_X\left(\frac{\partial \psi}{\partial q_r}(pq+\dot{r})\right) & +I_Y(0) & -I_Z\left(\frac{\partial \phi}{\partial q_r}(qr-\dot{p})\right) \\ -I_X\left(\frac{\partial \theta}{\partial q_r}(pr-\dot{q})\right) & +I_Y\left(\frac{\partial \phi}{\partial q_r}(qr+\dot{p})\right) & +I_Z(0) \end{array} \right] \\
 & + \left[\begin{array}{l} I_{XY}(r^2+q^2) \frac{\partial \psi}{\partial q_r} - I_{XZ}(r^2+q^2) \frac{\partial \theta}{\partial q_r} + I_{YZ}\left((pq-\dot{r}) \frac{\partial \theta}{\partial q_r} - (pr+\dot{q}) \frac{\partial \psi}{\partial q_r}\right) \\ -I_{XY}(r^2+p^2) \frac{\partial \psi}{\partial q_r} + I_{XZ}\left(-(pq+\dot{r}) \frac{\partial \phi}{\partial q_r} + (qr-\dot{p}) \frac{\partial \psi}{\partial q_r}\right) + I_{YZ}(r^2+p^2) \frac{\partial \phi}{\partial q_r} \\ I_{XY}\left((pr-\dot{q}) \frac{\partial \phi}{\partial q_r} - (qr+\dot{p}) \frac{\partial \theta}{\partial q_r}\right) + I_{XZ}(p^2+q^2) \frac{\partial \theta}{\partial q_r} - I_{YZ}(p^2+q^2) \frac{\partial \phi}{\partial q_r} \end{array} \right]_j
 \end{aligned}
 \tag{6-52}$$

where in this case the summation $\sum_{i=1}^N$ represents summation over the jth

rigid body element. With this in mind, substituting Equations 6-52 and 6-37 back into Equation 6-25 yields the complete form of the Lagrange energy equation in constrained coordinates with distributed elemental masses and forces from which the REXOR equations of motion are all developed. Also including these terms as well as the moment terms of Equation 6-37 in Equation 6-35 yields the final form of the equation as used in REXOR. This form will be presented following the development of the generalized mass damping and stiffness matrices.

From Equation 6-33 it is easily seen, by examining the coefficients of the corrective accelerations that generalized mass matrix elements,

M_{rk} , can be written as

$$M_{rk} = \sum_{i=1}^N m_i \left(\frac{\partial x_i}{\partial q_r} \frac{\partial x_i}{\partial q_k} + \frac{\partial y_i}{\partial q_r} \frac{\partial y_i}{\partial q_k} + \frac{\partial z_i}{\partial q_r} \frac{\partial z_i}{\partial q_k} \right) \quad (6-53)$$

This equation is for point masses. Actually, as discussed earlier, the REXOR equations model a set of distributed masses characterized by an overall mass, center of gravity, and moment of inertia values. As shown in the previous section, extension to the distributed mass form is made by describing the particle absolute coordinates in terms of the position of a relative coordinate set in inertial space and the particle position in terms of this relative set as developed in Section 5.4. For a rigid body the associated relative set and the particle associated with the body maintain a fixed relationship. The summing over the particles of the system then becomes a sum over products of masses and lengths yielding mass moment and moment of inertia terms.

The mass elements can be developed by substituting the partial derivatives developed in the preceding discussion. These partials describe both the motion of the mass element reference and also the distributed masses within the rigid body elemental masses.

Substituting these partials, Equations 6-47, 6-48 and 6-49 in the generalized mass expression, Equation 6-53 yields:

$$\begin{aligned}
 M_{rk} = \sum_{i=1}^N m_i & \left(\frac{\partial x_0}{\partial q_r} \frac{\partial x_0}{\partial q_k} - y_i \frac{\partial x_0}{\partial q_r} \frac{\partial x_0}{\partial q_k} + z_i \frac{\partial x_0}{\partial q_r} \frac{\partial \theta}{\partial q_k} - y_i \frac{\partial \psi}{\partial q_r} \frac{\partial x_0}{\partial q_k} \right. \\
 & + y_i^2 \frac{\partial \psi}{\partial q_r} \frac{\partial \psi}{\partial q_k} - y_i z_i \frac{\partial \psi}{\partial q_r} \frac{\partial \theta}{\partial q_k} + z_i \frac{\partial \theta}{\partial q_r} \frac{\partial x_0}{\partial q_k} + y_i z_i \frac{\partial \theta}{\partial q_r} \frac{\partial \psi}{\partial q_k} \\
 & + z_i^2 \frac{\partial \theta}{\partial q_r} \frac{\partial \theta}{\partial q_k} + \frac{\partial y_0}{\partial q_r} \frac{\partial y_0}{\partial q_k} + x_i \frac{\partial y_0}{\partial q_r} \frac{\partial \psi}{\partial q_k} - z_i \frac{\partial y_0}{\partial q_r} \frac{\partial \phi}{\partial q_k} \\
 & + x_i \frac{\partial \psi}{\partial q_r} \frac{\partial y_0}{\partial q_k} + x_i^2 \frac{\partial \psi}{\partial q_r} \frac{\partial \psi}{\partial q_k} - x_i z_i \frac{\partial \psi}{\partial q_r} \frac{\partial \phi}{\partial q_k} - z_i \frac{\partial \phi}{\partial q_r} \frac{\partial y_0}{\partial q_k} \\
 & - z_i x_i \frac{\partial \phi}{\partial q_r} \frac{\partial \psi}{\partial q_k} + z_i^2 \frac{\partial \phi}{\partial q_r} \frac{\partial \phi}{\partial q_k} + \frac{\partial z_0}{\partial q_r} \frac{\partial z_0}{\partial q_k} - x_i \frac{\partial z_0}{\partial q_r} \frac{\partial \phi}{\partial q_k} \\
 & + y_i \frac{\partial z_0}{\partial q_r} \frac{\partial \phi}{\partial q_k} - x_i \frac{\partial \theta}{\partial q_r} \frac{\partial z_0}{\partial q_k} + x_i^2 \frac{\partial \theta}{\partial q_r} \frac{\partial \theta}{\partial q_k} - x_i y_i \frac{\partial \theta}{\partial q_r} \frac{\partial \phi}{\partial q_k} \\
 & \left. + y_i \frac{\partial \phi}{\partial q_r} \frac{\partial z_0}{\partial q_k} - x_i y_i \frac{\partial \phi}{\partial q_r} \frac{\partial \theta}{\partial q_k} + y_i^2 \frac{\partial \phi}{\partial q_r} \frac{\partial \phi}{\partial q_k} \right) \quad (6-54)
 \end{aligned}$$

and using moment of inertia and mass moment definitions:

$$\begin{aligned}
M_{rk} = & M \left(\frac{\partial x}{\partial q_r} \frac{\partial x}{\partial q_k} + \frac{\partial y}{\partial q_r} \frac{\partial y}{\partial q_k} + \frac{\partial z}{\partial q_r} \frac{\partial z}{\partial q_k} \right) + I_{ZZ} \left(\frac{\partial \psi}{\partial q_r} \frac{\partial \psi}{\partial q_k} \right) \\
& + I_{XX} \left(\frac{\partial \phi}{\partial q_r} \frac{\partial \phi}{\partial q_k} \right) + I_{YY} \left(\frac{\partial \theta}{\partial q_r} \frac{\partial \theta}{\partial q_k} \right) + I_{XZ} \left(- \frac{\partial \psi}{\partial q_r} \frac{\partial \phi}{\partial q_k} - \frac{\partial \phi}{\partial q_r} \frac{\partial \psi}{\partial q_k} \right) \\
& + I_{XY} \left(- \frac{\partial \theta}{\partial q_r} \frac{\partial \phi}{\partial q_k} - \frac{\partial \phi}{\partial q_r} \frac{\partial \theta}{\partial q_k} \right) + I_{YZ} \left(- \frac{\partial \psi}{\partial q_r} \frac{\partial \theta}{\partial q_k} - \frac{\partial \theta}{\partial q_r} \frac{\partial \psi}{\partial q_k} \right) \\
& + M\bar{x} \left(\frac{\partial y}{\partial q_r} \frac{\partial \psi}{\partial q_k} + \frac{\partial \psi}{\partial q_r} \frac{\partial y}{\partial q_k} - \frac{\partial \theta}{\partial q_r} \frac{\partial z}{\partial q_k} - \frac{\partial z}{\partial q_r} \frac{\partial \theta}{\partial q_k} \right) \\
& + M\bar{y} \left(- \frac{\partial x}{\partial q_r} \frac{\partial \psi}{\partial q_k} - \frac{\partial \psi}{\partial q_r} \frac{\partial x}{\partial q_k} + \frac{\partial \phi}{\partial q_r} \frac{\partial z}{\partial q_k} + \frac{\partial z}{\partial q_r} \frac{\partial \phi}{\partial q_k} \right) \\
& + M\bar{z} \left(\frac{\partial x}{\partial q_r} \frac{\partial \theta}{\partial q_k} + \frac{\partial \theta}{\partial q_r} \frac{\partial x}{\partial q_k} - \frac{\partial \phi}{\partial q_r} \frac{\partial y}{\partial q_k} - \frac{\partial y}{\partial q_r} \frac{\partial \phi}{\partial q_k} \right)
\end{aligned} \tag{6-55}$$

and is identified as a generalized mass. For orthogonal systems M_{rk} is zero except for $r = k$. The development of REXOR is mostly nonorthogonal coordinates, therefore, the generalized mass matrix has many off-diagonal terms.

Similarly, terms can be developed for the strain (potential) energy and damping functions.

$$\begin{aligned}
U = & \frac{1}{2} \sum_{i=1}^N \left[\left(k_{x_i} x_i^2 + k_{y_i} y_i^2 + k_{z_i} z_i^2 \right) \right. \\
& \left. + \left(K_{\phi_i} \phi_i^2 + K_{\theta_i} \theta_i^2 + K_{\psi_i} \psi_i^2 \right) \right]
\end{aligned} \tag{6-56}$$

$$\begin{aligned}
\frac{\partial U}{\partial q_r} &= \sum_{i=1}^N \left(k_{x_i} x_i \frac{\partial x_i}{\partial q_r} + k_{y_i} y_i \frac{\partial y_i}{\partial q_r} + k_{z_i} z_i \frac{\partial z_i}{\partial q_r} \right. \\
&\quad \left. + K_{\phi_i} \phi_i \frac{\partial \phi_i}{\partial q_r} + K_{\theta_i} \theta_i \frac{\partial \theta_i}{\partial q_r} + K_{\psi_i} \psi_i \frac{\partial \psi_i}{\partial q_r} \right) \\
&= \sum_{i=1}^N \left[k_{x_i} \frac{\partial x_i}{\partial q_r} \sum_{k=1}^n \frac{\partial x_i}{\partial q_k} q_k + k_{y_i} \frac{\partial y_i}{\partial q_r} \sum_{k=1}^n \frac{\partial y_i}{\partial q_k} q_k \right. \\
&\quad \left. + k_{z_i} \frac{\partial z_i}{\partial q_r} \sum_{k=1}^n \frac{\partial z_i}{\partial q_k} q_k + k_{\phi_i} \frac{\partial \phi_i}{\partial q_r} \sum_{k=1}^n \frac{\partial \phi_i}{\partial q_k} q_k \right. \\
&\quad \left. + k_{\theta_i} \frac{\partial \theta_i}{\partial q_r} \sum_{k=1}^n \frac{\partial \theta_i}{\partial q_k} q_k + k_{\psi_i} \frac{\partial \psi_i}{\partial q_r} \sum_{k=1}^n \frac{\partial \psi_i}{\partial q_k} q_k \right] \quad (6-57)
\end{aligned}$$

Define

$$\begin{aligned}
\sum_{i=1}^N \left[k_{x_i} \frac{\partial x_i}{\partial q_r} \frac{\partial x_i}{\partial q_k} + k_{y_i} \frac{\partial y_i}{\partial q_r} \frac{\partial y_i}{\partial q_k} + k_{z_i} \frac{\partial z_i}{\partial q_r} \frac{\partial z_i}{\partial q_k} \right. \\
\left. + k_{\phi_i} \frac{\partial \phi_i}{\partial q_r} \frac{\partial \phi_i}{\partial q_k} + k_{\theta_i} \frac{\partial \theta_i}{\partial q_r} \frac{\partial \theta_i}{\partial q_k} + k_{\psi_i} \frac{\partial \psi_i}{\partial q_r} \frac{\partial \psi_i}{\partial q_k} \right] = K_{rk} \quad (6-58)
\end{aligned}$$

Similarly for damping:

$$\begin{aligned}
\sum_{i=1}^N \left[c_{x_i} \frac{\partial x_i}{\partial q_r} \frac{\partial x_i}{\partial q_k} + c_{y_i} \frac{\partial y_i}{\partial q_r} \frac{\partial y_i}{\partial q_k} + c_{z_i} \frac{\partial z_i}{\partial q_r} \frac{\partial z_i}{\partial q_k} \right. \\
\left. + c_{\phi_i} \frac{\partial \phi_i}{\partial q_r} \frac{\partial \phi_i}{\partial q_k} + c_{\theta_i} \frac{\partial \theta_i}{\partial q_r} \frac{\partial \theta_i}{\partial q_k} + c_{\psi_i} \frac{\partial \psi_i}{\partial q_r} \frac{\partial \psi_i}{\partial q_k} \right] = C_{rk} \quad (6-59)
\end{aligned}$$

The stiffness and damping matrix terms in REXOR are defined with reference to relative coordinates; which parallels the physical configuration. The coordinates used with these terms then should be on a relative basis. This statement at first appears to be contradictory to the premise of the equation development. However, if these matrix terms were defined on an absolute basis the terms other than those associated with a relative motion would be identically zero. The integration of the accelerations produces changes in velocity and position. These changes with the proper starting reference are the relative coordinates and velocities.

Equation 6-35 is now repeated here in a slightly expanded form to include the effect of applied elemental moments, Equation 6-37, and distributed elemental masses, Equation 6-52.

$$\begin{aligned}
 \left\{ \begin{array}{c} \ddot{q}_1 \\ \vdots \\ \ddot{q}_n \end{array} \right\}_{\text{CORR}} &= - \left[\begin{array}{c} M_{rk} \\ \text{MASS} \\ \text{MATRIX} \end{array} \right]^{-1} \left\{ \begin{array}{c} \sum_{i=1}^N \left[\left(m_i \ddot{x}_{i_{\text{EST}}} - F_{x_i} \right) \frac{\partial x_i}{\partial q_1} + M_{x_i} \frac{\partial \phi_i}{\partial q_1} + \dots \right] \\ \vdots \\ \sum_{i=1}^N \left[\left(m_i \ddot{x}_{i_{\text{EST}}} - F_{x_i} \right) \frac{\partial x_i}{\partial q_n} + M_{x_i} \frac{\partial \phi_i}{\partial q_1} + \dots \right] \end{array} \right\} \\
 &\quad \text{(Equation 6-55)} \qquad \qquad \qquad \text{(Sum of Equations 6-37 and 6-52)} \\
 &+ \left[\begin{array}{c} C_{rk} \\ \text{DAMPING} \\ \text{MATRIX} \end{array} \right] \left\{ \begin{array}{c} \dot{q}_1 \\ \vdots \\ \dot{q}_n \end{array} \right\} + \left[\begin{array}{c} K_{rk} \\ \text{STIFFNESS} \\ \text{MATRIX} \end{array} \right] \left\{ \begin{array}{c} q_1 \\ \vdots \\ q_n \end{array} \right\} \qquad (6-60) \\
 &\quad \text{(Equation 6-59)} \qquad \qquad \qquad \text{(Equation 6-58)}
 \end{aligned}$$

Even though Q_r was defined as the generalized forces of the system, for the purpose of further development and of the application of the above equation in the REXOR analysis, each line in the large brackets on the right side of Equation 6-60 will hereafter be referred to as a generalized force or a generalized delta force and will be referred to by the symbol, FR, in the following development.

6.4 OVERVIEW OF ROTOR-BLADE MODEL

Many elements of the rotorcraft can be directly modeled along the lines developed in Sections 6 through 6.2 and systematized in Section 6.5 without further ado. However, there are enough special considerations and concepts involved in modeling the individual blades and combined rotor to justify a separate section to address these topics.

6.4.1 Concept of Modes

The basic textbook principles governing solutions for eigenvalues (natural frequencies) and eigenvectors (mode shapes) for systems of several degrees of freedom can be applied to those of many degrees of freedom. For each independent degree of freedom there is an additional natural frequency and mode shape.

Free vibrations of continuous systems such as beams, or for example the helicopter fuselage, or rotor blades, are generally analyzed mathematically by reducing the system to a system of discrete masses and elastic constraints.

6.4.2 Blade Bending - Modal Variable

The blade is a twisted rotating beam and its analysis requires considering the coupled flapwise-chordwise-torsional response of the blade. For the REXOR analysis, coupled flapwise-chordwise mode shapes are used, upon which is superimposed one of a number of torsional response representations of varying complexity (Sections 5.3.4, 6.4.8, 6.6.5, and 6.6.6).

If one applies generalized coordinates, each blade mode in the analysis may be treated as a single degree of freedom. The generalized coordinates are called normal coordinates for the special case when the modes are orthogonal, in which case the generalized mass matrix reduces to a diagonal matrix, as does the generalized stiffness matrix.

The REXOR analysis uses blade modes calculated for the blade at a fixed rpm, fixed collective, and in an unswept, unconed orientation. Since the program allows for variation of all of these parameters, which is accounted for in the overall REXOR analysis, the predetermined modes become non-orthogonal as used in the program. Thus, blade motion is effectively described by a set of modal variables, each representing a characteristic

frequency, and a set of modal coefficients that describe the relative amplitude of oscillation for each blade segment and each frequency.

Since the modes are nonorthogonal, we will find in REXOR, as would be expected in such a case, off-diagonal coupling terms in both the generalized mass and stiffness matrices. It can readily be shown in cases where generalized or normal coordinates are applied, that relatively few modes need be taken to define accurately the time-history of blade deflection. This assumes that the primary frequencies of excitation fall within the range of modes considered.

Some caution should be applied, however, in interpreting time-histories of moment (stress) or shear. These variables generally represent the second and third spanwise derivatives of the deflection curve. The higher the degree of spanwise derivative, the greater the number of modes required to define it.

However, another unique feature of REXOR is that it actually makes spanwise integration of the blade element aerodynamic and inertial distributed loading functions to compute the moments and shears rather than using the second and third spanwise derivatives of the deflection curve. This approach greatly enhances the accuracy of the internal loads for a given number of modes.

6.4.3 Adapting Modal Description to Variable Geometry

It is noted that the selection of the modal description is such that the periodic reorientation of the structural axis, due to blade feathering and torsional deflection, with respect to the centrifugal force field stiffness is accounted for. This is accomplished by generating blade modes as rotating blade modes for input into the program, generating structural only generalized stiffness terms for each mode, and the couplings between modes. The centrifugal stiffness effects are then included separately within the REXOR program. Thus accounting for the effects of blade feathering, etc., as indicated above.

The blade equations developed in Section 6.6 permit the easy separation of structural and centrifugal stiffness type terms. Including the centrifugal terms in the blade element accelerations and the structural stiffness terms in the expression $\frac{\partial U}{\partial q_r}$ permits accurate simulation of the effect of rotor

speed. Secondly, due to the blade element motion description of Section 5.5.5, the modal structural stiffness, $\frac{\partial U}{\partial q_r}$, remains independent of blade feathering angle in each mode.

This modal development in conjunction with blade torsion as used in the REXOR analysis includes all of the principal terms of the blade motion equations (22, 23, 24) of Reference 9. These equations are repeated here, using the notation of that reference, with the underlined terms being those, amongst others, accounted for in REXOR.

$$\begin{aligned}
 & - \left\{ \left[\underline{\underline{GJ}} + \underline{\underline{Tk_A}}^2 + \underline{\underline{EB_1}}(\beta')^2 \right] \phi' - \underline{\underline{EB_2}}\beta'(v'' \cos\beta + w'' \sin\beta) \right\}' \\
 & + \underline{\underline{Te_A}}(v'' \sin\beta - w'' \cos\beta) + \underline{\Omega^2_{mxe}}(-v' \sin\beta + w' \cos\beta) \\
 & + \underline{\Omega^2_{me} \sin\beta v} + \underline{\Omega^2_m \left[\left(\underline{k_{m2}}^2 - \underline{k_{m1}}^2 \right) \cos 2\beta + \underline{ee_0} \cos\beta \right] \phi} + \underline{mk_m^2 \ddot{\phi}} \\
 & - \underline{me(\ddot{v} \sin\beta - \ddot{w} \cos\beta)} = \underline{M} + (\underline{\underline{Tk_A}}^2 \beta')' \\
 & - \underline{\Omega^2_m \left[\left(\underline{k_{m2}}^2 - \underline{k_{m1}}^2 \right) \sin\beta \cos\beta + \underline{ee_0} \sin\beta \right]} \quad (6-62)
 \end{aligned}$$

$$\begin{aligned}
 & \left[\underline{(\underline{EI_1} \cos^2\beta + \underline{EI_2} \sin^2\beta)w''} + \underline{(\underline{EI_2} - \underline{EI_1}) \sin\beta \cos\beta v''} \right. \\
 & \left. - \underline{\underline{Te_A}}\phi \cos\beta - \underline{\underline{EB_2}}\beta'\phi' \sin\beta \right]'' - \underline{(\underline{Tw'})}' - \underline{(\Omega^2_{mxe}\phi \cos\beta)'} \\
 & + \underline{m(\ddot{w} + e\ddot{\phi} \cos\beta)} = \underline{L_z} + \underline{(\underline{Te_A} \sin\beta)''} + \underline{(\Omega^2_{mxe} \sin\beta)'} \quad (6-63)
 \end{aligned}$$

$$\begin{aligned}
 & \left[\underline{(\underline{EI_2} - \underline{EI_1}) \sin\beta \cos\beta w''} + \underline{\underline{EI_1} \sin^2\beta + \underline{EI_2} \cos^2\beta} v'' \right. \\
 & \left. + \underline{\underline{Te_A}}\phi \sin\beta - \underline{\underline{EB_2}}\beta'\phi' \cos\beta \right]'' - \underline{(\underline{Tv'})}' + \underline{(\Omega^2_{mxe}\phi \sin\beta)'} \\
 & + \underline{\Omega^2_{me}\phi \sin\beta} + \underline{m(\ddot{v} - e\ddot{\phi} \sin\beta)} - \underline{\Omega^2_{mv}} = \underline{L_y} + \underline{(\underline{Te_A} \cos\beta)''} \\
 & + \underline{(\Omega^2_{mxe} \cos\beta)'} + \underline{\Omega^2_m(e_0 + e \cos\beta)} \quad (6-64)
 \end{aligned}$$

In addition to the above terms, a considerable number of nonlinear terms are included in REXOR. These include blade spanwise acceleration, nonlinear Coriolis type terms and feathering moments due to products of flapping loads times inplane deflection with respect to the feathering axis and inplane loads times flapping displacements relative to the feathering axis. Additionally, β as used in REXOR is time dependent and includes the effect of blade pretwist and the instantaneous blade feathering angle due to collective and cyclic including pitch-flap and pitch-lag coupling effects.

The effects of static precone, blade sweep, blade droop, jogs in the structural axis, feathering axis precone, etc., are also included.

6.4.4 Blade Mode Generation

The blade modes can be determined by any appropriate classical method of analysis for coupled flapwise-inplane bending beams. The only requirement is a cantilever (hinge or hingeless) boundary condition for the modes and that the terms included in the homogeneous part of equations 28 and 29 of Reference 9 be accounted for. These equations are repeated here for convenience. Flapwise:

$$\left[(EI_1 \cos^2 \beta + EI_2 \sin^2 \beta) w'' + (EI_2 - EI_1) \sin \beta \cos \beta v'' \right]'' - (Tv')' - \Omega^2 m v + m \ddot{v} = 0 \quad (6-65)$$

and inplanewise:

$$\left[(EI_2 - EI_1) \sin \beta \cos \beta w'' + (EI_1 \sin^2 \beta + EI_2 \cos^2 \beta) v'' \right]'' - (Tv')' - \Omega^2 m v + m \ddot{v} = 0 \quad (6-66)$$

6.4.5 Modal Coefficients

Several additional points need to be made regarding modes in order that the equation development be properly understood. First, the same modal coefficients apply to the first and second time derivatives of the function, since

$$\frac{\partial Z_S}{\partial A_i} = f(x) \quad (6-67)$$

$$\dot{Z}_S = \frac{\partial Z_S}{\partial A_1} \dot{A}_1 + \frac{\partial Z_S}{\partial A_2} \dot{A}_2 + \dots + \frac{\partial Z_S}{\partial A_n} \dot{A}_n \quad (6-68)$$

$$\ddot{Z}_S = \frac{\partial Z_S}{\partial A_1} \ddot{A}_1 + \frac{\partial Z_S}{\partial A_2} \ddot{A}_2 + \dots + \frac{\partial Z_S}{\partial A_n} \ddot{A}_n \quad (6-69)$$

Second, the motion is not necessarily confined to one direction. A given modal frequency may excite or couple with motions in other directions. For example:

$$Y_S = \frac{\partial Y_S}{\partial A_1} A_1 + \frac{\partial Y_S}{\partial A_2} A_2 + \dots + \frac{\partial Y_S}{\partial A_n} A_n \quad (6-70)$$

$$\dot{Y}_S = \frac{\partial Y_S}{\partial A_1} \dot{A}_1 + \frac{\partial Y_S}{\partial A_2} \dot{A}_2 + \dots + \frac{\partial Y_S}{\partial A_n} \dot{A}_n \quad (6-71)$$

$$\ddot{Y}_S = \frac{\partial Y_S}{\partial A_1} \ddot{A}_1 + \frac{\partial Y_S}{\partial A_2} \ddot{A}_2 + \dots + \frac{\partial Y_S}{\partial A_n} \ddot{A}_n \quad (6-72)$$

6.4.6 Independent Blades

In REXOR the blade motions are computed and tracked individually. One set of equations operates on a blade in BLE coordinates as explained in Section 6.4.11. The result for a time step is stored in BLn coordinates for that blade. The operating set in BLE coordinates then performs the computations for the next blade in turn.

6.4.7 Blade Element Aerodynamic Forces - Overview

The functions F_{X_i} , F_{Y_i} , F_{Z_i} , and moment terms from Section 6.2 are

primarily aerodynamic loads for the blade equations. These loads are derived from blade inertial velocity (equivalent to air velocity) and table lookup aerodynamic coefficients as given in Section 7.

6.4.8 Blade Torsional Response

6.4.8.1 Pitch Horn Bending

Several alternate approaches to modeling blade feathering dynamics exist in REXOR. The simplest is to assume the blade is torsionally rigid, and that the flexibility is in the pitch horn.

6.4.8.2 Quasi-Static Blade Torsion

The blade pitch horn bending description is improved by the addition of a blade twist dependent on the moment loading. This quasi-static torsion is computed by integrating the blade pitching moment times the torsional flexibility from tip into the root. (Developed in Sections 5.3.4 and 6.6.5.)

6.4.8.3 Dynamic Blade Torsion

A third approach to blade torsional response in REXOR is an uncoupled torsional mode which operates as additional blade twist. This material is developed in Section 6.6.

6.4.9 Radial Integration

For each element of a rotor blade the equations of motion are formed per Section 6.2.9. As briefly touched on in Section 6.4.6 these data are formed in BLE axis. These elements are summed to total equations for each blade in BLn coordinates at the blade root. This is explained in Section 6.6. These blade root summations are also used in the hub axis (Section 6.9).

6.5 EQUATION SYSTEM DEVELOPMENT

6.5.1 Reference to Base Operation Matrix

The equation of motion, as developed in Sections 6.2 and 6.3 and as presented in most general form by Equation 6-60, may be given in abbreviated form as

$$\left\{ \ddot{q}_r \right\}_{\text{CORR}} = \left[M_{rk} \right]^{-1} \left\{ F_r \right\}_{\text{EST}} \quad (6-73)$$

The M_{rk} 's are the generalized mass matrix elements, the F_r 's are the generalized forces, and the q_r 's the generalized coordinates or degrees of freedom. As explained previously, the F_r 's are the complete set of external forces and internal reactions computed with estimated values of the accelerations, \ddot{q}_{rEST} 's, at the next time point. The \ddot{q}_{rCORR} 's are

then corrections to the estimated values.

The generalized mass, M_{rk} , is developed in Section 6.3. The generalized force may be expanded as (using the point mass form):

$$F_r = - \sum_{i=1}^N \left[m_i \left(\ddot{x}_i \frac{\partial X_i}{\partial q_r} + \ddot{y}_i \frac{\partial Y_i}{\partial q_r} + \ddot{z}_i \frac{\partial Z_i}{\partial q_r} \right) \right] - \frac{\partial B}{\partial \dot{q}_r} - \frac{\partial U}{\partial q_r} + F_{FR_r} + F_{A_r} + F_{c_r} \quad (6-74)$$

The inertia, damping, and elastic terms are developed further in Section 6.3 (see Equation 6-60). The friction force F_{FR_r} , the aerodynamic external forces F_{A_r} , and the pilot control forces F_{c_r} are described as

needed. Note that the potential energy and dissipation terms have been directly included in the force expression. Where the stiffness and damping matrices are simple diagonals, this is done. In the case of the blade equations the distinct stiffness and damping matrix form (Section 6.3) is computed before combining all the applied forces, internal reactions, stiffness and damping terms into an overall force.

6.5.2 Organization by Degrees of Freedom

In developing the equations of motion there are three types of ingredients needed:

- Generalized masses
- Generalized forces
- Partial derivatives (used in both of the above items)

The equation development can then proceed with these ingredients along one of two lines of organization.

- For every major rotorcraft piece (fuselage, rotor, etc.), compute all the ingredients and sort according to degree of freedom for equation use.
- For every degree-of-freedom group, sort through the rotorcraft pieces for applicable ingredients. Sorting is minimal because of close association of degrees of freedom and component parts.

The latter development is used here. The degrees of freedom modeled are given in Figure 5-10.

The following subsections will describe the appropriate partial differentiations, the generalized masses, and the generalized forces in detail. Each generalized mass couples the inertia of one generalized coordinate with another or itself. The algebraic equations for each generalized mass will be given only once. If the reader cannot find a particular mass element under one subsection, he should look into the other subsection relating to the coupled generalized coordinate.

6.5.3 Partial Derivatives

The generalized masses and forces use partial derivatives which describe the variational motion of each physical mass element in rectangular coordinates relative to the motion of each generalized coordinate. The partial derivatives required are determined from the generalized mass and force expressions for distributed masses of Section 6.2. The partial derivatives are easily constructed from the coordinate transformations which have been developed.

In developing the motions of a physical mass element relative to a generalized coordinate, a number of transforms may be used. These can be categorized as either linear or Euler axes transforms which either displace without rotation or rotate without displacement. The overall partial will be the product of partials associated with each of these transforms. The typical form of these partials will now be illustrated.

To obtain the partials, the equations relating the velocities are obtained first. Reviewing Sections 5.4.1 and 5.4.2, the velocity relations of interest are restated. For linear transforms:

$$\begin{Bmatrix} \dot{X} \\ \dot{Y} \\ \dot{Z} \end{Bmatrix}_b = \begin{Bmatrix} \dot{X}_0 \\ \dot{Y}_0 \\ \dot{Z}_0 \end{Bmatrix}_b + \begin{Bmatrix} \dot{X} \\ \dot{Y} \\ \dot{Z} \end{Bmatrix}_a + \begin{bmatrix} 0 & Z_a & -Y_a \\ -Z_a & 0 & X_a \\ Y_a & -X_a & 0 \end{bmatrix} \begin{Bmatrix} p \\ q \\ r \end{Bmatrix}_a \quad (6-75)$$

$$\begin{Bmatrix} p \\ q \\ r \end{Bmatrix}_b = \begin{Bmatrix} p \\ q \\ r \end{Bmatrix}_a \quad (6-76)$$

and for Euler transforms

$$\begin{Bmatrix} \dot{X} \\ \dot{Y} \\ \dot{Z} \end{Bmatrix}_b = [T_{a-b}] \begin{Bmatrix} \dot{X} \\ \dot{Y} \\ \dot{Z} \end{Bmatrix}_a \quad (6-77)$$

$$\begin{Bmatrix} p \\ q \\ r \end{Bmatrix}_b = \begin{Bmatrix} 0 \\ 0 \\ \dot{\psi}_b \end{Bmatrix}_a + [T_\psi] \left\{ \begin{Bmatrix} 0 \\ \dot{\theta}_b \\ 0 \end{Bmatrix}_a + [T_\theta] \left\{ \begin{Bmatrix} \dot{\phi}_b \\ 0 \\ 0 \end{Bmatrix}_a + [T_\phi] \begin{Bmatrix} p \\ q \\ r \end{Bmatrix}_a \right\} \right\} \quad (6-78)$$

The partials of interest are conveniently organized into 3 by 3 matrices. They are for the linear transform:

$$\left[\frac{\partial}{\partial X_{Ob}} \begin{Bmatrix} X \\ Y \\ Z \end{Bmatrix}_b \mid \frac{\partial}{\partial Y_{Ob}} \begin{Bmatrix} X \\ Y \\ Z \end{Bmatrix}_b \mid \frac{\partial}{\partial Z_{Ob}} \begin{Bmatrix} X \\ Y \\ Z \end{Bmatrix}_b \right] = [I] = \begin{bmatrix} 1 & 0 & 0 \\ 0 & 1 & 0 \\ 0 & 0 & 1 \end{bmatrix} \quad (6-79)$$

$$\left[\frac{\partial}{\partial X_a} \begin{Bmatrix} X \\ Y \\ Z \end{Bmatrix}_b \mid \frac{\partial}{\partial Y_a} \begin{Bmatrix} X \\ Y \\ Z \end{Bmatrix}_b \mid \frac{\partial}{\partial Z_a} \begin{Bmatrix} X \\ Y \\ Z \end{Bmatrix}_b \right] = [I] \quad (6-80)$$

$$\left[\frac{\partial}{\partial \phi} \begin{Bmatrix} X \\ Y \\ Z \end{Bmatrix}_b \mid \frac{\partial}{\partial \theta} \begin{Bmatrix} X \\ Y \\ Z \end{Bmatrix}_b \mid \frac{\partial}{\partial \psi} \begin{Bmatrix} X \\ Y \\ Z \end{Bmatrix}_b \right] = \begin{bmatrix} 0 & Z_a & -Y_a \\ -Z_a & 0 & X_a \\ Y_a & -X_a & 0 \end{bmatrix} \quad (6-81)$$

$$\left[\frac{\partial}{\partial X_a} \begin{Bmatrix} \phi \\ \theta \\ \psi \end{Bmatrix}_b \mid \frac{\partial}{\partial Y_a} \begin{Bmatrix} \phi \\ \theta \\ \psi \end{Bmatrix}_b \mid \frac{\partial}{\partial Z_a} \begin{Bmatrix} \phi \\ \theta \\ \psi \end{Bmatrix}_b \right] = [0] \quad (6-82)$$

$$\left[\frac{\partial}{\partial \phi_a} \begin{Bmatrix} \phi \\ \theta \\ \psi \end{Bmatrix}_b \mid \frac{\partial}{\partial \theta_a} \begin{Bmatrix} \phi \\ \theta \\ \psi \end{Bmatrix}_b \mid \frac{\partial}{\partial \psi_a} \begin{Bmatrix} \phi \\ \theta \\ \psi \end{Bmatrix}_b \right] = [I] \quad (6-83)$$

For the Euler angles defined in Section 5.4.2:

$$\left[\frac{\partial}{\partial X_a} \begin{Bmatrix} X \\ Y \\ Z \end{Bmatrix}_b \mid \frac{\partial}{\partial Y_a} \begin{Bmatrix} X \\ Y \\ Z \end{Bmatrix}_b \mid \frac{\partial}{\partial Z_a} \begin{Bmatrix} X \\ Y \\ Z \end{Bmatrix}_b \right] = [T_{a-b}] \quad (6-84)$$

$$\left[\frac{\partial}{\partial \phi_a} \begin{Bmatrix} X \\ Y \\ Z \end{Bmatrix}_b \mid \frac{\partial}{\partial \theta_a} \begin{Bmatrix} X \\ Y \\ Z \end{Bmatrix}_b \mid \frac{\partial}{\partial \psi_a} \begin{Bmatrix} X \\ Y \\ Z \end{Bmatrix}_b \right] = [0] \quad (6-85)$$

$$\left[\frac{\partial}{\partial X_a} \begin{Bmatrix} \phi \\ \theta \\ \psi \end{Bmatrix}_b \mid \frac{\partial}{\partial Y_a} \begin{Bmatrix} \phi \\ \theta \\ \psi \end{Bmatrix}_b \mid \frac{\partial}{\partial Z_a} \begin{Bmatrix} \phi \\ \theta \\ \psi \end{Bmatrix}_b \right] = [0] \quad (6-86)$$

$$\left[\frac{\partial}{\partial \phi_a} \begin{Bmatrix} \phi \\ \theta \\ \psi \end{Bmatrix}_b \mid \frac{\partial}{\partial \theta_a} \begin{Bmatrix} \phi \\ \theta \\ \psi \end{Bmatrix}_b \mid \frac{\partial}{\partial \psi_a} \begin{Bmatrix} \phi \\ \theta \\ \psi \end{Bmatrix}_b \right] = [T_{a-b}] \quad (6-87)$$

$$\left[\frac{\partial}{\partial \phi_b} \begin{Bmatrix} \phi \\ \theta \\ \psi \end{Bmatrix}_b \mid \frac{\partial}{\partial \theta_b} \begin{Bmatrix} \phi \\ \theta \\ \psi \end{Bmatrix}_b \mid \frac{\partial}{\partial \psi_b} \begin{Bmatrix} \phi \\ \theta \\ \psi \end{Bmatrix}_b \right] = \begin{bmatrix} \cos\psi\cos\theta & \sin\psi & 0 \\ -\sin\psi\cos\theta & \cos\psi & 0 \\ 0 & 0 & 1 \end{bmatrix} \quad (6-88)$$

For Euler angles defined in reversed order or reversed sign the last matrix will differ. Note by inspection that rotary to linear derivatives such

as $\frac{\partial \theta}{\partial x}$ are all zero. The derivatives can be strung together to get motion

in a third axis c relative to motion in axis a . Abbreviating the matrices:

$$\begin{bmatrix} \frac{\partial r_c}{\partial \zeta_a} \end{bmatrix} = \begin{bmatrix} \frac{\partial r_c}{\partial r_b} \end{bmatrix} \begin{bmatrix} \frac{\partial r_b}{\partial \zeta_a} \end{bmatrix} + \begin{bmatrix} \frac{\partial r_c}{\partial \zeta_b} \end{bmatrix} \begin{bmatrix} \frac{\partial \zeta_b}{\partial \zeta_a} \end{bmatrix} \quad (6-89)$$

$$\begin{bmatrix} \frac{\partial r_c}{\partial r_a} \end{bmatrix} = \begin{bmatrix} \frac{\partial r_c}{\partial r_b} \end{bmatrix} \begin{bmatrix} \frac{\partial r_b}{\partial r_a} \end{bmatrix} \quad (6-90)$$

$$\begin{bmatrix} \frac{\partial \zeta_c}{\partial r_a} \end{bmatrix} = 0 \quad (6-91)$$

$$\begin{bmatrix} \frac{\partial \zeta_c}{\partial \zeta_a} \end{bmatrix} = \begin{bmatrix} \frac{\partial \zeta_c}{\partial \zeta_b} \end{bmatrix} \begin{bmatrix} \frac{\partial \zeta_b}{\partial \zeta_a} \end{bmatrix} \quad (6-92)$$

assuming in general

$$r_b = r_b(r_a, \zeta_a) \quad (6-93)$$

and

$$\zeta_c = \zeta_c(r_b, \zeta_b) \quad (6-94)$$

The abbreviations used are

$$r = \{X, Y, Z\} \quad (6-95)$$

and

$$\zeta = \{\phi, \theta, \psi\} \quad (6-96)$$

6.5.4 Generalized Masses

As discussed before, the helicopter is assumed composed of a finite number of mass elements. They are the

- fuselage
- tail rotor
- propeller
- engine rotor
- swashplate
- fixed hub
- k mass elements on each of b blades.

The reader should realize the mass matrix is symmetric from the definition of equation (6-33) and interchange of the order of differentiation.

$$M_{kr} = M_{rk} \quad (6-97)$$

Only the elements in the diagonal and the upper right triangle will be given in the following sections.

Each of these mass elements must be summed for each of the generalized mass matrix elements. Each mass is handled with the distributed mass M_{rk} relation of Section 6.2. Fortunately, only the fuselage requires the full equation. The center-of-gravity terms drop out if the mass motion is determined at the center of gravity. This situation is true for the blade line which passes through the center of gravity of the blade section mass elements. Only the fuselage and swashplate have reference axis origin off the center of gravity. Another simplification is that cross products of inertia exist only for the fuselage. Each blade mass element is considered to be in the shape of a rod lying along the chord at the blade station in question.

Certain small terms and factors are dropped from the generalized masses. As discussed in Section 6.3, the equations of motion are solved for small incremental corrections to the accelerations. With this formulation the masses can tolerate approximations as contrasted to the generalized forces. For example, some partials are assumed to be zero or one such as the hub to fuselage partials, which in effect, says the shaft bending deflections are small.

6.5.5 Generalized Forces

The equation formulation, Section 6.3, requires that precision be used in compiling the generalized forces per Equation 6-74, expanded per Section 6.3, Equation 6-60, to include rigid body distributed mass elements. This formulation includes for each degree of freedom:

- Summation over all mass elements of the mass times inertial acceleration times partial derivative. (Section 6.3 expression for distributed masses.)
- External (aerodynamic) loadings times a partial derivative.
- Potential energy and damping terms or assembled stiffness and damping terms with partial derivatives (Section 6.3).

For some degrees of freedom the applicable mass elements and the total integration are directly written as final results which can be verified by inspection. Degrees of freedom that properly include summation over the main rotor blades involve some extensive numerical integrations and complicated coordinate transformations.

6.6 BLADE BENDING AND TORSION EQUATIONS

6.6.1 Blade Radial Summation

The contribution from all the individual blade sections are summed to give the blade generalized masses and forces. These are given for blade root, bending, feathering, and torsion motions. The blade root values are then transformed to the final degree of freedom variables by partial derivatives. The summation is carried out over all elements of the rotorcraft, including the independent blades. Due to the relative isolation of one blade's modes from another, only the 4 by 4 submass matrices along the diagonal of the 4b by 4b rotor matrix are filled, where b is the number of blades.

6.6.2 Partial Derivatives

The generalized masses and forces utilize partials relating the X, Y, Z, ϕ , θ , and ψ linear and rotary motion of each blade element to the blade bending, blade torsion, body, rotor, and swashplate degrees of freedom.

Only the blade bending, torsion, and feathering partials are derived in this section; the blade partials for the body, rotor, and swashplate are to be found in their respective sections.

As developed in Section 5.3.4, the blade torsion may be modeled either as a pitch horn bending or an uncoupled dynamic torsion mode. For the former

case the partial $\frac{\partial \phi_{Fn}}{\partial \beta_{PHn}}$ is a blade spanwise constant multiplier to summa-

tions which couple in the feather angle. In the latter case, $\frac{\partial \phi_{BLE}}{\partial \beta_{PHn}}$ is a function of span and blade number.

The first partials to be considered are those relating motions at any point i on the blade to the rigid body motion of the blade root. These partials are:

$$\left[\frac{\partial (r_{BLE})_{BLn}}{\partial r_{OBLn}} \right] = \begin{bmatrix} \frac{\partial (X_{BLE})_{BLn}}{\partial X_{OBLn}} & \frac{\partial (X_{BLE})_{BLn}}{\partial Y_{OBLn}} & \frac{\partial (X_{BLE})_{BLn}}{\partial Z_{OBLn}} \\ \frac{\partial (Y_{BLE})_{BLn}}{\partial X_{OBLn}} & \frac{\partial (Y_{BLE})_{BLn}}{\partial Y_{OBLn}} & \frac{\partial (Y_{BLE})_{BLn}}{\partial Z_{OBLn}} \\ \frac{\partial (Z_{BLE})_{BLn}}{\partial X_{OBLn}} & \frac{\partial (Z_{BLE})_{BLn}}{\partial Y_{OBLn}} & \frac{\partial (Z_{BLE})_{BLn}}{\partial Z_{OBLn}} \end{bmatrix} = [I] \quad (6-98)$$

$$\left[\frac{\partial (r_{BLE})_{BLn}}{\partial \zeta_{BLn}} \right] = \begin{bmatrix} \frac{\partial (X_{BLE})_{BLn}}{\partial \phi_{BLn}} & \frac{\partial (X_{BLE})_{BLn}}{\partial \theta_{BLn}} & \frac{\partial (X_{BLE})_{BLn}}{\partial \psi_{BLn}} \\ \frac{\partial (Y_{BLE})_{BLn}}{\partial \phi_{BLn}} & \frac{\partial (Y_{BLE})_{BLn}}{\partial \theta_{BLn}} & \frac{\partial (Y_{BLE})_{BLn}}{\partial \psi_{BLn}} \\ \frac{\partial (Z_{BLE})_{BLn}}{\partial \phi_{BLn}} & \frac{\partial (Z_{BLE})_{BLn}}{\partial \theta_{BLn}} & \frac{\partial (Z_{BLE})_{BLn}}{\partial \psi_{BLn}} \end{bmatrix} = \begin{bmatrix} 0 & Z_{BLE} & -Y_{BLE} \\ -Z_{BLE} & 0 & X_{BLE} \\ Y_{BLE} & -X_{BLE} & 0 \end{bmatrix} \quad (6-99)$$

$$\begin{bmatrix} \frac{\partial \zeta_{BLE}}{\partial \zeta_{BLn}} \end{bmatrix} = \begin{bmatrix} \frac{\partial (\phi_{BLE})_{BLE}}{\partial \phi_{BLn}} & \frac{\partial (\phi_{BLE})_{BLE}}{\partial \theta_{BLn}} & \frac{\partial (\phi_{BLE})_{BLE}}{\partial \psi_{BLn}} \\ \frac{\partial (\theta_{BLE})_{BLE}}{\partial \phi_{BLn}} & \frac{\partial (\theta_{BLE})_{BLE}}{\partial \theta_{BLn}} & \frac{\partial (\theta_{BLE})_{BLE}}{\partial \psi_{BLn}} \\ \frac{\partial (\psi_{BLE})_{BLE}}{\partial \phi_{BLn}} & \frac{\partial (\psi_{BLE})_{BLE}}{\partial \theta_{BLn}} & \frac{\partial (\psi_{BLE})_{BLE}}{\partial \psi_{BLn}} \end{bmatrix} = \begin{bmatrix} T_{BLn-BLE} \end{bmatrix} \quad (6-100)$$

Note that X_{BLE} , Y_{BLE} and Z_{BLE} are expressed in blade root coordinates; while ϕ_{BLE} , θ_{BLE} and ψ_{BLE} are in terms of blade element axes aligned with the blade element principal axes.

Next consider the blade Y and Z bending response with respect to the blade bending modes. A number of equations can be used to develop the required expressions. The velocity equations from Section 5.5.5 are selected for ease of analysis. Using cancellation of the dots (Section 6.2):

$$\left(\frac{\partial \dot{Y}(i)_{BLE}}{\partial \dot{A}_{mn}} \right)_{BLn} = \left(\frac{\partial Y(i)_{BLE}}{\partial A_{mn}} \right)_{BLn} \quad (6-101)$$

$$\left(\frac{\partial \dot{Z}(i)_{BLE}}{\partial \dot{A}_{mn}} \right)_{BLn} = \left(\frac{\partial Z(i)_{BLE}}{\partial A_{mn}} \right)_{BLn} \quad (6-102)$$

gives:

$$\begin{aligned}
 & \left\{ \begin{array}{c} 0 \\ \frac{\partial Y_{BLE}}{\partial A_{mn}} \\ \frac{\partial Z_{BLE}}{\partial A_{mn}} \end{array} \right\}_{BLn} = \left[\begin{array}{l} \frac{\partial Z'_{FA}}{\partial A_m} \left[\begin{array}{c} \dot{T}_{Z',FA} \\ T_{Y',FA} \end{array} \right]^T \left[\begin{array}{c} T_{\Delta\phi_F} \\ T_{Y',FA} \end{array} \right]^T \left[\begin{array}{c} T_{Y',FA} \\ T_{Z',FA} \end{array} \right] \\ + \left[\begin{array}{c} T_{Z',FA} \\ T_{Y',FA} \end{array} \right]^T \left[\begin{array}{c} T_{\Delta\phi_f} \\ T_{Y',FA} \end{array} \right]^T \left[\begin{array}{c} T_{Y',FA} \\ \dot{T}_{Z',FA} \end{array} \right] \\ + \frac{\partial Y'_{FA}}{\partial A_m} \left[\begin{array}{c} T_{Z',FA} \\ \dot{T}_{Y',FA} \end{array} \right]^T \left[\begin{array}{c} T_{\Delta\phi_F} \\ T_{Y',FA} \end{array} \right]^T \left[\begin{array}{c} T_{Y',FA} \\ T_{Z',FA} \end{array} \right] \\ + \left[\begin{array}{c} T_{Z',FA} \\ T_{Y',FA} \end{array} \right]^T \left[\begin{array}{c} T_{\Delta\phi_f} \\ \dot{T}_{Y',FA} \end{array} \right]^T \left[\begin{array}{c} T_{Y',FA} \\ T_{Z',FA} \end{array} \right] \\ + \frac{\partial \phi_{Fn}}{\partial A_m} \left[\begin{array}{c} T_{Z',FA} \\ T_{Y',FA} \end{array} \right]^T \left[\begin{array}{c} \dot{T}_{\Delta\phi_F} \\ T_{Y',FA} \end{array} \right]^T \left[\begin{array}{c} T_{Y',FA} \\ T_{Z',FA} \end{array} \right] \end{array} \right] \\
 & \cdot \left\{ \left[\frac{\partial r_{BLE}}{\partial A_{mn}} \right] \left\{ A_{mn} \right\} + \left\{ r_{s_{BLE}} \right\} \right\} \\
 & + \left[\begin{array}{c} T_{Z',FA} \\ T_{Y',FA} \end{array} \right]^T \left[\begin{array}{c} T_{\Delta\phi_F} \\ T_{Y',FA} \end{array} \right]^T \left[\begin{array}{c} T_{Y',FA} \\ T_{Z',FA} \end{array} \right] \left\{ \frac{\partial r_{BLE}}{\partial A_{mn}} \right\} \\
 & - \left\{ \frac{\partial r_{IB}}{\partial A_{mn}} \right\} \right\} + \left\{ \frac{\partial r_{IB}}{\partial A_{mn}} \right\} \quad (6-103)
 \end{aligned}$$

where

$$\begin{aligned}
 \left\{ r_{S_{BLE}} \right\} = & \left[T_{\beta_{FA}} \right]^T \left[T_{\phi_{REF}} \right]^T \left[T_{\beta_{FA}} \right] \left\{ \left[T_{\tau_0} \right]^T \left[T_{\gamma} \right]^T \right. \\
 & \cdot \left\{ \left[T_{\beta_0} \right]^T \left\{ \left[T_{\phi_T} \right]^T \left\{ r_{CG_{BLE}} \right\} - \left[T_{\phi_{TW}} \right]^T - \left[T_{\phi_T} \right]^T \right\} \left\{ r_{sc} \right\} \right\} \\
 & - \left[T_{\beta_0} \right]^T \left\{ r_{SW} \right\} \left. \right\} + \left\{ \left[T_{\beta_0} \right]^T \left\{ r_{SW} \right\} + \left\{ r_{Jog} \right\} \right. \\
 & \left. - \left[T_{\beta_0} \right]^T \left\{ r_p \right\} \right\} + \left\{ \left[T_{\beta_0} \right]^T \left\{ r_p \right\} - \left\{ r_{IB} \right\} \right\} \quad (6-104)
 \end{aligned}$$

$$\left. \begin{aligned} & \frac{\partial Y'_{FA}}{\partial A_m} \\ & \frac{\partial Z'_{FA}}{\partial A_m} \end{aligned} \right\} \text{ Defined Section 5.5.8.} \quad (6-105)$$

and

$$\frac{\partial \phi_F}{\partial A_1} = - C_1 \frac{\partial Y'_{FA}}{\partial A_1} ; \quad \frac{\partial \phi_F}{\partial A_2} = - C_2 \frac{\partial Z'_{FA}}{\partial A_2} ; \quad \frac{\partial \phi_F}{\partial A_3} = - C_3 \frac{\partial Z'_{FA}}{\partial A_3} \quad (6-106)$$

The input coefficient C_1 is a pitch lag coupling. The coefficients,

C_2 and C_3 , are the pitch flap couplings for first and second flap modes.

The existence of two coefficients accounts for the difference in position of the flap (virtual) hinge for the two flap modes. These coefficients are developed further in Section 5.5.8.

Even though these coefficients are referenced to the inplane or flapping slope in the inplane or flapping modes, they are the total pitch-flap-lag coupling in each mode. Therefore, they must account for the effect of both the inplane and flapping feathering axis slope changes in each mode.

The angular derivatives with respect to the blade bending modes are also constructed in the velocity form.

$$\begin{Bmatrix} \frac{\partial p}{\partial \dot{A}_{mn}} \\ \frac{\partial q}{\partial \dot{A}_{mn}} \\ \frac{\partial r}{\partial \dot{A}_{mn}} \end{Bmatrix}_{BLE} = \begin{Bmatrix} \frac{\partial \phi_{BLE}}{\partial A_{mn}} \\ \frac{\partial \theta_{BLE}}{\partial A_{mn}} \\ \frac{\partial \psi_{BLE}}{\partial A_{mn}} \end{Bmatrix}_{BLE} \quad (6-107)$$

Note that the angular derivatives, being applied to local segments, are presented in BLE axis. Referring to Equation 5-125:

$$\begin{Bmatrix} \frac{\partial \phi_{BLE}}{\partial A_{mn}} \\ \frac{\partial \theta_{BLE}}{\partial A_{mn}} \\ \frac{\partial \psi_{BLE}}{\partial A_{mn}} \end{Bmatrix}_{BLE} = \begin{bmatrix} T_{\phi_T} \\ T_{\beta_O} \\ T_Y \\ T_{\tau_O} \\ T_{\beta_{FA}} \end{bmatrix}^T \begin{bmatrix} T_{\phi_{REF}} \\ T_{\beta_{FA}} \end{bmatrix} \cdot \left\{ \begin{Bmatrix} 0 \\ 0 \\ \frac{\partial Y'_{BEND}}{\partial A_{mn}} \end{Bmatrix} + \begin{bmatrix} T_{Y'_{BEND}} \end{bmatrix} \begin{Bmatrix} 0 \\ \frac{-\partial Z'_{BEND}}{\partial A_{mn}} \\ 0 \end{Bmatrix} + \begin{bmatrix} T_{Z'_{BEND}} \\ T_{Z'_{FA}} \\ T_{Y'_{FA}} \end{bmatrix} \begin{Bmatrix} \frac{\partial \phi_{Fn}}{\partial A_{mr}} \\ 0 \\ 0 \end{Bmatrix} \right\} \quad (6-108)$$

From:

$$\begin{Bmatrix} Y'_{\text{BEND}} \\ Z'_{\text{BEND}} \end{Bmatrix} = \begin{bmatrix} Y'_1 & Y'_2 & Y'_3 \\ Z'_1 & Z'_2 & Z'_3 \end{bmatrix} \begin{Bmatrix} A_{1n} \\ A_{2n} \\ A_{3n} \end{Bmatrix} \quad (6-109)$$

Gives:

$$\begin{Bmatrix} \frac{\partial Y'_{\text{BEND}}}{\partial A_{mn}} \\ \frac{\partial Z'_{\text{BEND}}}{\partial A_{mn}} \end{Bmatrix} = \begin{Bmatrix} Y'_m \\ Z'_m \end{Bmatrix} \quad (6-110)$$

Also note that in the same context and argument of Section 5.5.5 the feathering axis slopes, Y'_{FA} and Z'_{FA} have been neglected in the above angular partials.

Derivatives with respect to the blade feathering are also constructed using cancellation of the dots.

$$\begin{Bmatrix} \frac{\partial Y_{\text{BLE}}}{\partial \phi_{Fn}} \\ \frac{\partial Z_{\text{BLE}}}{\partial \phi_{Fn}} \end{Bmatrix} = \begin{Bmatrix} \frac{\partial \dot{Y}_{\text{BLE}}}{\partial \dot{\phi}_{Fn}} \\ \frac{\partial \dot{Z}_{\text{BLE}}}{\partial \dot{\phi}_{Fn}} \end{Bmatrix} \quad (6-111)$$

gives:

$$\begin{Bmatrix} 0 \\ \frac{\partial Y_{BLE}}{\partial \phi_{Fn}} \\ \frac{\partial Z_{BLE}}{\partial \phi_{Fn}} \end{Bmatrix}_{BLn} = \begin{bmatrix} T_{Z', FA} \\ T_{Y', FA} \\ \dot{T}_{\Delta \phi_F} \end{bmatrix}^T \begin{bmatrix} T_{Y', FA} \\ T_{Z', FA} \end{bmatrix} \cdot \left\{ \begin{bmatrix} \frac{\partial r_{BLE}}{\partial A_{mn}} \end{bmatrix} \begin{Bmatrix} A_{mn} \end{Bmatrix} + \begin{Bmatrix} r_{S_{BLE}} \end{Bmatrix} + \begin{Bmatrix} r_{IB} \end{Bmatrix} \right\} \quad (6-112)$$

Similarly, for angular motion:

$$\begin{Bmatrix} \frac{\partial \phi_{BLE}}{\partial \phi_{Fn}} \\ \frac{\partial \theta_{BLE}}{\partial \phi_{Fn}} \\ \frac{\partial \psi_{BLE}}{\partial \phi_{Fn}} \end{Bmatrix}_{BLE} = \begin{bmatrix} T_{\phi_T} \\ T_{\beta_O} \\ T_Y \\ T_{\tau_O} \\ T_{\beta_{FA}} \end{bmatrix}^T \begin{bmatrix} T_{\phi_{REF}} \\ T_{\beta_{FA}} \end{bmatrix} \cdot \begin{bmatrix} T_{Y', BEND} \\ T_{Z', BEND} \end{bmatrix} \begin{bmatrix} T_{Z', FA} \\ T_{Y', FA} \end{bmatrix}^T \begin{Bmatrix} 1 \\ 0 \\ 0 \end{Bmatrix} \approx \begin{Bmatrix} 1 \\ 0 \\ 0 \end{Bmatrix} \quad (\text{as programmed}) \quad (6-113)$$

The partials developed with respect to ϕ_{Fn} are used directly in swash-plate and rotor summations as well as some of the following mass and force

terms. Some terms require a further compounding derivative, $\frac{\partial \phi_{Fn}}{\partial \beta_{PHn}}$, for

the case of the pitch horn bending torsion option. Taking the degree of freedom to be pitch horn angular deflection about the feather axis, the constant is approximately 1/e. For the dynamic torsion option a different set of mass formulations is used in terms of BLE axis, obviating the

need for the compounded derivative. As indicated in Section 5.5.5, expressions inboard of X_{SW} equal expressions outboard of X_{SW} with

$$\begin{bmatrix} T_Y \end{bmatrix} \begin{bmatrix} T_{\tau_0} \end{bmatrix} = \begin{bmatrix} I \end{bmatrix} \quad (6-114)$$

and

$$\{r_{SW}\} = \{r_{jog}\} = \{0\} \quad (6-115)$$

Blade X motions must now be accounted for. The assumption of the neutral axis as the axis of no stretch is discussed in Section 5.5.5 and the derivation of the X motions shown. The equation for the partials in BLn axis for a point on the neutral axis is taken from the formulation for the X velocities:

$$\left(\frac{\partial X(i)_{NA}}{\partial A_{mn}} \right)_{BLn} = \sum_{i=1}^k \left(\frac{- \left(Y(i)_{NA} - Y(i-1)_{NA} \right) \left(\frac{\partial Y(i)_{NA}}{\partial A_{mn}} - \frac{\partial Y(i-1)_{NA}}{\partial A_{mn}} \right)}{X(i)_{NA} - X(i-1)_{NA}} - \left(Z(i)_{NA} - Z(i-1)_{NA} \right) \left(\frac{\partial Z(i)_{NA}}{\partial A_{mn}} - \frac{\partial Z(i-1)_{NA}}{\partial A_{mn}} \right)}{X(i)_{NA} - X(i-1)_{NA}} \right)_{BLn} \quad (6-116)$$

The program data, however, is at the blade center-of-gravity axis. The transfer is:

$$\begin{Bmatrix} \frac{\Delta \partial X(i)_{NA}}{\partial A_{mn}} \\ \frac{\partial Y(i)_{NA}}{\partial A_{mn}} \\ \frac{\partial Z(i)_{NA}}{\partial A_{mn}} \end{Bmatrix}_{BLn} = \begin{Bmatrix} 0 \\ \frac{\partial Y(i)_{BLE}}{\partial A_{mn}} \\ \frac{\partial Z(i)_{BLE}}{\partial A_{mn}} \end{Bmatrix}_{BLn} + \begin{bmatrix} T_{BLn-BLE} \end{bmatrix}^T \begin{Bmatrix} \left(- \frac{\partial \psi_{BLE}}{\partial A_{mr}} \right) Y(i)_{ONA} \\ 0 \\ \left(\frac{\partial \phi_{BLE}}{\partial A_{mn}} \right) Y(i)_{ONA} \end{Bmatrix} \quad (6-117)$$

where the right-hand side elements are from Section 5.5.5 and the previous development of this section. The distance $Y(i)_{ONA} = Y(i)_{NA} - Y(i)_{CG}$ BLE

is the distance the neutral axis is from the center-of-gravity axis,

positive forward. The partials $\frac{\partial Y(i)_{NA}}{\partial A_{mn}}$ and $\frac{\partial Z(i)_{NA}}{\partial A_{mn}}$ are used in the

preceding equation for $\frac{\partial X(i)_{NA}}{\partial A_{mn}}$. $\frac{\Delta \partial X(i)_{NA}}{\partial A_{mn}}$ is then the difference in X

motions between the reference and the neutral axis, and is subtracted from the neutral axis motions:

$$\left(\frac{\partial X(i)_{BLE}}{\partial A_{mn}} \right)_{BLn} = \left(\frac{\partial X(i)_{NA}}{\partial A_{mn}} \right)_{BLn} - \left(\Delta \frac{\partial X(i)_{NA}}{\partial A_{mn}} \right)_{BLn} \quad (6-118)$$

to obtain a center-of-gravity value.

The spanwise variation of X with feathering, $\frac{\partial X(i)_{BLE}}{\partial \phi_{Fn}}$, can be derived

in a manner similar to $\frac{\partial X(i)_{BLE}}{\partial A_{mn}}$. The formulations are:

$$\left(\frac{\partial X(i)_{BLE}}{\partial \phi_{Fn}} \right)_{BLn} = \left(\frac{\partial X(i)_{NA}}{\partial \phi_{Fn}} \right)_{BLn} - \left(\Delta \frac{\partial X(i)_{NA}}{\partial \phi_{Fn}} \right)_{BLn} \quad (6-119)$$

where

$$\begin{Bmatrix} \frac{\Delta \partial X(i)_{NA}}{\partial \phi_{Fn}} \\ \frac{\partial Y(i)_{NA}}{\partial \phi_{Fn}} \\ \frac{\partial Z(i)_{NA}}{\partial \phi_{Fn}} \end{Bmatrix}_{BLn} = \begin{Bmatrix} 0 \\ \frac{\partial Y(i)_{BLE}}{\partial \phi_{Fn}} \\ \frac{\partial Z(i)_{BLE}}{\partial \phi_{Fn}} \end{Bmatrix} + \left[T_{BLn-BLE} \right] \begin{Bmatrix} \left(-\frac{\partial \psi_{BLE}}{\partial \phi_{Fn}} \right) Y(i)_{ONA} \\ 0 \\ \left(\frac{\partial \phi_{BLE}}{\partial \phi_{Fn}} \right) Y(i)_{ONA} \end{Bmatrix} \quad (6-120)$$

and

$$\left(\frac{\partial X(i)_{NA}}{\partial \phi_{Fn}} \right)_{BLn} = \sum_{i=1}^k \left(\frac{- \left(Y(i)_{NA} - Y(i-1)_{NA} \right) \left(\frac{\partial Y(i)_{NA}}{\partial \phi_{Fn}} - \frac{\partial Y(i-1)_{NA}}{\partial \phi_{Fn}} \right)}{X(i)_{NA} - X(i-1)_{NA}} - \frac{\left(Z(i)_{NA} - Z(i-1)_{NA} \right) \left(\frac{\partial Z(i)_{NA}}{\partial \phi_{Fn}} - \frac{\partial Z(i-1)_{NA}}{\partial \phi_{Fn}} \right)}{X(i)_{NA} - X(i-1)_{NA}} \right)_{BLn} \quad (6-121)$$

The program assumes $\left(\frac{\partial X_{BLE}}{\partial \phi_{Fn}} \right)_{BLn}$ to be zero for generalized mass calculations.

This is done because of the latitude possible in the generalized masses and the second order nature of the term. In contrast, the derivative

$\left(\frac{\partial X_{BLE}}{\partial A_{mn}} \right)_{BLn}$ is retained. The partial $\frac{\partial \phi_{BLE}}{\partial \phi_{Fn}}$ is set to unity for

the generalized mass terms. The full equations are used for all these terms in determining the generalized forces.

A simple partial derivative is also needed when $\partial \beta_{PHn}$ is defined as dynamic torsion. Since torsion occurs along the bent and twisted blade line, in blade element axis BLE, only the vertical or normal to chord motion of the shear center is of interest, hence,

$$\frac{\partial Z(i)_{BLE}}{\partial \beta_{PHn}} = \frac{\partial Z(i)_{BLE}}{\partial \phi_{BLE}} \frac{\partial \phi_{BLE}}{\partial \beta_{PHn}} = \left(Y(i)_{SC} - Y(i)_{CG} \right)_{BLE} \frac{\partial \phi_{BLE}}{\partial \beta_{PHn}} \quad (6-122)$$

$\frac{\partial \phi_{BLE}}{\partial \beta_{PHn}}$ is program input for the torsion mode shape.

6.6.3 Generalized Masses

The blade generalized masses in conjunction with partial derivatives couple blade feathering, blade torsion, blade bending, body motions, and rotor tilt. All the blade generalized masses that are assumed to exist

are given in the following table. As mentioned before, $\frac{\partial X_{BLE}}{\partial \phi_{Fn}}$ is assumed

zero and $\frac{\partial \phi_{BLE}}{\partial \phi_{Fn}}$ is assumed one in the program, although it is given in

the table. The blade has a rotary inertia about the center of gravity axis $I_{XX_{BLE}}$. The blade also has inertia $I_{ZZ_{BLE}}$ about a vertical axis,

but its contribution is considered small to the generalized mass and is neglected. This contribution is not neglected in the generalized forces.

The coupling of the dynamic blade torsion with the body is assumed zero (but not for pitch horn bending). The dynamic torsion is taken as a high frequency mode, and is assumed effectively decoupled from rigid body motions of the hub or rotor.

Table 6-1 lists all the terms coupling rotary motion at the blade root,

$M_{\phi_{BLn} \phi_{BLn}}$ and similar terms. However, not all listed are used, as certain

approximations are made in developing the principal axis generalized masses which reduce the number of blade coupling generalized masses needed. Since the mass matrix operates on the acceleration error term rather than the total acceleration, these approximations do not detract from the validity of the results produced.

TABLE 6-1. BLADE GENERALIZED MASSES

Blade Root Coupling

$$M_{Y_{OBLn} \psi_{BLn}} = -M_{Z_{OBLn} \theta_{BLn}} = m_{BLn} X_{CG_{BLn}} = \sum_{i=1}^k \left(X_{BLE}^{(i)} \right)_{BLn} \left(m(i) \right) \quad (6-123)$$

$$M_{Z_{OBLn} \phi_{BLn}} = -M_{X_{OBLn} \psi_{BLn}} = m_{BLn} Y_{CG_{BLn}} = \sum_{i=1}^k \left(Y_{BLE}^{(i)} \right)_{BLn} \left(m(i) \right) \quad (6-124)$$

$$M_{X_{OBLn} \theta_{BLn}} = -M_{Y_{OBLn} \phi_{BLn}} = m_{BLn} Z_{CG_{BLn}} = \sum_{i=1}^k \left(Z_{BLE}^{(i)} \right)_{BLn} \left(m(i) \right) \quad (6-125)$$

$$M_{X_{OBLn} X_{OBLn}} = M_{Y_{OBLn} Y_{OBLn}} = M_{Z_{OBLn} Z_{OBLn}} = m_{BLn} = \sum_{i=1}^k m(i) \quad (6-126)$$

Feather Coupling

$$M_{X_{OBLn} \phi_{Fn}} = \sum_{i=1}^k m(i) \left(\frac{\partial X_{BLE}}{\partial \phi_{Fn}} \right)_{BLn} \quad (6-127)$$

$$M_{Y_{OBLn} \phi_{Fn}} = \sum_{i=1}^k m(i) \left(\frac{\partial Y_{BLE}}{\partial \phi_{Fn}} \right)_{BLn} \quad (6-128)$$

$$M_{Z_{OBLn} \phi_{Fn}} = \sum_{i=1}^k m(i) \left(\frac{\partial Z_{BLE}}{\partial \phi_{Fn}} \right)_{BLn} \quad (6-129)$$

$$M_{\phi_{BLn} \phi_{Fn}} = \sum_{i=1}^k \left[m(i) \left(\frac{\partial Y_{BLE}}{\partial \phi_{BLn}} \frac{\partial Y_{BLE}}{\partial \phi_{Fn}} + \frac{\partial Z_{BLE}}{\partial \phi_{BLn}} \frac{\partial Z_{BLE}}{\partial \phi_{Fn}} \right) + I_{XX_{BLE}} \left(\frac{\partial \phi_{BLE}}{\partial \phi_{BLn}} \frac{\partial \phi_{BLE}}{\partial \phi_{Fn}} \right) \right]_{BLn} \quad (6-130)$$

TABLE 6-1 - Continued

Feather Coupling (Continued)

$$M_{\theta_{BLn} \phi_{Fn}} = \sum_{i=1}^k \left[m(i) \left(\frac{\partial Y_{BLE}}{\partial \theta_{BLn}} \frac{\partial Y_{BLE}}{\partial \phi_{Fn}} + \frac{\partial Z_{BLE}}{\partial \theta_{BLn}} \frac{\partial Z_{BLE}}{\partial \phi_{Fn}} \right) + I_{XX_{BLE}} \left(\frac{\partial \phi_{BLE}}{\partial \theta_{BLn}} \frac{\partial \phi_{BLE}}{\partial \phi_{Fn}} \right) \right]_{BLn} \quad (6-131)$$

$$M_{\psi_{BLn} \phi_{Fn}} = \sum_{i=1}^k \left[m(i) \left(\frac{\partial Y_{BLE}}{\partial \psi_{BLn}} \frac{\partial Y_{BLE}}{\partial \phi_{Fn}} + \frac{\partial Z_{BLE}}{\partial \psi_{BLn}} \frac{\partial Z_{BLE}}{\partial \phi_{Fn}} \right) + I_{XX_{BLE}} \left(\frac{\partial \phi_{BLE}}{\partial \psi_{BLn}} \frac{\partial \phi_{BLE}}{\partial \phi_{Fn}} \right) \right]_{BLn} \quad (6-132)$$

$$M_{\phi_{Fn} \phi_{Fn}} = \sum_{i=1}^k \left[m(i) \left(\left(\frac{\partial X_{BLE}}{\partial \phi_{Fn}} \right)^2 + \left(\frac{\partial Y_{BLE}}{\partial \phi_{Fn}} \right)^2 + \left(\frac{\partial Z_{BLE}}{\partial \phi_{Fn}} \right)^2 \right) + I_{XX_{BLE}} \left(\frac{\partial \phi_{BLE}}{\partial \phi_{Fn}} \frac{\partial \phi_{BLE}}{\partial \phi_{Fn}} \right) \right]_{BLn} \quad (6-133)$$

$$M_{A_{mn} \phi_{Fn}} = \sum_{i=1}^k \left[m(i) \left(\frac{\partial X_{BLE}}{\partial A_{mn}} \frac{\partial X_{BLE}}{\partial \phi_{Fn}} + \frac{\partial Y_{BLE}}{\partial A_{mn}} \frac{\partial Y_{BLE}}{\partial \phi_{Fn}} + \frac{\partial Z_{BLE}}{\partial A_{mn}} \frac{\partial Z_{BLE}}{\partial \phi_{Fn}} \right) + I_{XX_{BLE}} \left(\frac{\partial \phi_{BLE}}{\partial A_{mn}} \frac{\partial \phi_{BLE}}{\partial \phi_{Fn}} \right) \right]_{BLn} \quad (6-134)$$

TABLE 6-1 - Continued

Blade Bending Coupling

$$M_{X_{OBLn} A_{mn}} = \sum_{i=1}^k m(i) \left(\frac{\partial X_{BLE}}{\partial A_{mn}} \right)_{BLn} \quad (6-135)$$

$$M_{Y_{OBLn} A_{mn}} = \sum_{i=1}^k m(i) \left(\frac{\partial Y_{BLE}}{\partial A_{mn}} \right)_{BLn} \quad (6-136)$$

$$M_{Z_{OBLn} A_{mn}} = \sum_{i=1}^k m(i) \left(\frac{\partial Z_{BLE}}{\partial A_{mn}} \right)_{BLn} \quad (6-137)$$

$$M_{\psi_{BLn} A_{mn}} = \sum_{i=1}^k \left[m(i) \left(\frac{\partial X_{BLE}}{\partial \psi_{BLn}} \frac{\partial X_{BLE}}{\partial A_{mn}} + \frac{\partial Y_{BLE}}{\partial \psi_{BLn}} \frac{\partial Y_{BLE}}{\partial A_{mn}} + \frac{\partial Z_{BLE}}{\partial \psi_{BLn}} \frac{\partial Z_{BLE}}{\partial A_{mn}} \right) + I_{XX_{BLE}} \left(\frac{\partial \phi_{BLE}}{\partial \psi_{BLn}} \frac{\partial \phi_{BLE}}{\partial A_{mn}} \right) \right]_{BLn} \quad (6-138)$$

$$M_{A_{mn} A_{mn}} = \sum_{i=1}^k \left[m(i) \left(\frac{\partial X_{BLE}}{\partial A_{mn}} \frac{\partial X_{BLE}}{\partial A_{mn}} + \frac{\partial Y_{BLE}}{\partial A_{mn}} \frac{\partial Y_{BLE}}{\partial A_{mn}} + \frac{\partial Z_{BLE}}{\partial A_{mn}} \frac{\partial Z_{BLE}}{\partial A_{mn}} \right) + I_{XX_{BLE}} \left(\frac{\partial \phi_{BLE}}{\partial A_{mn}} \frac{\partial \phi_{BLE}}{\partial A_{mn}} \right) \right]_{BLn} \quad (6-139)$$

 β_{PHn} Defined As Dynamic Pitch Horn Bending

$$M_{A_{mn} \beta_{PHn}} = M_{A_{mn} \phi_{Fn}} \frac{\partial \phi_{Fn}}{\partial \beta_{PHn}} \quad (6-140)$$

TABLE 6-1 - Continued

 β_{PHn} Defined As Dynamic Pitch Horn Bending (Continued)

$$M_{\beta_{PHn} \beta_{PHn}} = M_{\phi_{Fn} \phi_{Fn}} \left(\frac{\partial \phi_{Fn}}{\partial \beta_{PHn}} \right)^2 \quad (6-141)$$

$$M_{\beta_{PHn} \phi_{Fn}} = M_{\phi_{Fn} \phi_{Fn}} \left(\frac{\partial \phi_{Fn}}{\partial \beta_{PHn}} \right) \quad (\text{used in swashplate}) \quad (6-142)$$

 β_{PHn} Defined As Dynamic Torsion

$$M_{A_{mn} \beta_{PHn}} \approx \sum_{i=1}^k \left[m(i) \left(\frac{\partial Z_{BLE}}{\partial A_{mn}} \right) \left(\frac{\partial Z_{BLE}}{\partial \phi_{BLE}} \right) + I_{XX_{BLE}} \left(\frac{\partial \phi_{BLE}}{\partial A_{mn}} \right)_{BLn} \right] \left(\frac{\partial \phi_{BLE}}{\partial \beta_{PHn}} \right)_{BLn} \quad (6-143)$$

$$M_{\beta_{PHn} \beta_{PHn}} \approx \sum_{i=1}^k \left[m(i) \left(\frac{\partial Z_{BLE}}{\partial \phi_{BLE}} \right)^2 + I_{XX_{BLE}} \right]_{BLn} \left(\frac{\partial \phi_{BLE}}{\partial \beta_{PHn}} \right)_{BLn}^2 \quad (6-144)$$

$$M_{\beta_{PHn} \phi_{Fn}} \approx \sum_{i=1}^k \left[m(i) \left(\frac{\partial Z_{BLE}}{\partial \phi_{Fn}} \right) \left(\frac{\partial Z_{BLE}}{\partial \phi_{BLE}} \right) + I_{XX_{BLE}} \frac{\partial \phi_{BLE}}{\partial \phi_{Fn}} \right]_{BLn} \left(\frac{\partial \phi_{BLE}}{\partial \beta_{PHn}} \right)_{BLn} \quad (6-145)$$

(used in swashplate)

6.6.4 Generalized Forces

The development herein proceeds by first deriving the equations for the loads on an individual blade element. The blade element loads are composed of aerodynamic and inertial components conveniently found in either the blade root axes BLn or the blade element axes BLE. The loads will be summed in BLn axes with the appropriate transformation. The desired equations are:

$$\begin{Bmatrix} F_X^{(i)}_{BLE} \\ F_Y^{(i)}_{BLE} \\ F_Z^{(i)}_{BLE} \end{Bmatrix}_{BLn} = -m(i) \begin{Bmatrix} \ddot{X}^{(i)}_{BLE} \\ \ddot{Y}^{(i)}_{BLE} \\ \ddot{Z}^{(i)}_{BLE} \end{Bmatrix}_{BLn} + \begin{bmatrix} T_{BLn-BLE} \end{bmatrix}^T \begin{Bmatrix} F_{XA}^{(i)}_{BLE} \\ F_{YA}^{(i)}_{BLE} \\ F_{ZA}^{(i)}_{BLE} \end{Bmatrix} \quad (6-146)$$

$$\begin{aligned} \begin{Bmatrix} M_X^{(i)}_{BLE} \\ M_Y^{(i)}_{BLE} \\ M_Z^{(i)}_{BLE} \end{Bmatrix}_{BLn} &= \begin{bmatrix} T_{BLn-BLE} \end{bmatrix}^T \left\{ -I_{XX_{BLE}} \begin{Bmatrix} \dot{p}_{BLE} + \dot{q}_{BLE} r_{BLE} \\ 0 \\ \dot{r}_{BLE} - \dot{p}_{BLE} q_{BLE} \end{Bmatrix} \right. \\ &+ \left. \begin{Bmatrix} M_{XA}^{(i)}_{BLE} \\ 0 \\ 0 \end{Bmatrix}_{BLn} + \begin{Bmatrix} -Y_{CG}^{(i)}_{BLE} F_{ZA}^{(i)}_{BLE} \\ 0 \\ 0 \end{Bmatrix}_{BLn} \right\} \\ &+ \begin{bmatrix} 0 & -Z(i)_{BLE} & Y(i)_{BLE} \\ Z(i)_{BLE} & 0 & -X(i)_{BLE} \\ -Y(i)_{BLE} & X(i)_{BLE} & 0 \end{bmatrix}_{BLn} \begin{Bmatrix} F_X^{(i)}_{BLE} \\ F_Y^{(i)}_{BLE} \\ F_Z^{(i)}_{BLE} \end{Bmatrix}_{BLn} \end{aligned} \quad (6-147)$$

The aerodynamic loads are in BLE axes alignment about the blade reference datum line which is the quarter chord. A transfer through the distance $Y_{CG_{BLE}}$ is made to the aerodynamic moment. To put the data on a common

basis with dynamic terms. The blade aerodynamics is detailed in Section 7. Since only the blade section pitching moment is considered,

$M_{Y_{BLE}} = M_{Z_{BLE}} = 0$. Note the blade element is assumed configured as a

chordwise rod for inertia; hence

$$\left(I_{XX_{BLE}} = I_{ZZ_{BLE}} \text{ and } I_{YY_{BLE}} = 0 \right) \quad (6-148)$$

A number of blade summations are desired. All will be made in BLn axes along the center-of-gravity axis. The loads at the principal reference axes and for rotor tilt make use of the blade root shears and moment. These are simply the sum of the k total blade elements,

$$\begin{Bmatrix} F_{X_{OBLn}} \\ F_{Y_{OBLn}} \\ F_{Z_{OBLn}} \end{Bmatrix} = \sum_{i=1}^k \begin{Bmatrix} F_X^{(i)}_{BLE} \\ F_Y^{(i)}_{BLE} \\ F_Z^{(i)}_{BLE} \end{Bmatrix}_{BLn} \quad (6-149)$$

and likewise for root moments.

$$\begin{Bmatrix} M_{X_{BLn}} \\ M_{Y_{BLn}} \\ M_{Z_{BLn}} \end{Bmatrix} = \sum_{i=1}^k \begin{Bmatrix} M_X^{(i)}_{BLE} \\ M_Y^{(i)}_{BLE} \\ M_Z^{(i)}_{BLE} \end{Bmatrix}_{BLn} \quad (6-150)$$

The summations illustrated above are for the total inertial and aerodynamic components. In a similar manner, the blade root aerodynamic loads are derived. The blade root loads are summed over all the blade to give main aerodynamic loads for downwash computations (Section 7.2.2) in the manner the total main rotor loads are found in Section 6.9.

Feathering moments are used by the swashplate equations of motion. These moments are:

$$\begin{Bmatrix} M_{X_{Fn}} \\ - \\ - \end{Bmatrix} = [T_{BLn-Fn}] \left\{ \begin{Bmatrix} M_{X_{BLn}} \\ M_{Y_{BLn}} \\ M_{Z_{BLn}} \end{Bmatrix} + \begin{bmatrix} 0 & Z_{IB} & -Y_{IB} \\ -Z_{IB} & 0 & X_{IB} \\ Y_{IB} & -X_{IB} & 0 \end{bmatrix}_{BLn} \begin{Bmatrix} F_{X_{OBLn}} \\ F_{Y_{OBLn}} \\ F_{Z_{OBLn}} \end{Bmatrix} \right\} \quad (6-151)$$

where

$$[T_{BLn-Fn}] = \begin{bmatrix} \cos Y'_{FA} & \sin Y'_{FA} & 0 \\ -\sin Y'_{FA} & \cos Y'_{FA} & 0 \\ 0 & 0 & 1 \end{bmatrix} \begin{bmatrix} \cos Z'_{FA} & 0 & \sin Z'_{FA} \\ 0 & 1 & 0 \\ -\sin Z'_{FA} & 0 & \cos Z'_{FA} \end{bmatrix} \quad (6-152)$$

Only the X component is used by the program. The equations above transfer the summed blade loads to the inboard bearing, then transform them to feathering axes. Using the blade root loads is correct when one recalls that the blade is defined as those portions that are feathered; the fixed hub is excluded.

The blade bending generalized forces are now presented. They are:

$$F_{A_{mn}} = \sum_{i=1}^k \left[\left(\frac{\partial X(i)_{BLE}}{\partial A_{mn}} F_{X(i)_{BLE}} + \frac{\partial Y(i)_{BLE}}{\partial A_{mn}} F_{Y(i)_{BLE}} + \frac{\partial Z(i)_{BLE}}{\partial A_{mn}} F_{Z(i)_{BLE}} \right)_{BLn} \right. \\ \left. + \left(\frac{\partial \phi(i)_{BLE}}{\partial A_{mn}} M_{X(i)_{BLE}} + \frac{\partial \psi(i)_{BLE}}{\partial A_{mn}} M_{Z(i)_{BLE}} \right)_{BLn} \right] - \frac{\partial U}{\partial A_{mn}} - \frac{\partial B}{\partial A_{mn}} \quad (6-153)$$

The potential energy is given as:

$$\frac{\partial U}{\partial A_{mn}} = \sum_{j=1}^3 K_{mj} A_{jn} \quad (6-154)$$

where

$$K_{mj} = \int_{\text{ROOT}}^{\text{TIP}} \left(\frac{M_{Yi} M_{Yj}}{EI_{YY}} + \frac{M_{Zi} M_{Zj}}{EI_{ZZ}} \right) dS \quad (6-155)$$

are inputs calculated external to the program from a bending beam model.

EI_{YY} and EI_{ZZ} are the flapping and chord stiffness about axes aligned with the blade element principal axes. The chord and flapping moments, M_{Yi} and M_{Zi} reflect the contribution of the bending moment from the i

(or j) mode. The integration goes from root to tip. The K 's are evaluated for whatever normalized modes are used as program input.

The last equation can be derived from the Bernoulli-Euler law for bending beams:

$$M = \frac{EI}{r} \quad (6-156)$$

where r is a radius of curvature. The strain energy is

$$U = \int_{\text{ROOT}}^{\text{TIP}} \frac{1}{2} \left(M_Y \frac{d\theta}{dS} + M_Z \frac{d\psi}{dS} \right) dS \quad (6-157)$$

Substituting in from the Bernoulli-Euler law and noting that $dS = r_Y d\theta = r_Z d\psi$,

$$U = \int_{\text{ROOT}}^{\text{TIP}} \frac{1}{2} \left(\frac{M_Y^2}{EI_{YY}} + \frac{M_Z^2}{EI_{ZZ}} \right) dS \quad (6-158)$$

Partial differentiation gives

$$\frac{\partial U}{\partial A_{mn}} = \int_{\text{ROOT}}^{\text{TIP}} \left(\frac{M_Y}{EI_{YY}} \frac{M_Y}{A_{mn}} + \frac{M_Z}{EI_{ZZ}} \frac{M_Z}{A_{mn}} \right) dS \quad (6-159)$$

Considering the moments as a linear sum of components from each bending mode, one has:

$$M_Y = \frac{\partial M_Y}{\partial A_{1n}} A_{1n} + \frac{\partial M_Y}{\partial A_{2n}} A_{2n} + \frac{\partial M_Y}{\partial A_{3n}} A_{3n} = \sum_{i=1}^3 M_{Y_i} A_{in} \quad (6-160)$$

and likewise for M_Z . Then, by substitution, the desired equation is obtained.

The damping factor is assumed proportional to the spring rate. This assumption in conjunction with a mechanical lead-lag damper operating at the feather axis with respect to the fixed hub leads to:

$$\frac{\partial B}{\partial \dot{A}_{mn}} = C_S \sum_{j=1}^3 K_{mj} \dot{A}_{jn} + C_{\text{LAG}} \sum_{j=1}^3 \left(\frac{\partial Y'_{FA}}{\partial A_j} A_{jn} \right) \frac{\partial Y'_{FA}}{\partial A_n} \quad (6-161)$$

The coefficients K_{mj} used above can be directly identified with the coefficients K_{rk} developed in Section 6.3. Here the partial derivatives associated with the elemental springs are embodied in the mode shape determinations. The lag damper is restricted to respond only to inplane motion.

The generalized force is developed for pitch horn bending and dynamic torsion. For pitch horn bending,

$$F_{\beta_{PHn}} = M_{Fn} \frac{\partial \phi_{Fn}}{\partial \beta_{PHn}} - K_{\beta_{PHn}} \beta_{PHn} \quad (6-162)$$

where M_{Fn} is the total feather moment as derived in Section 6.10. For the uncoupled dynamic torsion option,

$$F_{\beta_{PHn}} = \sum_{i=1}^k \left(\frac{\partial Z(i)_{BLE}}{\partial \phi_{BLE}} F_Z(i)_{BLE} + M_X(i)_{BLE} \right)_{BLE} \frac{\partial \phi_{BLE}}{\partial \beta_{PHn}} - K_{\beta_{PHn}} \beta_{PHn} \quad (6-163)$$

in BLE axes. Since the blade elements loads are derived in BLn axes, the transform

$$\begin{Bmatrix} - \\ - \\ F_Z(i)_{BLE} \end{Bmatrix} = [{}^{m}_{BLn-BLE}] \begin{Bmatrix} F_X(i)_{BLE} \\ F_Y(i)_{BLE} \\ F_Z(i)_{BLE} \end{Bmatrix}_{BLn} \quad (6-164)$$

is needed. The spring constant can be interpreted as

$$K_{\beta_{PHn}} = M_{\beta_{PHn}} \omega_{\beta_{PHn}}^2 \quad (6-165)$$

where the generalized mass is computed continuously and $\omega_{\beta_{PH}}$ is the

nautral frequency of the uncoupled torsion mode, a program input constant.

6.6.5 Quasi-Static Blade Torsion

To improve the pitch horn bending blade feathering representation a quasi-static blade torsion distribution is introduced. Quasi-static torsion is computed from the structural stiffness, GJ_{SC} , at each station and the

torque $M_{X_{SC}}$ at the shear center. The torque is summed from the tip to

the blade station in question as shown in Section 5.3.4. The increment of twist produced at a blade station j can be displayed as:

$$\tau_T \dot{\phi}_{Tj} + \phi_{Tj} = \frac{M_{X_{SCj}}}{GJ_{SCj}} \quad (6-166)$$

assuming a first-order lag represents the torsional dynamics. The time constant τ_T is chosen to be representative of the blade first torsional mode frequency.

To obtain this result, the available computation elements require some further operations. First, REXOR conducts blade integrations from root to tip, in BL_n axes. To obtain tip to root values:

$$\begin{Bmatrix} F_{X_{BLEj}} \\ F_{Y_{BLEj}} \\ F_{Z_{BLEj}} \\ M_{X_{BLEj}} \\ M_{Y_{BLEj}} \\ M_{Z_{BLEj}} \end{Bmatrix}_{BL_n} = \begin{Bmatrix} F_{X0} \\ F_{Y0} \\ F_{Z0} \\ M_{X0} \\ M_{Y0} \\ M_{Z0} \end{Bmatrix}_{BL_n} - \sum_{i=1}^j \begin{Bmatrix} F_{X_{BLE}(i)} \\ F_{Y_{BLE}(i)} \\ F_{Z_{BLE}(i)} \\ M_{X_{BLE}(i)} \\ M_{Y_{BLE}(i)} \\ M_{Z_{BLE}(i)} \end{Bmatrix}_{BL_n} \quad (6-167)$$

Note the summation is conducted from root to the station j in question. Thus the j represents a summation whereas the i represents a blade station.

Second, these data are used to form the required torque at the shear center.

$$\begin{Bmatrix} M_{X_{SCj}} \\ - \\ - \end{Bmatrix}_{BL_n} = \begin{bmatrix} 1 & Y'_{SC} & Z'_{SC} \\ - & - & - \\ - & - & - \end{bmatrix} \begin{Bmatrix} M_{X_{BLEj}} \\ M_{Y_{BLEj}} \\ M_{Z_{BLEj}} \end{Bmatrix}_{BL_n} + \begin{bmatrix} 0 & Z_{SC} & -Y_{SC} \\ -Z_{SC} & 0 & X_{SC} \\ Y_{SC} & -X_{SC} & 0 \end{bmatrix}_{BL_n} \begin{Bmatrix} F_{X_{BLEj}} \\ F_{Y_{BLEj}} \\ F_{Z_{BLEj}} \end{Bmatrix}_{BL_n} \quad (6-168)$$

Small angles are assumed. The moments $\begin{pmatrix} M_{X_{BLE}} \\ M_{Y_{BLE}} \\ M_{Z_{BLE}} \end{pmatrix}_{BLn}$ etc., act along the

BLn axes and hence the matrix of lengths $\begin{pmatrix} X_{SC} \\ Y_{SC} \\ Z_{SC} \end{pmatrix}_{BLn}$ etc., are employed to

obtain moments at the shear center which are then transformed into shear center axes, subscripted SC, parallel to blade element center-of-gravity axes, subscripted BLE.

The blade deflections and slope in BLn are also needed for the above expressions.

$$\begin{Bmatrix} X_{SC} \\ Y_{SC} \\ Z_{SC} \end{Bmatrix}_{BLn} = \begin{Bmatrix} X_{BLE} \\ Y_{BLE} \\ Z_{BLE} \end{Bmatrix}_{BLn} + \begin{bmatrix} T_{BLn-BLE} \end{bmatrix}^T \begin{Bmatrix} 0 \\ Y_{SC} - Y_{CG} \\ 0 \end{Bmatrix}_{BLE} \quad (6-169)$$

and

$$\begin{Bmatrix} 0 \\ Y'_{SC} \\ Z'_{SC} \end{Bmatrix}_{BLn} \cong \begin{Bmatrix} 0 \\ Y'_{BLE} \\ Z'_{BLE} \end{Bmatrix}_{BLn} \quad (6-170)$$

6.6.6 Quasi-Static Pitch Horn Bending

To facilitate troubleshooting numerical instability problems an optional quasi-static pitch horn bending degree of freedom is available. The computation elements are the same as developed in Section 6.6.4 except that the solution does not use generalized masses, is therefore an uncoupled mode, and is calculated externally to the main computation flow. The formulation used is:

$$\tau_{PH} \dot{\phi}_{FnPH} + \phi_{FnPH} = \frac{M_{Fn}}{K_{\beta_{PH}}} \quad (6-171)$$

The dynamics are assumed represented by a first-order lag with τ_{PH} as the time constant. The variable ϕ_{FnPH} is used to distinguish this formulation from the usual β_{PHn} symbology.

6.7 ROTOR TILT EQUATIONS

As an interim measure, the capability to model teetering rotor systems has been included in REXOR by the partial redefinition of the available blade degrees of freedom. The methodology is to utilize blade positions $n=1$ and $n=3$ to represent the rotor and suppress blade matrix positions $n=2$ and $n=4$.

The four degrees of freedom per blade are used as follows:

- #1 First Inplane (no change)
- #2 Coning (first flap-collective)
- #3 Teetering (first flap-cyclic)
- #4 Blade Torsion (currently not used)

The inplane calculations proceed as usual. Currently the hard swashplate option is specified with the interim teetering modeling. This means kinematic relations are used between command functions and blade angles produced. The fourth mode, β_{PHn} , therefore is not used.

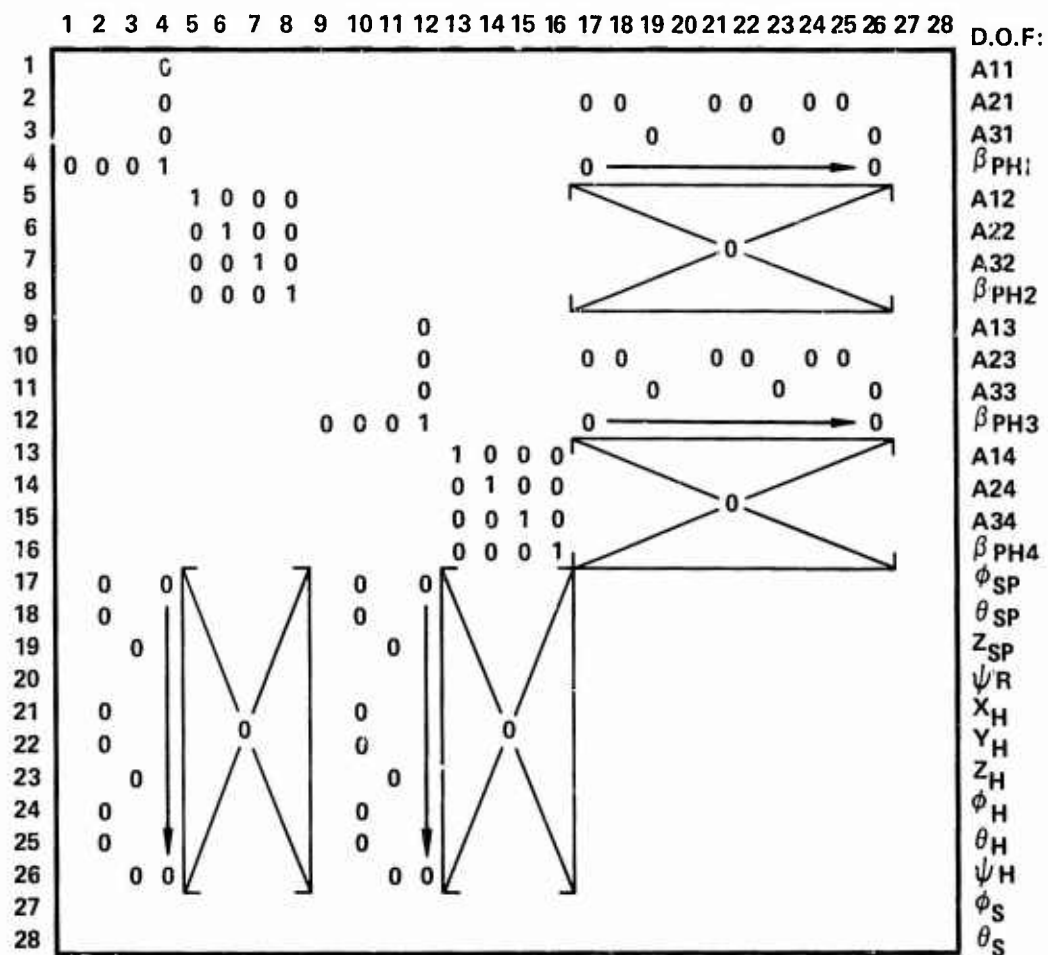
Positions 2 and 3 are programmed to be blade flapping modes, and proper generalized forces and masses will be generated assuming the modal data is entered. A fixed root restraint mode shape, coning, is used for mode #2, and a pinned connection pair mode shape (teetering) is used for mode #3. A rigid flapping mode (straight line) will also work for the teetering mode.

To generate coning preferentially in mode #2 and teetering in mode #3 the opposite type is nulled from each mode. This is done as follows:

- Coning Blade #1 = $1/2$ (Blade #1 + #3)
- Coning Blade #3 = $1/2$ (Blade #1 + #3)
- Teetering Blade #1 = $1/2$ (Blade #1 - #3)
- Teetering Blade #3 = $-1/2$ (Blade #1 - #3)

This procedure is used for the blade generalized forces and accelerations.

Modifications are made to the generalized mass matrix. As shown in Figure 6-2, the elements involved with the unused blade positions 2 and 4 are zeroed except for diagonal ones to prevent singularities. Note that the teetering is associated with roll, pitch, longitudinal, and lateral hub velocities; whereas coning gives rise to yaw and vertical velocities. The remaining zeroes shown in Figure 6-2 remove the teetering coupling with coning associated hub motions and vice versa.



ELEMENTS NOT MARKED (0) OR (1) ARE
USED AS CALCULATED

Figure 6-2. Teetering Rotor Mass Matrix Modifications

The remaining element of the teetering representation is the hub undersling (Z_{OBL}), which is taken positive above the teeter axis. The effect is approximately modeled by shifting the final blade X coordinate by the undersling times the teeter mode root angle.

$$\left(X(i)_{BLE} \right)_{BLn} = \left(X(i)_{BLE} \right)_{BLn} - Z_{OBL} \left(\frac{\partial Z'}{\partial A_3} \right)_{i=0} A_{3n} \quad (6-172)$$

$$\left(\dot{X}(i)_{BLE} \right)_{BLn} = \left(\dot{X}(i)_{BLE} \right)_{BLn} - Z_{OBL} \left(\frac{\partial Z'}{\partial A_3} \right)_{i=0} \dot{A}_{3n} \quad (6-173)$$

$$\left(\ddot{X}(i)_{BLE} \right)_{BLn} = \left(\ddot{X}(i)_{BLE} \right)_{BLn} - Z_{OBL} \left(\frac{\partial Z'}{\partial A_3} \right)_{i=0} \ddot{A}_{3n} \quad (6-174)$$

$$\left(\frac{\partial X(i)}{\partial A_3} \right)_{BLn} = \left(\frac{\partial X(i)}{\partial A_3} \right)_{BLn} - Z_{OBL} \left(\frac{\partial Z'}{\partial A_3} \right)_{i=0} \quad (6-175)$$

6.8 SHAFT BENDING EQUATIONS

6.8.1 Prime Contributions From Fuselage

The shaft equations of motion involve only the fuselage and shaft forces and masses. This simplification results from the hub axes being the principal axes. Therefore, only derivatives of elements physically connected to the shaft branch of the system, i.e., the fuselage, need be considered.

6.8.2 Partial Derivatives

The needed partial derivatives are those relating fuselage motions to shaft bending motions. The reader should recall that shaft roll right and nose up are positive for hub motions in fuselage axes. Here the interest is in fuselage motions in hub axes where fuselage roll left and nose down

are positive. The desired derivatives are obtained from the fuselage equations of Section 5.5.2.

$$\frac{\partial}{\partial \phi_S} \begin{Bmatrix} X_{OF} \\ Y_{OF} \\ Z_{OF} \end{Bmatrix} = [T_{H-F}] \begin{Bmatrix} 0 \\ \frac{\partial Y_F}{\partial \phi_S} \\ 0 \end{Bmatrix} \quad (6-176)$$

$$\frac{\partial}{\partial \theta_S} \begin{Bmatrix} X_{OF} \\ Y_{OF} \\ Z_{OF} \end{Bmatrix} = [T_{H-F}] \begin{Bmatrix} \frac{\partial X_F}{\partial \theta_S} \\ 0 \\ 0 \end{Bmatrix} \quad (6-177)$$

$$\frac{\partial}{\partial \phi_S} \begin{Bmatrix} \phi_F \\ \theta_F \\ \psi_F \end{Bmatrix} = \begin{Bmatrix} -1 \\ 0 \\ 0 \end{Bmatrix} \quad (6-178)$$

$$\frac{\partial}{\partial \theta_S} \begin{Bmatrix} \phi_F \\ \theta_F \\ \psi_F \end{Bmatrix} = \begin{Bmatrix} 0 \\ -\cos \phi_S \\ -\sin \phi_S \end{Bmatrix} \quad (6-179)$$

where the $[T_{H-F}]$ elements are given in Section 5.5.2.

6.8.3 Generalized Masses

Table 6-2 lists the generalized masses. It includes cross-coupling terms with the principal axis. Note that only upper diagonal terms are given. The lower diagonal terms are obtained by symmetry. Certain terms are judged negligible and are dropped.

TABLE 6-2. GENERALIZED MASSES

Shaft Axis Generalized Masses

$$M_{\phi_S \phi_S} = I_{XX_F} + m_F \left[\left(\frac{\partial Y_F}{\partial \phi_S} \right)^2 + 2Z_{CG_F} \frac{\partial Y_F}{\partial \phi_S} \right] + I_{XX_{ENG}} + I_{XX_{TR}} + I_{XX_P} \quad (6-180)$$

$$M_{\phi_S \theta_S} = - I_{XY_F} \quad (6-181)$$

$$M_{\phi_S X_H} = 0 \quad (6-182)$$

$$M_{\phi_S Y_H} = m_F \left(\frac{\partial Y_F}{\partial \phi_S} + Z_{CG_F} \right) \quad (6-183)$$

$$M_{\phi_S Z_H} = - m_F Y_{CG_F} \quad (6-184)$$

$$M_{\phi_S \phi_H} = - I_{XX_F} + m_F \left[\frac{\partial Y_F}{\partial \phi_S} \frac{\partial Y_F}{\partial \phi_H} + Z_{CG_F} \frac{\partial Y_F}{\partial \phi_H} - Z_{CG_F} \frac{\partial Y_F}{\partial \phi_S} \right] - I_{XX_{ENG}} - I_{XX_{TR}} - I_{XX_P} \quad (6-185)$$

$$M_{\phi_S \theta_H} = I_{XY_F} \quad (6-186)$$

$$M_{\phi_S \psi_H} = I_{XZ_F} + m_F X_{CG_F} \frac{\partial Y_F}{\partial \phi_S} \quad (6-187)$$

$$M_{\theta_S \theta_S} = I_{YY_F} + m_F \left[\left(\frac{\partial X_F}{\partial \theta_S} \right)^2 - 2Z_{CG_F} \frac{\partial X_F}{\partial \theta_S} - 2Y_{CG_F} \frac{\partial X_F}{\partial \theta_S} \frac{\partial \psi_F}{\partial \theta_S} \right] - 2I_{YZ_F} \frac{\partial \psi_F}{\partial \theta_S} + I_{YY_{ENG}} + I_{YY_{TR}} + I_{YY_P} \quad (6-188)$$

TABLE 6-2 - Continued

Shaft Axis Generalized Masses (Continued)

$$M_{\theta_S X_H} = m_F \left(\frac{\partial X_F}{\partial \theta_S} - Y_{CG_F} \frac{\partial \psi_F}{\partial \theta_S} - Z_{CG_F} \right) \quad (6-189)$$

$$M_{\theta_S Y_H} = m_F X_{CG_F} \frac{\partial \psi_F}{\partial \theta_S} \quad (6-190)$$

$$M_{\theta_S Z_H} = m_F X_{CG_F} \quad (6-191)$$

$$M_{\theta_S \phi_H} = I_{XY_F} + m_F X_{CG_F} \frac{\partial Y_F}{\partial \phi_H} \frac{\partial \psi_F}{\partial \theta_S} - I_{XZ_F} \frac{\partial \psi_F}{\partial \theta_S} \quad (6-192)$$

$$M_{\theta_S \theta_H} = -I_{YY_F} + m_F \left[\frac{\partial X_F}{\partial \theta_S} \frac{\partial X_F}{\partial \theta_H} - Y_{CG_F} \frac{\partial \psi_F}{\partial \theta_S} \frac{\partial X_F}{\partial \theta_H} + Z_{CG_F} \frac{\partial X_F}{\partial \theta_S} - Z_{CG_F} \frac{\partial X_F}{\partial \theta_H} \right] \\ - I_{YZ_F} \frac{\partial \psi_F}{\partial \theta_S} - I_{YY_{ENG}} - I_{YY_{TR}} - I_{YY_P} \quad (6-193)$$

$$M_{\theta_S \psi_H} = I_{YZ_F} + I_{ZZ} \frac{\partial \psi_F}{\partial \theta_S} - m_F Y_{CG} \frac{\partial X_F}{\partial \theta_S} \quad (6-194)$$

6.8.4 Generalized Forces

Table 6-3 gives the generalized forces for the shaft bending degrees of freedom. As mostly fuselage masses and inertias are involved, the contributions less the multiplying partial derivative are the same as those for the fuselage part of the principal axis generalized forces. The expansion of these terms is referred to in Section 6.9, and only referenced in the following table. The strain energy and dissipation terms are simple diagonals for shaft bending. Rather than carry these in the stiffness and damping matrices (Section 6.3), they are incorporated into the generalized force at this point.

TABLE 6-3. GENERALIZED FORCES

Shaft Axis Generalized Forces

$$F_{\phi_S} = F_{Y_F} \frac{\partial Y_{OF}}{\partial \phi_S} + M_{X_F} \frac{\partial \phi_F}{\partial \phi_S} + M_{Z_F} \frac{\partial \psi_F}{\partial \phi_S} - \frac{\partial U}{\partial \phi_S} - \frac{\partial B}{\partial \phi_S} \quad (6-195)$$

$$F_{\theta_S} = F_{X_F} \frac{\partial X_{OF}}{\partial \theta_S} + M_{X_F} \frac{\partial \phi_F}{\partial \theta_S} + M_{Z_F} \frac{\partial \psi_F}{\partial \theta_S} - \frac{\partial U}{\partial \theta_S} - \frac{\partial B}{\partial \theta_S} \quad (6-196)$$

where:

$$\frac{\partial U}{\partial \phi_S} = K_{\phi_S} \phi_S + R_{SPS} \frac{\partial U}{\partial \phi_{SP}} \quad (6-197)$$

$$\frac{\partial U}{\partial \theta_S} = K_{\theta_S} \theta_S + R_{SPS} \frac{\partial U}{\partial \theta_{SP}} \quad (6-198)$$

$$\frac{\partial B}{\partial \phi_S} = C_{\phi_S} \dot{\phi}_S + R_{SPS} \frac{\partial B}{\partial \phi_{SP}} \quad (6-199)$$

$$\frac{\partial B}{\partial \theta_S} = C_{\theta_S} \dot{\theta}_S + R_{SPS} \frac{\partial B}{\partial \theta_{SP}} \quad (6-200)$$

where K_{ϕ_S} , K_{θ_S} , C_{ϕ_S} , C_{θ_S} are constants and $R_{SPS} = \frac{\partial \phi'_{SP}}{\partial \phi_S} = \frac{\partial \theta'_{SP}}{\partial \theta_S} =$ constant where ϕ'_{SP} and θ'_{SP} are equivalent motions of the swashplate if the swashplate springs were infinite.

6.9 PRINCIPAL REFERENCE AXIS EQUATIONS

6.9.1 Nonzero Contributions From Most Vehicle Mass Elements

The principal reference axis equations of motion consider contributions from most of the physical elements of the rotorcraft. The elements involved are:

- Main rotor - defined as all portions that can be feathered
- Rotor hub - includes all portions of the main rotor assembly that cannot be feathered, and is treated as a rigid body
- Swashplate
- Tail rotor
- Propeller (if used)
- Fuselage
- Engine

The internal control gyro (if used) contribution is considered negligible.

The six rigid degrees of freedom: $X, Y, Z, \phi, \theta, \psi$ are taken with respect to the stationary hub axes which are also the principal axes. The origin lies on the main rotor shaft where it is intercepted by the rotor reference line.

The other elements considered are then referenced to the hub axes. The fuselage is subject to shaft bending motions relative to the principal axes. The tail rotor, the propeller, and the engine are installed on the fuselage and rotate at the main rotor speed times the appropriate gear ratio. Positive rotations are defined as:

- Hub
 - Swashplate
- } same as main rotor
- Propeller - Counterclockwise looking forward
 - Tail rotor - Clockwise looking right
 - Engine - Counterclockwise looking forward

The propeller and engine are treated as rigid rotating bodies; the tail rotor is also allowed to flap (teetering hinge, etc.). This flapping is considered secondary and enters only into the aerodynamic computations. The main rotor is allowed a variety of motions; teetering, feathering, bending, and twisting.

6.9.2 Partial Derivatives

A prime ingredient for the equations of motion, Section 6.3, as outlined in Section 6.5, are the partial derivatives. First considering partial derivatives concerning the fuselage set with respect to the hub set,

$$\begin{bmatrix} \frac{\partial r_{OF}}{\partial r_{OH}} \end{bmatrix} = \begin{bmatrix} \frac{\partial}{\partial X_{OH}} \begin{Bmatrix} X_{OF} \\ Y_{OF} \\ Z_{OF} \end{Bmatrix} \mid \frac{\partial}{\partial Y_{OH}} \begin{Bmatrix} X_{OF} \\ Y_{OF} \\ Z_{OF} \end{Bmatrix} \mid \frac{\partial}{\partial Z_{OH}} \begin{Bmatrix} X_{OF} \\ Y_{OF} \\ Z_{OF} \end{Bmatrix} \end{bmatrix} = [T_{H-F}] \quad (6-201)$$

$$\begin{bmatrix} \frac{\partial \zeta_F}{\partial \zeta_H} \end{bmatrix} = \begin{bmatrix} \frac{\partial}{\partial \phi_H} \begin{Bmatrix} \phi_F \\ \theta_F \\ \psi_F \end{Bmatrix} \mid \frac{\partial}{\partial \theta_F} \begin{Bmatrix} \phi_F \\ \theta_F \\ \psi_F \end{Bmatrix} \mid \frac{\partial}{\partial \psi_F} \begin{Bmatrix} \phi_F \\ \theta_F \\ \psi_F \end{Bmatrix} \end{bmatrix} = [T_{H-F}] \quad (6-202)$$

$$\begin{bmatrix} \frac{\partial r_{OF}}{\partial \zeta_H} \end{bmatrix} = \begin{bmatrix} \frac{\partial}{\partial \phi_H} \begin{Bmatrix} X_{OF} \\ Y_{OF} \\ Z_{OF} \end{Bmatrix} \mid \frac{\partial}{\partial \theta_H} \begin{Bmatrix} X_{OF} \\ Y_{OF} \\ Z_{OF} \end{Bmatrix} \mid \frac{\partial}{\partial \psi_H} \begin{Bmatrix} X_{OF} \\ Y_{OF} \\ Z_{OF} \end{Bmatrix} \end{bmatrix} = [T_{H-F}]$$

$$\begin{bmatrix} 0 & Z_{OF} & -\phi_S \frac{\partial Y_F}{\partial \phi_S} \\ -Z_{OF} & 0 & \theta_S \frac{\partial X_F}{\partial \theta_S} \\ \phi_S \frac{\partial Y_F}{\partial \phi_S} & -\theta_S \frac{\partial X_F}{\partial \theta_S} & 0 \end{bmatrix} \quad (6-203)$$

As usual, partials relating rotary motions to linear motions are zero. For certain applications, the shaft bending is small and some small terms

in the partial equation can be neglected. Note in the above, the axis notation is left off where the axis notation is the same as the mass element notation. For example,

$$\frac{\partial \left(X_{OF} \right)_F}{\partial \left(X_{OH} \right)_H} = \frac{\partial X_{OF}}{\partial X_{OH}} \quad (6-204)$$

Next the hub-to-blade root partial derivatives are given.

$$\begin{aligned} \left[\frac{\partial r_{OBLn}}{\partial r_H} \right] &= \left[\frac{\partial}{\partial X_H} \begin{Bmatrix} X_{OBLn} \\ Y_{OBLn} \\ Z_{OBLn} \end{Bmatrix} \mid \frac{\partial}{\partial Y_H} \begin{Bmatrix} X_{OBLn} \\ Y_{OBLn} \\ Z_{OBLn} \end{Bmatrix} \mid \frac{\partial}{\partial Z_H} \begin{Bmatrix} X_{OBLn} \\ Y_{OBLn} \\ Z_{OBLn} \end{Bmatrix} \right] = \left[T_{R-BLn} \right] \left[T_{H-R} \right] \\ &= \begin{bmatrix} -\cos(\psi_R + \psi_{BLn}) & \sin(\psi_R + \psi_{BLn}) & 0 \\ \sin(\psi_R + \psi_{BLn}) & \cos(\psi_R + \psi_{BLn}) & 0 \\ 0 & 0 & -1 \end{bmatrix} \end{aligned} \quad (6-205)$$

$$\left[\frac{\partial \zeta_{BLn}}{\partial \zeta_H} \right] = \left[\frac{\partial}{\partial \theta_H} \begin{Bmatrix} \phi_{BLn} \\ \theta_{BLn} \\ \psi_{BLn} \end{Bmatrix} \mid \frac{\partial}{\partial \theta_H} \begin{Bmatrix} \phi_{BLn} \\ \theta_{BLn} \\ \psi_{BLn} \end{Bmatrix} \mid \frac{\partial}{\partial \psi_H} \begin{Bmatrix} \phi_{BLn} \\ \theta_{BLn} \\ \psi_{BLn} \end{Bmatrix} \right] = \left[T_{R-BLn} \right] \left[T_{H-R} \right] \quad (6-206)$$

$$\left[\frac{\partial r_{OBLn}}{\partial \zeta_H} \right] = 0 \quad (6-207)$$

$$\left[\frac{\partial r_{BLE}}{\partial r_H} \right]_{BLn} = \left[\frac{\partial r_{BLE}}{\partial r_{OBLn}} \right]_{BLn} \left[\frac{\partial r_{OBLn}}{\partial r_H} \right] \quad (6-208)$$

$$\left[\frac{\partial r_{BLE}}{\partial \zeta_H} \right]_{BLn} = \left[\frac{\partial r_{BLE}}{\partial r_{OBLn}} \right]_{BLn} \left[\frac{\partial r_{OBLn}}{\partial \zeta_H} \right] + \left[\frac{\partial r_{BLE}}{\partial \zeta_{BLn}} \right]_{BLn} \left[\frac{\partial \zeta_{BLn}}{\partial \zeta_H} \right] \quad (6-209)$$

$$\left[\frac{\partial \zeta_{BLE}}{\partial \zeta_H} \right]_{BLn} = \left[\frac{\partial \zeta_{BLE}}{\partial \zeta_{BLn}} \right]_{BLn} \left[\frac{\partial \zeta_{BLn}}{\partial \zeta_H} \right] \quad (6-210)$$

$$\left[\frac{\partial \zeta_{SP}}{\partial \zeta_H} \right] = \left[T_{H-SP} \right] = \begin{bmatrix} \cos \theta_{SP} & \sin \theta_{SP} \sin \phi_{SP} & -\sin \theta_{SP} \cos \phi_{SP} \\ 0 & \cos \phi_{SP} & \sin \phi_{SP} \\ \sin \theta_{SP} & -\sin \phi_{SP} \cos \theta_{SP} & \cos \phi_{SP} \cos \theta_{SP} \end{bmatrix} \quad (6-211)$$

Note that all the rotary-to-linear partials like $\frac{\partial \phi(i)_{BLE}}{\partial X_{OH}}$ are zero. In

deriving these derivatives the relationship

$$\begin{bmatrix} 0 & -r & q \\ r & 0 & -p \\ -q & p & 0 \end{bmatrix} \begin{Bmatrix} X \\ Y \\ Z \end{Bmatrix} = \begin{bmatrix} 0 & Z & -Y \\ -Z & 0 & X \\ Y & -X & 0 \end{bmatrix} \begin{Bmatrix} p \\ q \\ r \end{Bmatrix} \quad (6-212)$$

is helpful in moving the rotary quantities from a matrix to a vector.

Derivatives properly ought to be taken for the other physical elements that have been considered for the principal axis degrees of freedom. Omission of the swashplate partials could be serious for swashplate mass and inertia that are significant compared to the fuselage and rotor. Derivatives for the other rotating elements are covered for the constant rotational speed in the fuselage derivatives. The variable rotational speed case is estimated to develop third or fourth order chain rule derivatives, and therefore can be safely neglected.

6.9.3 Generalized Masses

Table 6-4 lists the generalized masses. Note that small terms are dropped from the generalized mass equations but not from the generalized forces. This is justified because as discussed in Section 6.3, the equations of motion are solved for small increment corrections to the accelerations. With such a formulation, the generalized masses operate only on acceleration errors, and can tolerate approximations.

The swashplate and the hub motions are given in the principal axes. The hub motions apply to the hub center of gravity which is assumed to be at the origin of the principal axes. The swashplate, however, can be displaced vertically from that origin. The fuselage reference axis origin is taken to be directly below the principal axes. Note the fuselage mass and center of gravity include the propeller, tail rotor, and engine, but the moment of inertia excludes these items.

The terms can be checked by inspection from the overall generalized mass formulation of Section 6.3 and the preceding partial derivatives.

6.9.4 Generalized Forces

As pointed out in Section 6.5, the generalized forces contain both the external forcing terms (F_{x_i} , etc.) and the internal reaction terms

such as $m_i \ddot{x}_i$. The latter is entered with a negative sign so that terms such as $m_i \ddot{x}_i - F_{x_i}$ from Section 6.3 are properly compiled.

The loads associated with the six principal reference axis degrees of freedom are listed in Table 6-5. The propeller, tail rotor, main rotor, and engine are assumed to have shafts parallel to the fuselage reference axes. The transfer of the aerodynamic loads from tail rotor axes with origin at hub center and parallel to the fuselage reference axes is shown in the table. The propeller is similar. The fuselage aerodynamic loads are assumed to already be in the fuselage reference axes. Further development of the main rotor blade component loads is in Section 6.6.1 and the aerodynamics for all rotors and fixed surfaces is left to Section 7.

TABLE 6-4. PRINCIPAL AXIS GENERALIZED MASSES

$$M_{\phi_H^A mn} = \sum_{i=1}^k \left[m(i) \left(\frac{\partial X_{BLE}}{\partial \phi_H} \frac{\partial X_{BLE}}{\partial A_{mn}} + \frac{\partial Y_{BLE}}{\partial \phi_H} \frac{\partial Y_{BLE}}{\partial A_{mn}} + \frac{\partial Z_{BLE}}{\partial \phi_H} \frac{\partial Z_{BLE}}{\partial A_{mn}} \right) + I_{XX_{BLE}} \frac{\partial \phi_{BLE}}{\partial \phi_H} \frac{\partial \phi_{BLE}}{\partial A_{mn}} \right]_{BLn} \quad (6-213)$$

$$M_{\theta_H^A mn} = \sum_{i=1}^k \left[m(i) \left(\frac{\partial X_{BLE}}{\partial \theta_H} \frac{\partial X_{BLE}}{\partial A_{mn}} + \frac{\partial Y_{BLE}}{\partial \theta_H} \frac{\partial Y_{BLE}}{\partial A_{mn}} + \frac{\partial Z_{BLE}}{\partial \theta_H} \frac{\partial Z_{BLE}}{\partial A_{mn}} \right) + I_{XX_{BLE}} \frac{\partial \phi_{BLE}}{\partial \theta_H} \frac{\partial \phi_{BLE}}{\partial A_{mn}} \right]_{BLn} \quad (6-214)$$

$$M_{\psi_H^A mn} = \sum_{i=1}^k \left[m(i) \left(\frac{\partial X_{BLE}}{\partial \psi_H} \frac{\partial X_{BLE}}{\partial A_{mn}} + \frac{\partial Y_{BLE}}{\partial \psi_H} \frac{\partial Y_{BLE}}{\partial A_{mn}} + \frac{\partial Z_{BLE}}{\partial \psi_H} \frac{\partial Z_{BLE}}{\partial A_{mn}} \right) + I_{XX_{BLE}} \frac{\partial \phi_{BLE}}{\partial \psi_H} \frac{\partial \phi_{BLE}}{\partial A_{mn}} \right]_{BLn} \quad (6-215)$$

$$M_{X_H^A mn} = \frac{\partial X_{OBLn}}{\partial X_H} M_{X_{OBLn}^A mn} + \frac{\partial Y_{OBLn}}{\partial X_H} M_{Y_{OBLn}^A mn} \quad (6-216)$$

$$M_{Y_H^A mn} = \frac{\partial X_{OBLn}}{\partial Y_H} M_{X_{OBLn}^A mn} + \frac{\partial Y_{OBLn}}{\partial Y_H} M_{Y_{OBLn}^A mn} \quad (6-217)$$

$$M_{Z_H^A mn} = \frac{\partial Z_{OBLn}}{\partial Z_H} M_{Z_{OBLn}^A mn} \quad (6-218)$$

TABLE 6-4 - Continued

$$M_{\phi_H \phi_{Fn}} = \sum_{i=1}^k \left[m(i) \left(\frac{\partial Y_{BLE}}{\partial \phi_H} \frac{\partial Y_{BLE}}{\partial \phi_{Fn}} + \frac{\partial Z_{BLE}}{\partial \phi_H} \frac{\partial Z_{BLE}}{\partial \phi_{Fn}} \right) + I_{XX_{BLE}} \frac{\partial \phi_{BLE}}{\partial \phi_H} \frac{\partial \phi_{BLE}}{\partial \phi_{Fn}} \right]_{BLn} \quad (6-219)$$

$$M_{\theta_H \phi_{Fn}} = \sum_{i=1}^k \left[m(i) \left(\frac{\partial Y_{BLE}}{\partial \theta_H} \frac{\partial Y_{BLE}}{\partial \phi_{Fn}} + \frac{\partial Z_{BLE}}{\partial \theta_H} \frac{\partial Z_{BLE}}{\partial \phi_{Fn}} \right) + I_{XX_{BLE}} \frac{\partial \phi_{BLE}}{\partial \theta_H} \frac{\partial \phi_{BLE}}{\partial \phi_{Fn}} \right]_{BLn} \quad (6-220)$$

$$M_{\psi_H \phi_{Fn}} = \sum_{i=1}^k \left[m(i) \left(\frac{\partial Y_{BLE}}{\partial \psi_H} \frac{\partial Y_{BLE}}{\partial \phi_{Fn}} + \frac{\partial Z_{BLE}}{\partial \psi_H} \frac{\partial Z_{BLE}}{\partial \phi_{Fn}} \right) + I_{XX_{BLE}} \frac{\partial \phi_{BLE}}{\partial \psi_H} \frac{\partial \phi_{BLE}}{\partial \phi_{Fn}} \right] \quad (6-221)$$

$$M_{X_H X_H} = m_H \quad (6-222)$$

$$M_{Y_H Y_H} = m_H \quad (6-223)$$

$$M_{Z_H Z_H} = m_H \quad (6-224)$$

$$M_{X_H Y_H} = M_{X_H Z_H} = M_{Y_H Z_H} = 0 \quad (6-225)$$

TABLE 6-4 - Continued

$$M_{\phi_H \phi_H} = I_{XX_F} + m_F (Z_{OF}^2 + 2Z_{CG_F} Z_{OF}) + I_{XX_R} + I_{XX_{SP}} \\ + m_{SP} (Z_{SP} + Z_{OSP})^2 + I_{XX_H} + I_{XX_{ENG}} + I_{XX_{TR}} + I_{XX_P} \quad (6-226)$$

$$M_{\phi_H X_H} = 0 \quad (6-227)$$

$$M_{\phi_H Y_H} = -m_H Z_{CG_H} \quad (6-228)$$

$$M_{\phi_H Z_H} = m_H Y_{CG_H} \quad (6-229)$$

$$M_{\theta_H \phi_H} = -I_{XY_F} - I_{XY_R} \quad (6-230)$$

$$M_{\theta_H \theta_H} = I_{YY_F} + m_F (Z_{OF}^2 + 2Z_{CG_F} Z_{OF}) + I_{YY_R} + I_{YY_{SP}} \\ + m_{SP} (Z_{SP} + Z_{CSP})^2 + I_{YY_H} + I_{YY_{ENG}} + I_{YY_{TR}} + I_{YY_P} \quad (6-231)$$

where Z_{SP} , Z_{OSP} are explained in Section 5.5.6.

$$M_{\theta_H X_H} = m_H Z_{CG_H} \quad (6-232)$$

$$M_{\theta_H Y_H} = 0 \quad (6-233)$$

$$M_{\theta_H Z_H} = -m_H X_{CG_H} \quad (6-234)$$

$$M_{\psi_H \phi_H} = -I_{XZ_F} - m_F Z_{OF} X_{CG_F} - I_{XZ_R} \quad (6-235)$$

TABLE 6-4 - Continued

$$M_{\psi_H \theta_H} = -I_{YZ_F} - m_F Z_{OF} Y_{CG_F} - I_{YZ_R} \quad (6-236)$$

$$M_{\psi_H \psi_H} = I_{ZZ_F} + I_{ZZ_R} + I_{ZZ_{SP}} + I_{ZZ_H} + I_{ZZ_{ENG}} + I_{ZZ_{TR}} + I_{ZZ_P} \quad (6-237)$$

$$M_{\psi_H X_H} = -m_H Y_{CG_H} \quad (6-238)$$

$$M_{\psi_H Y_H} = m_H X_{CG_H} \quad (6-239)$$

$$M_{\psi_H Z_H} = 0 \quad (6-240)$$

where the following weight and balance relations hold.

$$m_R = \sum_{i=1}^n m_{BLn} \quad (6-241)$$

$$m_H = m_F + m_{SP} + m_{HUB} + m_R \quad (6-242)$$

$$I_{XX_H} = I_{YY_H} = I_{ZZ_H} / 2 \quad (6-243)$$

$$I_{XX_{SP}} = I_{YY_{SP}} = I_{ZZ_{SP}} / 2 \quad (6-244)$$

TABLE 6-4 - Continued

$$\begin{bmatrix} I_{XX_R} & -I_{XY_R} & -I_{XZ_R} \\ -I_{YX_R} & I_{YY_R} & -I_{YZ_R} \\ -I_{ZX_R} & -I_{ZY_R} & I_{ZZ_R} \end{bmatrix} = \begin{bmatrix} T_{H-R} \end{bmatrix}^T \sum_{n=1}^b \begin{bmatrix} T_{R-BLn} \end{bmatrix}^T$$

$$\cdot \begin{bmatrix} I_{XX} & 0 & 0 \\ 0 & I_{YY} & 0 \\ 0 & 0 & I_{ZZ} \end{bmatrix}_{BLn} \begin{bmatrix} T_{R-BLn} \end{bmatrix} \begin{bmatrix} T_{H-R} \end{bmatrix} \quad (6-245)$$

$$\begin{Bmatrix} I_{XX_{BLn}} \\ I_{YY_{BLn}} \\ I_{ZZ_{BLn}} \end{Bmatrix} \cong \sum_{i=1}^k m(i) \begin{Bmatrix} 0 \\ X^2(i)_{CG,BLE} \\ X^2(i)_{CG,BLE} \end{Bmatrix}_{BLn} \quad (6-246)$$

$$\begin{Bmatrix} X_{CG_{BLn}} \\ Y_{CG_{BLn}} \\ Z_{CG_{BLn}} \end{Bmatrix}_H = \begin{bmatrix} T_{H-R} \end{bmatrix}^T \begin{bmatrix} T_{R-BLn} \end{bmatrix}^T \begin{Bmatrix} X_{CG_{BLn}} \\ Y_{CG_{BLn}} \\ Z_{CG_{BLn}} \end{Bmatrix} \quad (6-247)$$

$$X_{CG_R} = \sum_{n=1}^b \left(X_{CG_{BLn}} \right)_H / b \quad (6-248)$$

TABLE 6-4 - Continued

$$Y_{CG_R} = \sum_{n=1}^b (Y_{CG_{BLn}})_H / b \quad (6-249)$$

$$Z_{CG_R} = \sum_{n=1}^b (Z_{CG_{BLn}})_H / b \quad (6-250)$$

$$X_{CG_H} = \left[m_R X_{CG_R} + m_F \left(X_{CG_F} + \theta_S \frac{\partial X_F}{\partial \theta_S} \right) \right] / m_H \quad (6-251)$$

$$Y_{CG_H} = \left[m_R Y_{CG_R} + m_F \left(Y_{CG_F} + \phi_S \frac{\partial Y_F}{\partial \phi_S} \right) \right] / m_H \quad (6-252)$$

$$Z_{CG_H} = \left[m_R Z_{CG_R} + m_F \left(Z_{CG_F} + Z_{OF} \right) + m_{SP} \left(Z_{SP} + Z_{OSP} \right) \right] / m_H \quad (6-253)$$

For pitch horn bending option:

$$M_{X_H \beta_{PHn}} = \frac{\partial Y_{OBLn}}{\partial X_H} \frac{\partial \phi_{Fn}}{\partial \beta_{PHn}} M_{Y_{OBLn} \phi_{Fn}} \quad (6-254)$$

$$M_{Y_H \beta_{PHn}} = \frac{\partial Y_{OBLn}}{\partial Y_H} \frac{\partial \phi_{Fn}}{\partial \beta_{PHn}} M_{Y_{OBLn} \phi_{Fn}} \quad (6-255)$$

$$M_{Z_H \beta_{PHn}} = \frac{\partial Z_{OBLn}}{\partial Z_H} \frac{\partial \phi_{Fn}}{\partial \beta_{PHn}} M_{Z_{OBLn} \phi_{Fn}} \quad (6-256)$$

TABLE 6-4 - Continued

$$M_{\phi_H^{\beta} PHn} = \frac{\partial \phi_{Fn}}{\partial \beta_{PHn}} \left[\frac{\partial \phi_{BLn}}{\partial \phi_H} M_{\phi_{BLn} \phi_{Fn}} + \frac{\partial \theta_{BLn}}{\partial \phi_H} M_{\theta_{BLn} \phi_{Fn}} \right] \quad (6-257)$$

$$M_{\theta_H^{\beta} PHn} = \frac{\partial \phi_{Fn}}{\partial \beta_{PHn}} \left[\frac{\partial \phi_{BLn}}{\partial \theta_H} M_{\phi_{BLn} \phi_{Fn}} + \frac{\partial \theta_{BLn}}{\partial \theta_H} M_{\theta_{BLn} \phi_{Fn}} \right] \quad (6-258)$$

$$M_{\psi_H^{\beta} PHn} = \frac{\partial \phi_{Fn}}{\partial \beta_{PHn}} \left[\frac{\partial \psi_{BLn}}{\partial \psi_H} M_{\psi_{BLn} \phi_{Fn}} \right] \quad (6-259)$$

$$M_{\psi_R^{\beta} PHn} = \frac{\partial \phi_{Fn}}{\partial \beta_{PHn}} M_{\psi_R \phi_{Fn}} \quad (6-260)$$

For dynamic torsion option:

$$\left[M_{r_H^{\beta} PHn} \right] = 0 \quad (6-261)$$

$$\left[M_{\zeta_H^{\beta} PHn} \right] = 0 \quad (6-262)$$

$$M_{\psi_R^{\beta} PHn} = 0 \quad (6-263)$$

TABLE 6-5. PRINCIPAL AXIS GENERALIZED FORCES

$$F_{X_H} = F_{X_F} \frac{\partial X_{OF}}{\partial X_{OH}} + F_{Y_F} \frac{\partial Y_{OF}}{\partial X_{OH}} + F_{Z_F} \frac{\partial Z_{OF}}{\partial X_{OH}} + \left(F_{X_{MR}} \right)_H - m_H \ddot{X}_H - m_{SP} \ddot{X}_H \quad (6-264)$$

$$F_{Y_H} = F_{X_F} \frac{\partial X_{OF}}{\partial Y_{OH}} + F_{Y_F} \frac{\partial Y_{OF}}{\partial Y_{OH}} + F_{Z_F} \frac{\partial Z_{OF}}{\partial Y_{OH}} + \left(F_{Y_{MR}} \right)_H - m_H \ddot{Y}_H - m_{SP} \ddot{Y}_H \quad (6-265)$$

$$F_{Z_H} = F_{X_F} \frac{\partial X_{OF}}{\partial Z_{OH}} + F_{Y_F} \frac{\partial Y_{OF}}{\partial Z_{OH}} + F_{Z_F} \frac{\partial Z_{OF}}{\partial Z_{OH}} + \left(F_{Z_{MR}} \right)_H - m_H \ddot{Z}_H - m_{SP} \ddot{Z}_{OSP} \quad (6-266)$$

$$\begin{aligned} F_{\phi_H} = & F_{X_F} \frac{\partial X_{OF}}{\partial \phi_H} + F_{Y_F} \frac{\partial Y_{OF}}{\partial \phi_H} + F_{Z_F} \frac{\partial Z_{OF}}{\partial \phi_H} + M_{X_F} \frac{\partial \phi_F}{\partial \phi_H} + M_{Y_F} \frac{\partial \theta_F}{\partial \phi_H} \\ & + M_{Z_F} \frac{\partial \psi_F}{\partial \phi_H} + \left(M_{X_{MR}} \right)_H - I_{XX_H} (\dot{p}_H + q_H r_H) + I_{ZZ_H} \dot{\psi}_R q_H \\ & - \left(\frac{I_{ZZ_{SP}}}{2} + m_{SP} (Z_{SP} + Z_{OSP})^2 \right) (\dot{p}_{SP} + q_{SP} r_{SP}) + I_{ZZ_{SP}} \dot{\psi}_R q_{SP} \end{aligned} \quad (6-267)$$

$$\begin{aligned} F_{\theta_H} = & F_{X_F} \frac{\partial X_{OF}}{\partial \theta_H} + F_{Y_F} \frac{\partial Y_{OF}}{\partial \theta_H} + F_{Z_F} \frac{\partial Z_{OF}}{\partial \theta_H} + M_{X_F} \frac{\partial \phi_F}{\partial \theta_H} + M_{Y_F} \frac{\partial \theta_F}{\partial \theta_H} \\ & + M_{Z_F} \frac{\partial \psi_F}{\partial \theta_H} + \left(M_{Y_{MR}} \right)_H - I_{ZZ_{SP}} \dot{\psi}_R p_{SP} - I_{YY_H} (\dot{q}_H - p_H r_H) \\ & - I_{ZZ_H} \dot{\psi}_R p_H - \left(\frac{I_{ZZ_{SP}}}{2} + m_{SP} (Z_{SP} + Z_{CSP})^2 \right) (\dot{q}_{SP} - p_{SP} r_{SP})_{NR} \end{aligned} \quad (6-268)$$

TABLE 6-5 - Continued

$$\begin{aligned}
F_{\psi_H} = & F_{X_F} \frac{\partial X_{OF}}{\partial \psi_H} + F_{Y_F} \frac{\partial Y_{OF}}{\partial \psi_H} + F_{Z_F} \frac{\partial Z_{OF}}{\partial \psi_H} + M_{X_F} \frac{\partial \phi_F}{\partial \psi_H} + M_{Y_F} \frac{\partial \theta_F}{\partial \psi_H} \\
& + M_{Z_F} \frac{\partial \psi_F}{\partial \psi_H} + \left(M_{Z_{MR}} \right)_H - I_{ZZ_H} (\dot{r}_H - \ddot{\psi}_R) - I_{ZZ_{SP}} (\dot{r}_{SP_{NR}} - \ddot{\psi}_R)
\end{aligned}
\tag{6-269}$$

where:

$$F_{X_F} = F_{X_{IF}} + F_{X_{AP}} + F_{X_{ATR}} + F_{X_{AF}} \tag{6-270}$$

$$M_{X_F} = M_{X_{IF}} + M_{X_{AP}} + M_{X_{ATR}} + M_{X_{AF}} \tag{6-271}$$

$$F_{Y_F} = F_{Y_{IF}} + F_{Y_{AP}} + F_{Y_{ATR}} + F_{Y_{AF}} \tag{6-272}$$

$$M_{Y_F} = M_{Y_{IF}} + M_{Y_{AP}} + M_{Y_{ATR}} + M_{Y_{AF}} \tag{6-273}$$

$$F_{Z_F} = F_{Z_{IF}} + F_{Z_{AP}} + F_{Z_{ATR}} + F_{Z_{AF}} \tag{6-274}$$

$$M_{Z_F} = M_{Z_{IF}} + M_{Z_{AP}} + M_{Z_{ATR}} + M_{Z_{AF}} \tag{6-275}$$

$$\begin{aligned}
F_{X_{IF}} = & -m_F \left(\ddot{X}_{OF} - X_{CG_F} (q_F^2 + r_F^2) - Y_{CG_F} (\dot{r}_F - p_F q_F) \right. \\
& \left. + Z_{CG_F} (\dot{q}_F + p_F r_F) \right)
\end{aligned}
\tag{6-276}$$

$$\begin{aligned}
F_{Y_{IF}} = & -m_F \left(\ddot{Y}_{OF} - Y_{CG_F} (p_F^2 + r_F^2) - Z_{CG_F} (\dot{p}_F - q_F r_F) \right. \\
& \left. + X_{CG_F} (\dot{r}_F + p_F q_F) \right)
\end{aligned}
\tag{6-277}$$

TABLE 6-5 - Continued

$$F_{Z_{IF}} = -m_F \left(\ddot{z}_{OF} - z_{CG_F} (\dot{p}_F^2 + \dot{q}_F^2) - x_{CG_F} (\dot{q}_F - p_F r_F) + y_{CG_F} (\dot{p}_F + q_F r_F) \right) \quad (6-278)$$

$$M_{X_{IF}} = M_{X_{IP}} + M_{X_{ITR}} + M_{X_{IENG}} - \left[I_{XX_F} \dot{p}_F + (I_{ZZ_F} - I_{YY_F}) q_F r_F + I_{XY_F} (p_F r_F - \dot{q}_F) + I_{XZ_F} (-p_F q_F - \dot{r}_F) + I_{YZ_F} (r_F^2 - q_F^2) + m_F (-z_{CG_F} \ddot{y}_F + y_{CG_F} \ddot{z}_F) \right] \quad (6-279)$$

$$M_{Y_{IF}} = M_{Y_{IP}} + M_{Y_{ITR}} + M_{Y_{IENG}} - \left[I_{YY_F} \dot{q}_F + (I_{XX_F} - I_{ZZ_F}) p_F r_F + I_{YZ_F} (q_F p_F - \dot{r}_F) + I_{XY_F} (-q_F r_F - \dot{p}_F) + I_{XZ_F} (p_F^2 - r_F^2) + m_F (-x_{CG_F} \ddot{z}_F + z_{CG_F} \ddot{x}_F) \right] \quad (6-280)$$

$$M_{Z_{IF}} = M_{Z_{IP}} + M_{Z_{ITR}} + M_{Z_{IENG}} - \left[I_{ZZ_F} \dot{r}_F + (I_{YY_F} - I_{XX_F}) q_F p_F + I_{XZ_F} (r_F q_F - \dot{p}_F) + I_{YZ_F} (-r_F p_F - \dot{q}_F) + I_{XY_F} (q_F^2 - p_F^2) + m_F (-y_{CG_F} \ddot{x}_F + x_{CG_F} \ddot{y}_F) \right] \quad (6-281)$$

$$M_{X_{IP}} = -I_{XX_P} (\dot{p}_F - G_P \ddot{\psi}_R) \quad (6-282)$$

$$M_{Y_{IP}} = -I_{YY_P} (\dot{q}_F + p_F r_F) + I_{XX_P} G_P \dot{\psi}_R r_F \quad (6-283)$$

TABLE 6-5 - Continued

$$M_{Z_{IP}} = - I_{ZZ_P} (\dot{r}_F - p_F q_F) - I_{XX_P} G_P \dot{\psi}_R q_F \quad (6-284)$$

$$M_{X_{ITR}} = 0 \quad (6-285)$$

$$M_{Y_{ITR}} = - I_{YY_{TR}} (\dot{q}_F + G_{TR} \ddot{\psi}_R) \quad (6-286)$$

$$M_{Z_{ITR}} = 0 \quad (6-287)$$

$$M_{X_{IENG}} = - I_{XX_{ENG}} (\dot{p}_F - G_{ENG} \ddot{\psi}_R) \quad (6-288)$$

$$M_{Y_{IENG}} = - I_{YY_{ENG}} (\dot{q}_F + p_F r_F) + I_{XX_{ENG}} G_{ENG} \dot{\psi}_R r_F \quad (6-289)$$

$$M_{Z_{IENG}} = - I_{ZZ_{ENG}} (\dot{r}_F - p_F q_F) - I_{XX_{ENG}} G_{ENG} \dot{\psi}_R q_F \quad (6-290)$$

$$\begin{pmatrix} M_{X_{ATR}} \end{pmatrix}_F = \begin{pmatrix} M_{X_{ATR}} \end{pmatrix}_{TR} - \begin{pmatrix} Z_{TR} \end{pmatrix}_F F_{Y_{ATR}} + \begin{pmatrix} Y_{TR} \end{pmatrix}_F F_{Z_{ATR}} \quad (6-291)$$

$$\begin{pmatrix} M_{Y_{ATR}} \end{pmatrix}_F = \begin{pmatrix} M_{Y_{ATR}} \end{pmatrix}_{TR} - \begin{pmatrix} X_{TR} \end{pmatrix}_F F_{Z_{ATR}} + \begin{pmatrix} Z_{TR} \end{pmatrix}_F F_{X_{ATR}} \quad (6-292)$$

$$\begin{pmatrix} M_{Z_{ATR}} \end{pmatrix}_F = \begin{pmatrix} M_{Z_{ATR}} \end{pmatrix}_{TR} - \begin{pmatrix} Y_{TR} \end{pmatrix}_F F_{X_{ATR}} + \begin{pmatrix} X_{TR} \end{pmatrix}_F F_{Y_{ATR}} \quad (6-293)$$

$$\begin{pmatrix} M_{X_{AP}} \end{pmatrix}_F = \begin{pmatrix} M_{X_{AP}} \end{pmatrix}_P - \begin{pmatrix} Z_P \end{pmatrix}_F F_{Y_P} + \begin{pmatrix} Y_P \end{pmatrix}_F F_{Z_{AP}} \quad (6-294)$$

$$\begin{pmatrix} M_{Y_{AP}} \end{pmatrix}_F = \begin{pmatrix} M_{Y_{AP}} \end{pmatrix}_P - \begin{pmatrix} X_P \end{pmatrix}_F F_{Z_{AP}} + \begin{pmatrix} Z_P \end{pmatrix}_F F_{X_{AP}} \quad (6-295)$$

$$\begin{pmatrix} M_{Z_{AP}} \end{pmatrix}_F = \begin{pmatrix} M_{Z_{AP}} \end{pmatrix}_P - \begin{pmatrix} Y_P \end{pmatrix}_F F_{X_{AP}} + \begin{pmatrix} X_P \end{pmatrix}_F F_{Y_{AP}} \quad (6-296)$$

The main rotor shaft loads are simply found from the blade root loads. The approximate equations are:

$$\begin{Bmatrix} F_{rMR} \end{Bmatrix}_H = \begin{Bmatrix} F_{XMR} \\ F_{YMR} \\ F_{ZMR} \end{Bmatrix}_H = \begin{bmatrix} T_{H-R} \end{bmatrix}^T \sum_{i=1}^K \begin{bmatrix} T_{R-BLn} \end{bmatrix}^T \begin{Bmatrix} F_X \\ F_Y \\ F_Z \end{Bmatrix}_{BLn} \quad (6-297)$$

$$\begin{Bmatrix} M_{rMR} \end{Bmatrix}_H = \begin{Bmatrix} M_{XMR} \\ M_{YMR} \\ M_{ZMR} \end{Bmatrix}_H = \begin{bmatrix} T_{H-R} \end{bmatrix}^T \begin{Bmatrix} M_{XMR} \\ M_{YMR} \\ M_{ZMR} \end{Bmatrix}_R \quad (6-298)$$

The $\begin{bmatrix} T_{H-R} \end{bmatrix}$ matrix accounts for rotor gimballing, the transfer between stationary and rotating axes, and the switch between Z up and Z down axes. The $\begin{bmatrix} T_{R-BLn} \end{bmatrix}$ matrix accounts for the individual blade azimuth. These matrices were developed in Section 5.5.5. Z_{OBLn} is the amount of undersling (negative value).

6.10 SWASHPLATE EQUATIONS

6.10.1 Use as a Pure Swashplate or a Feathering Feedback Control Gyro

The swashplate converts the nonrotating system (hub axis) collective and cyclic blade commands into first-harmonic Fourier components in the rotating system (rotor coordinates). For a conventional swashplate system the command signal operates open loop from input to blade feathering. The swashplate formulation used in REXOR handles this case, but this original, and prime, use is for the external control gyro with feathering feedback. This is a closed-loop system where the command input torques the control gyro, which in turn feathers the blades. Response rates of the principal axes and rotor moment via hub geometry form a control system loop closure. Both systems, as well as the swashplate element of the isolated control gyro, are handled merely by changing the system constants input.

6.10.2 Partial Derivatives

The swashplate partial derivatives are readily obtained from Section 5.3.5. Using matrix notation

$$\left[\begin{array}{c} \frac{\partial}{\partial \phi_{SP}} \begin{Bmatrix} \phi_{SP} \\ \theta_{SP} \\ \psi_{SP} \end{Bmatrix} \mid \frac{\partial}{\partial \theta_{SP}} \begin{Bmatrix} \phi_{SP} \\ \theta_{SP} \\ \psi_{SP} \end{Bmatrix} \mid - \end{array} \right] = \begin{bmatrix} \cos \theta_{SP} & 0 & - \\ 0 & 1 & - \\ \sin \theta_{SP} & 0 & - \end{bmatrix} \quad (6-299)$$

Also:

$$\frac{\partial z_{OSP}}{\partial z_{SP}} = 1 \quad (6-300)$$

Since the swashplate axis is directly referenced to the principal (hub) set, the above derivatives are complete. The lack of translation to angular derivatives is explained by the parallelogram linkages used with swashplates to isolate the collective and cyclic inputs. The terms left out of the matrix indicate that the swashplate does not have a yaw degree of freedom.

The reader should be aware that the angular notation ϕ , θ , and ψ have two meanings, depending on whether they are in the numerator or the denominator of the partial. The numerator is the displacement of the mass element with respect to the principal reference axis, whereas the denominator is the degree of freedom incremental variable.

Swashplate motions pick up large inertia loads from the rotor due to blade feathering. Partials relating feathering to swashplate motions are assembled by first relating the feathering motion in the rotating system with feathering in the stationary system:

$$\frac{\partial \phi_{Fn}}{\partial \theta_0} = 1 \quad (6-301)$$

$$\frac{\partial \phi_{Fn}}{\partial A_{1S}} = -\cos(\psi_{BLn} + \psi_R) \quad (6-302)$$

$$\frac{\partial \phi_{Fn}}{\partial \psi_{1S}} = -\sin(\psi_{BLn} + \psi_R) \quad (6-303)$$

From Section 5.5.8, equations relating swashplate motions to the stationary feather angles give

$$\begin{bmatrix} \frac{\partial A_{1S}}{\partial \phi_{SP}} & \frac{\partial A_{1S}}{\partial \theta_{SP}} \\ \frac{\partial B_{1S}}{\partial \phi_{SP}} & \frac{\partial B_{1S}}{\partial \theta_{SP}} \end{bmatrix} = \frac{d}{e} \begin{bmatrix} T_{\psi_{PH}} \end{bmatrix} \quad (6-304)$$

and

$$\begin{Bmatrix} \frac{\partial A_{1S}}{\partial \theta_0} \\ \frac{\partial B_{1S}}{\partial \theta_0} \end{Bmatrix} = \left(\frac{d}{e}\right)_1 \begin{bmatrix} T_{\psi_{PH}} \end{bmatrix} \begin{Bmatrix} \phi_{SP} \\ \theta_{SP} \end{Bmatrix} \quad (6-305)$$

where

$$\begin{bmatrix} T_{\psi_{PH}} \end{bmatrix} = \begin{bmatrix} \sin \psi_{PH} & \cos \psi_{PH} \\ \cos \psi_{PH} & -\sin \psi_{PH} \end{bmatrix} \quad (6-306)$$

Also

$$\frac{\partial \theta_0}{\partial Z_{SP}} = -\frac{1}{e} \quad (6-307)$$

The $\begin{bmatrix} T_{\psi} \\ \psi_{PH} \end{bmatrix}$ matrix does not follow the conventional Euler angle notation since a desire existed to define ψ_{PH} as the angle the pitch horn to pitch link attachment point leads the blade. The overall derivatives can be put together as:

$$\frac{\partial \phi_{Fn}}{\partial \phi_{SP}} = \frac{\partial \phi_{Fn}}{\partial A_{1S}} \frac{\partial A_{1S}}{\partial \phi_{SP}} + \frac{\partial \phi_{Fn}}{\partial B_{1S}} \frac{\partial B_{1S}}{\partial \phi_{SP}} \quad (6-308)$$

$$\frac{\partial \phi_{Fn}}{\partial \theta_{SP}} = \frac{\partial \phi_{Fn}}{\partial A_{1S}} \frac{\partial A_{1S}}{\partial \theta_{SP}} + \frac{\partial \phi_{Fn}}{\partial B_{1S}} \frac{\partial B_{1S}}{\partial \theta_{SP}} \quad (6-309)$$

$$\frac{\partial \phi_{Fn}}{\partial \dot{z}_{SP}} = \left(\frac{\partial \phi_{Fn}}{\partial \theta_0} + \frac{\partial \phi_{Fn}}{\partial A_{1S}} \frac{\partial A_{1S}}{\partial \theta_0} + \frac{\partial \phi_{Fn}}{\partial B_{1S}} \frac{\partial B_{1S}}{\partial \theta_0} \right) \frac{\partial \theta_0}{\partial \dot{z}_{SP}} \quad (6-310)$$

6.10.3 Generalized Masses

Table 6-6 presents the generalized masses which couple the swashplate motions with one and another, with the rotor, blade, and body degrees of freedom. The table uses summations of the blade that are described in detail in Section 6.6.1.

TABLE 6-6. SWASHPLATE GENERALIZED MASSES

$$M_{\phi_{SP}^A mn} = \frac{\partial \phi_{Fn}}{\partial \phi_{SP}} M_{A mn} \phi_{Fn} \quad (6-311)$$

$$M_{\phi_{SP}^{\beta} PHn} = \frac{\partial \phi_{Fn}}{\partial \phi_{SP}} M_{\beta PHn} \phi_{Fn} \quad (6-312)$$

$$M_{\phi_{SP}^{\phi} SP} = \sum_{n=1}^b \left(\frac{\partial \phi_{Fn}}{\partial \phi_{SP}} \right)^2 M_{\phi_{Fn} \phi_{Fn}} + I_{XX_{SP}} \left(\frac{\partial \phi_{SP}}{\partial \phi_{SP}} \right)^2 + I_{ZZ_{SP}} \left(\frac{\partial \psi_{SP}}{\partial \phi_{SP}} \right)^2 \quad (6-313)$$

$$M_{\phi_{SP}^{X_H}} = \sum_{n=1}^b \left[\frac{\partial Y_{OBLn}}{\partial X_H} \frac{\partial \phi_{Fn}}{\partial \phi_{SP}} M_{Y_{OBLn} \phi_{Fn}} + \frac{\partial Z_{OBLn}}{\partial X_H} \frac{\partial \phi_{Fn}}{\partial \phi_{SP}} M_{Z_{OBLn} \phi_{Fn}} \right] \quad (6-314)$$

$$M_{\phi_{SP}^{Y_H}} = \sum_{n=1}^b \left[\frac{\partial Y_{OBLn}}{\partial Y_H} \frac{\partial \phi_{Fn}}{\partial \phi_{SP}} M_{Y_{OBLn} \phi_{Fn}} + \frac{\partial Z_{OBLn}}{\partial Y_H} \frac{\partial \phi_{Fn}}{\partial \phi_{SP}} M_{Z_{OBLn} \phi_{Fn}} \right] \quad (6-315)$$

$$M_{\phi_{SP}^{Z_H}} = \sum_{n=1}^b \left[\frac{\partial Y_{OBLn}}{\partial Z_H} \frac{\partial \phi_{Fn}}{\partial \phi_{SP}} M_{Y_{OBLn} \phi_{Fn}} + \frac{\partial Z_{OBLn}}{\partial Z_H} \frac{\partial \phi_{Fn}}{\partial \phi_{SP}} M_{Z_{OBLn} \phi_{Fn}} \right] \quad (6-316)$$

$$M_{\phi_{SP}^{\phi_H}} = \sum_{n=1}^b \frac{\partial \phi_{Fn}}{\partial \phi_{SP}} M_{\phi_H \phi_{Fn}} + I_{XX_{SP}} \frac{\partial \phi_{SP}}{\partial \phi_{SP}} \frac{\partial \phi_{SP}}{\partial \phi_H} + I_{ZZ_{SP}} \frac{\partial \psi_{SP}}{\partial \phi_{SP}} \frac{\partial \psi_{SP}}{\partial \phi_H} \quad (6-317)$$

$$M_{\phi_{SP}^{\theta_H}} = \sum_{n=1}^b \frac{\partial \phi_{Fn}}{\partial \phi_{SP}} M_{\theta_H \phi_{Fn}} + I_{XX_{SP}} \frac{\partial \phi_{SP}}{\partial \phi_{SP}} \frac{\partial \phi_{SP}}{\partial \theta_H} + I_{ZZ_{SP}} \frac{\partial \psi_{SP}}{\partial \phi_{SP}} \frac{\partial \psi_{SP}}{\partial \theta_H} \quad (6-318)$$

TABLE 6-6 - Continued

$$M_{\phi_{SP}\psi_H} = \sum_{n=1}^b \frac{\partial \phi_{Fn}}{\partial \phi_{SP}} M_{\psi_H \phi_{Fn}} + I_{XX_{SP}} \frac{\partial \phi_{SP}}{\partial \phi_{SP}} \frac{\partial \phi_{SP}}{\partial \psi_H} + I_{ZZ_{SP}} \frac{\partial \psi_{SP}}{\partial \phi_{SP}} \frac{\partial \psi_{SP}}{\partial \psi_H} \quad (6-319)$$

$$M_{\phi_{SP}\psi_R} = \sum_{n=1}^b \frac{\partial \phi_{Fn}}{\partial \phi_{SP}} M_{\psi_R \phi_{Fn}} \quad (6-320)$$

$$M_{\theta_{SP}A_{mn}} = \frac{\partial \phi_{Fn}}{\partial \theta_{SP}} M_{A_{mn} \phi_{Fn}} \quad (6-321)$$

$$M_{\theta_{SP}\beta_{PHn}} = \frac{\partial \phi_{Fn}}{\partial \theta_{SP}} M_{\beta_{PHn} \phi_{Fn}} \quad (6-322)$$

$$M_{\theta_{SP}\phi_{SP}} = \sum_{n=1}^b \frac{\partial \phi_{Fn}}{\partial \theta_{SP}} \frac{\partial \phi_{Fn}}{\partial \phi_{SP}} M_{\phi_{Fn} \phi_{Fn}} \quad (6-323)$$

$$M_{\theta_{SP}\theta_{SP}} = \sum_{n=1}^b \left(\frac{\partial \phi_{Fn}}{\partial \theta_{SP}} \right)^2 M_{\phi_{Fn} \phi_{Fn}} + I_{YY_{SP}} \quad (6-324)$$

$$M_{\theta_{SP}X_H} = \sum_{n=1}^b \left[\frac{\partial Y_{OBLn}}{\partial X_H} \frac{\partial \phi_{Fn}}{\partial \theta_{SP}} M_{Y_{OBLn} \phi_{Fn}} + \frac{\partial Z_{OBLn}}{\partial X_H} \frac{\partial \phi_{Fn}}{\partial \theta_{SP}} M_{Z_{OBLn} \phi_{Fn}} \right] \quad (6-325)$$

TABLE 6-6 - Continued

$$M_{\theta_{SP}^Y H} = \sum_{n=1}^b \left[\frac{\partial Y_{OBLn}}{\partial Y_H} \frac{\partial \phi_{Fn}}{\partial \theta_{SP}} M_{Y_{OBLn} \phi_{Fn}} + \frac{\partial Z_{OBLn}}{\partial Y_H} \frac{\partial \phi_{Fn}}{\partial \theta_{SP}} M_{Z_{OBLn} \phi_{Fn}} \right] \quad (6-326)$$

$$M_{\theta_{SP}^Z H} = \sum_{n=1}^b \left[\frac{\partial Y_{OBLn}}{\partial Z_H} \frac{\partial \phi_{Fn}}{\partial \theta_{SP}} M_{Y_{OBLn} \phi_{Fn}} + \frac{\partial Z_{OBLn}}{\partial Z_H} \frac{\partial \phi_{Fn}}{\partial \theta_{SP}} M_{Z_{OBLn} \phi_{Fn}} \right] \quad (6-327)$$

$$M_{\theta_{SP} \phi_H} = \sum_{n=1}^b \frac{\partial \phi_{Fn}}{\partial \theta_{SP}} M_{\phi_H \phi_{Fn}} \quad (6-328)$$

$$M_{\theta_{SP} \theta_H} = \sum_{n=1}^b \frac{\partial \phi_{Fn}}{\partial \theta_{SP}} M_{\theta_H \phi_{Fn}} + I_{YY_{SP}} \frac{\partial \theta_{SP}}{\partial \theta_{SP}} \frac{\partial \theta_{SP}}{\partial \theta_H} \quad (6-329)$$

$$M_{\theta_{SP} \psi_H} = \sum_{n=1}^b \frac{\partial \phi_{Fn}}{\partial \psi_{SP}} M_{\psi_H \phi_{Fn}} + I_{YY_{SP}} \frac{\partial \theta_{SP}}{\partial \theta_{SP}} \frac{\partial \theta_{SP}}{\partial \psi_H} \quad (6-330)$$

$$M_{\theta_{SP} \psi_R} = \sum_{n=1}^b \frac{\partial \phi_{Fn}}{\partial \theta_{SP}} M_{\psi_R \phi_{Fn}} \quad (6-331)$$

$$M_{Z_{SP}^A mn} = \frac{\partial \phi_{Fn}}{\partial Z_{SP}} M_{A_{mn} \phi_{Fn}} \quad (6-332)$$

TABLE 6-6 - Continued

$$M_{Z_{SP} \beta_{PHn}} = \frac{\partial \phi_{Fn}}{\partial Z_{SP}} M_{\beta_{PHn} \phi_{Fn}} \quad (6-333)$$

$$M_{Z_{SP} Z_{SP}} = \sum_{n=1}^b \left(\frac{\partial \phi_{Fn}}{\partial Z_{SP}} \right)^2 M_{\phi_{Fn} \phi_{Fn}} + m_{SP} \quad (6-334)$$

$$M_{Z_{SP} \phi_{SP}} = \sum_{n=1}^b \left(\frac{\partial \phi_{Fn}}{\partial Z_{SP}} \right) \left(\frac{\partial \phi_{Fn}}{\partial \phi_{SP}} \right) M_{\phi_{Fn} \phi_{Fn}} \quad (6-335)$$

$$M_{Z_{SP} \theta_{SP}} = \sum_{n=1}^b \left(\frac{\partial \phi_{Fn}}{\partial Z_{SP}} \right) \left(\frac{\partial \phi_{Fn}}{\partial \theta_{SP}} \right) M_{\phi_{Fn} \phi_{Fn}} \quad (6-336)$$

$$M_{Z_{SP} X_H} = \sum_{n=1}^b \left[\frac{\partial Y_{OBLn}}{\partial X_H} \frac{\partial \phi_{Fn}}{\partial Z_{SP}} M_{Y_{OBLn} \phi_{Fn}} + \frac{\partial Z_{OBLn}}{\partial X_H} \frac{\partial \phi_{Fn}}{\partial Z_{SP}} M_{Z_{OBLn} \phi_{Fn}} \right] \quad (6-337)$$

$$M_{Z_{SP} Y_H} = \sum_{n=1}^b \left[\frac{\partial Y_{OBLn}}{\partial Y_H} \frac{\partial \phi_{Fn}}{\partial Z_{SP}} M_{Y_{OBLn} \phi_{Fn}} + \frac{\partial Z_{OBLn}}{\partial Y_H} \frac{\partial \phi_{Fn}}{\partial Z_{SP}} M_{Z_{OBLn} \phi_{Fn}} \right] \quad (6-338)$$

$$M_{Z_{SP} Z_H} = \sum_{n=1}^b \left[\frac{\partial Y_{OBLn}}{\partial Z_H} \frac{\partial \phi_{Fn}}{\partial Z_{SP}} M_{Y_{OBLn} \phi_{Fn}} + \frac{\partial Z_{OBLn}}{\partial Z_H} \frac{\partial \phi_{Fn}}{\partial Z_{SP}} M_{Z_{OBLn} \phi_{Fn}} \right] + m_{SP} \quad (6-339)$$

TABLE 6-6 - Continued

$$M_{Z_{SP}\phi_H} = \sum_{n=1}^b \frac{\partial \phi_{Fn}}{\partial Z_{SP}} M_{\phi_H \phi_{Fn}} \quad (6-340)$$

$$M_{Z_{SP}\theta_H} = \sum_{n=1}^b \frac{\partial \phi_{Fn}}{\partial Z_{SP}} M_{\theta_H \phi_{Fn}} \quad (6-341)$$

$$M_{Z_{SP}\psi_H} = \sum_{n=1}^b \frac{\partial \phi_{Fn}}{\partial Z_{SP}} M_{\psi_H \phi_{Fn}} \quad (6-342)$$

$$M_{Z_{SP}\psi_R} = \sum_{n=1}^b \frac{\partial \phi_{Fn}}{\partial Z_{SP}} M_{\psi_R \phi_{Fn}} \quad (6-343)$$

$$M_{\psi_R \phi_{Fn}} = M_{\psi_{BLn} \phi_{Fn}} + \frac{\partial \phi_{Fn}}{\partial \psi_R} M_{\phi_{Fn} \phi_{Fn}} \quad (6-344)$$

where $\frac{\partial \phi_{Fn}}{\partial \psi_R}$ is given in Section 6.12.3.

6.10.4 Generalized Forces

As explained earlier, the swashplate generalized forces are obtained by similar formulation, whether the swashplate is used in the normal manner or as an external control gyro. The forces are: (assuming a constant speed drive)

$$F_{\phi_{SP}} = - \frac{\partial \phi_{SP}}{\partial \phi_{SP}} \left(\dot{p}_{SP} I_{XX_{SP}} + q_{SP} r_{SP} I_{ZZ_{SP}} \right) - \frac{\partial \psi_{SP}}{\partial \phi_{SP}} \dot{r}_{SP} I_{ZZ_{SP}} + \sum_{n=1}^b M_{Fn} \frac{\partial \phi_{Fn}}{\partial \phi_{SP}} - \frac{\partial U}{\partial \phi_{SP}} - \frac{\partial B}{\partial \phi_{SP}} - M_{FR, \phi_{SP}} \quad (6-345)$$

$$F_{\theta_{SP}} = - \frac{\partial \theta_{SP}}{\partial \theta_{SP}} \left(\dot{q}_{SP} I_{YY_{SP}} - r_{SP} p_{SP} I_{ZZ_{SP}} \right) + \sum_{n=1}^b M_{Fn} \frac{\partial \theta_{Fn}}{\partial \theta_{SP}} - \frac{\partial U}{\partial \theta_{SP}} - \frac{\partial B}{\partial \theta_{SP}} - M_{FR, \theta_{SP}} \quad (6-346)$$

Note p, q terms are the same for R and NR systems.

$$F_{Z_{SP}} = - (\ddot{z}_{SP} + \ddot{z}_H) m_{SP} + \sum_{n=1}^b M_{Fn} \frac{\partial \phi_{Fn}}{\partial z_{SP}} - \frac{\partial U}{\partial z_{SP}} - \frac{\partial B}{\partial z_{SP}} \quad (6-347)$$

where

$$\begin{Bmatrix} \dot{p} \\ \dot{q} \\ \dot{r} \end{Bmatrix}_{SP, NR} = \begin{Bmatrix} \dot{p} \\ \dot{q} \\ \dot{r} \end{Bmatrix}_{SP} - \begin{Bmatrix} \dot{\psi} q \\ -\dot{\psi} p \\ \dot{\psi} \end{Bmatrix}_{SP} \quad (6-348)$$

The moments used in these formulas are developed below.

The feathering moment, M_{Fn} , is taken to be composed of blade loads, friction, and tension-torsion pack loads.

$$M_{Fn} = M_{X_{Fn}} + M_{FR_{Fn}} + M_{TT_{Fn}} \quad (6-349)$$

The detailing of $M_{X_{Fn}}$, feathering moments due to blade loads, is accomplished in Section 6.6.4. The friction load, $M_{FR_{Fn}}$, follows the function shown in Figure 6-3. By reducing $\phi_{Fn,BK}$ to near zero, stiction

is obtained. Otherwise, if $\phi_{Fn,BK}$ is large, the ratio $\frac{M_{FR_{Fn,BK}}}{\phi_{Fn,BK}}$ determines the amount of viscous friction.

The first part of the tension-torsion pack, $M_{TT_{Fn}}$, has a simple spring contribution of

$$K_{TT}(\phi_{Fn} - \phi_{Fn_{TT}}) \quad (6-350)$$

from the torsion spring K_{TT} ; $\phi_{Fn_{TT}}$ being the blade angle for zero spring

load. The tension contribution from the tension-torsion pack requires a knowledge of the locations of the inboard and outboard feather bearings and the inboard and outboard pin ends of the tension-torsion pack. The locations of the bearings are described in Section 5.5.5. The inboard end of the pack is the sum of the static and blade bending contributions:

$$\begin{Bmatrix} X_{TTI} \\ Y_{TTI} \\ Z_{TTI} \end{Bmatrix}_{BLn} = \begin{Bmatrix} X_{S_{TTI}} \\ Y_{S_{TTI}} \\ Z_{S_{TTI}} \end{Bmatrix}_{BLn} + \begin{bmatrix} 0 & 0 & 0 \\ Y_{TTI_1} & Y_{TTI_2} & Y_{TTI_3} \\ Z_{TTI_1} & Z_{TTI_2} & Z_{TTI_3} \end{bmatrix} \begin{Bmatrix} A_{1n} \\ A_{2n} \\ A_{3n} \end{Bmatrix} \quad (6-351)$$

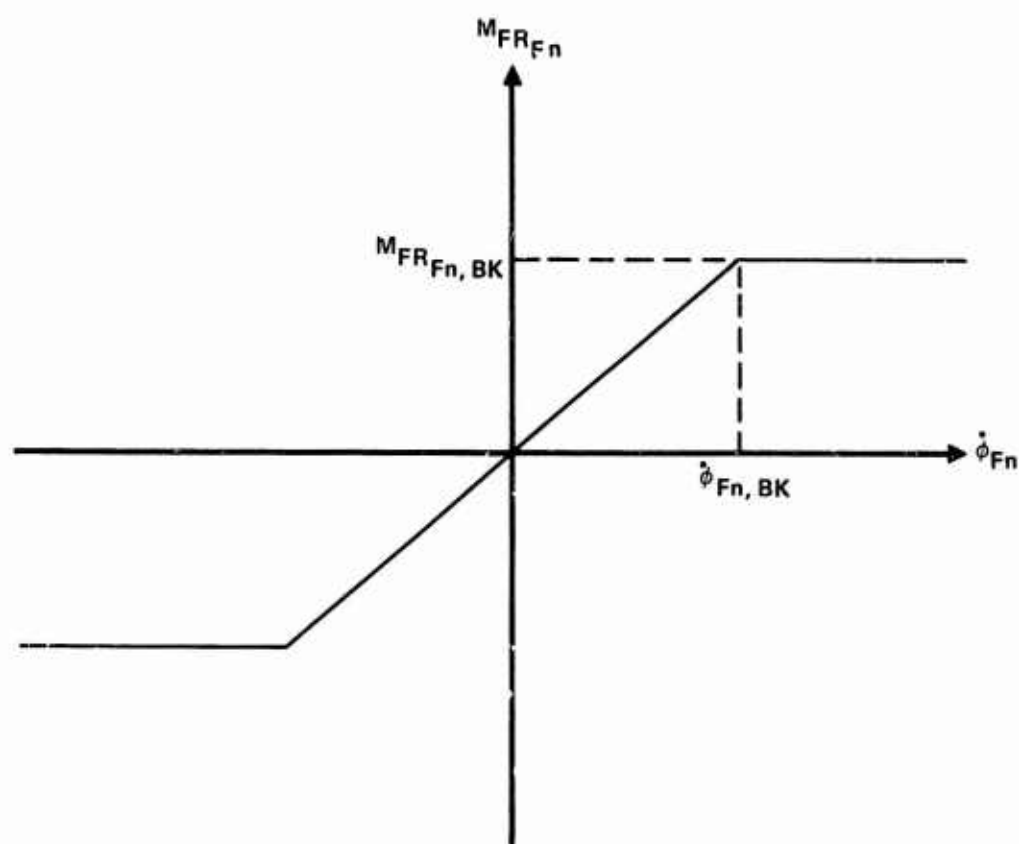


Figure 6-3. Swashplate Friction

The symbols Y_{TTI_1} , . . . represent partials $\frac{\partial Y_{TTI}}{\partial A_1}$. . . , etc. The static positions are:

$$\begin{Bmatrix} X_{S_{TTI}} \\ Y_{S_{TTI}} \\ Z_{S_{TTI}} \end{Bmatrix}_{BLn} = \begin{Bmatrix} \ell_{TTI} \cos \beta_0 \\ 0 \\ \ell_{TTI} \sin \beta_0 + Z_{0TTI} \end{Bmatrix} \quad (6-352)$$

where Z_{0TTI} is the vertical offset at a distance ℓ_{TTI} out the coned reference line. See Figure 6-4.

For the outboard end of the tension-torsion pack:

$$\begin{Bmatrix} X_{TTO} \\ Y_{TTO} \\ Z_{TTO} \end{Bmatrix}_{BLn} = \begin{bmatrix} T_{Z', FA} \\ T_{Y', FA} \\ T_{\Delta\phi_F} \\ T_{Y', FA} \\ T_{Z', FA} \end{bmatrix}^T \begin{Bmatrix} X_{S_{TTO}} \\ Y_{S_{TTO}} \\ Z_{S_{TTO}} \end{Bmatrix}_{BLn} + \begin{bmatrix} 0 & 0 & 0 \\ Y_{TTO_1} & Y_{TTO_2} & Y_{TTO_3} \\ Z_{TTO_1} & Z_{TTO_2} & Z_{TTO_3} \end{bmatrix} \begin{Bmatrix} A_{1n} \\ A_{2n} \\ A_{3n} \end{Bmatrix} \quad (6-353)$$

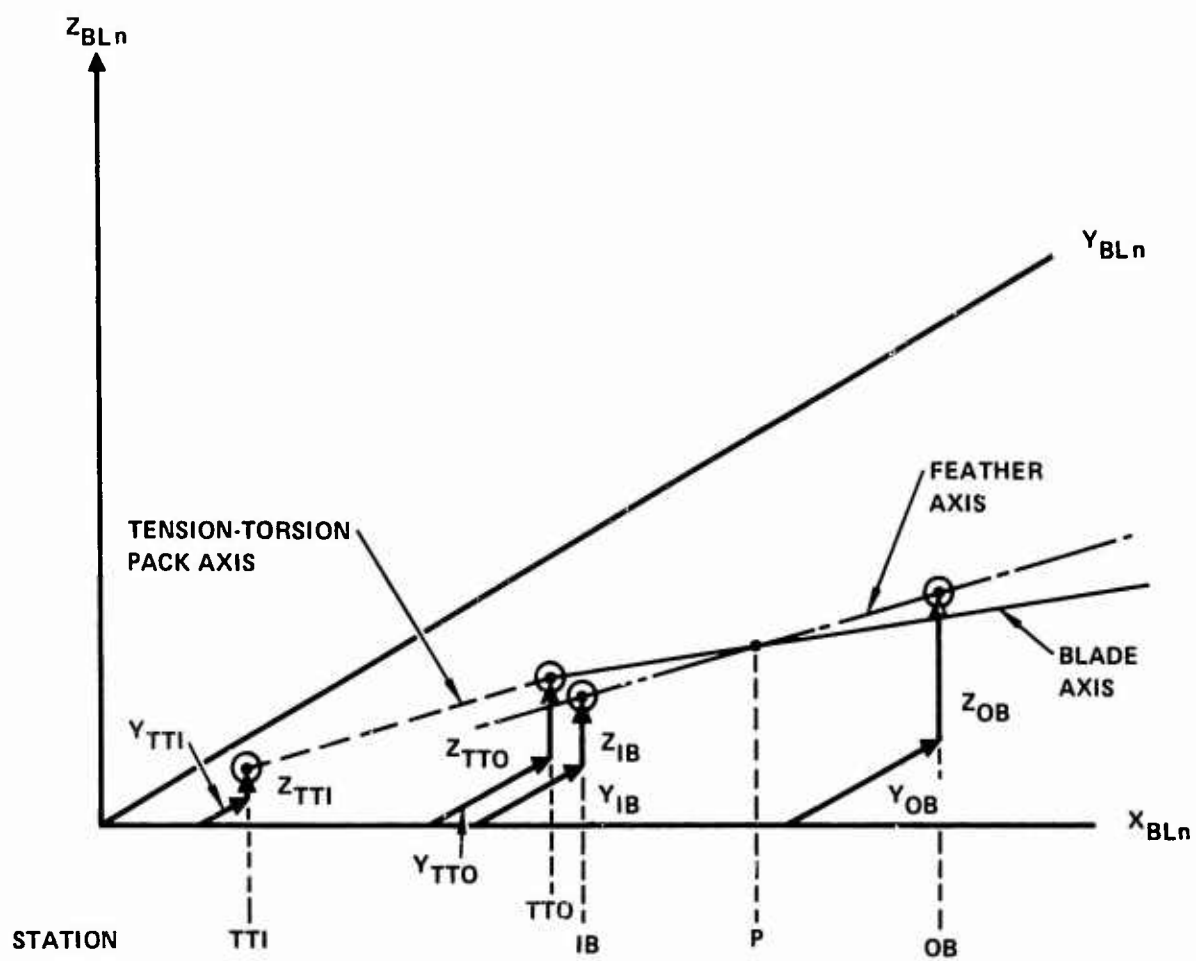


Figure 6-4. Tension-Torsion Pack Geometry

The static position formulation follows the development of Section 5.5.5 inboard of X_{SW} (blade attack point to movable hub) except that geometric twist is not included.

$$\begin{Bmatrix} X_{S_{TTO}} \\ Y_{S_{TTO}} \\ Z_{S_{TTO}} \end{Bmatrix}_{BLn} = \begin{bmatrix} T_{\beta_{FA}} \end{bmatrix}^T \begin{bmatrix} T_{\phi_{REF}} \end{bmatrix}^T \begin{bmatrix} T_{\beta_{FA}} \end{bmatrix} \begin{Bmatrix} X_{TTO} \cos \beta_0 \\ 0 \\ X_{TTO} \sin \beta_0 + Z_{TTO} \end{Bmatrix} - \begin{Bmatrix} l_p \cos \beta_0 \\ 0 \\ l_p \sin \beta_0 \end{Bmatrix} + \begin{Bmatrix} l_p \cos \beta_0 \\ 0 \\ l_p \sin \beta_0 \end{Bmatrix} \quad (6-354)$$

Knowing the location of the tension-torsion pack and the feather bearings, the total contribution from the pack is

$$M_{TT_{Fn}} = K_{TT}(\phi_{Fn} - \phi_{FnTT}) + \{\sin(X'_{FA}), \sin(Y'_{FA}), \sin(Z'_{FA})\} \cdot \begin{bmatrix} 0 & (Z_{TTO} - Z_{IB}) & -(Y_{TTO} - Y_{IB}) \\ -(Z_{TTO} - Z_{IB}) & 0 & (X_{TTO} - X_{IB}) \\ (Y_{TTO} - Y_{IB}) & -(X_{TTO} - X_{IB}) & 0 \end{bmatrix} \cdot \begin{Bmatrix} -T_{TT} X'_{TT} \\ -T_{TT} Y'_{TT} \\ -T_{TT} Z'_{TT} \end{Bmatrix} \quad (6-355)$$

where for each blade:

$$\sin(X'_{FA}) \approx \frac{(X_{OB} - X_{IB})}{(\ell_{OB} - \ell_{IB})} \quad (6-356)$$

$$\sin(Y'_{FA}) \approx \frac{(Y_{OB} - Y_{IB})}{(\ell_{OB} - \ell_{IB})} \quad (6-357)$$

$$\sin(Z'_{FA}) \approx \frac{(Z_{OB} - Z_{IB})}{(\ell_{OB} - \ell_{IB})} \quad (6-358)$$

$$X_{TT'} = \frac{(X_{TTO} - X_{TTI})}{(\ell_{TTO} - \ell_{TTI})} \quad (6-359)$$

$$Y_{TT'} = \frac{(Y_{TTO} - Y_{TTI})}{(\ell_{TTO} - \ell_{TTI})} \quad (6-360)$$

$$Z_{TT'} = \frac{(Z_{TTO} - Z_{TTI})}{(\ell_{TTO} - \ell_{TTI})} \quad (6-361)$$

If no stretch is assumed, the ℓ 's can be treated as constants. Directional cosines are used for convenience. The negative value of the tension in the feather moment equation indicates a tension-torsion pack reaction force acting through the small arms $X_{TTO} - X_{IB}$, $Y_{TTO} - Y_{IB}$, and $Z_{TTO} - Z_{IB}$ to produce a feathering moment.

The tension is equal to the component of the root shear lying along the tension-torsion pack axis. The lateral components of the shears reacted at the feather bearing are ignored. Using directional cosines

$$T_{TT} = X'_{TT} F_{X_{BLn}} + Y'_{TT} F_{Y_{BLn}} + Z'_{TT} F_{Z_{BLn}} \quad (6-362)$$

The remaining portions of the generalized force are the potential energy and dissipation functions. First consider the angular potential energy terms which model the swashplate tilt spring rate. This spring rate has a center dead-band, an operating range spring rate, and a high spring rate to simulate a travel limit stop.

Consider the normal operating range spring rate first. The swashplate springs are defined in control axes (Figure 6-5) as $K_{\phi_{SP}}$ and $K_{\theta_{SP}}$ (can be unequal in size). To find the elastic spring loads, the swashplate motions are first found in control axes as:

$$\begin{Bmatrix} \phi_{SP} + R_{SPS}\phi_S \\ \theta_{SP} + R_{SPS}\theta_S \end{Bmatrix}_C = \begin{bmatrix} \cos\psi_C & \sin\psi_C \\ -\sin\psi_C & \cos\psi_C \end{bmatrix} \begin{Bmatrix} \phi_{SP} + R_{SPS}\phi_S \\ \theta_{SP} + R_{SPS}\theta_S \end{Bmatrix} \quad (6-363)$$

The geometric interpretation of ψ_C is shown in Figure 6-5.

A shaft bending to swashplate coupling ratio, R_{SPS} , is allowed. This coupling exists for the unloaded swashplate in much the same way as the blade bending to feathering coupling exists for the unloaded pitch horn and defines a modal component.

Taking the swashplate deflections in the control axes, subtracting control inputs ϕ_C and θ_C , and using the inverse transform, the swashplate spring terms in swashplate axes become:

$$\begin{Bmatrix} \frac{\partial U}{\partial \phi_{SP}} \\ \frac{\partial U}{\partial \theta_{SP}} \end{Bmatrix}_1 = \begin{bmatrix} \cos\psi_C & -\sin\psi_C \\ \sin\psi_C & \cos\psi_C \end{bmatrix} \begin{Bmatrix} K_{\phi_{SP}} (\phi_{SP} + R_{SPS}\phi_S - \phi_C)_C \\ K_{\theta_{SP}} (\theta_{SP} + R_{SPS}\theta_S - \theta_C)_C \end{Bmatrix} \quad (6-364)$$

where the subscript (1) is used to distinguish these values (used in subsequent logic calculations) from the final expressions developed below.

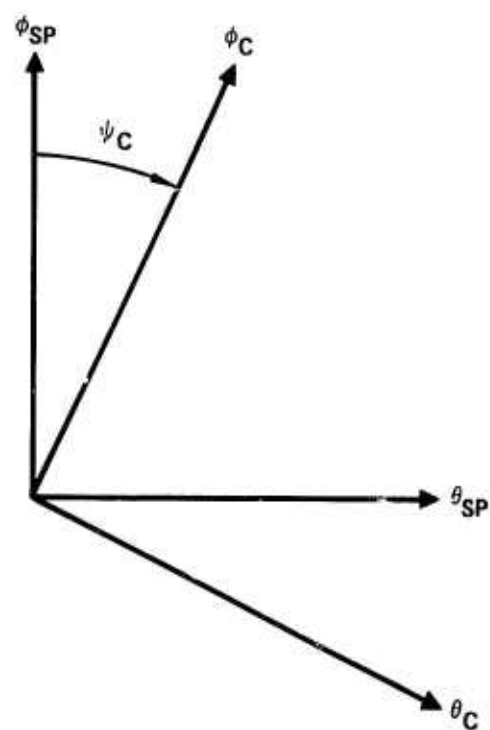


Figure 6-5. Control Axis

Substituting for the swashplate motions in terms of the swashplate axes and rearranging:

$$\begin{Bmatrix} \frac{\partial U}{\partial \phi_{SP}} \\ \frac{\partial U}{\partial \theta_{SP}} \end{Bmatrix}_1 = [K_{SP}] \begin{Bmatrix} \phi_{SP} + R_{SPS} \phi_S \\ \theta_S + R_{SPS} \theta_S \end{Bmatrix} - [T_{\psi_C}]^T \begin{Bmatrix} K_{\phi_{SP}} \phi_C \\ K_{\theta_{SP}} \theta_C \end{Bmatrix} \quad (6-365)$$

where

$$[T_{\psi_C}]^T = \begin{bmatrix} \cos \psi_C & -\sin \psi_C \\ \sin \psi_C & \cos \psi_C \end{bmatrix} \quad (6-366)$$

and

$$[K_{SP}] = \begin{bmatrix} K_{\phi_{SP}} \cos^2 \psi_C + K_{\theta_{SP}} \sin^2 \psi_C & (K_{\phi_{SP}} - K_{\theta_{SP}}) \sin \psi_C \cos \psi_C \\ K_{\phi_{SP}} - K_{\theta_{SP}} \sin \psi_C \cos \psi_C & K_{\phi_{SP}} \sin^2 \psi_C + K_{\theta_{SP}} \cos^2 \psi_C \end{bmatrix} \quad (6-367)$$

Note: $[K_{SP}]$ is a symmetric matrix of constants.

The spring constants, $K_{\phi_{SP}}$, $K_{\theta_{SP}}$, exist as springs in the usual sense

when the swashplate serves strictly as a swashplate. When the swashplate is used as a control gyro, the springs may be composed of springs operating in the usual sense plus a preloaded on center spring, which counteracts the other spring (positive spring) when the system is viewed from the swashplate. The preloaded spring is called the negative spring. With this arrangement, it is possible to have zero spring rate of the swashplate motion while having a very stiff input spring rate.

The center dead band is modeled by the following logic.

$$\frac{\partial U}{\partial \phi_{SP}} = 0 \quad \text{if} \quad \left| \left(\frac{\partial U}{\partial \phi_{SP}} \right)_1 \right| \leq K_{SP}^{(1,1)} \delta \phi_{SP} \quad (6-368)$$

$$\text{ELSE} = \left(\frac{\partial U}{\partial \phi_{SP}} \right)_1 - K_{SP}^{(1,1)} \delta \phi_{SP} \text{SIGN} \left(\frac{\partial U}{\partial \phi_{SP}} \right)_1 \quad (6-369)$$

$$\frac{\partial U}{\partial \theta_{SP}} = 0 \quad \text{if} \quad \left| \left(\frac{\partial U}{\partial \theta_{SP}} \right)_1 \right| \leq K_{SP}^{(2,2)} \delta \theta_{SP} \quad (6-370)$$

$$\text{ELSE} = \left(\frac{\partial U}{\partial \theta_{SP}} \right)_1 - K_{SP}^{(2,2)} \delta \theta_{SP} \text{SIGN} \left(\frac{\partial U}{\partial \theta_{SP}} \right)_1 \quad (6-371)$$

$\delta \phi_{SP}$ and $\delta \theta_{SP}$ are input constants giving swashplate angular freeplay.

Swashplate stops are also allowed with spring rate $K_{S,SP}$. A load

$$K_{S,SP} \left(\left(\phi_{SP}^2 + \theta_{SP}^2 \right)^{1/2} - \delta_{S,SP} \right) \begin{Bmatrix} \phi_{SP} \\ \theta_{SP} \end{Bmatrix} / \left(\phi_{SP}^2 + \theta_{SP}^2 \right)^{1/2} \quad (6-372)$$

is added to

$$\begin{Bmatrix} \frac{\partial U}{\partial \phi_{SP}} \\ \frac{\partial U}{\partial \theta_{SP}} \end{Bmatrix} \quad (6-373)$$

to account for a limit travel stop. The limit deflection for the swashplate is

$$\left(\phi_{SP}^2 + \theta_{SP}^2 \right)^{1/2} \leq \delta_{S,SP} \quad (6-374)$$

where $\delta_{S,SP}$ is the circular stop swashplate deflection limit.

The angular damping term is analogous to the spring load:

$$\begin{Bmatrix} \frac{\partial B}{\partial \dot{\phi}_{SP}} \\ \frac{\partial B}{\partial \dot{\theta}_{SP}} \end{Bmatrix} = [C_{SP}] \begin{Bmatrix} \dot{\phi}_{SP} + R_{SPS} \dot{\phi}_S \\ \dot{\theta}_{SP} + R_{SPS} \dot{\theta}_S \end{Bmatrix} - [T_{\psi_C}]^T \begin{Bmatrix} C_{\phi_C} \dot{\phi}_C \\ C_{\theta_C} \dot{\theta}_C \end{Bmatrix} \quad (6-375)$$

where $[C_{SP}]$ has the same formulation as $[K_{SP}]$,

Control friction is treated as having rotating and nonrotating components. The rotating component has already been discussed as part of the feathering moment. The nonrotating component is applied to the swashplate. It has the formulation shown in Figure 6-3 with a change in labels such that $\dot{\phi}_{Fn}$ is either $\dot{\phi}_{SP}$ or $\dot{\theta}_{SP}$, and $M_{FR_{Fn}}$ is either $M_{FR,\phi_{SP}}$ or $M_{FR,\theta_{SP}}$.

The vertical potential energy term is described as:

$$\frac{\partial U}{\partial Z_{SP}} = K_{1Z_{SP}} Z_{SP} + F_C \quad \text{if} \quad |Z_{SP}| < Z_{1_{SP}} \quad (6-376)$$

Otherwise

$$\frac{\partial U}{\partial Z_{SP}} = K_{1Z_{SP}} Z_{1_{SP}} + K_{2Z_{SP}} (Z_{SP} - Z_{1_{SP}}) + F_C \quad (6-377)$$

F_C is a constant to center the gyro springs.

The spring rate is taken to be $K_{1Z_{SP}}$ out to deflection Z_{1SP} and $K_{2Z_{SP}}$ beyond.

A simple coupling from the rotary dampers gives the vertical dissipation function.

$$\frac{\partial B}{\partial \dot{Z}_{SP}} = C_{Z_{SP}} \dot{Z}_{SP} - R_{Z\phi} C_{\phi_{SP}} \dot{\phi}_{SP} \phi_{SP} - R_{Z\theta} C_{\theta_{SP}} \dot{\theta}_{SP} \theta_{SP} \quad (6-378)$$

where $R_{Z\phi}$, $R_{Z\theta}$ are coupling ratios. Note the effect of vertical motion on the swashplate tilt loads through the rotary dampers is assumed zero.

To correlate with flight test records and/or to force the swashplate vertical response to cross the spring rate changeover a force offset constant is used. Introducing this constant into the swashplate vertical degree of freedom equation line, causes the variables, primarily the swashplate vertical motion, to shift and rebalance the equation.

6.10.5 Control Inputs

The swashplate angular input is controlled by the pilot's lateral stick for either a pure swashplate or use as a control gyro. The input torques are:

$$\begin{Bmatrix} K_{\phi_C} \phi_C \\ K_{\theta_C} \theta_C \end{Bmatrix} = \begin{Bmatrix} -K_{X_C} X_C \\ K_{Y_C} Y_C \end{Bmatrix} \quad (6-379)$$

The inputs are aligned with the control axis (Figure 6-5).

Note the equivalence of forms in terms of angular commands ϕ_C , θ_C , or longitudinal stick (aft) X_C and lateral stick (right) Y_C .

The controls are frequently linked to the swashplate through actuators which, as a first-order approximation, can be simulated by a first-order lag. For illustration, consider the longitudinal stick. Its rate becomes:

$$\dot{X}_C = \frac{(X_P - X_C)}{\tau_{X_C}} \quad (6-380)$$

The position is found by a time integration. The pilot's input is X_P and τ_{X_C} is the time constant. The actuator may be rate limited:

$$\left| \dot{X}_C \right| \leq \dot{X}_{C_{MAX}}, \quad (6-381)$$

or displacement limited:

$$\left| X_C \right| \leq X_{C_{MAX}} \quad (6-382)$$

Similar formulations can be applied to Y_C , ϕ_C , θ_C . For the vertical or collective system, the command input is $Z_C = -\theta_C e$ and the actual, true value is $Z_{SP} = -\theta_O e$ in terms of the collective angle and the pitch horn arm. The vertical system is typically fully powered, and θ_{OC} is modeled similarly to the technique just described for X_C .

6.11 CONTROL GYRO EQUATIONS

6.11.1 Introduction

As developed briefly in Section 6.10.1, REXOR models three cyclic control configurations. The first two types are the conventional swashplate and the feathering feedback external control gyro. Both of these systems use the same modeling in REXOR; the type being set by the selection of the system constants. The third configuration is an isolated direct flap feedback control gyro which operates a swashplate, as modeled in Section 6.10, via irreversible actuators.

This configuration, and the associated degrees of freedom, ϕ_G , θ_G , are defined somewhat differently in that no generalized mass couplings are assumed with the other degrees of freedom. The generalized masses involved are simply the diametral moments of inertia of the control gyro.

This simplification is possible because the inertia of the gyro is so small the principal axis loads do not include the control gyro contributions. This leads to zero generalized mass coupling, and advantage is taken of this fact to decouple the gyro degrees of freedom. Being decoupled, the control gyro can be handled apart from the main stream of the computations.

The following development also differs from other sections in that the control gyro interface with the other rotorcraft elements (feedback and phasing) are treated as separate subsections.

6.11.2 Partial Derivatives

Partials are required to relate the motions in the instantaneous gyro axes to the gyro Euler angle degrees of freedom. The desired partials are extracted from the rotary velocities relationship of Section 5.5.7 and the geometry shown in Figure 5-9. They are:

$$\begin{bmatrix} \frac{\partial \phi_G}{\partial \phi_G} & \frac{\partial \phi_G}{\partial \theta_G} & - \\ \frac{\partial \theta_G}{\partial \phi_G} & \frac{\partial \theta_G}{\partial \theta_G} & - \\ \frac{\partial \psi_G}{\partial \phi_G} & \frac{\partial \psi_G}{\partial \theta_G} & - \end{bmatrix} = \begin{bmatrix} \cos \theta_G & 0 & - \\ 0 & 1 & - \\ \sin \theta_G & 0 & - \end{bmatrix} \quad (6-383)$$

The values of the above partials are the same for axes rotating with the rotor or nonrotating axes attached to the gimbal. As shown in Section 5.5.7, this is due to the rotor axes being inertial axes defined to be momentarily attached body axes at $\psi_G = 0$ and therefore coincident with gimbal axes.

The difference between the inner and outer gimbals is ignored and the gimbal supporting the gyro rotor is taken to contain all the inertia.

6.11.3 Generalized Forces

The control gyro loads result from inertia, springs and dampers, pilot input and rotor flap feedback. The detailing of the feedback is extensive enough for a separate section. The net loads are:

$$\begin{aligned} F_{\phi_G} = 0 = & - \frac{\partial \phi_G}{\partial \phi_G} \left[I_{XX_G} \dot{p}_G + (I_{ZZ_G} - I_{YY_G}) q_G r_{G,NR} - I_{ZZ_{G,R}} q_G \dot{\psi}_R \right] \\ & - \frac{\partial \psi_G}{\partial \phi_G} I_{ZZ_{G,NR}} \dot{r}_G - \frac{\partial U}{\partial \phi_G} - \frac{\partial B}{\partial \phi_G} + M_{X_{GUB}} + M_{X_{GFB}} + M_{X_{GFR}} \end{aligned} \quad (6-384)$$

where subscript R is rotating component only, and NR is nonrotating component only.

and

$$F_{\theta_G} = 0 = -\frac{\partial \theta_G}{\partial \theta_G} \left[I_{YY_G} \dot{q}_G + (I_{XX_G} - I_{ZZ_G}) p_G r_{G,NR} + I_{ZZ_{G,R}} p_G \dot{\psi}_R \right] - \frac{\partial U}{\partial \theta_G} - \frac{\partial B}{\partial \dot{\theta}_G} + M_{Y_{GUB}} + M_{Y_{GFB}} + M_{Y_{GFR}} \quad (6-385)$$

Stiction is allowed in the feedback load, and viscous friction can be equivalenced to damping.

The equations can be solved for $\ddot{\phi}_G$ and $\ddot{\theta}_G$ by substituting in the expression for angular accelerations derived in Section 5.5.7. These are:

$$\begin{Bmatrix} \dot{p}_G \\ \dot{q}_G \\ \dot{r}_G \end{Bmatrix} = \begin{Bmatrix} \cos \theta_G \ddot{\phi}_G \\ \ddot{\theta}_G \\ \sin \theta_G \ddot{\phi}_G \end{Bmatrix} + \begin{Bmatrix} \ddot{G} \end{Bmatrix} \quad (6-386)$$

where:

$$\begin{aligned} \begin{Bmatrix} \ddot{G} \end{Bmatrix} &= \ddot{\theta}_G \begin{bmatrix} -\sin \theta_G & 0 & -\cos \theta_G \\ 0 & 0 & 0 \\ \cos \theta_G & 0 & -\sin \theta_G \end{bmatrix} \begin{Bmatrix} \dot{\phi}_G \\ 0 \\ 0 \end{Bmatrix} + \begin{bmatrix} 1 & 0 & 0 \\ 0 & \cos \phi_G & \sin \phi_G \\ 0 & -\sin \phi_G & \cos \phi_G \end{bmatrix} \begin{Bmatrix} p \\ q \\ r \end{Bmatrix}_F \\ &\cdot \begin{bmatrix} \cos \theta_G & 0 & -\sin \theta_G \\ 0 & 1 & 0 \\ \sin \theta_G & 0 & \cos \theta_G \end{bmatrix} \begin{Bmatrix} \dot{\phi}_G \\ 0 \\ 0 \end{Bmatrix} + \begin{bmatrix} 0 & 0 & 0 \\ 0 & -\sin \phi_G & \cos \phi_G \\ 0 & -\cos \phi_G & -\sin \phi_G \end{bmatrix} \begin{Bmatrix} p \\ q \\ r \end{Bmatrix}_F \\ &+ \begin{bmatrix} 1 & 0 & 0 \\ 0 & \cos \phi_G & \sin \phi_G \\ 0 & -\sin \phi_G & \cos \phi_G \end{bmatrix} \begin{Bmatrix} \dot{p} \\ \dot{q} \\ \dot{r} \end{Bmatrix}_F \end{aligned} \quad (6-387)$$

Substituting the values of the partials and the above into the gyro equations of motion and rearranging yields:

$$\ddot{\phi}_G = \frac{1}{\cos^2 \phi_G I_{XX_G} + \sin^2 \phi_G I_{ZZ_{G,NR}}} \left\{ -\cos \phi_G \left[I_{XX_G} \ddot{G}(1) + (I_{ZZ_G} - I_{YY_G}) q_\theta r_{G,NR} - I_{ZZ_{G,R}} q_\theta \dot{\psi}_R \right] - \sin \phi_G I_{ZZ_{G,NR}} \ddot{G}(3) - \frac{\partial U}{\partial \phi_G} - \frac{\partial B}{\partial \dot{\phi}_G} + M_{X_{GUB}} + M_{X_{GFB}} + M_{X_{GFR}} \right\} \quad (6-388)$$

$$\ddot{\theta}_G = \frac{1}{I_{YY_G}} \left\{ - \left[I_{YY_G} \ddot{G}(2) + (I_{XX_G} - I_{ZZ_G}) p_G r_{G,NR} + I_{ZZ_{G,R}} p_G \dot{\psi}_R \right] - \frac{\partial U}{\partial \theta_G} - \frac{\partial B}{\partial \dot{\theta}_G} + M_{Y_{GUB}} + M_{Y_{GFB}} + M_{Y_{GFR}} \right\} \quad (6-389)$$

Expanding the inertia load, the general formulation for the moments generated by a body along principal axes are:

$$M_X = I_{XX} \dot{p} + (I_{ZZ} - I_{YY})qr \quad (6-390)$$

$$M_Y = I_{YY} \dot{q} + (I_{XX} - I_{ZZ})rp \quad (6-391)$$

$$M_Z = I_{ZZ} \dot{r} + (I_{YY} - I_{XX})pq \quad (6-392)$$

where the moments, the velocities, and the accelerations are all along the principal axes. If the body is axially symmetric about the Z axis,

$$M_X = I_{XX}(\dot{p} + qr) = I_{ZZ}(\dot{p} + qr)/2 \quad (6-393)$$

$$M_Y = I_{YY}(\dot{q} - rp) = I_{ZZ}(\dot{q} - rp)/2 \quad (6-394)$$

$$M_Z = I_{ZZ} \dot{r} \quad (6-395)$$

Next, the motions are conveniently described as composed of a nonrotating component plus a spin ψ .

In addition, the body motions are assumed referenced to inertia axes which are instantaneously attached to the body at $\psi = 0$. Specifically for the gyro rotor the relations are:

$$\begin{Bmatrix} p \\ q \\ r \end{Bmatrix}_G = \begin{Bmatrix} p \\ q \\ r \end{Bmatrix}_{G, NR} + \begin{Bmatrix} 0 \\ 0 \\ \dot{\psi}_G \end{Bmatrix} \quad (6-396)$$

and

$$\begin{Bmatrix} \dot{p} \\ \dot{q} \\ \dot{r} \end{Bmatrix}_G = \begin{Bmatrix} \dot{p} \\ \dot{q} \\ \dot{r} \end{Bmatrix}_{G, NR} + \begin{Bmatrix} \dot{\psi}_G q_{NR} \\ -\dot{\psi}_G p_{NR} \\ \dot{\psi}_G \end{Bmatrix} \quad (6-397)$$

Therefore, for the gyro gimbals which do not rotate, the moments are:

$$M_{XG, NR} = I_{XXG, NR} (\dot{p}_{G, NR} + q_{G, NR} r_{G, NR}) \quad (6-398)$$

$$M_{YG, NR} = I_{YYG, NR} (\dot{q}_{G, NR} - r_{G, NR} p_{G, NR}) \quad (6-399)$$

and

$$M_{ZG, NR} = I_{ZZG, NR} (\dot{r}_{G, NR}) \quad (6-400)$$

Next, recalling that all the gimbal inertia is in the gimbals that hold the rotor, we have for the gyro rotor:

$$M_{X_G} = I_{XX_G} (\dot{p}_{G,NR} + q_{G,NR} r_{G,NR}) + 2I_{XX_G} q_{G,NR} \dot{\psi}_G \quad (6-401)$$

$$M_{Y_G} = I_{YY_G} (\dot{q}_{G,NR} - r_{G,NR} p_{G,NR}) - 2I_{YY_G} p_{G,NR} \dot{\psi}_G \quad (6-402)$$

and

$$M_{Z_G} = I_{ZZ_G} (\dot{r}_{G,NR} + \ddot{\psi}_G) \quad (6-403)$$

The contribution from spin thrust appear as add-on terms. Collecting terms:

$$M_{X_G} = I_{XX_G} (\dot{p}_{G,NR} + q_G r_{G,NR}) + I_{ZZ_G} q_G \dot{\psi}_G \quad (6-404)$$

$$M_{Y_G} = I_{YY_G} (\dot{q}_{G,NR} - r_{G,NR} p_G) - I_{ZZ_G} p_G \dot{\psi}_G \quad (6-405)$$

$$M_{Z_G} = I_{ZZ_G} \dot{r}_{G,NR} + I_{ZZ_G} \ddot{\psi}_G \quad (6-406)$$

The NR notation was dropped from p_G and q_G since $p_G = p_{G,NR}$ and $q_G = q_{G,NR}$. The control gyro rotation is assumed to be independent of rotor-engine speed variations, and driven through a constant speed coupling. These assumptions are reasonable even with rotor shaft driven configurations because the coupling of drive torque equation into the required roll and pitch equations is a second-order effect. The yaw moment reduces to

$$M_{Z_G} = I_{ZZ_{G,NR}} \dot{r}_{G,NR} \quad (6-407)$$

The spring and dampers are taken to be defined in control axes. The formulation follows the corresponding formulation for the swashplate:

$$\begin{Bmatrix} \frac{\partial U}{\partial \phi_G} \\ \frac{\partial U}{\partial \theta_G} \end{Bmatrix} = [K_G] \begin{Bmatrix} \phi_G \\ \theta_G \end{Bmatrix} - [T_{\psi_{c,G}}]^T \begin{Bmatrix} -K_{XC} X_C \\ K_{YC} Y_C \end{Bmatrix}_G \quad (6-408)$$

and

$$\begin{Bmatrix} \frac{\partial B}{\partial \dot{\phi}_G} \\ \frac{\partial B}{\partial \dot{\theta}_G} \end{Bmatrix} = [C_G] \begin{Bmatrix} \dot{\phi}_G \\ \dot{\theta}_G \end{Bmatrix} - [T_{\psi_{c,G}}]^T \begin{Bmatrix} -K_{XC} \dot{X}_C \\ K_{YC} \dot{Y}_C \end{Bmatrix}_G \quad (6-409)$$

The development of the $[K_G]$ and $[C_G]$ follows precisely the formulation presented for the swashplate in Section 6.10.5 or can be directly supplied as input. Note the cross coupling terms only exist if the spring and damper are not symmetric. The stick positions X_c and Y_e are the equivalent position output of first-order servos modeled in the manner of Section 6.10.5.

The gimbals are allowed to be unbalanced. A simple formulation couples hub vertical motion into the gyro, and is included in the previous generalized force expressions.

$$M_{X_{GUB}} = -m_{GUB} Y_{UB} \ddot{Z}_{OH} \quad (6-410)$$

$$M_{Y_{GUB}} = m_{GUB} X_{UB} \ddot{Z}_{OH} \quad (6-411)$$

Gyro tilt transforms are ignored. The distances X_{UB} and Y_{UB} are positive if the imbalance mass is to the right or forward of the gyro spin axis.

6.11.4 Control Gyro Feedback

The feedback is highly important to the direct feedback gyro control concept, and is detailed with care. For steady flight, when the gyro is not precessing, the pilot input counters the moments from the feedback and the gyro spring. The spring contribution is minor. Since the feedback is proportional to blade flap displacements, the resulting rotor shaft moment is proportional to the pilot's stick displacement.

Typically, to achieve a feedback proportional to the rotor shaft moment, a feedback lever is mounted part way out on the fixed hub. Displacement and tilt of the lever mount with blade bending causes the tip of the lever to move, driving a rod that is attached to the gyro feedback spring. The displacement of the tip of the lever is:

$$Z_{J_n} = Z_{RM_n} - Z'_{RM_n} (X_{RM} - X_J) \quad (6-412)$$

Where the subscript RM and J refer to the lever moment and tip, respectively. The lever spanwise length is then $X_{RM} - X_J$. The linear and slope displacements of the lever mount are given as:

$$Z_{RM_n} = \sum_{m=1}^3 \frac{\partial Z_{RM}}{\partial A_{mn}} A_{mn} \quad (6-413)$$

and

$$Z'_{RM_n} = \sum_{m=1}^3 \frac{\partial Z'_{RM}}{\partial A_{mn}} A_{mn} \quad (6-414)$$

for blade n due to modes 1, 2 and 3. The displacement does not depend on feathering, and the mount is taken to be at the same waterline as the hub origin. Polarity of the motion needs to be observed. For instance, the construction of the lever for the AH-56A helicopter caused the slope displacement contribution to Z_{J_n} to be greater than Z_{RM_n} . Therefore,

the tip of the lever went down as the blade flapped up.

A feedback spring preload is used to preclude deadband. Friction exists and is modeled by letting the point J_n reverse direction an incremental amount, ΔZ_{J_LIMIT}

$$\Delta Z_{J_LIMIT} = \frac{M_{FB_FR}}{K_{FB}} \quad (6-415)$$

This acts without changing the applied gyro moment. M_{FB_FR} is the gyro stiction moment and K_{FB} the feedback spring. The feedback spring displacement becomes:

$$Z_{FB_n} = Z_{J_n} - \left(\int_0^T \dot{Z}_{J_n} dt \right)_{LIMIT} \quad (6-416)$$

where:

$$\left(\int_0^T \dot{Z}_{J_n} dt \right)_{LIMIT} = \text{SIGN} \left[\left| \int_0^T \dot{Z}_{J_n} dt \right| \leq \Delta Z_{J_LIMIT}, \int_0^T \dot{Z}_{J_n} dt \right] \quad (6-417)$$

The action of stiction on the feedback displacement during a reversal of velocity is shown in Figure 6-6.

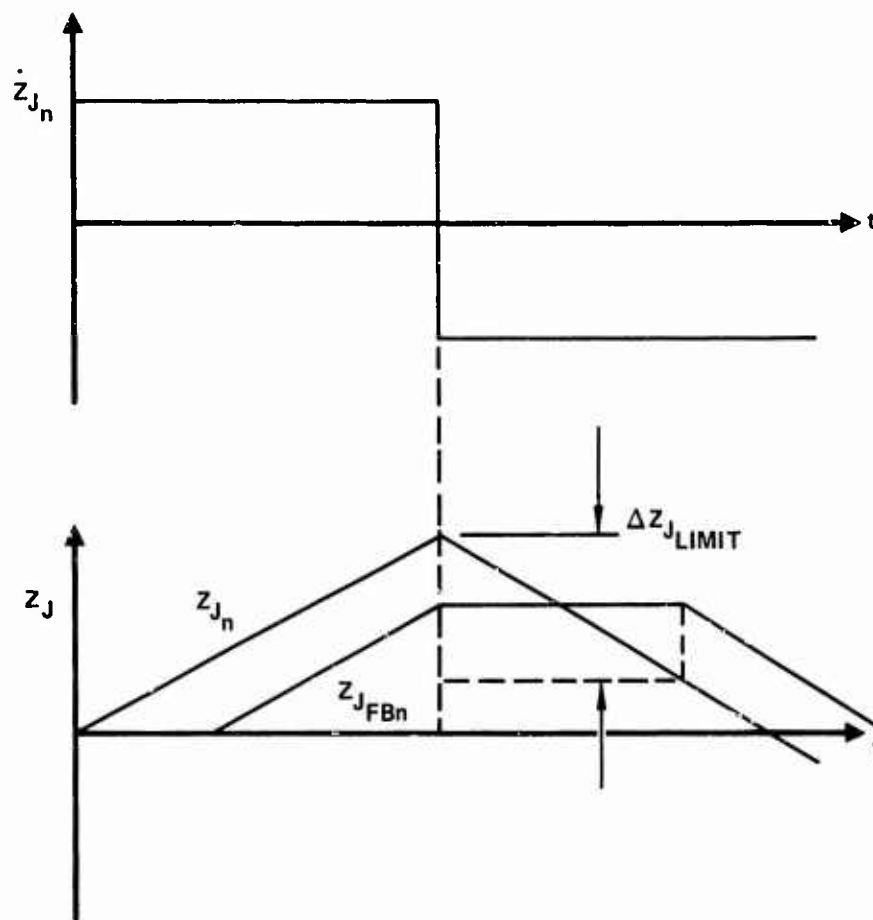


Figure 6-6. Effect of Stiction of Feedback Lever Displacement

Point J_n on the feedback lever is located at an azimuth ψ_{FB} ahead of the blade reference and a distance X_{FB} from the rotor shaft center. The point J_n in fuselage axis becomes

$$\begin{Bmatrix} J_n \\ \end{Bmatrix}_F = \begin{Bmatrix} - \\ - \\ Z_{FBn} \end{Bmatrix}_F = [T_{H-F}] \left\{ \left\{ [T_{H-R}]^T [T_{R-BLn}]^T [T_{BLn-FBn}]^T \begin{Bmatrix} X_{FBn} \\ 0 \\ Z_{FBn} \end{Bmatrix} \right\} - \begin{Bmatrix} 0 \\ 0 \\ Z_F \end{Bmatrix}_H \right\} \quad (6-418)$$

where

$$[T_{BLn-FBn}]^T = \begin{bmatrix} \cos\psi_{FBn} & -\sin\psi_{FBn} & 0 \\ \sin\psi_{FBn} & \cos\psi_{FBn} & 0 \\ 0 & 0 & 1 \end{bmatrix} \quad (6-419)$$

The other end of the feedback spring is grounded to the gyro at a radius of X_{FBG} which leads the blade by the angle ψ_{FBG} . Hence,

$$\begin{Bmatrix} X_{FBGn} \\ Y_{FBGn} \\ Z_{FBGn} \end{Bmatrix}_F = [T_{\phi_G}]^T [T_{\theta_G}]^T [T_{\psi_R}]^T [T_{FBG}]^T \begin{Bmatrix} X_{FBG} \\ 0 \\ 0 \end{Bmatrix} \quad (6-420)$$

in fuselage axes where

$$\begin{bmatrix} T_{\psi_R} \end{bmatrix}^T = \begin{bmatrix} \cos(\psi_R + \psi_{BLn}) & -\sin(\psi_R + \psi_{BLn}) & 0 \\ \sin(\psi_R + \psi_{BLn}) & \cos(\psi_R + \psi_{BLn}) & 0 \\ 0 & 0 & 1 \end{bmatrix} \quad (6-421)$$

and

$$\begin{bmatrix} T_{\psi_{FBG}} \end{bmatrix} = \begin{bmatrix} \cos\psi_{FBG} & -\sin\psi_{FBG} & 0 \\ \sin\psi_{FBG} & \cos\psi_{FBG} & 0 \\ 0 & 0 & 1 \end{bmatrix} \quad (6-422)$$

The feedback spring force is assembled as:

$$\left(F_{FBn} \right)_F = K_{FB} \left(Z_{FBn} - \ell_{FB} \right) \quad (6-423)$$

The length ℓ_{FB} serves as the preload constant. It does not affect the cyclic spring feedback to the gyro. The vertical displacement Z_{FBn} of

the lower end of the spring is excluded. It produces a force proportional to gyro tilt and this force is best considered to be a component of the gyro spring value.

The feedback moment is the spring force times the gyro attachment arm. The moment becomes:

$$\begin{Bmatrix} M_{X_{GFB}} \\ M_{Y_{GFB}} \\ - \end{Bmatrix}_G = \sum_{n=1}^b \begin{bmatrix} T_{\phi_G} \end{bmatrix} \begin{Bmatrix} Y_{FBG_n} F_{FBn} \\ -X_{FBG_n} F_{FBn} \\ 0 \end{Bmatrix} \quad (6-424)$$

which is taken about the gyro Euler axes.

To close the gyro-swashplate-rotor blade loop, a relation is needed between gyro motions and swashplate motions. Assuming a power actuator between the gyro and swashplate gives:

$$\tau_{\text{GSP}} \dot{\phi}_{\text{SP}_C} + \phi_{\text{SP}_C} = G_{\phi_{\text{GSP}}} \phi_G \quad (6-425)$$

and

$$\tau_{\text{GSP}} \dot{\theta}_{\text{SP}_C} + \theta_{\text{SP}_C} = G_{\theta_{\text{GSP}}} \theta_G \quad (6-426)$$

The subscript C refers to the command or control value.

The actuator variables can have rate and displacement limits in the manner described in Section 6.10.5.

6.11.5 Summary Description of Phase Angles

A number of phase angles were introduced in this section and Section 6.10 on the swashplate. Figure 6-7 shows the relationship between all these phase angles as they apply to the Direct-Flap Feedback Control System. The values indicated are for the AH-56A Cheyenne helicopter. The pilot is assumed to have pulled the stick back, precessing the gyro until the flap feedback was sufficient to react against the pilot input. The vehicle is assumed fixed, otherwise it would pitch up and relieve the flapping. The gyro spring load is minor and is not shown. Swashplate to blade linkage is made with a trailing pitch horn, hence ψ_{PH} is 180 degrees minus the

actual pitch horn angle to account for the reversal in feathering going from a leading to a trailing pitch horn. The pitch horn phasing is chosen to place feathering at an azimuth that will produce flapping at the desired direction, in this case up flap forward for a nose up pitching moment.

Note the gyro precesses up in an axis perpendicular to the applied moment F_{ϕ_G} , but that the swashplate displacement is in the same axis as the

applied moment F_{θ_G} . The swashplate control acts through very stiff

spring rate which prevents the rotating swashplate from responding in a low-frequency precession mode.

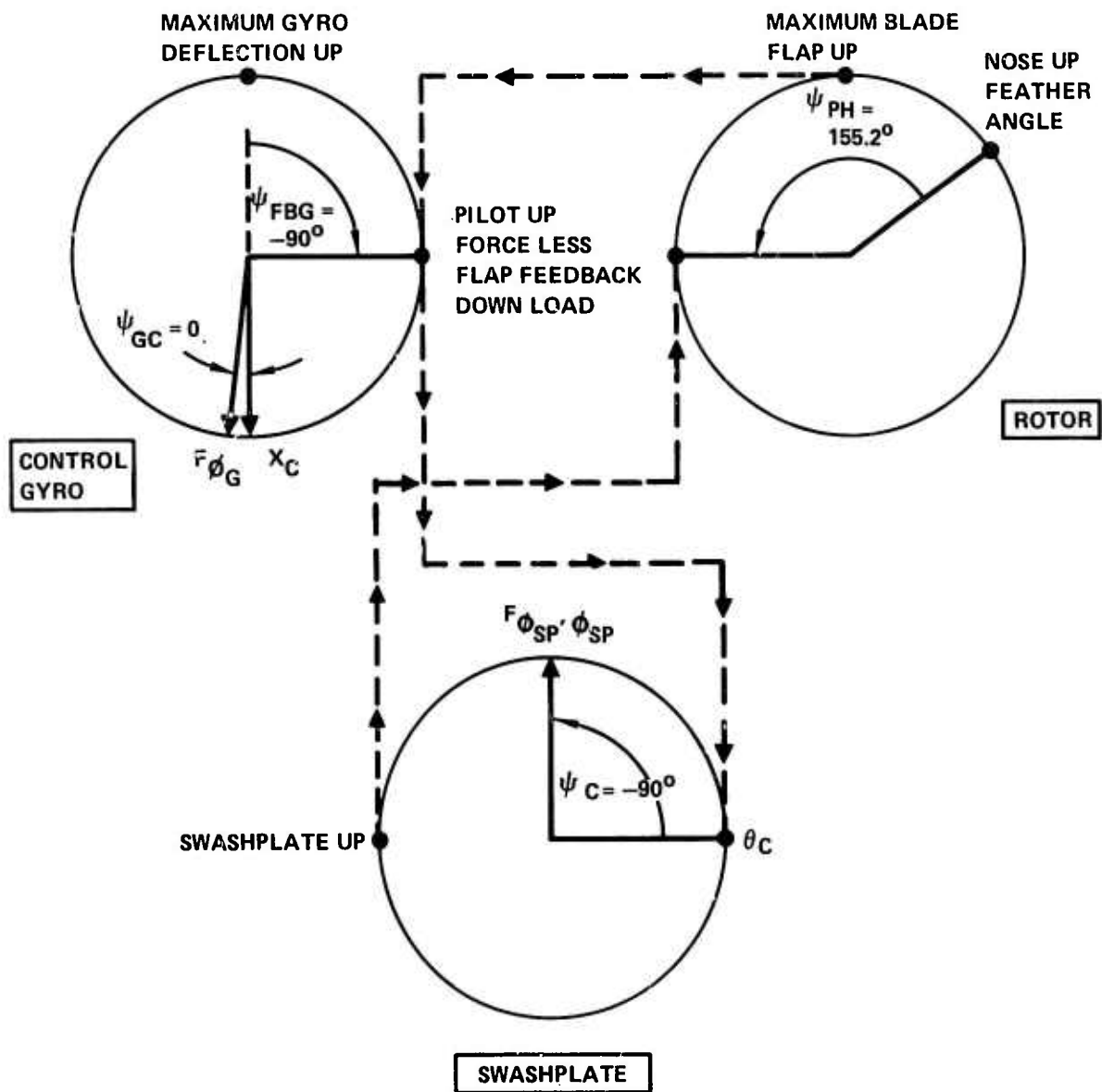


Figure 6-7. Phasing For Direct-Flap Feedback Control System

6.12 ENGINE EQUATIONS

6.12.1 Rotor Azimuth and Rotation Rate

The program allows a variation of rotor speed in maneuvers due to variations in the torque required by the various rotors and in the torque supplied by the engine. The dynamic system rotates as a rigid, geared unit. That is, the shafts are not allowed elastic windup. The main rotor speed, $\dot{\psi}_R$ and hence the engine speed, is referenced to the fuselage, and not to inertial space. The displacement ψ_R is the azimuth of the number one blade.

6.12.2 Engine Model

Figure 6-8 illustrates the engine model used in the program. The figure also plots typical engine torque characteristics. The model represents the first-order lag power response characteristics of the free turbine powerplants commonly used in rotorcraft applications.

Being a perturbation model, the engine is referenced to its trim position. The change in engine torque in a maneuver is

$$M_{XA_ENG} - M_{XA_ENG,TRIM} = \frac{\partial M_{ENG}}{\partial \dot{\psi}_{GEN}} \dot{\psi}_{GEN} - \frac{\partial M_{ENG}}{\partial \dot{\psi}_{ENG}} (\dot{\psi}_{ENG} - \dot{\psi}_{ENG,TRIM}) \quad (6-427)$$

where $0 \leq M_{XA_ENG} \leq M_{XA_ENG,MAX}$. The zero limit occurs if the overrunning

clutch disconnects the engine in the transition to autorotation. The maximum value corresponds to the engine shaft torque limit.

The gas generator, speed, $\dot{\psi}_{GEN}$, is a degree of freedom. It is considered a "secondary" degree of freedom in that the coupling through the generalized masses with the "primary" degrees of freedom can be neglected. An equation for the generation speed can be supplied from its torque characteristics:

$$I_{GEN} \ddot{\psi}_{GEN} + C_{GEN} \dot{\psi}_{GEN} = -K_{ENG1} \ddot{\psi}_{ENG} - K_{ENG2} (\dot{\psi}_{ENG} - \dot{\psi}_{ENG,TRIM}) \quad (6-428)$$

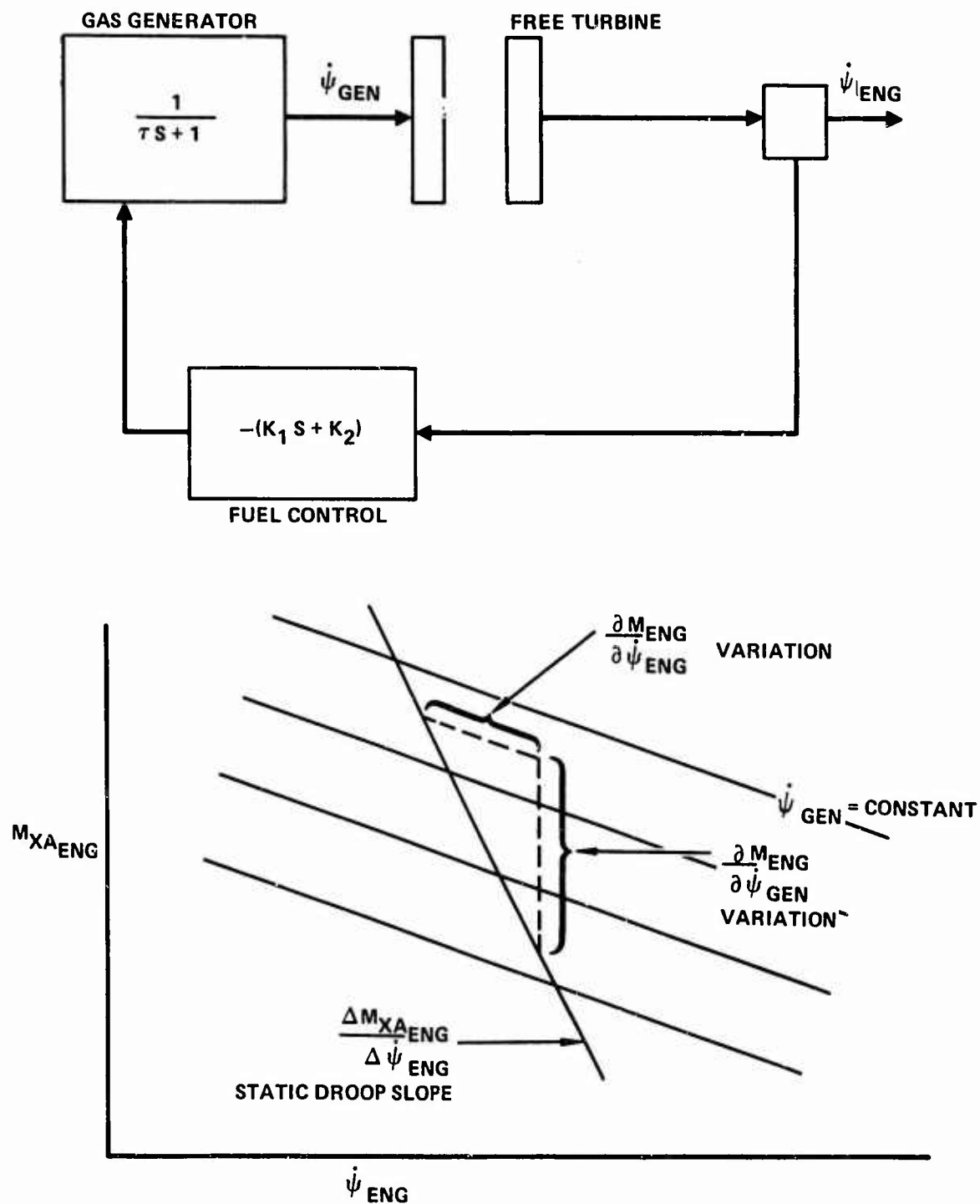


Figure 6-8. Engine Model and Torque-Speed Characteristics

The terms on the left represent acceleration inertia torque and steady-state torque. On the right, the fuel control causes torque to be added if the engine speed drops below the trim value. The $\ddot{\psi}_{ENG}$ term exists since the control is modeled with simple lag. Restating this equation, using rotor speed and a generator time constant, gives:

$$\ddot{\psi}_{GEN} = \frac{-\dot{\psi}_{GEN} - K_{R1} \ddot{\psi}_R - K_{R2}(\dot{\psi}_R - \dot{\psi}_{R,TRIM})}{\tau_{GEN}} \quad (6-429)$$

where $\psi_{GEN} = \frac{I_{GEN}}{C_{GEN}}$ is the order of a second.

The engine droop characteristic can be used to size the engine constants. With $\ddot{\psi}_{GEN} = \ddot{\psi}_R = 0$, substituting the generator equation into the engine equation and rearranging,

$$\frac{\Delta(M_{XA_{ENG}})_R}{\Delta\dot{\psi}_F} = \frac{\partial(M_{ENG})_R}{\partial\dot{\psi}_{GEN}} K_{R2} - \frac{\partial(M_{ENG})_R}{\partial\dot{\psi}_R} \quad (6-430)$$

Only Δ incremental changes are of interest. The bracket subscripted R indicates the torque is determined at the rotor speed and includes the engine gear ratio. The term on the right is the static droop line shown in Figure 6-8. This plot also geometrically interprets the partial derivatives on the left.

The generator speed $\dot{\psi}_{GEN}$ is not given a reference. Its value is zero when trim is completed.

6.12.3 Partial Derivatives

Partial derivatives relating linear motions of the blade elements to shaft rotations are needed:

$$\left\{ \frac{\partial r_{BLE}}{\partial \psi_R} \right\}_{BLn} = - \left\{ \frac{\partial r_{BLE}}{\partial \psi_H} \right\}_{BLn} + \left\{ \frac{\partial r_{BLE}}{\partial \phi_{Fn}} \right\}_{BLn} \left(\frac{\partial \phi_{Fn}}{\partial \psi_R} \right) \quad (6-431)$$

Shaft rotation not only involves blade root rotation ψ_H , but also feathering motions. The feathering partial is obtained by differentiating the feather angle equation in Section 5.5.8:

$$\frac{\partial \phi_{Fn}}{\partial \psi_R} = A_{1S} \sin(\psi_{BLn} + \psi_R) - B_{1S} \cos(\psi_{BLn} + \psi_R) \quad (6-432)$$

6.12.4 Generalized Masses

The engine degree of freedom couples in with every other degree of freedom except those for shaft bending. Equations for the engine generalized masses are given in Table 6-7.

TABLE 6-7. ENGINE GENERALIZED MASSES

$$M_{\psi_R \chi_H} = \sum_{n=1}^b \left[\frac{\partial Y_{OBLn}}{\partial X_H} \frac{\partial \phi_{Fn}}{\partial \psi_R} M_{Y_{OBLn} \phi_{Fn}} + \frac{\partial Z_{OBLn}}{\partial X_H} \frac{\partial \phi_{Fn}}{\partial \psi_R} M_{Z_{OBLn} \phi_{Fn}} \right] \quad (6-433)$$

$$M_{\psi_R Y_H} = \sum_{n=1}^b \left[\frac{\partial Y_{OBLn}}{\partial Y_H} \frac{\partial \phi_{Fn}}{\partial \psi_R} M_{Y_{OBLn} \phi_{Fn}} + \frac{\partial Z_{OBLn}}{\partial Y_H} \frac{\partial \phi_{Fn}}{\partial \psi_R} M_{Z_{OBLn} \phi_{Fn}} \right] \quad (6-434)$$

$$M_{\psi_R Z_H} = \sum_{n=1}^b \left[\frac{\partial Y_{OBLn}}{\partial Z_H} \frac{\partial \phi_{Fn}}{\partial \psi_R} M_{Y_{OBLn} \phi_{Fn}} + \frac{\partial Z_{OBLn}}{\partial Z_H} \frac{\partial \phi_{Fn}}{\partial \psi_R} M_{Z_{OBLn} \phi_{Fn}} \right] \quad (6-435)$$

$$M_{\psi_R \phi_H} = \sum_{n=1}^b \left(M_{\psi_R \phi_H} \right)_{BLn} - I_{XX_{ENG}} G_{ENG} - I_{XX_P} G_P \quad (6-436)$$

$$M_{\psi_R \theta_H} = \sum_{n=1}^b \left(M_{\psi_R \theta_H} \right)_{BLn} + I_{YY_{TR}} G_{TR} \quad (6-437)$$

$$M_{\psi_R \psi_H} = - I_{ZZ_R} - I_{ZZ_H} - I_{ZZ_{SP}} \quad (6-438)$$

$$M_{\psi_R \psi_R} = I_{ZZ_R} + I_{ZZ_{SP}} + I_{ZZ_H} + I_{XX_{ENG}} G_{ENG}^2 + I_{XX_P} G_P^2 + I_{YY_{TR}} G_{TR}^2 \quad (6-439)$$

$$M_{\psi_R \beta_{PHn}} = \frac{\partial \phi_{Fn}}{\partial \beta_{PHn}} \left(M_{\psi_{BLn} \phi_{Fn}} + \frac{\partial \phi_{Fn}}{\partial \psi_R} M_{\phi_{Fn} \phi_{Fn}} \right) \quad (6-440)$$

TABLE 6-7 - Continued

$$M_{\psi_R A_{mn}} = M_{\psi_{BLn} A_{mn}} + \frac{\partial \phi_{Fn}}{\partial \psi_R} M_{\phi_{Fn} A_{mn}} \quad (6-441)$$

$$\left(M_{\psi_R \phi_H} \right)_{BLn} = \sum_{i=1}^k \left[m(i) \left(\frac{\partial X_{BLE}}{\partial \psi_R} \frac{\partial X_{BLE}}{\partial \phi_H} + \frac{\partial Y_{BLE}}{\partial \psi_R} \frac{\partial Y_{BLE}}{\partial \phi_H} + \frac{\partial Z_{BLE}}{\partial \psi_R} \frac{\partial Z_{BLE}}{\partial \phi_H} \right)_{BLn} \right] \quad (6-442)$$

$$\left(M_{\psi_R \theta_H} \right)_{BLn} = \sum_{i=1}^k \left[m(i) \left(\frac{\partial X_{BLE}}{\partial \psi_R} \frac{\partial X_{BLE}}{\partial \theta_H} + \frac{\partial Y_{BLE}}{\partial \psi_R} \frac{\partial Y_{BLE}}{\partial \theta_H} + \frac{\partial Z_{BLE}}{\partial \psi_R} \frac{\partial Z_{BLE}}{\partial \theta_H} \right)_{BLn} \right] \quad (6-443)$$

6.12.5 Generalized Forces

Only one generalized force is needed:

$$F_{\psi_R} = - \left(M_{Z_{MR}} \right)_H - \left(M_{X_{IP}} + M_{X_{AP}} \right) G_P + \left(M_{Y_{ITR}} + M_{Y_{ATR}} \right) G_{TR} \\ - \left(M_{X_{IENG}} - M_{X_{AENG}} \right) G_{ENG} - \left(J_{ZZ_H} + I_{ZZ_{SP}} \right) (\dot{\psi}_R - \dot{r}_H) \quad (6-444)$$

The inertia component of the propeller, the tail rotor and the engine are formulated in Section 6.9.4. The aerodynamic description follows in Section 7. The positive direction of these moments are right roll, nose up, and yaw right per fuselage axes.

7. AERODYNAMICS

7.1 INTRODUCTION

Other than gravity, the external loadings acting on the REXOR equations of motion can be traced to aerodynamic sources. The following subsections trace the source, nature and use of these aerodynamic loads.

7.1.1 Aerodynamic Forces Producing Surfaces Considered

The aerodynamic loads considered in REXOR are divided into the categories of (1) associated with the main rotor, or (2) the rest of the rotorcraft (nonrotating surfaces, tail rotor and propeller). In view of the stated objectives of REXOR the program development emphasis is on the main rotor.

7.1.2 Use of Forces Generated

As mentioned, the aerodynamic loads are in essence the external forcing functions of the equations of motion. Generally the developed loads are in the axis of the apparent air velocity of the loaded element. Thus transformations are required to put the loads into the reference axes of the equation of motion considered.

7.2 MAIN ROTOR

7.2.1 Overview

To generate a main rotor model with sufficient detail to do dynamic investigations, a reasonably good quality aerodynamics presentation is required. To this end a table lookup of blade section properties, multifunction inflow model, quasi-steady aerodynamics, and dynamic stall are used in REXOR.

7.2.1.1 Blade Flow Field

As developed in the following subsections, the instantaneous blade air-flow is the inertial velocity of the blade element. This velocity includes the motion of the principal reference set and the motion of the blade element with respect to the principal reference set. The calculation assumes the air mass is at rest, which is reasonable for dynamics investigations.

7.2.1.2 Air Pressure and Angle of Attack

The dynamic pressure used for these calculations is based on sea level standard density. The loads are ratioed to the actual air density.

The angle of attack is the sum of geometric pitch angle and the instantaneous air velocity. The rate of angle of attack is also calculated and used for the transient blade aero loads, Sections 7.2.3.3 and 7.2.3.4.

7.2.1.3 Forces and Moments Produced

The steady blade loads are produced from the air velocity components of Section 7.2.3.1 and the coefficient data (C_L , C_D , C_M) of Section 7.2.4. The transient lift and moment effects are developed in Sections 7.2.3.3 (quasi-steady aerodynamics) and 7.2.3.4 (dynamic stall).

7.2.2 Concept of Rotor Inflow Model

The main rotor inflow model used in REXOR is based on the air flow incident upon the rotor disc plus the air velocity imparted due to momentum exchange due to integrated blade span loading. This is to be contrasted with a formulation which tracks the rotor blade positions and the attendant trailing vortices

The incident air flow is the inertial velocity of the rotor coordinates, and is directly available from the preceeding mechanical development. However a number of assumptions need to be stated and utilized to arrive at the induced velocity component of the inflow model.

7.2.2.1 Induced Velocity Assumptions

1. Only the vertical downwash and its variations radially and azimuthally over the rotor disk are considered. Induced swirl, and lateral downwash components are considered minor and therefore neglected.
2. Downwash effects due to unsteady aerodynamics are not treated here as an overall effect, but as a blade segment condition in Section 7.2.3.3.
3. Rotor-induced flow distribution in hover and forward flight is patterned after Reference 10. This reference assumes a uniform loading in hover. Figure 7-1, from Reference 11, shows this distribution compared with typical loading and a triangular loading model. Figure 7-2 from Reference 10 shows the theoretical induced velocity distribution in forward flight as a consequence of a uniform hover distribution. This data is fitted to slopes or a longitudinal skew as a function of speed in REXOR. Lateral distribution remains uniform in accord with Reference 12, which corrects the lateral distribution work of Reference 10.
4. A variation in lateral and longitudinal induced velocity is included to account for roll and pitch aerodynamic shaft moments.

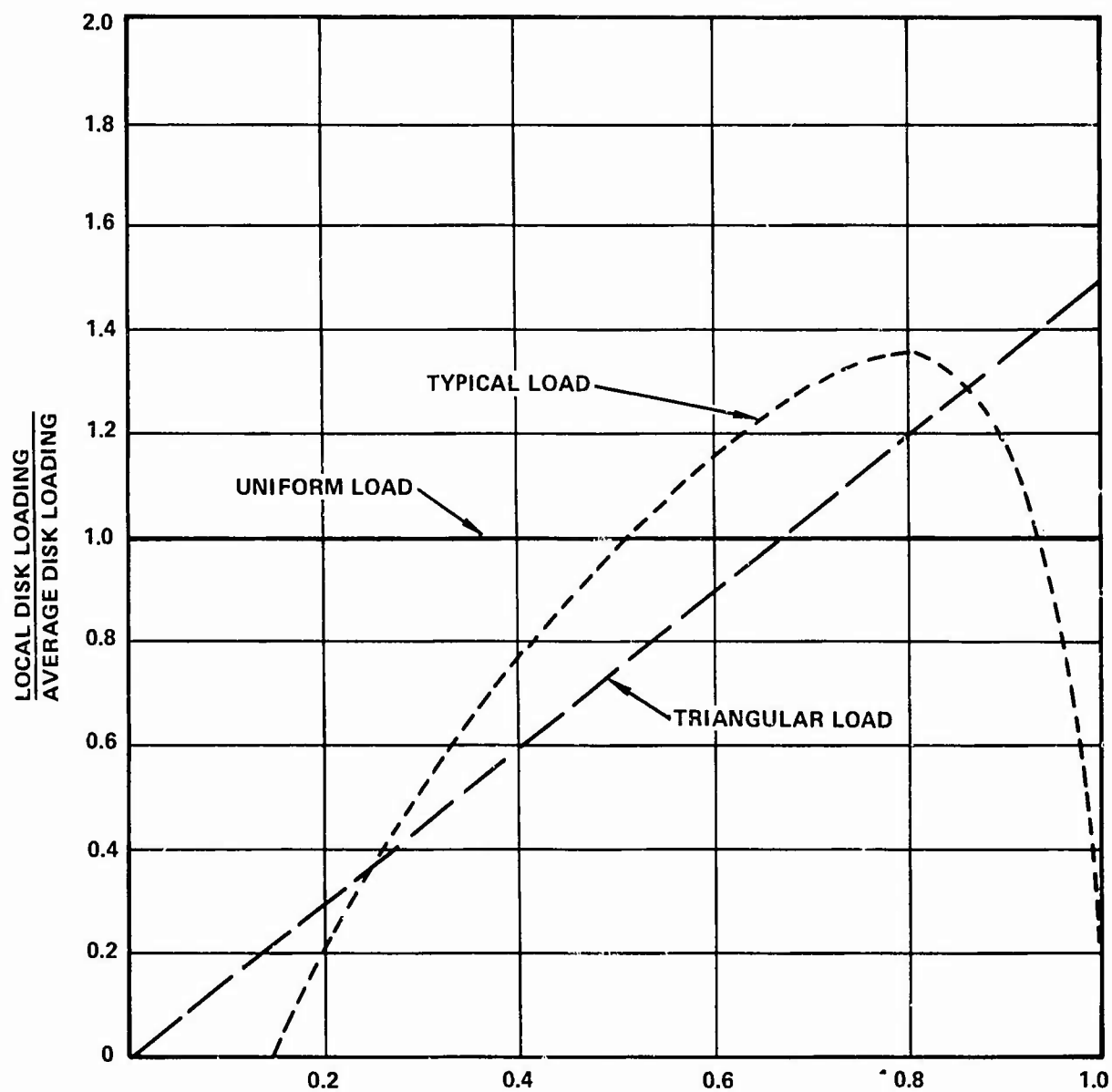


Figure 7-1. Blade Loading Distributions in Hover

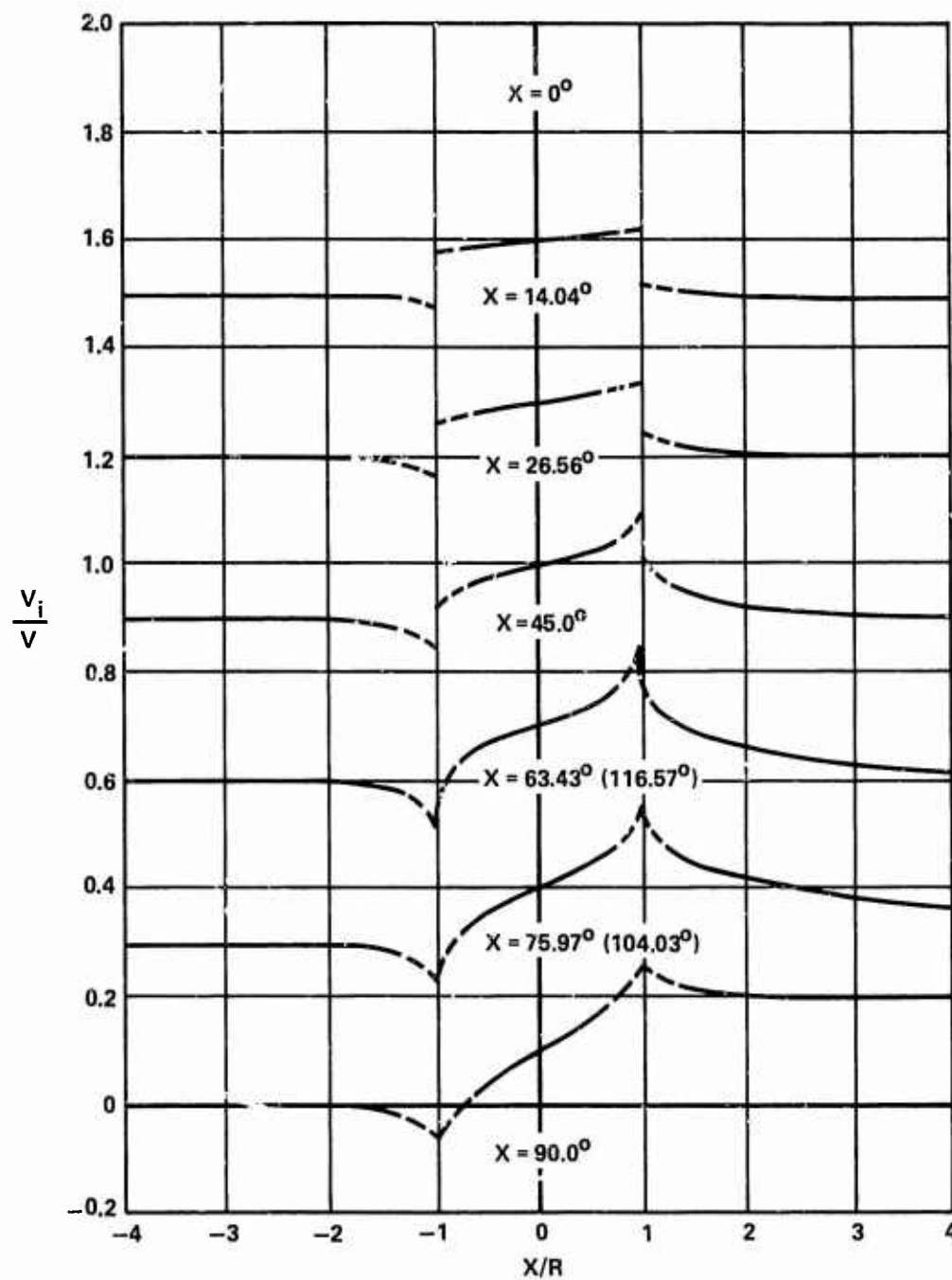


Figure 7-2. Induced Velocity Distribution as a Function of Wake Angle (Forward Flight)

5. Lifting line theory correction, rotor tip loss, and root cut-out effects are ignored.
6. Transient effects are simulated by a single time lag.

7.2.2.2 Steady State Values

The starting point for determining the downwash is momentum theory as applied to an elementary area dA :

$$\begin{aligned} dT &= \left(\frac{dm}{dt} \right) 2w_i = \left(\rho V_{iMR} dA \right) 2w_i \\ &= \rho \sqrt{u_H^2 + v_H^2 + (w_H - w_i)^2} dA 2w_i \end{aligned} \quad (7-1)$$

The thrust increment is dT , dm/dt is the flow of air through the rotor disk with resultant velocity V_{iMR} , ρ is the air density and w_i the downwash velocity. The velocities are taken in hub coordinates and no effort is made to account for rotor tilt.

The thrust expression above is used to define the following induced velocity components.

- Average component, w_i
- Longitudinal variation with pitching aerodynamic moment, q_{iMR}
- Lateral variation with roll aerodynamic moment, p_{iMR}

The downwash velocity becomes

$$w_i = w_{iMR} + r q_{iMR} \cos \psi_R + r p_{iMR} \sin \psi_R \quad (7-2)$$

The coefficients can be evaluated by equating the thrust and moment values for the main rotor equations to the integrals of the momentum expressions at hand. First consider the thrust expression. The evaluating task can be reduced by employing some boundary conditions. For rotor thrust only (no moment), q_{iMR} and $p_{iMR} = 0$. A convenient expression for the elementary area, dA , is shown in Figure 7-3. While radial annuli would serve for thrust integration, the form selected is particularly suited for the moment expressions.

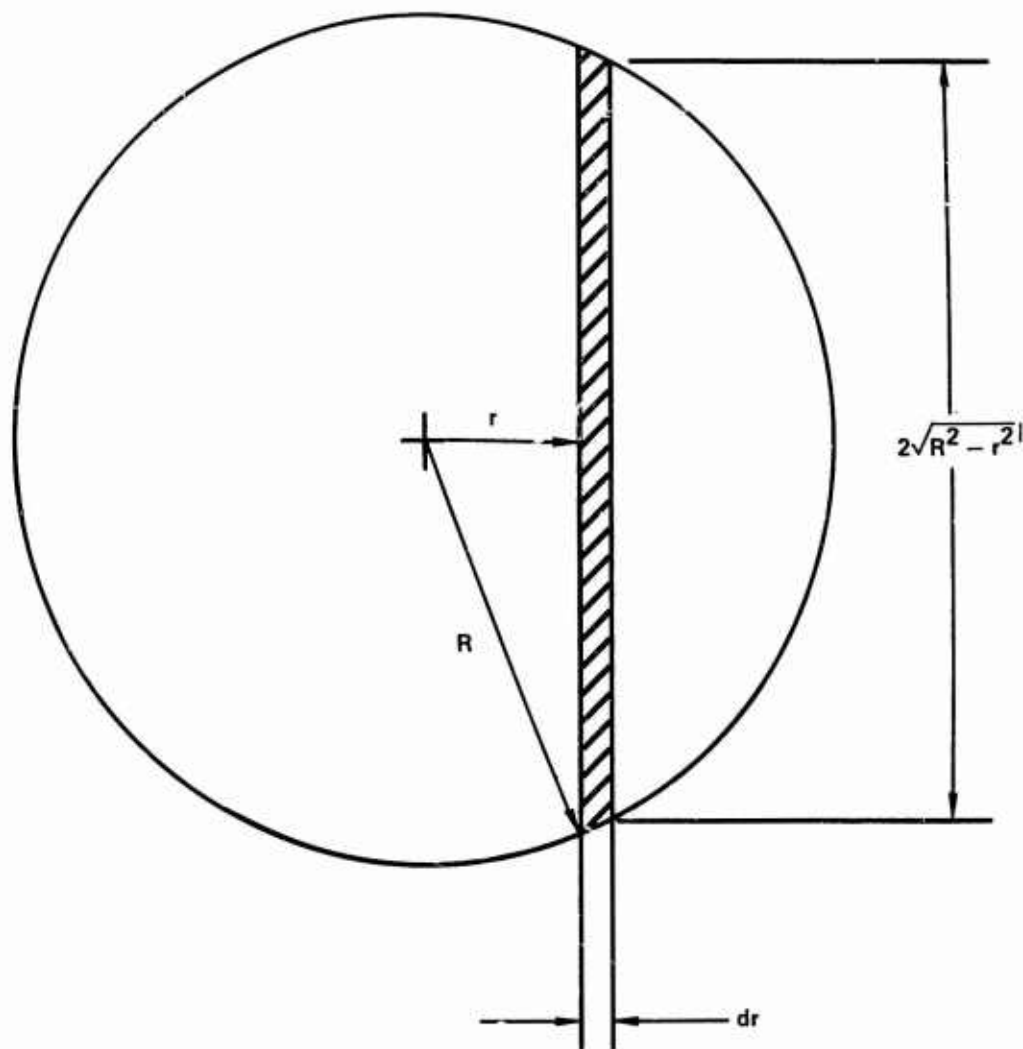


Figure 7-3. Incremental Area for Shaft Moment Integration

For the average rotor thrust,

$$-F_{ZA_{MR,H}} = T = \int_{-R}^R \rho \sqrt{u_H^2 + v_H^2 + (w_H - w_{iMR})^2} (2\sqrt{R^2 - r^2} dr)^2 w_{iMR} \quad (7-3)$$

A further assumption is required to solve the square root of this expression and the corollary momentum equations.

For forward flight

$$w_i \ll v_{iMR} = \sqrt{u_H^2 + v_H^2 + (w_H - w_{iMR})^2} = (\text{constant}) \quad (7-4)$$

Completing the integration gives

$$-F_{ZA_{MR,H}} = \rho \pi R^2 v_{iMR}^2 w_{iMR} \quad (7-5)$$

Next consider the case of no rolling moment; i.e., only thrust and pitching moment. Figure 7-3 is used with the incremental strip considered to be right-left oriented so that all equal values of q_{iMR} are integrated at once.

Then,

$$\begin{aligned} M_{YA_{MR,H}} &= \int_{-R}^R r dT \\ &= \int_{-R}^R r \rho \sqrt{u_H^2 + v_H^2 + (w_H - w_{iMR} - r q_{iMR})^2} \\ &\quad \cdot (2\sqrt{R^2 - r^2} dr)^2 (w_{iMR} + r q_{iMR}) \end{aligned} \quad (7-6)$$

or

$$M_{YA_{MR,H}} = \rho \frac{\pi R^4}{4} V_{iMR}^2 q_{iMR} \quad (7-7)$$

Likewise for rolling moment, and using fore-aft increment strips gives

$$M_{XA_{MR,H}} = \rho \frac{\pi R^4}{4} V_{iMR}^2 P_{iMR} \quad (7-8)$$

Note the subscript A on $F_{ZA_{MR,H}}$, $M_{XA_{MR,H}}$, and $M_{YA_{MR,H}}$ denotes the aerodynamic component only of main rotor loads in hub axes.

The foregoing expressions are now developed for hovering and low-speed flight. In this condition,

$$u_H^2 + v_H^2 \ll (w_H - w_{iMR})^2 \quad (7-9)$$

Integrating gives

$$-F_{ZA_{MR,H}} = \rho \pi R^2 (w_H - w_{iMR})^2 w_{iMR} \quad (7-10)$$

and

$$M_{YA_{MR,H}} = \left(\frac{\rho \pi R^4}{4} (w_H - w_{iMR}) \right) q_{iMR} \left(1 - \frac{w_{iMR} (w_H - w_{iMR})}{(w_H - w_{iMR})^2} \right) \quad (7-11)$$

$$M_{XA_{MR,H}} = \left(\frac{\rho \pi R^4}{4} (w_H - w_{iMR}) \right) P_{iMR} \left(1 - \frac{w_{iMR} (w_H - w_{iMR})}{(w_H - w_{iMR})^2} \right) \quad (7-12)$$

The consequence of cyclic, first-harmonic downwash was explored in Reference 13. Their conclusion, which parallels Lockheed's experience, is that the phase and magnitude of the flap response of a hingeless blade to cyclic feathering is markedly affected by cyclic downwash. The shaft moments variation with feathering angle and the phase angle between flap and feathering are both reduced with cyclic downwash, the effect being greater in hover than in forward flight.

A physical interpretation can be rationalized for the formula above, at least in hover, in that the aerodynamic thrust and moment produces a flow of linear and angular momentum. Imagine the flow as a continuous stack of disks having a mass per unit thickness $\rho \pi R^2$ and dimetral inertia per unit thickness $\rho (\pi R^4/4)$. $2 w_{iMR}$, $2 p_{iMR}$ and $2 q_{iMR}$ are the final, for downstream position, values of induced velocities obtained by these disks orientated with the flow. The terms $\rho \pi R^2 V_i$ and $\rho \pi R^4/4 V_i$ are the mass flow per unit time, and the moment of inertia flow per unit time through the "actuator" disk, which times $2 w_{iMR}$, $2 p_{iMR}$ or $2 q_{iMR}$ is the gain of momentum.

For programming purposes, an empirical blend of the forward flight and hovering sets of expressions is used. The limiting cases of the empirical set give the derived cases. The expressions used are:

$$-F_{ZA_{MR,H}} = \rho \pi R^2 V_{iMR} 2 w_{iMR} \quad (7-13)$$

$$M_{YA_{MR,H}} = \frac{\rho \pi R^4}{4} V_{iMR} 2 q_{iMR} \left[1 - \frac{w_{iMR} (w_H - w_{iMR})}{V_{iMR}^2} \right] \quad (7-14)$$

$$M_{XA_{MR,H}} = \frac{\rho \pi R^4}{4} V_{iMR} 2 p_{iMR} \left[1 - \frac{w_{iMR} (w_H - w_{iMR})}{V_{iMR}^2} \right] \quad (7-15)$$

7.2.2.3 Variations in Forward Flight and In Ground Effects

The previous development can be assembled and combined with linearized forward flight distribution and ground effect factors.

$$\begin{aligned} (w_{BLE})_{DW,BLn} &= w_{iMR} f_{iMR} \left[1 + K_{iMR} \frac{r}{R} \cos(\psi_R + \psi_{BLn} + \psi_w) \right. \\ &\quad \left. + r p_{iMR} \sin(\psi_R + \psi_{BLn}) + r q_{iMR} \cos(\psi_R + \psi_{BLn}) \right] \quad (7-16) \end{aligned}$$

The ground effect factor, f_{iMR} , and the longitudinal linear gradient factor, K_{iMR} , accounts for forward flight.

Note this formula is in rotating coordinates, and that the forward flight distribution actually is applied along the line of the apparent airflow, ψ_W . In doing this the distribution is valid for forward flight, sideward flight and sideslip conditions. The angle ψ_W is

$$\psi_W = \tan^{-1} \left(\frac{v_H}{u_H} \right) \quad (7-17)$$

as shown in Figure 5-4.

The aerodynamic moment factors, q_{iMR} and p_{iMR} , remain attached to the hub axis.

The downwash factor K_{iMR} , as explained in assumption 3, is given as a function of the wake angle defined as

$$\chi_{iMR} = \tan^{-1} \frac{\sqrt{u_H^2 + v_H^2}}{w_{iMR} - w_H} \quad (7-18)$$

which is zero in hover and near 90 degrees in high-speed flight. The function can be constrained by a number of factors. In hover, the value is zero. A 90-degree value of about 1.6 can be read from Figure 7-2. Also from this figure a set of linearized distributions is read, and plotted as Figure 7-4.

The ground effect factor,

$$f_{iMR} = 1 - \frac{1}{16} \left(\frac{R}{h} \right)^2 \frac{1}{1 + \frac{u_H^2 + v_H^2}{w_{iMR}^2}} \quad (7-19)$$

is taken from Reference 14. Where $h = -(Z_{O_H})_E$ from Section 5.5.1.

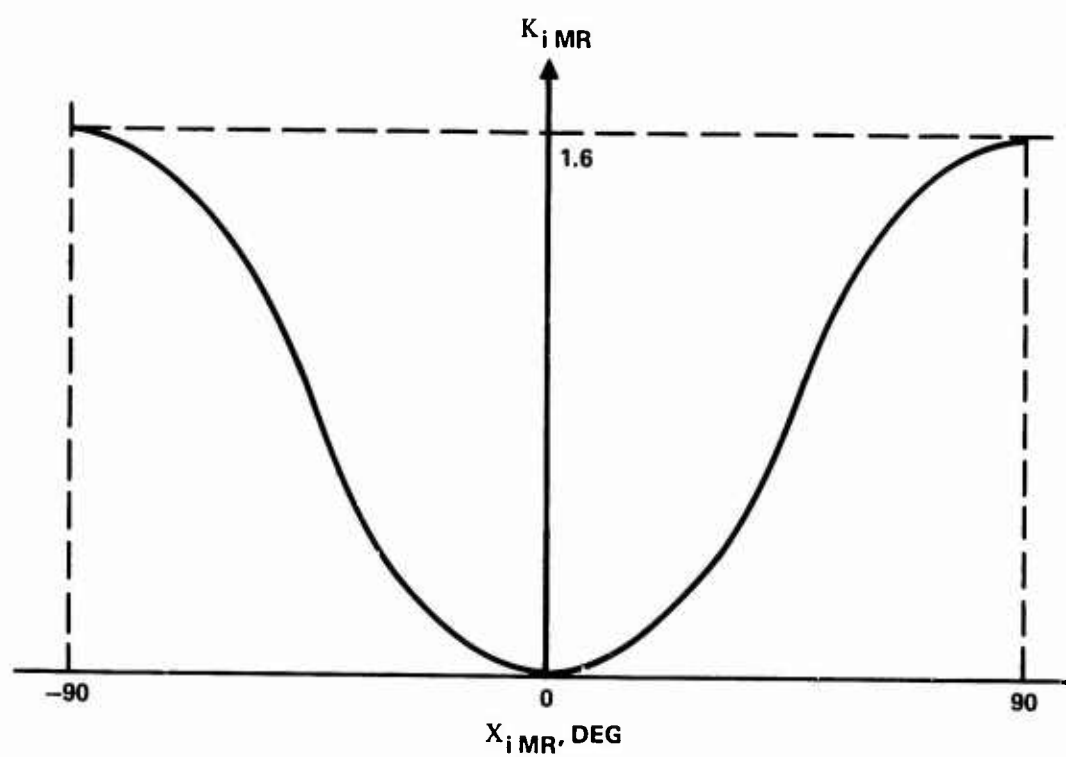


Figure 7-4. Typical Shape of Longitudinal Factor Curve

7.2.2.4 Downwash Transients

The downwash velocities are assumed subject to simple time lags:

$$\dot{w}_{iMR} = (w_{iMR,N} - w_{iMR})/\tau_{iMR} \quad (7-20)$$

and similarly for p_{iMR} and q_{iMR} . The value $w_{iMR,N}$ is the new value obtained from the steady-state formulation of the previous sections. The time lag τ_{iMR} is difficult to estimate. It probably should be related to a length such that $\tau_{iMR} = l_{iMR} V_{iMR}$. Suppose there is a sudden change in collective or cyclic. The characteristic length at which the old trailing vortices are having a minor effect on the rotor would be expected to be of the order of a small fraction, roughly 1/3, of the rotor diameter.

Also, de facto, the time lag serves as an averager which has some effect in assisting the convergence of the solution.

7.2.2.5 Iteration of Downwash Solution

As is the case with any rotary-wing loading calculation, there is an interplay between the downwash variance from calculating the loading and a variance in the loading from recomputing the downwash. A common practice is to solve an iterative loop to satisfy both equations (i.e., lift and momentum). In REXOR the iteration does not take place independently, but proceeds stepwise with the rotor azimuthal advance. With the normal, rapid convergence of the iteration the solution will essentially be complete with the step advance. However, large step sizes will incur an additional downwash time lag.

7.2.3 Blade Element Velocity Components

In the following subsections the blade aerodynamic loading is categorized and developed along two lines. They are:

- Steady-state aerodynamics
- Transient phenomena consisting of quasi-steady aerodynamics and dynamic stall.

7.2.3.1 Sources and Resolution from Blade Motion

The steady aerodynamics are based on the air velocities while the quasi-steady aerodynamics (from flutter theory) and dynamic stall depend on accelerations.

The air velocity is the blade mechanical velocities summed with a component due to downwash. In a similar manner, the air acceleration is taken to be the mechanical blade accelerations minus the downwash accelerations. The downwash formulation as developed in Section 7.2.2 allows for lags, and it is these lags that result in downwash acceleration terms.

7.2.3.2 Steady Aerodynamics

The air velocities relative to a blade section are desired for an axis system with origin at the quarter chord to match the airfoil table data. From Section 5.5.5, the mechanical blade velocities relative to the free stream or earth axes are available as $\{\dot{x}_{BLE}, \dot{y}_{BLE}, \dot{z}_{BLE}\}^I$. The desired relative air velocities at the quarter chord (or blade BLn reference axis) are:

$$\left\{ \begin{array}{c} \dot{x}_{1/4 \text{ c}} \\ \dot{y}_{1/4 \text{ c}} \\ \dot{z}_{1/4 \text{ c}} \end{array} \right\}_{BLE} = [T_{BLn - BLE}] \left\{ \begin{array}{c} \left\{ \begin{array}{c} \dot{x}_{BLE} \\ \dot{y}_{BLE} \\ \dot{z}_{BLE} \end{array} \right\}_{BLn}^I + \left\{ \begin{array}{c} 0 \\ 0 \\ w_{BLE} \end{array} \right\}_{DW, BLn} \end{array} \right\} + \left\{ \begin{array}{c} r \ Y_{CG} \\ 0 \\ -p \ Y_{CG} \end{array} \right\}_{BLE} \quad (7-21)$$

Where the second vector on the right is the downwash velocity developed in Section 7.2.2, and the third transfers the velocity from the BLE reference point at the blade center of gravity back to the quarter chord. The distance Y_{CG} is positive with the center of gravity ahead of the quarter chord. For notational convenience,

$$\left\{ \begin{array}{c} U_S \\ U_C \\ U_N \end{array} \right\} = \left\{ \begin{array}{c} -\dot{x}_{1/4 \text{ c}} \\ \dot{y}_{1/4 \text{ c}} \\ -\dot{z}_{1/4 \text{ c}} \end{array} \right\} \quad (7-22)$$

The angle of attack is defined as

$$\alpha_{1/4 \text{ c}} = \sin^{-1} \left(U_N / \sqrt{U_C^2 + U_N^2} \right) \quad (7-23)$$

Airflow aspects of quasi-steady aerodynamic formulation are developed at this point for convenience. The quasi-steady aerodynamic contribution is conceived as composed of circulatory and noncirculatory components. The circulatory components are taken to be equivalent to finding the aerodynamic force, and moment coefficients are based on an angle of attack at the three-quarter chord:

$$\alpha_{3/4 c} = \alpha_{1/4 c} + \frac{p_{BLE} \frac{c}{2}}{\sqrt{U_N^2 + U_C^2}} \quad (7-24)$$

As such, the effect of angular rates is included in deriving the steady aerodynamic coefficients. The formulation above does not attempt to account for local downwash rotation or curvature and its chordwise variation. The net result is that aerodynamic coefficients determined in Section 7.2.4 are computed with $\alpha_{3/4 c}$.

A number of quantities used in the dynamic stall computations, Section 7.2.3.4, are also available from the previous mechanical development. They are also defined here for convenience. First, the angle of sideslip appears only in the dynamic stall formulation. For this purpose it is defined as

$$\Lambda = \tan^{-1} \left(\frac{U_S}{U_C} \right) \quad (7-25)$$

Also, dynamic stall is based on the time derivative of the angle of attack at the three-quarter chord:

$$\begin{aligned} \dot{\alpha}_{3/4 c} = & \frac{1}{1 + (U_N/U_C)^2} \left[\frac{\dot{U}_N}{U_C} - \frac{U_N}{U_C} \frac{\dot{U}_C}{U_C} \right] \\ & + \frac{c}{2} \left[\frac{\dot{p}_{BLE}}{\sqrt{U_C^2 + U_N^2}} - p_{BLE} \left(\frac{U_C \dot{U}_C + U_N \dot{U}_N}{(U_C^2 + U_N^2) \frac{3}{2}} \right) \right] \end{aligned} \quad (7-26)$$

The above equation requires \dot{U}_C and \dot{U}_N .

$$\begin{Bmatrix} \dot{U}_S \\ \dot{U}_C \\ \dot{U}_N \end{Bmatrix} = + \left[T_{BLn} - BLE \right] \left\{ \begin{Bmatrix} -\ddot{X}_{BLE} \\ \ddot{Y}_{BLE} \\ -\ddot{Z}_{BLE} \end{Bmatrix}^I + \begin{Bmatrix} -g_X \\ g_Y \\ -g_Z \end{Bmatrix}_{BLn} + \begin{Bmatrix} 0 \\ 0 \\ -\dot{w}_{BLE} \end{Bmatrix}_{DW,BLE} \right\} \\ + \begin{Bmatrix} (\dot{r}-pq)Y_{CG} \\ 0 \\ -(\dot{p}+qr)Y_{CG} \end{Bmatrix}_{BLE} \quad (7-27)$$

The subscript I has been used to define motions to earth axes. The additive of the gravity term places these accelerations in a true inertial axis system, not earth inertial axes, as appropriate for aerodynamic calculations. See Section 5.5.1. Gravity does cause bouyancy forces, but these can be ignored. The gravity vector can be obtained from hub values as

$$\begin{Bmatrix} g_X \\ g_Y \\ g_Z \end{Bmatrix}_{BLE} = \begin{bmatrix} \frac{\partial \zeta_{BLn}}{\partial \zeta_R} \\ \frac{\partial \zeta_R}{\partial \zeta_H} \end{bmatrix} \begin{Bmatrix} g_X \\ g_Y \\ g_Z \end{Bmatrix}_H \quad (7-28)$$

By differentiating the downwash velocities, the downwash accelerations are obtained:

$$\begin{aligned}
 \left(\dot{w}_{BLE} \right)_{DW,BLn} = & \dot{w}_{iMR} \frac{\left(w_{BLE} \right)_{DW,BLn}}{w_{iMR}} \\
 & - w_{iMR} f_{iMR} K_{iMR} \frac{x_{BLn}}{R} \sin(\psi_R + \psi_{BLn} + \psi_W) \dot{\psi}_R \\
 & + r \dot{p}_{iMR} \sin(\psi_R + \psi_{BLn}) + r \dot{q}_{iMR} \cos(\psi_R + \psi_{BLn}) \\
 & + r \left[p_{iMR} \cos(\psi_R + \psi_{BLn}) - q_{iMR} \sin(\psi_R + \psi_{BLn}) \right] \dot{\psi}_R
 \end{aligned}
 \tag{7-29}$$

7.2.3.3 Quasi-Steady Aerodynamics

Quasi-steady aerodynamics is accounted for in REXOR by incorporating the terms from the two-dimensional flutter theory of Theodorsen (reference 15). In the REXOR analysis, Theodorsen's lift deficiency function $C(k)$ is taken as unity. This means that the flutter theory presently incorporated neglects shed wake effects, or in physical terms does not account for the phase change between blade element lift (or pitching moment) and angle of attack, due to shed vorticity, or the assumption of quasi-steady aerodynamics is expressed by $C(k) = 1$.

Referring to the classic text on aeroelasticity by Bisplinghoff, Ashley, and Halfman (Reference 16), the expressions for lift and pitching moment are given as:

$$L = \pi \rho b^2 [\ddot{h} + U \dot{\alpha} - b a \ddot{\alpha}] + 2 \pi \rho U b C(k) \left[\dot{h} + U \alpha + b \left(\frac{1}{2} - a \right) \dot{\alpha} \right]
 \tag{7-30}$$

and

$$M = \pi \rho b^2 \left[b a \ddot{h} - U b \left(\frac{1}{2} - a \right) \dot{\alpha} - b^2 \left(\frac{1}{8} + a^2 \right) \ddot{\alpha} \right] \\ + 2 \pi \rho U b^2 \left(a + \frac{1}{2} \right) C(k) \left[\dot{h} + U \alpha + b \left(\frac{1}{2} - a \right) \dot{\alpha} \right] \quad (7-31)$$

In REXOR, the blade aerodynamics and quasi-steady aerodynamics are referenced to the local section quarter-chord properties. This is done because the majority of available airfoil data uses this reference. Note that the final aerodynamic loads are translated to the local BLE axis (cg location) for use in the equations of motion.

Reviewing the above expressions, and referencing the rotation point to the quarter chord gives $a = -1/2$. If we take $C(k)$ as unity, replace 2π for circulatory lift by $(dC_{LR}/d\alpha)$, and substitute $c/2$ for the semi-chord b , these equations become

$$L = \frac{\pi \rho c^2}{4} \left[\ddot{h} + U \dot{\alpha} + \frac{c}{4} \ddot{\alpha} \right] + \left(\frac{d C_{LR}}{d \alpha} \right) \frac{\rho c U}{2} \left[\dot{h} + U \alpha + \frac{c \dot{\alpha}}{2} \right] \quad (7-32)$$

and:

$$M = \frac{\pi \rho c^2}{4} \left[-\frac{c}{4} \ddot{h} - \frac{U c}{2} \dot{\alpha} - \frac{c^2}{4} \left(\frac{3}{8} \ddot{\alpha} \right) \right] \quad (7-33)$$

Note that the entire last term in the moment equation vanishes with $a = -1/2$. Referring to the lift expression, noncirculatory aerodynamic lift is accounted for in REXOR by the first term in which $\dot{h} + U\alpha$ are combined into \dot{U}_N in blade element coordinates. The second term results from table lookup where

$$\Delta L = \frac{1}{2} \rho U^2 c \left(\frac{d C_{LR}}{d \alpha} \right) \alpha = \frac{1}{2} \rho U^2 c C_{LR} \quad (7-34)$$

in which the angle of attack is previously computed from

$$\alpha_{3/4c} = \left[\frac{\dot{h}}{U} + \alpha + \frac{c\dot{\alpha}}{2U} \right] \quad (7-35)$$

The α within the brackets is identified as θ , the actual physical angle of the blade with respect to the freestream direction. The α on the left hand is that due to the air velocities which include the plunging velocity \dot{h} and rotation component $c/2\dot{\alpha}$. Hence $p_{BLE} = \dot{\alpha}$.

The total aerodynamic pitching moment is the sum of the quasi-steady loads computed above and the table lookup blade section properties (Section 7.2.4).

7.2.3.4 Dynamic Stall

Dynamic stall is included in REXOR based upon the Boeing-Vertol formulation set forth in References 17, 18, and 19. It is similar to the treatment of dynamic stall in the Bell C-81 program. A comparison of REXOR with the C-81 program is given in Appendix IV, pages 393-404, of Reference 4. Dynamic stall is specifically addressed with respect to the two programs beginning on page 395 of that report. A significant point of difference between the treatment of dynamic stall in the two programs is that C-81 puts a 20-percent limit on the angle-of-attack overshoot in obtaining the dynamic maximum lift coefficient, whereas REXOR has no limit. The correctness of the treatment of dynamic stall in either program is difficult to assess since the consensus of researchers in this area is that current methods are empirical at best, and much research still remains to be done in this area.

Reference 17 notes that, "The trends show that compressibility effects reduce dynamic-stall delay, and at about $M = 0.6$ no dynamic-stall delay is evident." For this reason an upper Mach number limit of 0.6 was implemented in the dynamic stall calculations for REXOR. The test data obtained by Boeing Vertol and given in the references cited was for the Mach number range 0.2 to 0.6. As implemented in REXOR if $M < 0.25$, the value $M = 0.25$ is used in the analytic expression for developing the stall hysteresis loop.

Reference 18 notes that it was found that, "airfoils used currently by the helicopter industry had stalling dominated by leading edge stall. For this type of stalling process, the dynamic C_L extension was proportional to the time rate of change of the angle of attack."

In that reference, so as to use static airfoil data as much as possible, static stall and dynamic stall are empirically related by developing a reference angle of attack given by

$$\alpha_{REF} = \alpha - \left(\gamma \sqrt{\left| \frac{c\dot{\alpha}}{2V} \right|} \text{sign}(\dot{\alpha}) \right) \quad (7-36)$$

in which,

$$\gamma = \log_e \frac{0.601}{M} \quad (7-37)$$

and is physically related to dynamic stall delay. α is identified as $\alpha_{3/4c}$ and

$$M = \alpha_s / \sqrt{U_N^2 + U_C^2} \quad (7-38)$$

As noted in Reference 19 in regard to dynamic stall..." as a blade element reaches and exceeds the static angle of attack, stall does not occur as long as a sufficient, positive time rate of change of the airfoil angle of attack, $\dot{\alpha}$, is present." The experimentally derived equation for dynamic stall delay is given in the reference as

$$\text{dynamic stall delay} = \gamma \sqrt{\frac{c\dot{\alpha}}{2V}} \quad (7-39)$$

where

$$\frac{c\dot{\alpha}}{2V} = k \quad (7-40)$$

the blade element reduced frequency.

Referring to the gamma expression, we note that $\gamma \rightarrow 0$ as $M \rightarrow 0.601$, which is the upper limit for Mach number values for dynamic stall calculations. Also, note that $\gamma \rightarrow 1$ as $M \rightarrow 0.2211$, which is approximated by the value of $M = 0.25$, the lower limit in REXOR for dynamic stall simulation.

The term α_{REF} given above is also called the dynamic angle of attack (Reference 19) and given by the notation α_{DYN} .

7.2.3.4.1 Lift Accounting for Dynamic Stall

Using the reference or dynamic angle of attack computed from α_{REF} , the REXOR program implements the "Fast Aerodynamic Table", Section 7.2.4, subroutine and determines the lift coefficient, C_L , corresponding to α_{REF} and the freestream Mach number for the specified blade element and blade azimuth position. Also computed at the given Mach number are the C_L for zero angle of attack and the C_L for a small increment $\Delta\alpha$ with respect to zero. Yawed or radial flow is accounted for by computing the yaw angle of the flow given by:

$$\Lambda = \tan^{-1} \left(\frac{U_S}{U_C} \right) \quad (7-41)$$

where U_S and U_C represent blade spanwise and chordwise components of flow respectively.

The slope of the lift curve is then found from:

$$\left(\frac{\partial C_L}{\partial \alpha} \right)_{DYN} = \frac{C_L(\alpha_{REF}, M) - C_L(0, M)}{\alpha_{REF} \cos \Lambda} \quad (7-42)$$

It can be argued from physical reasonings that the dynamic lift-curve slope cannot exceed the static lift-curve slope. As a check, REXOR also calculates:

$$\left(\frac{\partial C_L}{\partial \alpha} \right)_{0, M} = \frac{C_L(\Delta\alpha, M) - C_L(0, M)}{\Delta\alpha} \quad (7-43)$$

Only in the event $(\partial C_L / \partial \alpha)_{DYN}$ is greater than $(\partial C_L / \partial \alpha)_{0, M}$ is the latter value used to calculate C_L . Otherwise C_L is calculated by

$$C_L = \left(\frac{\partial C_L}{\partial \alpha} \right)_{DYN} \alpha + C_L(0, M) \quad (7-44)$$

The ability of this approximation to describe mathematically the lift hysteresis characterized by dynamic stall is shown in Figure 7-5, which compares analytical results with experimental two-dimensional airfoil data. (From Reference 19).

The component of the lift force per unit span acting normal to the blade chord axis and including dynamic stall effects is then calculated from

$$\Delta F_{NC} = C_L c \frac{\rho V^2}{2} \cos \alpha \quad (7-45)$$

The total normal force is determined by adding to this term the drag component, $C_D c \rho V^2 / 2 \sin \alpha$, and the unsteady aerodynamic terms discussed in the previous section. To account for dynamic stall effects on drag, two-dimensional drag coefficient data are used, but as determined at α_{REF} , not α . This is consistent with Reference 18.

The component of the lift force per unit span parallel to the blade chord axis is found correspondingly from:

$$\Delta F_C = \frac{C_L c \rho V^2}{2} \sin \alpha \quad (7-46)$$

The total chordwise force is then obtained by adding the corresponding drag coefficient term multiplied by $\cos \alpha$.

7.2.3.4.2 Pitching Moment Accounting for Dynamic Stall

For determining pitching moments due to dynamic stall (see Reference 17), the reference or dynamic angle of attack given by α_{REF} must be modified. In REXOR, this is accomplished by multiplying the second term by an empirical constant, K . Hence,

$$\alpha'_{REF} = \alpha'_{DYN} = \alpha - K \left(\gamma \sqrt{\left| \frac{c \dot{\alpha}}{2V} \right|} \text{sign}(\alpha) \right) \quad (7-47)$$

K is selected based upon the dynamic stall characteristics of the airfoil. In general it has been found for conventional rotor blade airfoils that K should be selected so that

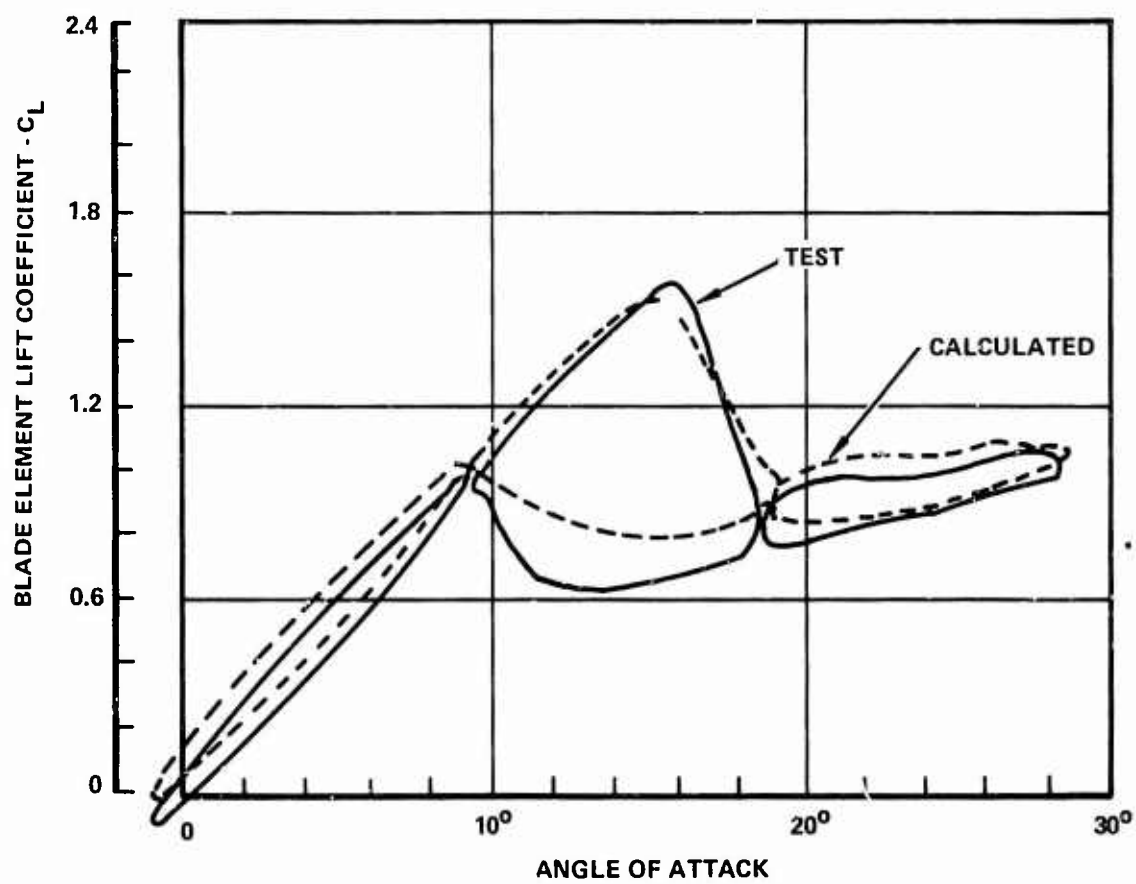


Figure 7-5. Dynamic Stall-Lift Coefficient vs Angle-of-Attack Hysteresis Loop

$$\alpha'_{REF} = \alpha_{REF} + \Delta \alpha \quad (7-48)$$

where $\Delta \alpha$ is of the order of 2.5 degrees. With α'_{REF} calculated from the above equation, the moment coefficient is determined from tables such that,

$$C_M = C_M(\alpha'_{REF}, M) \quad (7-49)$$

A comparison of test and theoretical dynamic C_M from Reference 19 is shown in Figure 7-6.

The total pitching moment acting per unit span on a blade element is then given by:

$$T(i) = - C_M c'^2 \frac{\rho V^2}{2} - F_{NO} S_Y(i) + \left[\begin{array}{c} \text{quasi-steady} \\ \text{aero} \\ \text{terms} \end{array} \right] \quad (7-50)$$

(Section 7.2.3.3)

where $S_Y(x)$ represents the distance from the aerodynamic center to the blade elastic axis, and the quasi-steady aerodynamic terms are included as described in Section 7.2.3.3.

7.2.4 Coefficient Table Lookup - Overview

In cataloging blade section aerodynamic data, C_L , C_D and C_M , there are two procedures available.

- Curve fit the aerodynamic data to the specific airfoil geometry being investigated for the range of Mach number and angle of attack to be considered.
- Tabulate the data as a function of performance and geometric parameters, and interpolate to the exact conditions at hand.

REXOR uses the second procedure. The data consist of a series of synthesized airfoil data for five digit series airfoils. The synthesizing process takes measured rotor data, and by means of numerical integration performance formulae, determines the equivalent two-dimensional airfoil section properties required.

Two-dimensional airfoil data from Lockheed tests and technical literature were used at a starting point to synthesize the data. Data for thickness

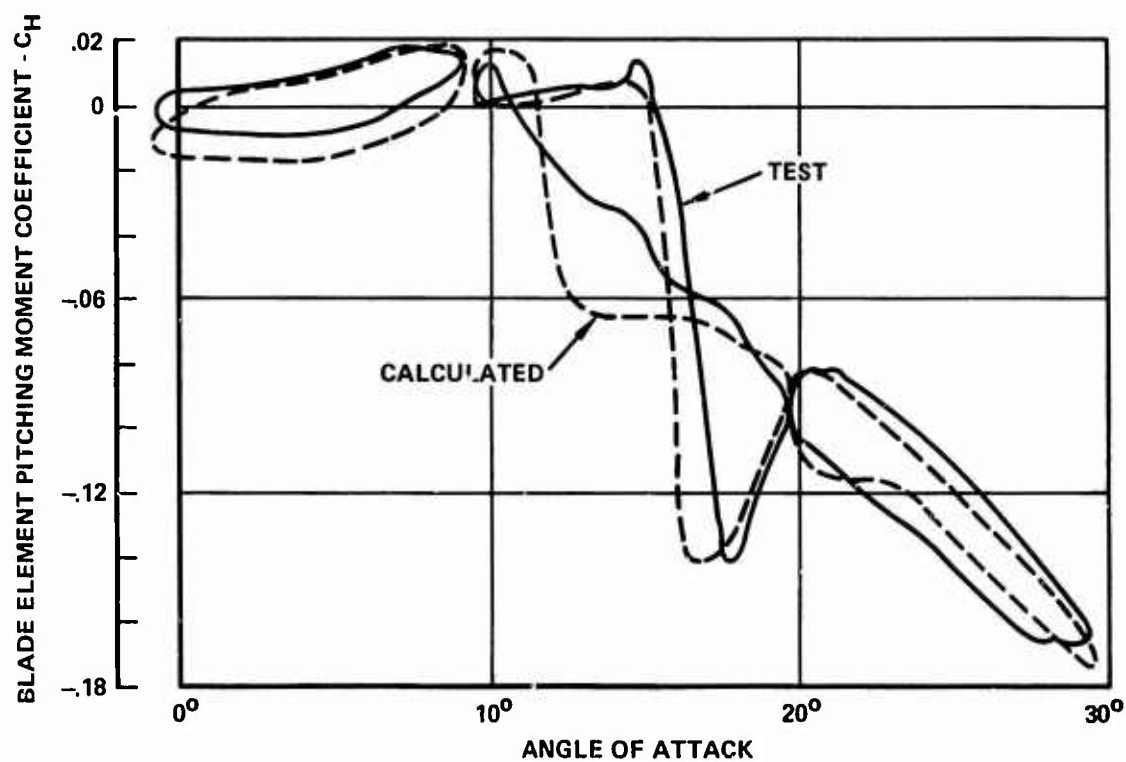


Figure 7-6. Dynamic Stall - Moment Coefficient vs Angle-of-Attack Hysteresis Loop

ratios and camber combinations, not previously available, were developed by using transonic similar rules as indicated in Reference 20. These data were cross checked for consistency with the data of the many sources noted in the bibliography of that reference. The rotor airfoil data synthesizing process from two-dimensional C_L and C_D data included the tip Mach relief and C_L and C_D adjustments for rotor applications in a manner consistent with the synthesized rotor airfoil data of Reference 21.

The C_L , C_D data covers uncambered thicknesses ratios from 6 to 12 percent and design lift coefficients of 0.09 to 0.69 for cambered sections of the same range of thickness ratio. For angles of attack within ± 30 degrees the data is also presented as a function of Mach number to account for compressibility. For large angles (above ± 30 degrees) compressibility effects are ignored. Blade element pitching moment data is also arranged along these lines, and is available for an uncambered 12 percent thickness ratio section and a 2-percent camber, 8-percent-thick section.

7.2.4.1 Inputs and Outputs

Two alternate methods are available in REXOR to use the data bank described above. First a lengthy, but generalized procedure, uses the data bank directly. From the spanwise design lift coefficient variation, the existing span station angle of attack and Mach number the tables are multiple interpolated to yield a C_L and C_D . The C_M coefficient is selected from one of the two sections available.

The second and the most common method of table usage, is to pre-interpolate the base tables described into a set keyed to the required geometry and arranged for rapid access. Currently the data take advantage of blade geometry characterized by either being constant thickness, camber or possessing a linear relationship between span - thickness and span - camber to specify only thickness ratio and automatically specify the other ingredients. The C_M data have been curve fitted for arbitrary variations in camber again specified as a function of thickness ratio. The data sets referred to in this second manner are known as the fast aero tables.

Note that by proper substitution, other tables and lookup procedures may be employed in REXOR.

7.2.4.2 Organization of Data in Tables

The base data bank contains a total of 31 tables. These are primarily referenced by design lift coefficient (and coincidentally camber) and thickness ratio. Secondary sorting is according to angle of attack range and if applicable, Mach number.

The fast aero tables are a set of six tables, two each for lift, drag and pitching moment coefficients. The double tables are for angles of attack below ± 30 degrees (also a function of Mach number) and above

± 30 degrees. These tables are generated for a specific blade configuration and referenced by thickness ratio.

Detailed contents of the tables are covered in Section 4 of Volume II.

7.2.4.3 Accession Method

As mentioned, the base data set is referenced to the desired C_L , C_D and C_M by a multiple interpolation scheme. The fast aero tables require a single trivariant interpolation (with Mach effects) to arrive at the required coefficient. By making the table entries at equally spaced intervals, an entry index is simply the entry value divided by the spacing value. The trivariant interpolation scheme is shown in Figure 7-7.

7.2.5 Blade Element and Rotor Aerodynamic Loads Summary

The required loads for use in the equations of motion are in B&n axis. Development to this form from BLE axis about this quarter chord point is covered in Section 6.6.4. The BLE axis form is:

$$\begin{aligned}
 \begin{Bmatrix} F_{X_A}(i) \\ F_{Y_A}(i) \\ F_{Z_A}(i) \\ M_{X_A}(i) \\ M_{Y_A}(i) \\ M_{Z_A}(i) \end{Bmatrix}_{BLE} &= \begin{bmatrix} [T_{\alpha-BLE}] & [0] \\ [0] & [T_{\alpha-BLE}] \end{bmatrix} \begin{Bmatrix} 0 \\ -\frac{1}{2} \rho (U_C^2 + U_N^2) C_D(i) \\ \frac{1}{2} \rho (U_C^2 + U_N^2) C_L(i) \\ \frac{1}{2} \rho_c (U_C^2 + U_N^2) C_M(i) \\ 0 \\ 0 \end{Bmatrix} + \\
 &+ \begin{Bmatrix} 0 \\ 0 \\ F_{Z_A}(i) \\ M_{X_A}(i) \\ 0 \\ 0 \end{Bmatrix}_{Unsteady, BLE}
 \end{aligned} \tag{7-51}$$

where,

$$\begin{bmatrix} T_{\alpha-BLE} \end{bmatrix} = \begin{bmatrix} 1 & 0 & 0 \\ 0 & \cos(\alpha_{3/4} c) & -\sin(\alpha_{3/4} c) \\ 0 & \sin(\alpha_{3/4} c) & \cos(\alpha_{3/4} c) \end{bmatrix} \quad (7-52)$$

7.3 INTERFERENCE TERMS

7.3.1 Nature of the Phenomenon

In the process of producing lift, the various parts of the rotorcraft impart a net momentum change to the air mass opposite to the direction of the force produced. This induced air velocity from the momentum change impinges upon other elements of the rotorcraft changing their aerodynamic behavior.

The sources of interest are the main rotor and wing (or lifting body characteristics of the fuselage). The surfaces being affected are the wing plus fuselage and horizontal tail. The impinging velocity is expressed in Z_F (fuselage verticle) axis as a percentage of the source flow and a function of the wake angle of this flow.

A second interference velocity source is to consider the circulation part of the Theodorsen function. Here the wing or wing equivalent of the fuselage is producing lift at the quarter-chord point according to the air velocity at the 3/4-chord location. Accordingly, the vertical component of air velocity at the wing includes a component,

$$\frac{1}{2} C_{wing} q_F \quad (7-53)$$

Here the wing quarter chord is assumed to lie on the Y_F axis. This component is also effective at the horizontal tail via the wing to horizontal tail downwash factor.

7.3.2 Rotor to Wing/Fuselage

The downwash function (percentage of source flow) used in REXOR is a lookup table of downwash factor, $F_{\chi_{MR-2}}$, and idealized main rotor wake angle χ_{MR}

where,

$$\chi_{MR} = \tan^{-1} \left(\frac{w_H - w_{iMR}}{u_H} \right) \quad (7-54)$$

The table data is linearly interpolated to the required wake angle value.

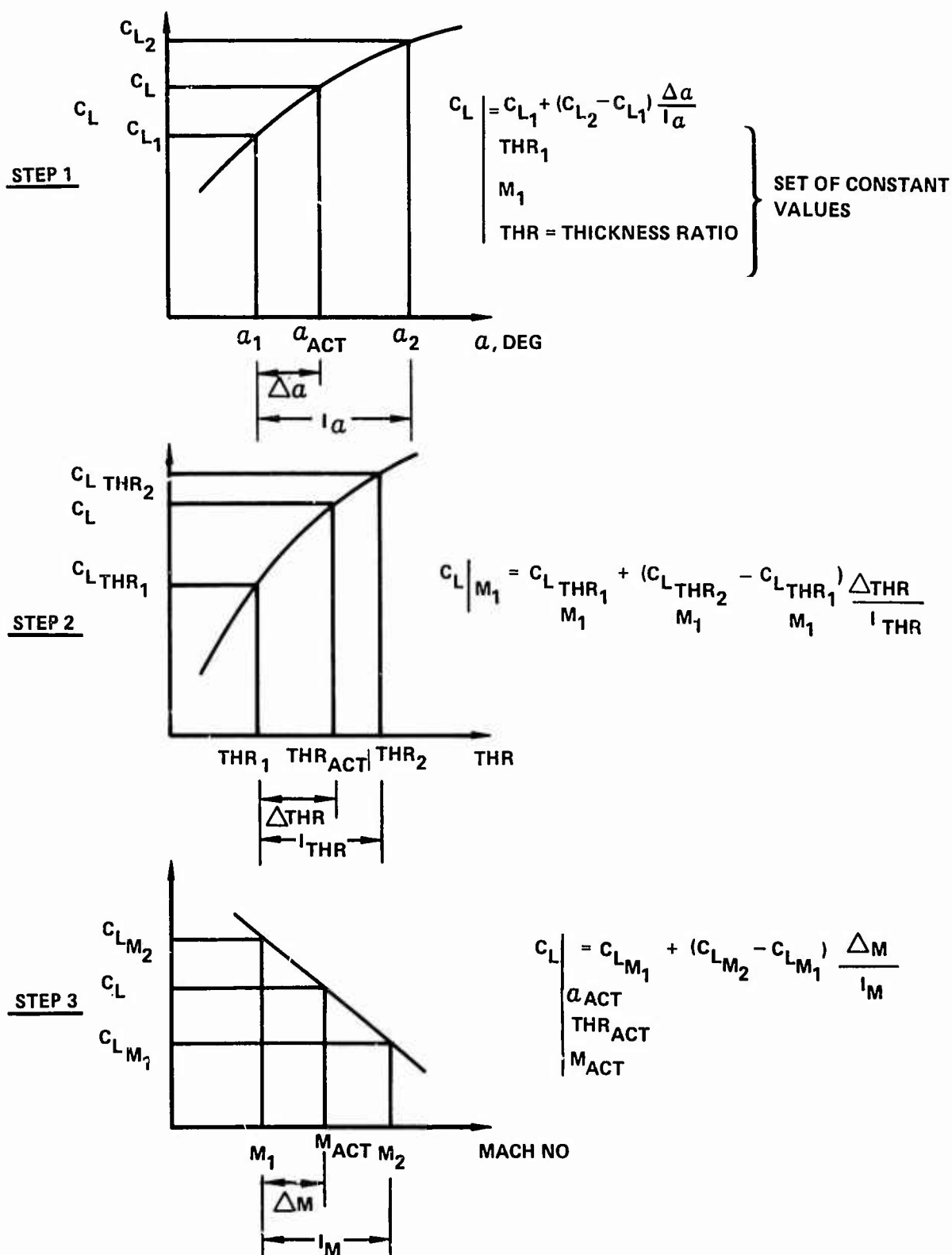


Figure 7-7. Trivariant Linear Interpolation

The fuselage reference downwash velocity at the wing (or equivalent) then is

$$w_{WING} = w_F - w_{iMR} F_{X_{MR-W}} + \frac{1}{2} C_{WING} q_F \quad (7-55)$$

and taking time derivatives,

$$\dot{w}_{WING} = \dot{w}_F - \dot{w}_{iMR} F_{X_{MR-W}} + \frac{1}{2} C_{WING} \dot{q}_F \quad (7-56)$$

The total air velocity to the wing/fuselage is

$$V_{T_{WING}} = \left(u_F^2 + v_F^2 + w_{WING}^2 \right)^{1/2} \quad (7-57)$$

and the angle of attack is

$$\alpha_{WING} = \tan^{-1} \left(\frac{w_{WING}}{u_F} \right) \quad (7-58)$$

The total velocity in the fuselage XZ plane is used in the horizontal tail computations:

$$V_{X_Z} = \left(u_F^2 + v_{WING}^2 \right)^{1/2} \quad (7-59)$$

7.3.3 Rotor to Horizontal Tail

A downwash factor $F_{X_{MR-HT}}$ between the main rotor and horizontal tail is computed in the same manner as $F_{X_{MR-W}}$ from the main rotor wake angle X_{MR} . This data in conjunction with the wing to horizontal tail downwash factor is used to compute incremental air velocities at the horizontal tail. The fuselage lift, drag and moment data, Section 7.4, is assumed to be complete, less the downwash factors. Hence, only incremental correction velocities, which in turn will be used in computing load increments, are needed.

Evaluating the main rotor increment,

$$w_{iMR_I} = w_{iMR} \left(F_{\chi_{MR-HT}} - F_{\chi_{MR-W}} \right) \quad (7-60)$$

7.3.4 Wing to Horizontal Tail

The wing to horizontal tail downwash factor appears explicitly as a quasi-unsteady aerodynamic term. The steady term is accounted in an overall fuselage aerodynamic characteristic set. An airflow time delay from the wing to horizontal tail is computed as

$$\Delta t = \frac{l_{HT}}{V_{X_Z}} \quad (7-61)$$

Using the downwash factor $\partial \epsilon / \partial \alpha$ the vertical airflow component at the horizontal tail is

$$\Delta t \dot{w}_{WING} \frac{\partial \epsilon}{\partial \alpha} = \frac{l_{HT}}{V_{X_Z}} \dot{w}_{WING} \frac{\partial \epsilon}{\partial \alpha} \quad (7-62)$$

The total incremental velocity components at the horizontal tail are

$$\Delta w_{HT} = - w_{iMR_I} + l_{HT} \left(q_F + \frac{\partial \epsilon}{\partial \alpha} \dot{w}_{WING} / V_{X_Z} \right) \quad (7-63)$$

$$\Delta V_{HT} = - l_{VT} r_F + h_{VT} p_F$$

No fuselage - wing induced side wash is modeled in REXOR.

7.3.5 Data Sources

The theoretical downwash factor ranges from 0 at $\chi = 0, 180$ degrees to 2 at $\chi = 90$ in the fully contracted rotor wake. Several sources of measured data are available to construct a distribution for a given configuration. Reference 11 gives isolated rotor data for field distances and wake angle

ranges suitable for F_{XMR-W} and F_{XMR-HT} . Reference 22 gives a good data set for typical wing locations.

7.4 BODY LOADS

7.4.1 Nonrotating Airframe Airloads

The required loads are computed in REXOR as the sum of steady-state forces and moments plus loads arising from stability derivative type terms. The steady-state data are formed in terms of overall C_L , C_D , and C_M for the fuselage, wing, and empennage assembly. Typically these data are from wind tunnel tests.

The static body loads are:

$$\left\{ \begin{array}{c} F_{X_B} \\ F_{Y_B} \\ F_{Z_B} \\ M_{X_B} \\ M_{Y_B} \\ M_{Z_B} \end{array} \right\}_{W,STATIC} = \left\{ \begin{array}{c} -C_{D_I} Q_A \\ 0 \\ -C_{L_I} Q_A \\ 0 \\ C_{M_I} Q_A C_{WING} \\ 0 \end{array} \right\} \quad (7-64)$$

where:

$$Q_A = \frac{1}{2} \rho S_{WING} V_{X_Z}^2 \quad (7-65)$$

The wing area, S_{WING} , and chord, C_{WING} , are actual or the equivalent of the lifting fuselage. Alternately, they may be the reference length and area used for the available wind tunnel data. C_{D_I} , C_{L_I} and C_{M_I} are linearly interpolated from input data tables of C_L , C_D , C_M , versus angle of attack. The data are interpolated on α_{WING} from Section 7.3.2. The loads developed are in wind axis.

The stability derivative load contributions are computed as a 6 by 6 derivative matrix postmultiplied by a velocity component vector.

$$\left\{ \begin{array}{c} F_{X_B} \\ F_{Y_B} \\ F_{Z_B} \\ M_{X_B} \\ M_{Y_B} \\ M_{Z_B} \end{array} \right\}_{W, \text{DERIV}} = \left[F_{MN} \right] \left\{ \begin{array}{c} u_F^2 \\ v_F^2 \\ u_F v_F \\ u_F p_F \\ u_F \Delta w_{HT} \\ u_F \Delta v_{HT} \end{array} \right\} \quad (7-66)$$

where,

$$F_{MN}(1, 2) = \frac{1}{2} \rho S_{WING} C_{D_0} V = \text{Drag due to side slip squared.} \quad (7-67)$$

$$F_{MN}(2, 3) = \frac{1}{2} \rho S_{WING} \frac{dC_Y}{d\beta} = \text{Side force due to side slip.} \quad (7-68)$$

$$F_{MN}(2, 6) = \frac{1}{2} \rho S_{WING} \frac{dC_Y}{dV} = \text{Side force due to lateral velocity} \quad (7-69)$$

$$F_{MN}(3, 5) = \frac{1}{2} \rho S_{WING} \frac{dC_Z}{dW} = \text{Vertical force due to vertical velocity} \quad (7-70)$$

$$F_{MN}(4, 1) = \frac{1}{2} \rho S_{WING} b_{WING} C_{L_0} = \text{Roll moment due to wing incidence differential.} \quad (7-71)$$

$$F_{MN}(4, 3) = \frac{1}{2} \rho S_{WING} b_{WING} \frac{dC_L}{d\beta} = \text{Roll moment due to yaw-dihedral.} \quad (7-72)$$

$$F_{MN}(4, 4) = \frac{1}{4} \rho S_{WING} b_{WING}^2 \frac{dC_L}{d\left(\frac{Pb}{2V}\right)} = \text{Wing roll damping.} \quad (7-73)$$

$$F_{MN}(4, 6) = \frac{1}{2} \rho S_{WING} b_{WING} \frac{dC_L}{dV} = \text{Roll moment - lateral velocity coupling.} \quad (7-74)$$

$$F_{MN}(5, 2) = \frac{1}{2} \rho S_{WING} c_{WING} C_{M_0} V = \text{Pitching moment due to side slip.} \quad (7-75)$$

$$F_{MN}(5, 5) = \frac{1}{2} \rho S_{WING} c_{WING} \frac{dC_M}{dW} = \text{Pitching moment due to vertical velocity.} \quad (7-76)$$

$$F_{MN}(6, 3) = \frac{1}{2} \rho S_{WING} b_{WING} \frac{dC_N}{d\beta} = \text{Yawing moment due to side slip.} \quad (7-77)$$

$$F_{MN}(6, 6) = \frac{1}{2} \rho S_{WING} b_{WING} \frac{dC_N}{dV} = \text{Yawing moment due to lateral velocity.} \quad (7-78)$$

These terms also produce forces and moments in wind axes.

The static and derivative terms are added to form the total body loads and transformed into fuselage axes.

$$\begin{Bmatrix} F_{X_B} \\ F_{Y_B} \\ F_{Z_B} \\ M_{X_B} \\ M_{Y_B} \\ M_{Z_B} \end{Bmatrix}_F = \begin{bmatrix} [T_{\alpha_W}] & [T_{\beta_W}]^T & [0] \\ \hline [0] & [T_{\alpha_W}] & [T_{\beta_W}]^T \end{bmatrix} \begin{Bmatrix} F_{X_B} \\ F_{Y_B} \\ F_{Z_B} \\ M_{X_B} \\ M_{Y_B} \\ M_{Z_B} \end{Bmatrix}_{W, \text{STATIC}} + \begin{Bmatrix} F_{X_B} \\ F_{Y_B} \\ F_{Z_B} \\ M_{X_B} \\ M_{Y_B} \\ M_{Z_B} \end{Bmatrix}_{W, \text{DERIV}} \quad (7-79)$$

where,

$$[T_{\alpha_W}] = \begin{bmatrix} \cos(\alpha_W) & 0 & -\sin(\alpha_W) \\ 0 & 1 & 0 \\ \sin(\alpha_W) & 0 & \cos(\alpha_W) \end{bmatrix} \quad (7-80)$$

$$\begin{bmatrix} T_{\beta_W} \end{bmatrix}^T = \begin{bmatrix} \cos(\beta_W) & -\sin(\beta_W) & 0 \\ \sin(\beta_W) & \cos(\beta_W) & 0 \\ 0 & 0 & 1 \end{bmatrix} \quad (7-81)$$

and

$$\cos(\alpha_W) = u_F / V_{X_Z} \quad (7-82)$$

$$\sin(\alpha_W) = w_{WING} / V_{X_Z} \quad (7-83)$$

$$\cos(\beta_W) = V_{X_Z} / V_{T_{WING}} \quad (7-84)$$

$$\sin(\beta_W) = v_F / V_{T_{WING}} \quad (7-85)$$

The air velocities w_{WING} , V_{X_Y} , $V_{T_{WING}}$, are defined in Section 7.3.2.

7.4.2 Component Additional Airloads

A total array, $\{QLOADS\}$, of non main rotor air loads is computed in fuselage axes.

$$\{QLOADS\}_F = \begin{Bmatrix} F_{X_B} \\ F_{Y_B} \\ F_{Z_B} \\ M_{X_B} \\ M_{Y_B} \\ M_{Z_B} \end{Bmatrix}_F + \begin{Bmatrix} F_{X_{TR}} \\ F_{Y_{TR}} \\ F_{Z_{TR}} \\ M_{X_{TR}} \\ M_{Y_{TR}} \\ M_{Z_{TR}} \end{Bmatrix}_F + \begin{Bmatrix} F_{X_P} \\ F_{Y_P} \\ F_{Z_P} \\ M_{X_P} \\ M_{Y_P} \\ M_{Z_P} \end{Bmatrix}_F \quad (7-86)$$

The first component is described above. The tail rotor load vector and propeller load vector are developed in the following sections.

7.5 TAIL ROTOR

A number of different levels of aerodynamic presentation accuracy and axis of representation may be used for tail rotor computations. In line with the stated objectives of REXOR, a linear aerodynamic approach is used. A shaft axis reference is used for the analysis. In this system, the air velocity quantities involved are easy to visualize. Also, the flapping and feathering motions are the true, measureable quantities.

7.5.1 Formulations

First, consider the airflow quantities available in fuselage axis, Figure 7-8. Note the tail rotor axes align with the fuselage axis system. The detailed velocity components are given in Figure 7-9. Constructing the blade element tangential (U_T) and perpendicular (U_P) components,

$$U_T = (r \Omega)_{TR} + u_F \sin \psi_{TR} \quad (7-87)$$

$$U_P = -v_F + \ell_{TR} \dot{\psi}_F - w_{iTR} - r\dot{\beta} - u_F \beta \cos \psi_{TR} \quad (7-88)$$

where,

w_{iTR} is the tail rotor induced velocity

and

$$V_{TR} = -v_F + \ell_{TR} \dot{\psi}_F - w_{iTR} \quad (7-89)$$

Expressing the blade element angle of attack as a small angle of approximation,

$$\alpha_{TR} = \theta + \frac{U_P}{U_T} \quad (7-90)$$

where,

$$\theta = \theta_{TR} - A_1 \cos \psi_{TR} - B_1 \sin \psi_{TR} \quad (7-91)$$

A δ_{3TR} coupling is used to minimize tail rotor flapping. Defining $+\delta_{3TR}$ as a reduction in feathering for positive flapping gives

$$\theta = \theta_{TR} + \delta_{3TR} a_{1TR} \cos \psi_{TR} + \delta_{3TR} b_{1TR} \sin \psi_{TR} \quad (7-92)$$

The tail rotor analysis assumes no coning.

The blade flapping, β , is then

$$\beta = - a_{1TR} \cos \psi_{TR} - b_{1TR} \sin \psi_{TR} \quad (7-93)$$

The tail rotor expressions of interest are the prime forces added to the fuselage system. First looking at the tail rotor thrust. For a blade element we have

$$d T_{TR} = \left[\frac{1}{2} \rho a b c \alpha U_T^2 dr \right]_{TR} \quad (7-94)$$

where a is the lift curve slope, b is the number of tail rotor blades, and c is the blade chord (assumed constant).

Substituting,

$$d T_{TR} = \left[\frac{1}{2} \rho a b c (\theta U_T^2 + U_P U_T) dr \right]_{TR} \quad (7-95)$$

Integrating for the entire rotor,

$$T_{TR} = \left[\frac{1}{2\pi} \frac{1}{2} \rho a b c \int_0^{2\pi} \int_0^{BR} (\theta U_T^2 + U_P U_T) dr d\psi \right]_{TR} \quad (7-96)$$

where B is the finite airfoil lift factor expressed as a so-called tip loss factor.

Noting only even functions contribute to the integrand.

$$T_{TR} = \frac{1}{2} \rho a (b c R)_{TR} \left(\theta_{TR} \frac{B^3}{3} (\Omega R)_{TR}^2 + \theta_{TR} \frac{B}{2} u_F^2 + \frac{B^2}{2} (\Omega R)_{TR} V_{TR} + (\Omega R)_{TR} u_F b_{1TR} \frac{B^2}{2} \delta_{3TR} \right) \quad (7-97)$$

Note the thrust is independent of the longitudinal flapping, but is a function of lateral cyclic shown as lateral flapping times delta 3.

The required lateral flapping angle is obtained by equating the lateral flapping moment equal to zero.

$$0 = \left[\frac{1}{2\pi} \frac{1}{2} \rho a b c \int_0^{2\pi} \int_0^{BR} (\theta U_T^2 + U_P U_T) \cos \psi r dr d\psi \right]_{TR} \quad (7-98)$$

gives

$$b_{1TR} = - a_{1TR} \delta_{3TR} \quad (7-99)$$

To obtain the longitudinal flapping angle, the longitudinal rotor moment is formed and set equal to zero.

$$0 = \left[\frac{1}{2\pi} \frac{1}{2} \rho a b c \int_0^{2\pi} \int_0^{BR} (\theta U_T^2 + U_P U_T) \sin \psi r dr d\psi \right]_{TR} \quad (7-100)$$

gives

$$a_{1TR} = \frac{2 u_F \left(\theta_{TR}(\Omega R)_{TR} \frac{3B}{4} + v_{TR} u_F \right)}{\delta_{3TR} \left(B^2(\Omega R)_{TR}^2 + \frac{3}{2} u_F^2 \right) + B^2(\Omega R)_{TR}^2 - \frac{1}{2} u_F^2} \quad (7-101)$$

In formulating the tail rotor drive torque, the blade profile drag is expressed as

$$\bar{C}_D = C_{D0} + k \bar{C}_L^4 \quad (7-102)$$

where \bar{C}_L is the average lift coefficient. Reviewing the thrust equation with a constant (average) lift coefficient gives

$$T_{TR} = \left[\frac{1}{2\pi} \frac{1}{2} \rho b c \bar{C}_L \int_0^{2\pi} \int_0^{BR} U_T^2 dr d\psi \right]_{TR}$$

gives

$$C_L = 6 T_{TR} / \left(\rho \sigma_{TR} A_{TR} \left(B^3 (\Omega R)_{TR}^2 + \frac{3}{2} B u_F^2 \right) \right) \quad (7-103)$$

The drive torque is expressed as the reaction to turning the tail rotor shaft. The sense of rotation is clockwise, facing a left-hand mounted tail rotor.

$$d Q_{TR} = \left[-\frac{1}{2} \rho c b r U_T^2 \bar{C}_D + \frac{1}{2} \rho a b c \alpha \phi r U_T^2 \right]_{TR} dr \quad (7-104)$$

where

$$\phi = \frac{U_P}{U_T} \quad (7-105)$$

•

TR (7-106)

The remaining load term in X_{TP} . Using the same formulation methodology,

(7-107)

Making small angle approximations,

$$\begin{aligned}
 d X_{TR} = & \frac{1}{2} \rho(b, c)_{TR} \left[-\overline{C}_D U_T^2 \sin \psi \right. \\
 & + a(\theta U_T U_P + U_P^2) \sin \psi \\
 & \left. - a(\theta U_T^2 + U_P U_T) (a_1 \cos^2 \psi + b_1 \sin \psi \cos \psi) \right]_{TR} dr
 \end{aligned}
 \tag{7-108}$$

integrating

$$\begin{aligned}
 X_{TR} = & \frac{1}{2\pi} \frac{1}{2} \rho(b, c)_{TR} \left[\int_0^2 \left(\int_0^R -\overline{C}_D U_T^2 \sin \psi \, dr \right. \right. \\
 & + \int_0^{BR} \left(a(\theta U_T U_P + U_P^2) \sin \psi \right. \\
 & - a(\theta U_T^2 + U_P U_T) (a_1 \cos^2 \psi \\
 & \left. \left. + b_1 \sin \psi \cos \psi) \right) dr \right) d\psi \Big]_{TR} \\
 = & \frac{1}{2} \rho a(b, c, R)_{TR} \left(-a_1 \theta (\Omega R)^2 \frac{B^3}{3} - a_1 \frac{B^2}{2} V_{TR} \right. \\
 & + R V u_F \theta \frac{B^2}{2} - a_1^2 \left(1 - \delta_3^2 \right) R^2 u_F \frac{B^2}{4} \\
 & \left. - a_1 \left(1 + \delta_3^2 \right) R^2 \Omega V \frac{B^2}{4} - \frac{\overline{C}_D}{a} \frac{R^2}{4} \Omega u_F \right)_{TR}
 \end{aligned}
 \tag{7-109}$$

The induced velocity is calculated from simplified momentum balance.

$$w_{iTR} = T_{TR} / \left((2 \rho \pi R^2 B^2)_{TR} (v_{TR}^2 + u_F^2)^{1/2} \right) \quad (7-110)$$

Normally, the thrust, flapping, and induced velocity equations are solved as an iterative set. In REXOR, these equations are solved for every pass (azimuth step) of the main rotor, and the tail rotor set convergence is assumed a priori.

Note that the pitch-flap coupling does not appear in the expressions developed. This is due to the equivalence of flapping and feathering, coupled with the absence of lateral flapping.

7.5.2 Airloads - Control Settings

The force and moment terms are assembled for use in the overall body loads, Section 7.4. The pilot control is the rudder pedals to θ_{TR} .

$$\begin{Bmatrix} F_{X_{TR}} \\ F_{Y_{TR}} \\ F_{Z_{TR}} \\ M_{X_{TR}} \\ M_{Y_{TR}} \\ M_{Z_{TR}} \end{Bmatrix}_F = \begin{Bmatrix} X_{TR} \\ T_{TR} \\ 0 \\ h_{TR} T_{TR} \\ -Q_{TR} - h_{TR} X_{TR} \\ -Y_{TR} X_{TR} - l_{TR} T_{TR} \end{Bmatrix} \quad (7-111)$$

7.6 PROPELLER

7.6.1 Formulations

A pusher propeller is modeled in REXOR, and is referenced to the fuselage axis as shown in Figure 7-10. The forces and moments generated by the propeller are added to the $\{F_{NW}\}$ vector of total fuselage forces and moments. These components are transformed to the principal reference set for use in the equations of motion.

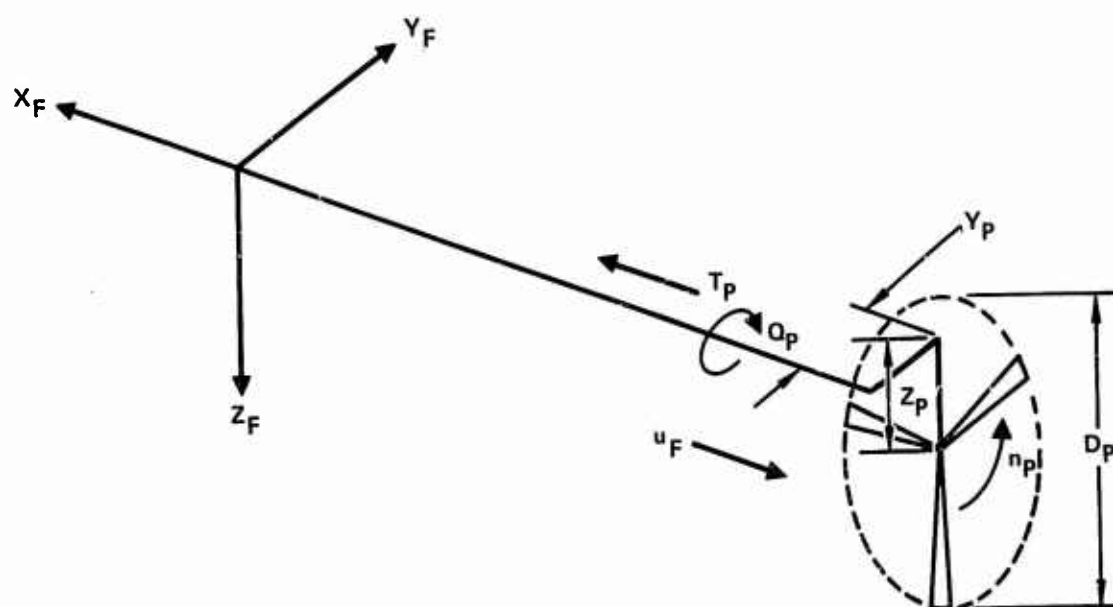


Figure 7-10. Propeller - Fuselage Geometry

The propeller aerodynamics are not calculated from blade theory, but instead are interpolated from performance data in the form of nondimensional thrust and power curves. See Figure 7-11. These curves are in terms of a thrust and power coefficient scheme unique to propeller work. Defining these coefficients:

$$J = \text{Advance Ratio} = \frac{V_P}{N_P D_P} \quad (7-112)$$

$$C_T = \text{Thrust coefficient} = \frac{T_P}{\rho N_P^2 D_P^4} \quad (7-113)$$

$$C_P = \text{Power coefficient} = \frac{2\pi Q_P}{\rho N_P^2 D_P^5} \quad (7-114)$$

where:

N_P = rotational speed, revolutions/second

D_P = propeller diameter, feet

V_P = axial inflow velocity, feet/second

ρ = air density slug/feet³

In REXOR, the fuselage inertial X velocity v_H is used for V . The rotational speed is ψ_R times the main rotor to tail rotor gear ratio less the gear case (fuselage) inertial roll rate.

7.6.2 Airloads - Control Settings

The coefficient curves are entered with the calculated advance ratio and command prop blade angle. The curves are bivariant interpolated to the required C_T and C_P . These quantities are then dimensionalized as shown above.

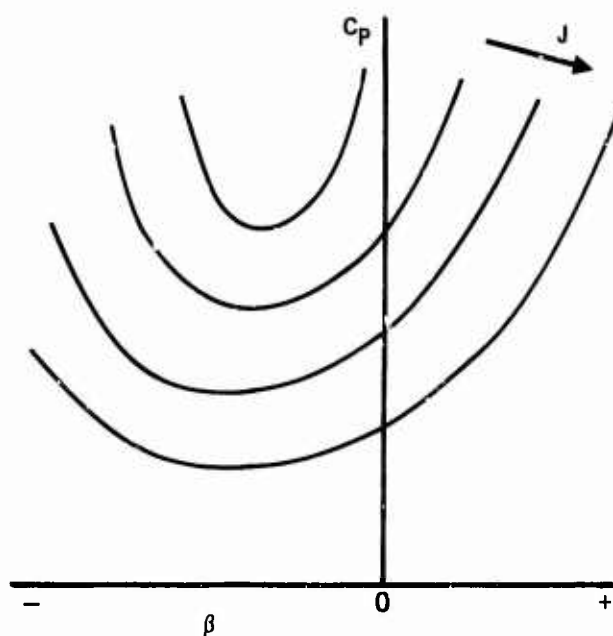
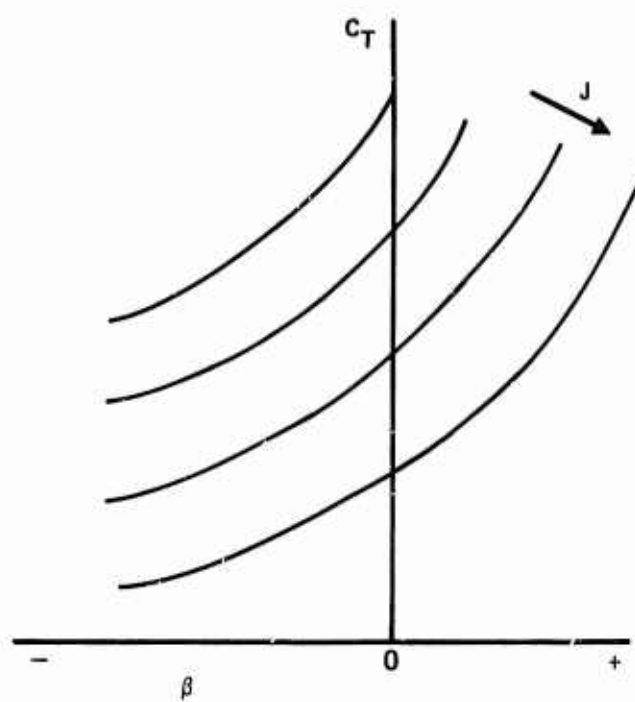


Figure 7-11. Typical Nondimensional Propeller Data

The required prop vector is

$$\begin{Bmatrix} F_X \\ F_Y \\ F_Z \\ M_X \\ M_Y \\ M_Z \end{Bmatrix}_P = \begin{Bmatrix} T_P \\ 0 \\ 0 \\ Q_P \\ Z_P T_P \\ -Y_P T_P \end{Bmatrix} \quad (7-115)$$

where Y_P and Z_P are prop shaft offsets from the fuselage axis.

8. REFERENCES CITED

1. Kerr, A. W., Potthast, A. J., Anderson, W. D., AN INTERDISCIPLINARY APPROACH TO INTEGRATED ROTOR/BODY MATHEMATICAL MODELING, Presented at the Symposium on the Status of Testing and Modeling for V/STOL Aircraft, American Helicopter Society, Philadelphia, Pa., Oct. 1972.
2. Anderson, W. D., INVESTIGATION OF REACTIONLESS MODE STABILITY CHARACTERISTICS OF A STIFF INPLANE HINGELESS ROTOR SYSTEM, American Helicopter Society, 29th Annual National Forum, May 1973, Preprint 734.
3. Gorenberg, N. B., Harvick, W. P., ANALYSIS OF MANEUVERABILITY EFFECTS ON ROTOR/WING DESIGN CHARACTERISTICS, Lockheed Report LR 24051, USAAVLABS Contract DAAJ02-70-C-0032, March 1971.
4. Anderson, W. D., Conner, F., Kerr, A. W., APPLICATION OF AN INTERDISCIPLINARY ROTARY-WING AIRCRAFT ANALYSIS TO THE PREDICTION OF HELICOPTER MANEUVER LOADS, USAAMRDL Technical Report 73-83, Dec. 1973.
5. Hoffman, J. A., ANALYSIS OF FLYING QUALITIES OF ROTARY WING AIRCRAFT, Lockheed Aerodynamics Memorandum Report No. 25, Oct. 1965.
6. Bailey, F. J., Jr., A SIMPLIFIED THEORETICAL METHOD OF DETERMINING THE CHARACTERISTICS OF A LIFTING ROTOR IN FORWARD FLIGHT, NACA Report 716, 1941.
7. Hoffman, J. A., Conner, F., ROTOR SENIOR ANALYSIS USING ASSUMED MODES, Lockheed Report LR 21619, June 1968.
8. Conner, F., ROTOR SENIOR BLADE AERODYNAMICS, Lockheed Rotary Wing Technical Memo TM-67-44-2, July 1969.
9. Houbolt, J. C. and Brooks, G. W., DIFFERENTIAL EQUATIONS OF MOTION FOR COMBINED FLAPWISE BENDING, CHORDWISE BENDING, AND TORSION OF TWISTED NONUNIFORM ROTOR BLADES, NACA Report 1346, Langley Aeronautical Laboratory, Langley Field, Va., 1959.
10. Castles, W., Jr., and De Leeuw, J. H., THE NORMAL COMPONENT OF THE INDUCED VELOCITY IN THE VICINITY OF A LIFTING ROTOR AND SOME EXAMPLES OF ITS APPLICATION, NACA Report 1184, 1954.
11. Heyson, H. H., and Katzoff, S., INDUCED VELOCITIES NEAR A LIFTING ROTOR WITH NONUNIFORM DISK LOADING, NACA Report 1319, 1957.
12. Castles, W., Jr., and Durham, H. L., Jr., DISTRIBUTION OF NORMAL COMPONENT OF INDUCED VELOCITY IN LATERAL PLANE OF A LIFTING ROTOR, NACA TN 3841, December 1956.

13. Curtiss, H. C., Jr., and Shope, N. K., A STABILITY AND CONTROL THEORY FOR HINGELESS ROTORS, 27th Annual Nat. V/STOL Forum, American Helicopter Society Preprint 541, May 1971.
14. Cheesman, I. C. and Bennett, W. E., THE EFFECT OF THE GROUND ON A HELICOPTER IN FORWARD FLIGHT, A.R.C. R.&M. No. 3021, 1957.
15. Theordorsen, T., GENERAL THEORY OF AERODYNAMIC INSTABILITY AND THE MECHANISM OF FLUTTER, NACA Report 496, 1935.
16. Bisplinghoff, R. L., Ashley, H., and Hoffman, R. L., AEROELASTICITY, Addison-Wesley Publishing Company, 1957.
17. Gross, D. M. and Harris, F. D., PREDICTION OF INFLIGHT STALLED AIR-LOADS FROM OSCILLATING AIRFOIL DATA, Proceedings 25th Annual National Forum, American Helicopter Society, Washington, D. C., May 14-16, 1969.
18. Harris, F. D., Tarzanin, F. J., Jr., and Fisher, R. K., Jr., ROTOR HIGH SPEED PERFORMANCE, THEORY VS. TEST, Journal of the American Helicopter Society, pp. 35-44, July 1970.
19. Tarzanin, F. J., Jr., PREDICTION OF CONTROL LOADS DUE TO BLADE STALL, Journal of the American Helicopter Society, pp. 33-46, April 1972.
20. Sipe, O. E., Jr., and Gorenberg, N. B., EFFECT OF MACH NUMBER, REYNOLDS NUMBER, AND THICKNESS RATIO ON THE AERODYNAMIC CHARACTERISTICS OF NACA 63A - SERIES AIRFOIL SECTIONS, Lockheed-California Company; USAAML Technical Report 65-28, U. S. Army Aviation Materiel Laboratories, Fort Eustis, Virginia, June 1965, AD 619153.
21. Carpenter, P. J., LIFT AND PROFILE DRAG CHARACTERISTICS OF AN NACA 0012 AIRFOIL SECTION AS DERIVED FROM MEASURED HELICOPTER ROTOR HOVERING PERFORMANCE, NACA Technical Note 4357, National Advisory Committee for Aeronautics, September 1958.
22. Bain, L. J., and Landgrebe, A. J., INVESTIGATION OF COMPOUND HELICOPTER AERODYNAMIC INTERFERENCE EFFECTS, United Technologies, Sikorsky Aircraft Div.; Technical Report 67-44, U.S. Army Aviation Materiel Labs, Fort Eustis, Virginia, 1967.

LIST OF SYMBOLS

The symbols used in the REXOR equations are quite numerous. In order to keep the catalog of symbols to manageable proportions the following list is divided according to the discussion in Section 4. Namely, a list of basic symbols is given, followed by subscripts, superscripts, and postscripts. Nonconforming cases of usage together with complicated or obscure subscripting are fully annotated in the basic list.

SYMBOLS

a	arbitrary vector
a_s	speed of sound
\ddot{a}_0	acceleration vector, ft/sec ²
a_1	longitudinal component of blade first harmonic flapping, rad
$[A]$	generalized mass element matrix
$A_{1,2,3}$	modal variables
A_{1n}	generalized displacement of <u>nth</u> blade, first mode
A_{2n}	generalized displacement of <u>nth</u> blade, second mode
A_{3n}	generalized displacement of <u>nth</u> blade, third mode
A_{1S}	cosine component of blade first harmonic cyclic, rad
b	number of main rotor blades; arbitrary vector
B	dissipation function
B_{1S}	sine component of blade first harmonic cyclic, rad
c	blade segment chord, ft
$[C]$	damping matrix
C_D	aerodynamic drag coefficient
C_L	aerodynamic lift coefficient
C_M	aerodynamic pitching moment coefficient
C_P	power coefficient
C_T	thrust coefficient

$C_{X,Y,Z}$	linear damping, lb/ft/sec
$C_{\phi,\theta,\psi}$	rotary damping, ft-lb/rad/sec
$C_{1,2,3}$	blade bending to feathering couplings
$C(k)$	lift deficiency function
d	infinitesimal increment
dr	increment in rotor, radius, ft
dt	increment in time, sec
d/dt	derivative with respect to time
$(d/e)_0$	swashplate to feather gear ratio, zero collective
$(d/e)_1$	swashplate to feather gear ratio slope with collective
e	pitch horn effective crank arm, ft
EI	blade bending stiffness distribution, lb-ft ²
f_{iMR}	ground effect factor for main rotor
F	factor; force, lb
$F_{X,Y,Z}$	force components along X,Y,Z directions, lb
$F_{\phi,\theta,\psi}$	generalized force about ϕ, θ, ψ axis
$F_{\beta PH}$	feathering mode generalized force
g	gravity, ft/sec ²
$g_{X,Y,Z}$	gravity components along X,Y,Z directions
G	gear ratio
$\{G\}$	generalized force vector
\ddot{G}	gyro angular acceleration partial product
GJ	blade torsional stiffness, lb-ft ²
I_X	$= \sum m_i X_i^2$, slug-ft ²
I_Y	$= \sum m_i Y_i^2$, slug-ft ²

I_Z	$= \sum m_i Z_i^2, \text{ slug-ft}^2$
I_{XX}	$= \sum m_i (Y_i^2 + Z_i^2), \text{ slug-ft}^2$
I_{YY}	$= \sum m_i (X_i^2 + Z_i^2), \text{ slug-ft}^2$
I_{ZZ}	$= \sum m_i (X_i^2 + Y_i^2), \text{ slug-ft}^2$
I_{XY}	$= \sum m_i X_i Y_i, \text{ slug-ft}^2$
I_{XZ}	$= \sum m_i X_i Z_i, \text{ slug-ft}^2$
I_{YZ}	$= \sum m_i Y_i Z_i, \text{ slug-ft}^2$
i	unit vector
j	unit vector
J	advance ratio
k	number of blade radial stations; reduced frequency, rad/sec; unit vector
$[K]$	spring matrix
K_{mj}	blade spring matrix element
$K_{X,Y,Z}$	spring constants along X,Y,Z direction, lb/ft
$K_{\phi,\theta,\psi}$	spring rates about ϕ, θ, ψ axis, ft-lb/rad
l_{IB}	location inboard feather bearing, ft
l_{OB}	location outboard feather bearing, ft
l_p	radial location of intersection of precone and feather axis, ft
l_{TTI}	tension torsion pack length, ft
L	rolling moment, ft-lb
m	mass of element, slugs
m_F	summed fuselage coordinate mass, slugs
m_H	summed hub axis mass, slugs
m_i	mass of <u>ith</u> particle or blade segment, slugs

m_{SP}	swashplate summed mass, slugs
M	pitching moment, ft-lb; $= \sum m_i$, slugs; mach number
$[M]$	generalized mass matrix
M_{rk}	generalized mass matrix element
$M_{\bar{X}}$	$= \sum m_i X_i$, slug-ft
$M_{\bar{Y}}$	$= \sum m_i Y_i$, slug-ft
$M_{\bar{Z}}$	$= \sum m_i Z_i$, slug-ft
$M_{X,Y,Z}$	moments about X,Y,Z axis, ft-lb
M_{ϕ}	blade torsional moment, ft-lb/ft
N	number of system particles
p	angular velocity about X axis, rad/sec; particle
P_{iMR}	main rotor pitch moment inflow, ft/sec
q	generalized coordinate; angular velocity about Y axis, rad/sec
q_{iMR}	main rotor roll moment inflow, ft/sec
Q	generalized forcing function
Q_A	aerodynamic pressure times reference wing area, lb
$QLOADS$	total nonmain rotor aerodynamic loads matrix
Q_{TR}	tail rotor torque, ft-lb
r	general vector; radius of curvature, ft; angular velocity about Z axis, rad/sec; notation for (X,Y,Z)
r_S	static blade shape
R	vector displacement of particle p in X,Y,Z axis system
R_0	vector displacement of x,y,z origin in X,Y,Z system
$R_{Z\phi,Z\theta}$	gyro damper coupling ratios

S	Laplace variable, path of motion of particle p
S_{NA}	blade spline length along neutral axis locii, ft
t	time
T	kinetic energy, ft-lb
[T]	transformation of coordinates matrix
T_{TT}	tension in tension - torsion pack, lb
u	velocity in X direction, ft/sec
U	potential energy function, ft-lb; strain energy, ft-lb
$U_{C,P,S,T}$	air velocity on blade element, ft/sec
v	velocity in Y direction, ft/sec
V_T	trajectory velocity
w	velocity in Z direction, ft/sec
w_{iMR}	main rotor collective inflow, ft/sec
w_{iTR}	tail rotor collective inflow, ft/sec
x	motion in X direction, ft; blade span location
X	coordinate direction; axis; deflection, ft; location, ft; cross product
X_{SW}	blade radial station of sweep and jog, ft
X_T	trajectory path, ft
X_{TR}	tail rotor longitudinal force, lb
y	motion in Y direction, ft
Y	coordinate direction; axis; deflection, ft; location, ft
$Y_{TTO_{1,2,3}}$	tension torsion pack outboard end modal coefficients
Y_{ONA}	difference between Y direction locations of cg and neutral axis points of blade element, ft

z	motion in Z direction
Z	coordinate direction; axis; deflection, ft; location, ft
Z_{SP}	relative swashplate vertical displacement with respect to the hub, ft
$Z_{TTO_{1,2,3}}$	tension-torsion pack outboard end modal coefficients
Z_{OBL}	teetering rotor undersling, ft
Z_{OF}	hub set distance above fuselage set, ft
Z_{OSP}	hub set distance above swashplate set, ft
Z_{OTTI}	blade vertical offset at outboard end of tension - torsion pack, ft
α	angle of attack, rad
α_2	angle of attack with hub set, rad
β	sideslip angle, rad
β_{FA}	blade feathering angle, rad
β_{PHn}	feathering/pitch-horn bending or dynamic torsion generalized coordinate displacement
β_0	blade droop relative to precone angle, rad
γ	blade sweep angle, rad; dynamic stall delay, sec
γ_T	trajectory path angle with E set, rad
δ	limit deflection, rad; freeplay, rad; small increment
δ_{3TR}	tail rotor pitch - flap coupling
$\partial \epsilon / \partial \alpha$	downwash factor of wing on horizontal tail
ζ	vector notation of ϕ, θ, ψ
θ	rotation about Y axis, rad
θ_0	collective blade angle, rad
Λ	sideslip at blade element, rad
ρ	air density, slugs/ft ³

τ	time constant, sec; natural period, sec
τ_0	feathering axis precone, rad
ϕ	rotation about X axis, rad
ϕ_F	feathering angle, rad
ϕ_{Fn}	feathering angle of blade element of <u>n</u> th blade, rad
ϕ_{REF}	blade root reference feather angle, rad
ϕ_T	blade torsion, rad
ϕ_T	sum of blade twist and torsion, rad
χ_{iMR}	wake angle of main rotor, deg
ψ	rotation about Z axis, rad; sideslip angle with hub set, rad
ψ_c	control input axis rotation from swashplate, rad
ψ_{PH}	pitch lead angle, deg
ψ_T	trajectory path yaw with E set, rad
ψ_W	main rotor apparent airflow angle, rad
ω	rotational speed, rad/sec; angular velocity, rad/sec; natural frequency, rad/sec
∂	partial derivative, derivation

SUBSCRIPTS

a	arbitrary coordinate set a
A	due to aerodynamics
b	arbitrary coordinate set b
BEND	associated with blade elastic bending
BLE	blade element coordinate system
BLn	blade reference axis system for the <u>n</u> th blade

C	associated with pilot control input, chordwise
CG	associated with center of gravity location
CORR	corrective, correction
DW	referring to downwash
DYN	referring to dynamic component
E	earth axis
ENG	associated with powerplant - engine
EST	estimated
F	fuselage axis; associated with blade feathering
FA	referring to blade feather axis
FB	associated with feedback
Fn	associated with feathering of the <u>nth</u> blade
FR	due to friction
G	referring to gyro or gyro coordinate system
GEN	associated with gas generator section of powerplant
GFB	associated with gyro control feedback
GSP	gyro to swashplate connection
GUB	relating to gyro gimbal unbalance
H	referring to hub or principal reference axis system
HT	associated with horizontal tail
i	referring to inflow, particle
IB	referring to inboard feather bearing location
J	spring matrix index
jog	associated with blade attachment joggle
J	associated with gyro end of feedback rod linkage

Jn	associated with feedback rod coming from the <u>n</u> th blade
k	generalized mass index
LAG	associated with lead-lag damper
LIMIT	signifying limiting value
m	blade mode index, spring matrix index
MR	associated with main rotor
n	blade number index
NA	referring to blade segment neutral axis
NEW	newly determined value
NO	normal (to airflow) component
NR	pertaining to nonrotating value
OB	referring to outboard feather bearing location
OLD	value from previous time step
P	associated with propeller; perpendicular blade component
PH	referring to pitch horn
r	generalized mass index
R	referring to rotor axis system
REF	associated with blade feather reference value
RM	referring to control gyro feedback lever moment
S	referring to blade spanwise velocity; general mode; static; structural; shaft
SC	referring to blade segment shear center
SP	referring to swashplate
SP _c	command to swashplate
S, SP	referring to swashplate limit stop

STEADY	steady component
SW	referring to blade sweep angle location
T	associated with trajectory path relating to E axis; tangential blade component; blade torsion; blade twist
TR	associated with the tail rotor
TRIM	initial or trim value
TT	associated with tension torsion pack
TTI	referring to inboard end of tension torsion pack
TTO	referring to outboard end of tension torsion pack
TW	associated with blade twist (built in)
UB	relating to control gyro unbalance
UNSTEADY	associated with unsteady component
VT	associated with vertical tail
WING	associated with the wing
X	relating to component in X direction
Y	relating to component in Y direction
YA	relating to aerodynamic component in Y direction
Z	relating to component in Z direction
ZA	relating to aerodynamic component in Y direction
0	(nought) associated with collective value, coordinate axis value, with respect to principal reference axis, blade root summation
1,2,3	with respect to blade modes 1, 2, or 3
1S	first harmonic component shaft axis feathering
1/4 c	with respect to blade 1/4 chord
3/4 c	with respect to blade 3/4 chord

β_{PHn}	associated with the feathering mode of the <u>n</u> th blade
ϕ	relating to component in the ϕ direction
θ	relating to component in the θ direction
ψ	relating to component in the ψ direction

SUPERSCRIPTS

I	referring to inertial reference
T	matrix transpose
(-)	(bar) average quantity
(')	(prime) slope with respect to blade span
(.)	(dot) time derivative of basic quantity
(..)	(double dot) second time derivative
(-1)	matrix inverse
(→)	vector quantity

POSTSCRIPTS

(i)	blade radial station index
(n)	blade number index